Homeostasis of Langerhans and Dendritic Cells in Health and Disease

Venetia Hart Bigley

Submitted in partial fulfillment of the requirements
for the degree of Doctor of Philosophy
Newcastle University

May 2011

Dedication

To my loved ones

Acknowledgements

My ardent thanks are given to Matthew Collin, without whose inspiration, steadfast guidance, abiding enthusiasm and boundless generosity, none of this would have been possible. I am also indebted to Muzlifah Haniffa who, with infinite patience and dedicated time, smoothed my initiation into the world of experimental science. All members of the laboratory have contributed to the exciting three years of research but specific thanks to Sarah Pagan for always being a willing, cheery and helpful pair of hands, Xiao Nong Wang for help with all things technical, Rachel Dickinson and Naomi McGovern for taking the reigns whilst I wrote up and Jean Norden for holding my hand at difficult moments in molecular biology.

Many people have been exceptionally generous with their time and help but I would particularly like to recognise my co-supervisors Stephen O'Brien, who provided both clinical and research support and Peter Middleton, who provided health and safety and procedural pearls of wisdom. Anne Dickinson and Graham Jackson have taken the trouble to keep me on the right academic tracks over the three years and shown enthusiastic support of the work.

For help with research material my heartfelt thanks go to the patients who have contributed to these studies and to the clinicians who have facilitated this: Jonathan Wallis whose sharp eyes and ear to the ground have lead us to identification of a number of subjects, Sophie Hambleton and Ignatius Chua who provided details and tissues from further subjects, Carl Allen and Kenneth McClain for a productive LCH collaboration and Kevin Windebank who not only put me in touch with LCH patients, but who also induced me into the clinical world of LCH. Without the help of the plastic surgery department of Newcastle Hospitals NHS Trust there would be no control skin.

For clinical and research help with subjects, I am grateful to Cliff Morgan and Jim Lordan. For technical support, guidance and practical help in flow cytometry and FACS, my greatest appreciation to Ian Dimmick and Rebecca Stewart and for making things visible with fluorescence microscopy, Trevor Booth.

For taking the ramblings of a PhD student seriously, for a trusted collaboration and for their generosity, I would like to thank John Dick and Sergei Doulatov.

Financial support for this work has been generously provided by the Medical Research Council, the Histiocytosis Association of America, The Newcastle Health Care Charity, Tyneside Leukaemia Research Association and the British Society of Haematology.

Finally, I am forever grateful for the broad-shouldered support of my husband, Mark Baker, close family and friends who have shared the excitements and struggles of the last few years.

Publications arising from Thesis

1. **Bigley V**, Haniffa M, Doulatov S, Wang XN, Dickinson R, McGovern N, Spence L, Pagan S, Dimmick I, Chua I, Wallis J, Lordan J, Morgan C, Kumararatne DS, Doffinger R, van der Burg M, van Dongen J, Cant A, Dick JE, Hampbleton S, Collin M. 2011. The human syndrome of dendritic cell, monocyte, B and NK cell deficiency. J Exp Med. Online publication Jan 17th 2011.

2. Hambleton S*, Salem S*, Bustamante J#, **Bigley V#**, Boisson-Dupuis S#, Azevedo J#, Fortin A, Haniffa M, Ceron-Gutierrez L, Bacon C, Menon G, Trouillet C, McDonald D, Carey P, Ginhoux F, Alsina L, Zumwalt T, Kong X, kumararatne D, Butler K, Hubeau M, Feinberg J, Al-Muhsen S, Cant A, Abel L, Chaussabel D, Doffinger R, Talesnik E, Grumach A, Duarte A, Abarca K, Moraes-Vasconcelos D, Burk D, Berguis A, Geissmann F!, Collin M!, Casanova JL!, Gros P!. 2011. Human IRF8 deficiency restricts monocyte and dendritic cell development and anti-mycobacterial immunity. NEJM in press. *Joint 1st authors. #Joint 2nd authors. ! Joint last authors.

3. **Bigley, VH**; Spence, LE; Collin, MP. 2010. Connecting the dots: monocyte/DC and NK subsets in human peripheral blood. Blood. 116: 2859-60

4. Haniffa, M; Ginhoux, F; Wang, XN; **Bigley, V**; Abel, M; Dimmick, I; Bullock, S; Grisotto, M; Booth, T; Taub, P; Hilkens, C; Merad, M; Collin, M. 2009. Differential rates of replacement of human dermal dendritic cells and macrophages during hematopoietic stem cell transplantation. J Exp Med. 206(2):371-85

5. **Bigley, V**; Haniffa, M; Pagen, S; Dimmick, I; Booth, T; Ginhoux, F; Allen, C; McClain, K; Merad, M; Collin, M. 2009. Human Langerin positive dermal dendritic cells constitute a population distinct from epidermal langerhans cells. *Manuscript in preparation.*

List of Abbreviations

AF	Autofluorescence
AML	Acute myeloid leukaemia
APC	Antigen presenting cell(s)
APC	Allophycocyanin
Baso	Basophil(s)
BM	Bone marrow
CD(number)	Cluster of differentiation (number)
CLA	Cutaneous Lymphocyte Antigen
CLP	Common lymphoid progenitor
CML	Chronic myeloid leukaemia
CMP	Common myeloid progenitor
CSF	Colony stimulating factor
DAPI	4',6-diamidino-2-phenylindole
DC	Dendritic cell(s)
DCML	Dendritic cell, monocyte and mixed lymphoid
DDC	Dermal dendritic cell(s)
EC	Endothelial cell(s)
EDTA	Ethylenediaminetetracetic acid
ELISA	Enzyme linked immunosorbent assay
Eosin	Eosinophil(s)
FACS	Fluorescence activated cell sorting
FCS	Fetal Calf Serum
FISH	Fluorescence in situ hybridization
FITC	Fluorescein isothiocyanate
Flt3	FMS-like tyrosine kinase 3
Flt3L	Flt3 ligand
GM-CSF	Granulocyte macrophage colony stimulating factor
GM-CSF-R	Granulocyte macrophage colony stimulating factor Receptor
GMP	Granulocyte monocyte progenitor
GvHD	Graft versus Host Disease
GvL	Graft versus Leukaemia
Hb	Haemoglobin
HLA-DR	Human leukocyte antigen – DR
HSC	Haematopoietic stem cell

HSCT	Haematopoietic stem cell transplant
IF	Immunofluorescence
IFN!	Interferon gamma
IL-(number)	Interleukin-(number)
Iso	Isotype control
Lang	Langerin
LC	Langerhans cell(s)
LCH	Langerhans cell histiocytosis
LDC	Langerin positive dermal dendritic cell(s)
LPS	Lipopolysaccharide
Lymph	Lymphocyte(s)
M-CSF	Macrophage colony stimulating factor (CSF-1)
M-CSF-R	Macrophage colony stimulating factor receptor (CSF1-R)
MEP	Megakaryocyte erythroid progenitor
MHC	Major Histocompatibility Complex
MLP	Multi-lymphoid progenitor
MLR	Mixed Lymphocyte Reaction
MoDC	Monocyte derived dendritic cell
Mono	Monocyte(s)
MPP	Multipotential progenitor
Neut	Neutrophil(s)
NK	Natural Killer Cell(s)
PB	Peripheral blood
PBMC	Peripheral Blood Mononuclear Cells
PBSC	Peripheral Blood Stem Cells
PCR	Polymerase chain reaction
pDC	Plasmacytoid dendritic cell
PE	Phycoerythrin
PerCP	Peridinin chlorophyll protein
Ph	Philadelphia Chromosome
Plt	Platelets
Preps	Preparations
Q-PCR	Quantitative polymerase chain reaction
RBC	Red blood cells
RNA	Ribonucleic acid

RPMI	Roswell Park Memorial Institute
RT	Room temperature
SCF	Stem cell factor
SCID	Severe combined immunodeficiency
SD	Standard deviation
TCR	T cell receptor
TLR	Toll-like receptor
TNF!	Tumour necrosis factor alpha
TGF	Transforming growth factor beta
TKI	Tyrosine kinase inhibitor
Treg	Regulatory T cell(s)
UV	Ultraviolet
WBC	While blood cell

Abstract: Homeostasis of Langerhans and Dendritic Cells in Health and Disease

Dendritic Cells (DC) play a pivotal role in both the initiation of immunity and its regulation through tolerance induction. They represent potential targets or tools of therapy in autoimmunity, allergy, cancer, and transplant medicine. Despite recent progress in mapping tissue DC subsets in human, their ontogeny and mechanisms of homeostasis remain elusive.

The conventional view is that maintenance of tissue DC and macrophages is dependent on constant replenishment from circulating monocyte precursors. This concept was derived from *in vitro* data and mouse models under perturbed conditions. While these observations may reflect events in inflammation, studies in murine steady-state biology have challenged this, with data indicating at least three ways in which DC may persist independently of monocytes: 1, tissue DC are replaced by non-monocyte, blood-borne precursors; 2, embryological cells seed tissues and persist in adulthood; 3, DC, or their immediate precursors, self-renew in tissues. These mechanisms may not be mutually exclusive.

Although much has been gained from the study of DC kinetics in human transplant, these conditions are, at least in part, inflammatory. To understand the steady-state homeostasis of DC and epidermal Langerhans cells (LC) in human tissues, a number of approaches were taken.

Firstly, a comprehensive 'DC profile' of normal human tissues was developed, starting with detailed characterization of DC, monocyte and macrophage populations in human peripheral blood (PB) and skin. This lead to the identification of new DC subsets in peripheral tissue. Cells with DC precursor potential were then sought, through analysis of their growth factor receptor expression and ability to enter into cell cycle. Correlative data was gathered to suggest relationships between potential blood borne DC precursors and skin APC. The $CD34^+$ haematopoietic compartment was examined to identify potential DC progenitors. The granulocyte/macrophage progenitor (GMP) and a

more recently described multilymphoid progenitor (MLP) were identified and shown also to be present in PB. $CD34^+$ cells were identified in peripheral tissue.

While cell and gene knockout experiments have significantly advanced understanding of murine DC, these experiments are not possible in human. The second approach was therefore to undertake a search for subjects with spontaneous DC or monocyte deficiencies. Two novel syndromes were identified; Dendritic Cell, Monocyte, B and NK Lymphoid (DCML) deficiency (4 subjects) and autosomal recessive IRF8 deficiency (1 subject). In both cases, severe depletion of peripheral blood monocyte and DC subsets was associated with absence of tissue DC but preservation of LC and some tissue macrophages. Examination of $CD34^+$ stem cell compartments revealed distinct stem cell defects resulting in loss of MLP and depletion of GMP in DCML deficiency, but accumulation of these subsets in IRF8 deficiency. As predicted by mouse models, DC deficiency was associated with a reduction in circulating regulatory T cells, in the context of elevated Flt3-ligand.

Finally, lesions of Langerhans Cell Histiocytosis (LCH), a histiocytic disorder presenting with pathological accumulation of $langerin^+$ DC in tissues, were studied. Analysis of langerin distribution in normal skin and lung identified a $langerin^+$ DC, independent of LC. In keeping with *in vitro* culture data, preliminary observations show that langerin may be up-regulated on mDC in inflammatory conditions. These data suggest that langerin expression in LCH lesions may reflect its upregulation, rather than determine the LC origin of LCH cells.

A variety of techniques have been used to explore DC in normal tissue, novel syndromes of DC deficiency and Langerhans cell histiocytosis. These studies provide new insights into the ontogeny and homeostasis of human DC and LC.

List of Tables and Figures

Tables

Figures

Table of Contents

Chapter 1. Introduction

Dendritic cells (DC) are key sentinels of the immune system, specialised in antigen capture and presentation. They are found in almost all tissues where they encounter antigen prior to migrating to lymph nodes to initiate immunity or tolerance. From where they derive and how they are maintained in sites of antigen exposure remain important unresolved questions. Elucidating the homeostasis of human DC is vital to understanding the induction of immunity and tolerance in health, the role of DC in pathology and how to harness their therapeutic potential in treatments.

1.1 Introduction to Dendritic Cells

1.1.1 DC as Antigen Presenting Cells

The major cells classified as professional antigen presenting cells (APC) include DC, macrophages and B cells. These cells have the ability to internalise, process and present antigen as peptide in the context of MHC Class II. B cells are relatively weak APC and differ from DC and Macs in their possession of specific antigen receptors, surface immunoglobulins. They will not be considered further here. Macrophages are long lived in tissue and are generally responsible for clearance of debris and tissue repair after inflammation (1). However, various tissue macrophages are able to adopt specialised functions depending on their anatomical locations (reviewed in (2)). For example, alveolar macrophages are responsible for clearing respiratory pathogens and debris from the lung so express high levels of scavenger receptors (3), while osteoclasts in bone are responsible for bone remodeling (4).

Many cell types can become ‘non-professional’ antigen presenting cells through up-regulation of MHC class II expression, usually under inflammatory conditions. This is commonly seen in response to Interferon gamma (IFNγ) and can be seen in cells including T cells, NK cells, endothelial cells and fibroblasts (5). In contrast, DC express MHC Class II constitutively, are specialised to capture and process antigens *in vivo* (6) and are able to up-regulate co-

stimulatory molecules required for efficient stimulation of T cells. They orchestrate responses in both the innate and adaptive immune systems to initiate either immunity or tolerance. The pivotal nature of DC in the immune system is indicated by their ability to recognise a broad range of potentially pathogenic antigens and harness an array of appropriate responses (7).

1.1.2 Historical perspective

Although the epidermal Langerhans Cell (LC) was the first described APC, identified in 1868 by Paul Langerhans, it was originally thought to be of neuronal origin. It was not until 1979 that it was recognised as a bone marrow derived cell (8). By then, the initial description had been made in 1972 (published in 1973) by Ralph Steinman et al., of adherent stellate cells, distinct from macrophages, in mouse spleen (9). The first indication that DC were potent stimulators of T cells was seen in the *in vitro* Mixed Lymphocyte Reaction (MLR) in which context DC were described as 'accessory cells'. They were found to be 100 times more effective than total spleen cells (containing approximately 1% DC) at stimulating a T cell response (10).

Through the study of murine Langerhans Cells it was noted that freshly isolated LC could present antigen but were poor stimulators in an MLR, while the reverse was true of LC cultured with GM-CSF (11) (12). This lead to the concept of the necessity of DC maturation following antigen capture, prior to migration and efficient interaction with T cells (13).

1.1.3 Role of DC in Innate Immunity

The innate immune system is phylogenically the oldest form of host defense against infection. It relies on a limited number of germ line encoded receptors which recognise conserved microbial antigens, including pathogen recognition receptors (PRR), Tol-like receptors (TLR) and lectins (14), expressed by many cells including neutrophils, monocytes and macrophages. Signaling via these receptors leads to the rapid induction of antimicrobial genes and inflammatory cytokines. Specific to DC, signaling via TLRs leads to the up-regulation of co-stimulatory molecules and increased antigen-presenting capacity (15). This links the DC to the adaptive arm of immunity.

1.1.4 Role of DC in Adaptive Immunity

The two key features of the adaptive immune system are: i) the exquisite specificity for antigens and ii) the development of memory leading to improved function on re-exposure to antigen. This is largely controlled through the interaction between DC and naïve $CD4^+$ T cells. The presentation of antigen in the context of Class II expression on DC allows the activation of T cells with specificity for that antigen. After clonal selection, T cells undergo extensive expansion and differentiation to helper or killer phenotypes (16). T cell memory is also acquired (17). The secretion of selective cytokines by DC is thought to regulate these processes. For example, secretion of IL-12, the major cytokine of activated DC, leads to a T helper (Th) type 1 response (18), while secretion of IL-23 induces Th17 responses (19).

The steps involved in DC activation of T cells within a lymph node were summarised by Kapsenberg in a 'three signal model' (20). Following antigen capture in the periphery and migration of DC to the LN, DC present the pathogenic antigen in the context of MHC class-II to the T cell via its T cell receptor (TCR); Signal 1. Signal 2 is co-stimulatory involving CD80 or CD86 expressed on activated DC, and CD28 on T cells. Signal 3 is a polarizing signal, mediated by soluble or membrane-bound factors, instructing T cells to develop a T-helper type I (Th1) or type II response. It is determined by the nature of the original antigen-DC interaction where the antigen binding of specific PRRs or TLRs will lead to the production of specific molecules to drive either a Th1 or Th2 response (**Figure 1.1**).

Figure 1.1

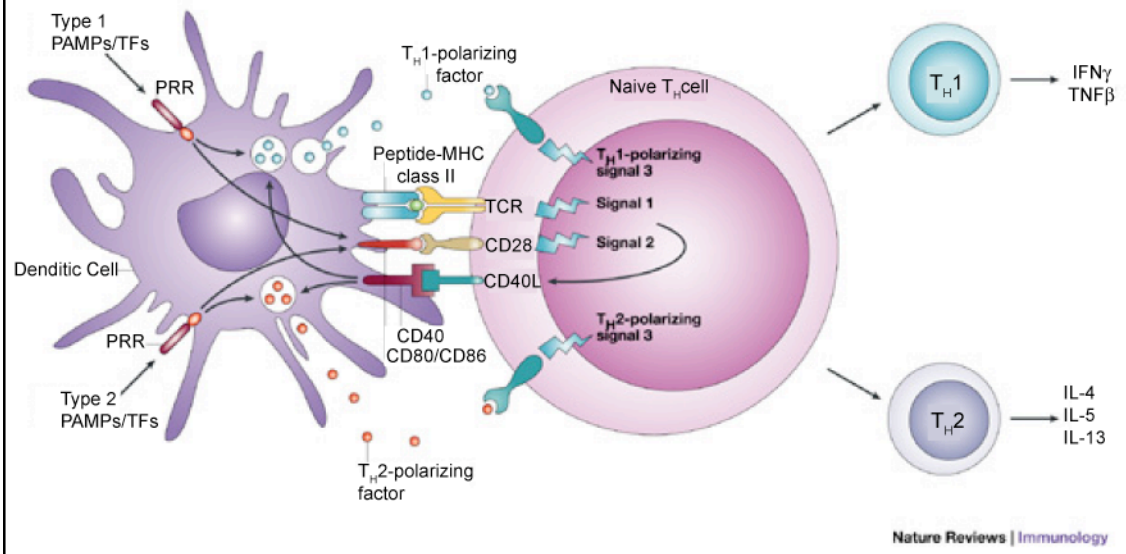

{Kapsenberg, 2003, Nat Rev Immunol, 3, 984-93}

Figure 1.1: Three signal model of DC-T cell interaction
Signal 1 is the antigen-specific signal that is mediated through T-cell receptor (TCR) triggering by MHC class-II-associated peptides processed from pathogens after internalization through specialized pattern recognition receptors (PRRs). Signal 2 is the co-stimulatory signal, mainly mediated by triggering of CD28 by CD80 and CD86 that are expressed by DC after ligation of PRRs, such as Toll-like receptors (TLRs) that are specialized to sense infection through recognition of pathogen-associated molecular patterns (PAMPs) or inflammatory tissue factors (TFs). Signal 3 is the polarizing signal that is mediated by various soluble or membrane-bound factors, such as interleukin-12 (IL-12) and CC-chemokine ligand 2 (CCL2), that promote the development of TH1 or TH2 cells, respectively. The nature of signal 3 depends on the activation of particular PRRs by PAMPs or TFs. Type 1 and type 2 PAMPs and TFs can be defined as those that selectively prime DCs for the production of high levels of TH1-cell-polarizing or TH2-cell-polarizing factors. Whereas, the profile of T-cell-polarizing factors is primed by recognition of PAMPs, optimal expression of this profile often requires feedback stimulation by CD40 ligand (CD40L) expressed by T cells after activation by signals 1 and 2. IFN-γ, interferon-γ; TNF-α, tumour-necrosis factor-α

1.1.5 Antigen presentation by DC

Like almost all cells, DC are able to present endogenous proteins in the context of MHC Class I through proteasome processing of cytosolic components. This includes the presentation of viral antigens in the setting of direct viral infection of the cell. Endogenous or exogenous antigens processed in the endosomal compartment are presented in the context of MHC Class II. These may include endogenous components of the endocytic pathway or exogenous antigens captured through pinocytosis, phagocytosis or receptor mediated endocytosis.

However, specific to some subsets of DC is the ability to 'cross-present' antigen, a mechanism whereby extracellular antigen is not presented in the context of MHC-Class II but is transferred to the MHC-Class I antigen presentation pathway (21) (**Figure 1.2**). This facilitates the activation of $CD8^+$ T cells through stimulation by extracellular antigen. This route may be important for the induction of tolerance to self-antigen and immunity to viral and bacterial pathogens, where DC are not directly infected.

Figure 1.2

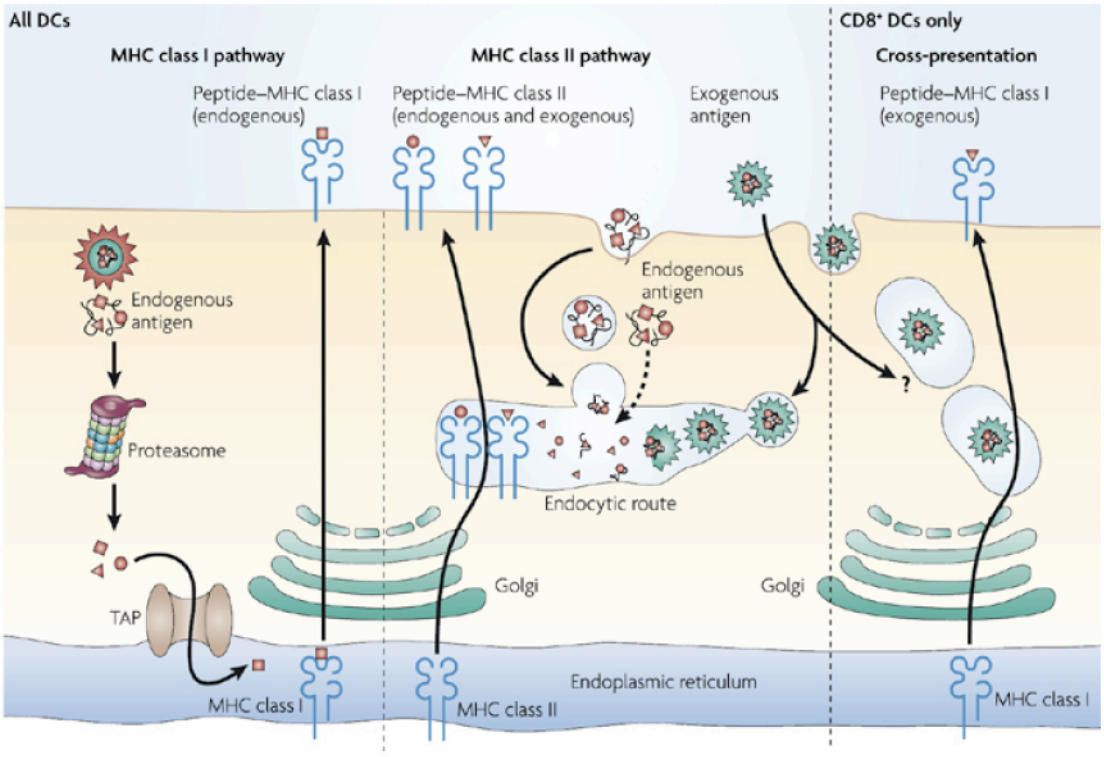

{Villadangos and Schnorrer, 2007, Nat Rev Immunol, 7, 543-55}

Figure 1.2 DC Antigen Presentation mechanisms
All dendritic cells (DCs) have functional MHC class I and MHC class II presentation pathways. MHC class I molecules present peptides that are derived from proteins degraded mainly in the cytosol, which in most DC types comprise almost exclusively endogenous proteins (synthesized by the cell itself). MHC class II molecules acquire peptide cargo that is generated by proteolytic degradation in endosomal compartments. The precursor proteins of these peptides include exogenous material that is endocytosed from the extracellular environment, and also endogenous components, such as plasma membrane proteins, components of the endocytic pathway and cytosolic proteins that access the endosomes by autophagy. CD8+ DCs have a unique ability to deliver exogenous antigens to the MHC class I (cross-presentation) pathway, although the mechanisms involved in this pathway are still poorly understood. The bifurcated arrow indicates that the MHC class II and the MHC class I cross-presentation pathways may 'compete' for exogenous antigens in CD8+ DCs, or that the endocytic mechanism involved in internalization of a given antigen may determine whether it is preferentially delivered to the MHC class II pathway or the MHC class I cross-presentation pathway. TAP, transporter associated with antigen processing.

1.1.6 Role of DC in Tolerance

As well as immunogenic responses, DC-T cell interactions can result in tolerance. This may occur either through the deletion or suppression of reactive T cells (22) or the induction of regulatory T cells (Treg).

T cell deletion is seen particularly in the induction of central tolerance in the thymus. Here, apoptosis is induced in thymocytes that recognise self-antigen with high affinity and is mediated by thymic DC (23). Peripheral tolerance is also thought to be mediated by DC but the exact mechanism is debated. Some propose that immature DC mediate tolerance through T cell anergy, while mature DC stimulate immune responses (24). However, this has been revised to suggest that tolerance is induced by DC that are mature but quiescent where as immunity requires additional danger signals from pathogens (25).

Naturally occurring Tregs not only prevent autoimmunity but also suppress a number of pathological immune responses to non-self antigens, such as allergy (26). Recently, an intimate association between the homeostasis of DC and Tregs has been seen in mice, linked to FMS-like tyrosine kinase 3 ligand (Flt3L) concentrations. Depletion of Tregs increases DC proliferation in a Flt3L-dependent manner (27) (28), administration of exogenous FL induces Treg proliferation as a direct result of DC expansion, and DC depletion in Flt3L KO mice leads to reduced numbers of Treg, with autoimmune sequelae (29). The proliferation of Treg *in vivo* is dependent on MHC Class II expression on DC (30). This leads to a model proposed by Nussenzweig's Group (**Figure 1.3**) whereby a feedback loop exists which allows reciprocal regulation of Treg and DC in a Flt3L and MHC Class-II dependent fashion.

The homeostatic balance between DC, Treg and Flt3L has not been tested in humans. This is discussed in Chapter 5.

Figure 1.3

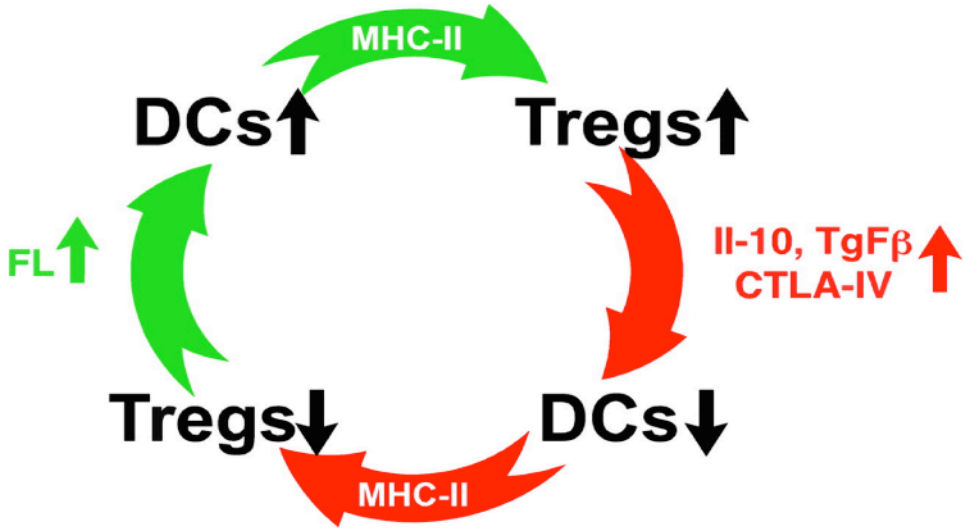

{Darrasse-Jeze et al., 2009, J Exp Med, 206, 1853-62}

Figure 1.3 DC and Treg homeostasis
Proposed homeostatic feedback loop between DCs and T reg cells. Increased numbers of DCs result in increased numbers of T reg cells. An increase in Treg cells leads to a decrease in DCs, which in turn decreases the number of Treg cells, which then increases DCs. MHCII expression by DCs is required for these effects. A loss of T reg cells increases DCs by a mechanism that requires FL.

1.1.7 Classification of DC

DC can be very broadly divided into two categories, relating to their tissue distribution (31): i) Migratory DC which act as sentinels of the immune system. In peripheral tissues they capture foreign- and self- antigen and migrate, via lymphatics, to lymph nodes (LN) where they communicate with T cells to initiate immunity or tolerance. They are particularly abundant at surfaces that interface with the environment, for example epidermal LC form a continuous network across the entire body. ii) lymphoid resident DC which present antigen encountered within the LN. An independent population of thymic DC is also described, which derive from thymic precursors and remain for their entire life within the thymus (32).

There is a third group of DC which are not present in steady state but can be found after inflammation. These include ‘tumour-necrosis factor and inducible nitric-oxide synthase-producing DC’ (Tip DC). DC homeostasis in inflammation is discussed below.

1.1.8 Classification of Murine DC

Murine DC can be similarly classified into migratory and lymphoid resident DC, reviewed in (33). Of these, the lymphoid resident cells are the most studied. These cells are peripheral blood-derived and can be divided into $CD8^+$, $CD4^+$ and $CD8^-CD4^-$subsets. These subsets vary in their anatomical location and antigen presenting capabilities. $CD8^+$ DC are found in the T cell zone and are able to cross-present antigen, where $CD4^+$ DC are mainly in the marginal zone and specialise in Class II dependent antigen presentation. Lymph node tissue contains similar populations but also those DC migrated from associated tissue.

Most murine tissues, including dermis, lung, liver and kidney, contain at least two migratory DC subsets; $CD103^+Lang^+CD11b^{low}$ and $CD11b^{++}CD103^-Lang^-$ cells (34), (35). Again, these populations appear to have differing antigen presenting capabilities with $CD103^+$ DC possessing the ability to cross-present antigen. Similarly to human, the murine epidermis contains a continuous network of Langerhans Cells.

Table 1.1 summaries the currently recognised murine DC and monocyte subsets. Comparison of these subsets with human DC is discussed in the relevant sections below.

Table 1.1

APC subset	Tissue					
	Blood	Dermis/Lung/ Liver/Kidney	Epidermis	GI Tract	(Skin draining) Lymph node	Spleen
Myeloid DC	pre-DC (ClassII+, CD11c+)	CD8-,11c+,11b++, 103-,Lang- Mig DC		CD8-,11c+,11b++, 103-,Lang- Mig DC	CD8-,Lang- Mig DC	CD8-,4+, Lang- 11b+,11c+ Blood derived DC
	pre-DC (ClassII-, CD11c+)	CD8-,11c+,11b+, 103+,Lang+ Mig DC		CD8-,11c+,11b+, 103+,Lang+ Mig DC	CD8-,Lang++ Mig DC	
			CD8-, Lang++ LC		CD8-,Lang++ Mig DC	
				CD103+,Lang-		
					CD8+,Lang+ Blood derived DC	CD8+,4-, Lang+ 11b-,11c+ Blood derived DC
pDC	ClassII+, CD11c+	PDCA1+ in liver	None	None	PDCA1+	PDCA1+
Monocyte	Gr1-high	?	None	?	?	?
	Gr1-low	?	None	?	?	?

1.2 Peripheral Blood Monocyte heterogeneity

In order to study the homeostasis of human DC, a detailed knowledge of currently recognised subsets in peripheral blood (PB) and tissue is required. Human PB monocytes and DC are now well described (36), (37), (38) and include at least two subsets of monocytes based on CD14 (part of LPS receptor) and CD16 (FcγRIII) expression, $CD123^{+}$,BDCA2/$CD303^{+}$, BDCA4/$CD304^{+}$ plasmacytoid DC (pDC) and $CD11c^{+}$ myeloid DC (mDC). mDC can be further subdivided into CD141/$BDCA3^{low}$,CD1c/$BDCA1^{+}$ DC and $CD141^{high}$,$CD1c^{-}$ DC (37). A recent consensus paper (39) has suggested the following nomenclature:

Monocytes: Classical $CD14^{++}CD16^{-}$, Intermediate $CD14^{++}CD16^{+}$ and Non-classical $CD14^{+}CD16^{+}$ Monocytes, The latter two groups are both included in the term $CD16^{+}$ Monocyte.

DC: plasmacytoid $CD303^{+}$ DC, myeloid $CD1c^{+}$DC and myeloid $CD141^{high}$DC.

However, despite attempts to harmonise nomenclature, controversy still remains, particularly as to the nature of the $CD14^{+}CD16^{+}$ cell, which shares properties in common with both $CD14^{+}$monocytes and mDC and in the literature is variably classed with either cell type. For the purposes of this thesis, the nomenclature shown in **figure 1.4** will be employed, based on the antigen

expression of cells in flow cytometric analysis, initially identified by negativity for lymphoid markers and positivity for MHC Class II expression.

Figure 1.4

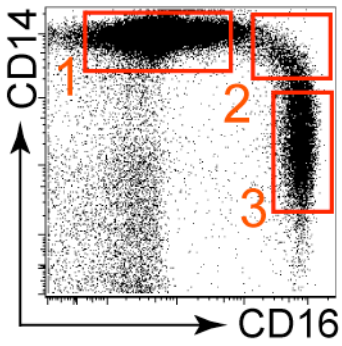

1: CD14⁺monocytes
2: CD14⁺CD16⁺monocytes
3: CD16⁺monocytes

Figure 1.4 Peripheral blood monocyte subsets
Flow cytometric classification of PB cells negative for lymphoid markers and positive for MHC Class II expression. Three monocyte subsets can be identified based on theirexpression of CD14 and CD16.

1.2.1 CD14⁺monocytes

The link between monocytes and macrophages was initially described following the observation that bone marrow precursors gave rise to circulating cells which were able to migrate to tissue to form macrophages (40). Monocytes were initially identified by their morphology and cytochemistry but more modern automated blood counters rely on their light scatter properties. The use of surface markers in flow cytometry, including CD14 and CD16, lead to the identification of monocyte subsets (41). CD14⁺monocytes constitute approximately 90% of total peripheral blood monocytes.

1.2.2 CD16⁺monocytes

CD16⁺monocytes express lower levels of CD14. Whether the CD16⁺monocyte is actually more closely related to a monocyte or a DC is debated (reviewed in (2)). Almeida et al (42) showed morphological, cytochemical, immunophenotypic and functional differences between the CD16⁺ cell and both the CD14⁺monocyte and mDC. Unlike CD14⁺monocytes CD16⁺ cells have cytoplasmic veils, are negative for myeloperoxidase staining and lack CD64

expression. They have higher HLA-DR, CD32 and CD86 expression. However, when compared to mDC they have lower HLA-DR and CD4 expression. Functionally, their Ig/complement mediated phagocytosis ability (as determined by E coli phagocytosis) was intermediary between $CD14^+$monocytes (high phagocytosis) and mDC (low phagocytosis).

In vitro, both $CD14^+$monocytes and $CD16^+$monocytes form DC-like cells when cultured with GM-CSF and IL-4 (43) (44) and both can become macrophage-like with the addition of M-CSF to the culture medium (45) (46). However, Randolph et al (47) showed different migratory properties of $CD14^+$monocytes and '$CD16^+DR^+$' cells (equivalent to $CD16^+$monocytes) in an *in vitro* transendothelial migration model, where $CD16^+DR^+$ cell was more likely to become DC-like as defined by reverse transmigration. In contrast, the $CD14^+$monocyte, in this set up, was more likely to differentiate into a macrophage. More recently, Geissmann's group demonstrated, through adoptive transfer experiments, the patrolling behaviour of the $CD16^+$ human monocyte in murine vessels (48).

Gene expression profiling (49) has shown the $CD16^+$monocyte to be more closely related to $CD14^+$monocyte and neutrophils, than to the lymph node resident DC, despite the possession of features in common with LN-DC and distinct from $CD14^+$monocytes. However, direct comparison of $CD14^+$monocytes and $CD16^+$monocyte (50) has shown a more DC-like expression profile in the $CD16^+$ cells. *In vivo*, numbers of $CD16^+$monocytes can be expanded in acute inflammation (51) and reduced by corticosteroid therapy (52).

1.2.3 SLAN DC

A further subdivision of $CD16^+$monocytes is by surface expression of 6-Sulfo LacNAc (53), so called 'slanDC'. This population produces IL-12p70 on LPS stimulation via TLR4 signaling and may be critical in the programming of Th1 cells and activation of NK cells. However, gene expression profiling has revealed no distinction other than SLAN expression between $slan^+$ and $slan^-$

$CD16^+$monocytes (48). Higher numbers of slanDC have been seen in patients with psoriasis or rheumatoid arthritis.

1.2.4 $CD14^+CD16^+$monocytes

A third monocyte subset is identified in humans as $CD14^+CD16^+$ (54). In this study, $CD14^+CD16^+$ cells showed increased phagocytic activity and decreased antigen presentation compared to $CD16^+DR^+(CD16^+)$monocytes. After LPS stimulation both $CD16^+$ subsets produced TNFα but only $CD14^+CD16^+$monocytes produced IL-10. Increased frequencies of this subset have been reported in patients with severe asthma (55) and in some with atherosclerosis (56).

It remains to be seen whether the $CD14^+CD16^+$ subset is derived from the $CD14^+$monocyte, the $CD16^+$monocyte, or constitutes it's own subpopulation with a physiological role distinct from these cells. However, it is conceivable that the fate and function of monocytes *in vivo* will depend on the physiological context. The remainder of this study considers only the $CD14^+$monocytes and $CD16^+$monocytes.

1.2.5 Comparison with mouse monocyte subsets

The $CD14^+$monocyte and $CD16^+$monocyte, by their CCR2 and CX_3CR1 expression, have been shown to be analogous to the two monocyte subsets described in the mouse; the $Gr1^+,Ly6C^{high},CCR2^+,CX_3CR1^{low}$ 'inflammatory monocyte' and $Gr1^-,Ly6C^{low},CCR2^-$, CX_3CR1^+ 'patrolling monocyte' respectively (57). More recently, genome wide expression analysis has confirmed this association (48). In the mouse, in inflammation, the $Gr1^+$ monocyte can become a 'TipDC', producing TNFα, nitrogen oxide and reactive oxygen species where the patrolling monocyte surveys the luminal side of vascular endothelium (58).

1.3 Peripheral Blood DC

PB DC, when freshly isolated, appear to be in an 'immature' state. They lack dendrites and the expression of maturation markers such as CD80 and CD83. Whether they have a specific function in blood is unknown, but it is unlikely that

they present antigen to T cells in this medium, as close cell-cell contact is required. It is therefore possible that these circulating cells represent a pool of immature DC, able to populate lymphoid or non-lymphoid tissues, where they may encounter antigens or maturation signals (59).

1.3.1 Plasmacytoid DC

This has been demonstrated in the case of plasmacytoid DC. They were initially identified as HLA-DR$^+$ cells which, in response to virus, produce large amounts of IFNα (60), leading to the term 'interferon-producing cells' (IPC). After receiving maturation signals, they are able to enter LN directly from blood, through high endothelial venules, to prime T cells (61). However, they are either absent from, or found at only low levels in. healthy human peripheral tissues (62) (63). They can be positively distinguished from mDC by their expression of CD123, CD303 and CD304 and by their lack of CD11c, CD1c and myeloid markers CD13 and CD33.

1.3.2 Myeloid DC

Two mDC subsets circulate in blood; CD1c$^+$DC and CD141^{high} DC. *In vitro*, up-regulation of maturation markers such as CMRF 44/56 and CD83 can be seen after incubation over night with serum, IL-3 and GM-CSF, and both subsets can induce T cell proliferation in an MLR (38) (64). However, they also show some features in keeping with a DC precursor status, such as the inability to mature in response to TNFα (65), and the expression of early myeloid markers CD13 and CD33 (39).

1.3.3 CD141^{high} mDC as Cross-Presenter

The CD141^{high} mDC have recently been shown to be efficient at cross-presenting antigen in response to TLR3 ligation (66) (67) (68) (69). This mechanism is thought to be specific to some DC subsets, including the murine CD8$^+$ LN resident DC and dermal CD103$^+$DC. A further similarity of these cross presenting cells is their expression of CLEC9A and XCR1. Whether a cell with cross presenting capacity exists in human tissues is unknown.

1.3.4 mDC as pre-tissue DC

If PB DC are able to act as tissue pre-DC, it might be expected that cells of a similar phenotype would be found, even if transiently, in peripheral tissues. However, human tissue has never been examined in this way. As mouse counterparts to these circulating DC are less well recognised, comparison with mouse models may be misleading. The question as to whether cells analogous to circulating mDC can be found in normal human skin is addressed in Chapter 3.

1.3.5 Comparison with mouse blood DC

Most studies of murine DC have concentrated on cells isolated in a relatively mature form from lymphoid tissues, due to the relative abundance of this tissue in comparison to mouse blood and non-lymphoid tissue. However, when blood was initially studied, two populations of immature DC were identified as $CD11c^{low}CD11b^{-}CD45RA^{high}$ cells resembling human pDC in morphology and production of type 1 interferons on stimulation, and $CD11c^{intermediate}CD45RA^{-}$ $CD11b^{+}$ cells which developed DC-like morphology after 8hr culture and matured rapidly on contact with TNFα, similarly to human mDC (70). In this paper, mouse 'pDC' and 'mDC' represented 0.025 and 0.07% of PBMC, respectively, in comparison with human 0.57% and 0.42% (unpublished). Another notable difference between species is the high expression of Class II on human PB DC but extremely low expression on these described mouse DC. $CD11c^{high}$Class-II^{high} cells have not been found in mouse PB (31).

1.4 Skin DC subsets

Dissecting the DC subsets in human tissue has lagged behind studies in mice. Skin is the most easily and non-invasively accessible tissue from patients and relatively large quantities of normal material is available from that discarded at plastic surgery. For these reasons, skin is the chosen peripheral tissue for DC analysis in this work.

1.4.1 Langerhans Cells

Epidermal Langerhans Cells (LC) were the first APC to be identified in 1868 by Paul Langerhans. Initially thought to be neuronal in origin, they were shown to be of haematopoietic origin in 1979 (8). They have a number of apparently distinguishing features including the expression of langerin, a C-type lectin and mannose receptor (71), and CD1a, a protein related structurally to MHC-Class I and involved in the presentation of lipid antigen (72). They contain Birbeck Granules, intracellular organelles associated with the endocytosis of langerin.

1.4.2 Dermal Antigen Presenting Cells

A recent paper from the laboratory describes three dermal myeloid APC when freshly isolated from digested tissue; $CD1a^+$DC, $CD14^+$DC and $CD14^+$ macrophages (73). APC are identified as $CD45^+$, HLA-DR^+ and all express CD11c. The key to distinguishing between $CD14^+$DC and macrophages in flow cytometry is the higher side scatter and inherent autofluorescence of macrophages, particularly in channels excited by the 488 laser, related to their ingestion of melanin. An important functional distinction between $CD14^+$DC and macrophages is the ability of DC (including $CD1a^+$DC) to migrate out of tissue in 40-72hr culture, while macrophages remain in the tissue 'remnant'. Also present in digested dermis is a population of $CD1a^{bright}Lang^+$ cells representing LC migrating from the epidermis, via the dermis, to draining LNs (74).

1.4.3 Unidentified Dermal DC population

When analyzing $CD45^+$HLA-DR^+AF^- cells by CD14 and CD1a expression, populations of $CD14^-CD1a^-$ and $CD14^+CD1a^+$ cells can always be seen. A similar phenomenon is observed in the differentiation of $CD34^+$ progenitors to DC *in vitro* (75). Although the identity and physiological relevance of these populations are currently unknown, it is possible that division of skin DC by CD14 and CD1a alone may not be the most physiologically relevant system. This is particularly the case when considering the potential blood-borne cellular origin of these cells, where CD1a expression is not seen.

Another complicating factor is the necessity for enzyme treatment and some time in culture to release the cells for analysis. Even with minimisation of both

parameters, it is possible that culture artifacts are introduced, such as alterations in antigen expression, particularly compared to PB that can be analyzed within an hour or so of sampling, with no enzyme treatment or culture steps.

1.4.4 Mouse skin DC populations

When mouse skin DC are selected as $CD45^+CD11c^+Class\text{-}II^+$, two major subsets can then be identified as $CD103^+$ and $CD11b^+$. These populations are present in other peripheral tissues including lung, liver and kidney, but in all cases, cells negative for both CD103 and CD11b can be found (35). There are both functional and developmental distinctions between the two classified subsets as $CD103^+$, but not $CD11b^+$ DC, are able to cross present antigen and are dependent developmentally on Flt3L, inhibitor of DNA protein 2 (Id2) and IFN regulatory protein 8 (IRF8). How these subsets relate to the present classification of human skin DC and whether any as yet unidentified human functional counterparts to mouse DC exist is an area of intrigue.

1.5 Langerin as a DC antigen

The relationship between DC phenotype, function, origin, tissue location and species homology is one that continues to add complexity to the field. The idea that the expression of a specific marker may correlate to all of these may be misleading. Langerin expression, once considered to be specific to epidermal LC and preserved in mouse and man, is now recognised on additional and distinct murine populations of peripheral and lymphoid tissue DC.

1.5.1 Langerin expression in murine tissues

In the mouse, it was know that $CD8^-Lang^{bright}$ migratory LC could be found in skin draining lymph nodes. In addition, all lymph nodes, as well as spleen and thymus, contain a population of $CD8^+Lang^{low}$ resident DC, distinct from migratory LC (76). This suggested that langerin expression was not specific to LC. In 2007 a number of groups published the description of murine $CD8^-Lang^+$ dermal DC (34) (77) (78), distinct from both epidermal LC and LC migrating through the dermis (79). Murine LC had previously been shown to self-renew

throughout life in steady-state (80) (81) but in transplant and parabiosis experiments $CD8^{-}Lang^{+}$ dermal DC were dependent on blood-borne precursors which traveled via the dermis to skin-draining LN where they formed a population of $CD8^{-}Lang^{bright}$ migratory DC. These cells were subsequently show to be $CD103^{+}$ and of the same lineage derivation as $CD8^{+}Lang^{+}$ LN resident DC, by their reliance on IRF8 and Flt3 for differentiation and their ability to cross-present antigen (35). Whether $Lang^{+}$DC, distinct from LC, exist in human tissue is unknown.

1.5.2 Induction of Langerin expression in vitro

Langerin expression can be induced on human $CD34^{+}$ cells and PB monocytes in culture. Prior to the description of langerin, LC-like cells were identified by CD1a or E-Cadherin expression. Caux et al, cultured cord blood $CD34^{+}$ progenitors cells for 12 days with GM-CSF and TNFα and found up to 50% $CD1a^{+}$ cells, 20% of which were found to contain Birbeck Granules by electron microscopy (EM) conferring an LC-like phenotype (82). PB $CD14^{+}$ monocytes cultured with GM-CSF, IL-4 and TGFβ (83) develop LC-like characteristics of CD1a and E-Cadherin expression and the presence BGs. More recently Klechevsky examined langerin expression on *in vitro* derived LC-like cells; PB $CD34^{+}$ cells cultured with GM-CSF, Flt3 and TNFα (75). A proportion of the resultant $CD1a^{+}$ cells expressed langerin. However, in comparison to LC isolated from epidermis, both the CD1a and langerin expression were lower on the cultured cells. Similarly to isolated dermal $CD1a^{+}$ DC and unlike LC, they had bright CD1c and CD11c expression and only very marginal expression of E-cadherin. These cultured cells, therefore, perhaps more closely resemble DC than LC, with the exception of langerin expression.

1.6 The origin and homeostasis of tissue DC

Understanding the origin of DC and how they are maintained in tissues, is critical to unraveling their role in disease and particularly to harnessing their therapeutic potential. The challenge is to map the ontogeny of migratory DC from the haematopoietic stem cell in BM, to circulating progenitors, to peripheral tissues and on to lymphoid organs. Understanding the conditions required for

these processes and how the steps are regulated will greatly increase the potential to manipulate DC for the purposes of immunotherapy.

The study of human DC development is complicated by the scarcity of tissue available for study and the inability to perform specific manipulations *in vivo*. However, the development of several techniques has allowed the exponential expansion in the understanding of DC ontogeny and homeostasis over the last twenty years.

1.6.1 Models of DC development

Models of DC development that have enabled this process include: i) The discovery that bone marrow or peripheral blood $CD34^+$ progenitors, and subsequently of human monocytes, can be differentiated into DC-like cells (moDC) *in vitro* (84) (43). This allowed not only the generation of large numbers of DC for functional or clinical studies, but also the initial mapping of cytokine requirements for DC differentiation. ii) The development of mouse models. Understanding of DC ontogeny at the cellular, cytosolic and genetic level has been hugely advanced by the use of genetic mouse models. Recombinant DNA technology facilitated the development of gene knock-out or knock-in models which have allowed the study of the effect of single genes on DC ontogeny (85). The ability to conditionally or constitutively ablate specific cell lineages has allowed studies of the kinetics of DC homeostasis (86) (76) (34) and genetic tagging has allowed tracking of cellular origins of APC (87). iii) Adoptive transfer of human progenitors to immune deficient mice allows the *in vivo* study of the differentiation of stem cells (88) (89) and more recent humanization of mouse models has increased the efficiency of this process (90).

1.6.2 The Monocyte precept

The precept that the monocyte is the immediate tissue DC precursor derived mainly from experiments showing the *in vitro* differentiation of monocytes to DC (43) (91). *In vitro* functional data showing phenotypic changes towards DC-like cells during reverse-transmigration (mimicking trafficking from tissue to lymphatic vessel) also lent weight to this argument (92).

Evidence to suggest that the monocyte may not be the immediate DC precursor was found through the bead-labeling of intracutaneous monocytes in a murine model. This showed that although labeled cells were found in draining lymph nodes they lacked some phenotypic features characteristic of classical lymphoid DC (93). Transfer experiments have shown that purified monocytes are unable to repopulate DC compartments in mice (94) (95). This inevitably leads to the questions; i) what is the tissue DC precursor? ii) at what point in haematopoiesis is it distinguishable from a monocyte precursor?

1.6.3 Advances in murine biology

Several observations in murine DC biology have suggested an alternative ontogeny of tissue DC. These include:

1. The existence of committed DC precursors with separation of monocyte and DC lineages early in ontogeny.
2. Differences in DC homeostatic mechanisms between steady-state and inflammatory conditions.
3. Differential dependence of DC and monocytes/macrophages on growth factors.
4. Selective effect of signaling molecule deficiencies on DC/monocyte subsets
5. The seeding and maintenance of some macrophage populations directly from embryonic cells, prior to the development of the haematopoietic system.

These observations suggest that steady-state DC homeostasis may be independent from the PB monocyte and that homeostatic mechanisms may vary between individual APC populations. They also highlight the necessity to distinguish between inflammatory and steady-state conditions in the study of DC ontogeny. How these observations relate to human DC biology is the focus of work presented here.

1.7 DC ontogeny and the haematopoietic stem cell compartment

In order to study haematopoietic lineage relationships, DC ontogeny may be traced back to the stem cell compartment. Studies of DC potential in mutant

mice have provided valuable insights into lineage dependence on, for example, transcription factors (33). However, the isolation of clonogenic precursors allows the direct identification of lineage relationships (96). These studies have challenged the basic concept of early segregation of myeloid and lymphoid lineages and allowed the mapping of populations with DC potential.

1.7.1 Lymphoid versus myeloid DC development

The categorization of human DC into myeloid and lymphoid subsets occurred early in attempts to classify these cells. Human plasmacytoid DC (pDC) were recognised as interferon producing cells (IPC) before their mouse counterparts were identified (97). They were labeled as plasmacytoid due to their morphological appearance and the presence of characteristic immunoglobulin rearrangements in a proportion of cells (98) and presumed to arise solely from lymphoid progenitors. The myeloid/lymphoid division of DC subsets was encouraged by *in vitro* culture experiments which revealed the myeloid DC potential of $CD34^+$ progenitors and monocytes. IPC were not found in these cultures. This concept was in keeping with the classical description of haematopoiesis involving an early and irreversible division of myeloid and lymphoid lineages (**Figure 1.5**).

Figure 1.5

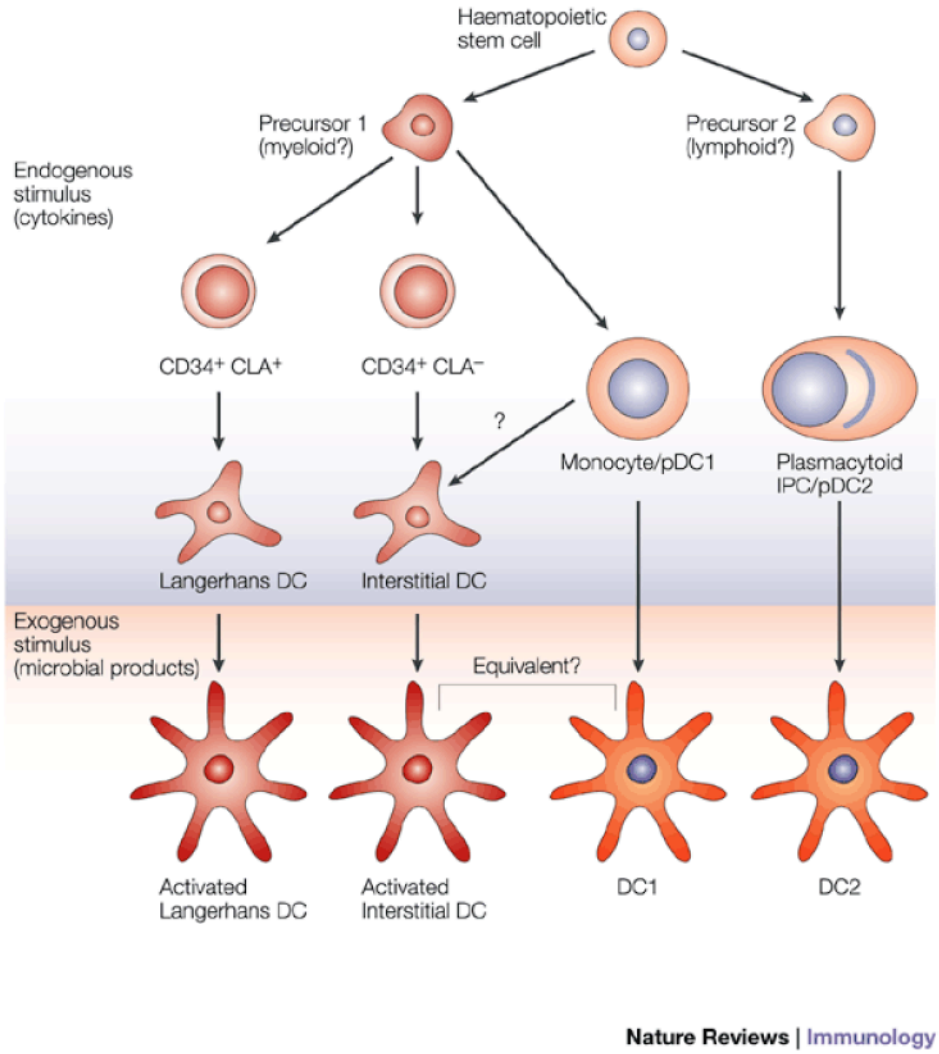

{Shortman and Liu, 2002, Nat Rev Immunol, 2, 151-61}

Figure 1.5 Pathways of human DC development 2002
Plasmacytoid DC develop from a lymphoid precursor while myeloid DC and monocytes are derived from a myeloid progenitor.
CLA, cutaneous lymphocyte antigen; pDC, pre-DC; DC1, myeloid DC; DC2, plasmacytoid DC

Subsequently, murine studies have led to the questioning of this early myeloid/lymphoid divide in haematopoiesis (99), and, through the study of individual precursor populations, murine plasmacytoid DC were found to arise from apparently committed myeloid precursors (100) (101). A new model was therefore proposed whereby a myeloid progenitor (MP) gives rise to a macrophage dendritic cell progenitor (MDP) which gives rise to a common

dendritic cell precursor (CDP) and monocyte (102). The CDP may then produce both lymphoid and myeloid (or conventional/classical) DC (103) (**Figure 1.6**).

Figure 1.6

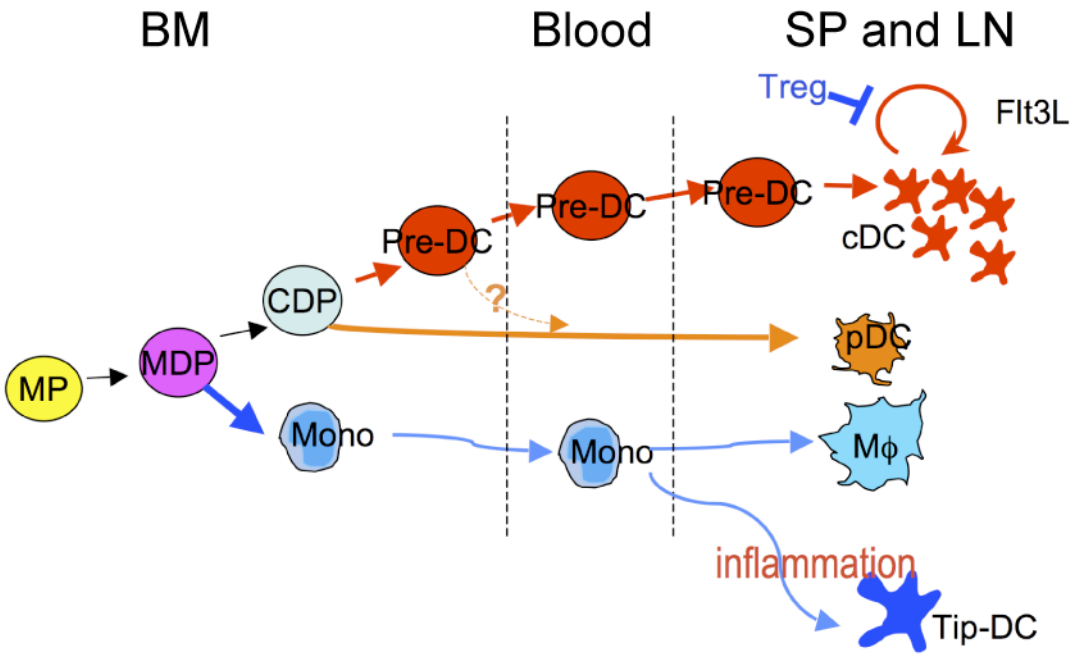

Liu and Nussenzweig, 2010, Immunol Rev, 234, 45-54. Fig 1

Figure 1.6 DC development from myeloid progenitors 2010
pDC and mDC and monocytes can develop from myeloid progenitors. MP, myeloid progenitor; MDP, macrophage dendritic cell progenitor; Mono, monocyte; CDP, common dendritic cell precursor; pre-DC, pre-dendritic cell; cDC, conventional Dendritic Cell;pDC, plasmacytoid dendritic cell; Mϕ, macrophage; Treg, regulatory T cell; Tip-DC; TNFα iNOS producting dendritic cell; Flt3L, Fms-like tyrosine kinase 3 Ligand; BM, bone marrow; SP, spleen; LN, lymph node.

However, the earliest murine precursors apparently committed to the lymphoid lineage (common lymphoid progenitors, CLP) have been found to have some myeloid potential and the ability to differentiate in mice to both myeloid and plasmacytoid DC subsets (104) (105). A link was made between lymphoid and DC ontogeny in humans cells as early as 1995 (106) when $CD34^{+}CD38^{+}CD10^{+}$ cells with B, T and NK cell potential were also seen to differentiate to CD33+HLA-DR+ cells with DC-like morphology in liquid culture. A second paper described the differentiation of DC, B and NK cells from a $CD34^{+}Lin^{-}$

$CD38^-$ population (107). Here it was shown that 2% of single cells from this population could give rise to all three lineages *in vitro*.

Authors of a more recent paper (89) have demonstrated the existence of a $CD34^+CD38^-CD90^-CD45RA^+$ MLP and shown that it can give rise to T, B, NK and $CD33^+CD11b^+$ myeloid cells, either $CD14^+$ monocyte/macrophages when cultured with M-CSF, or DC-like cells if cultured with GM-CSF and IL-4. MLP were also able to give rise, albeit transiently, to B, NK cells and monocytes when transferred into a NOD-SCID mouse. In contrast to the MLP, a granulocyte macrophage progenitor (GMP) gives rise exclusively to myeloid (granulocyte and $CD14^+$ monocyte/macrophage) colonies. From this, and in keeping with mouse models, was formed the hypothesis that there may be two routes of differentiation to monocyte or DC; the first via GMP and the second via MLP. Whether MLP plays a role in adult human monocyte or DC homeostasis, and in what relationship to GMP, is entirely unknown. (**Figure 1.7**).

Figure 1.7

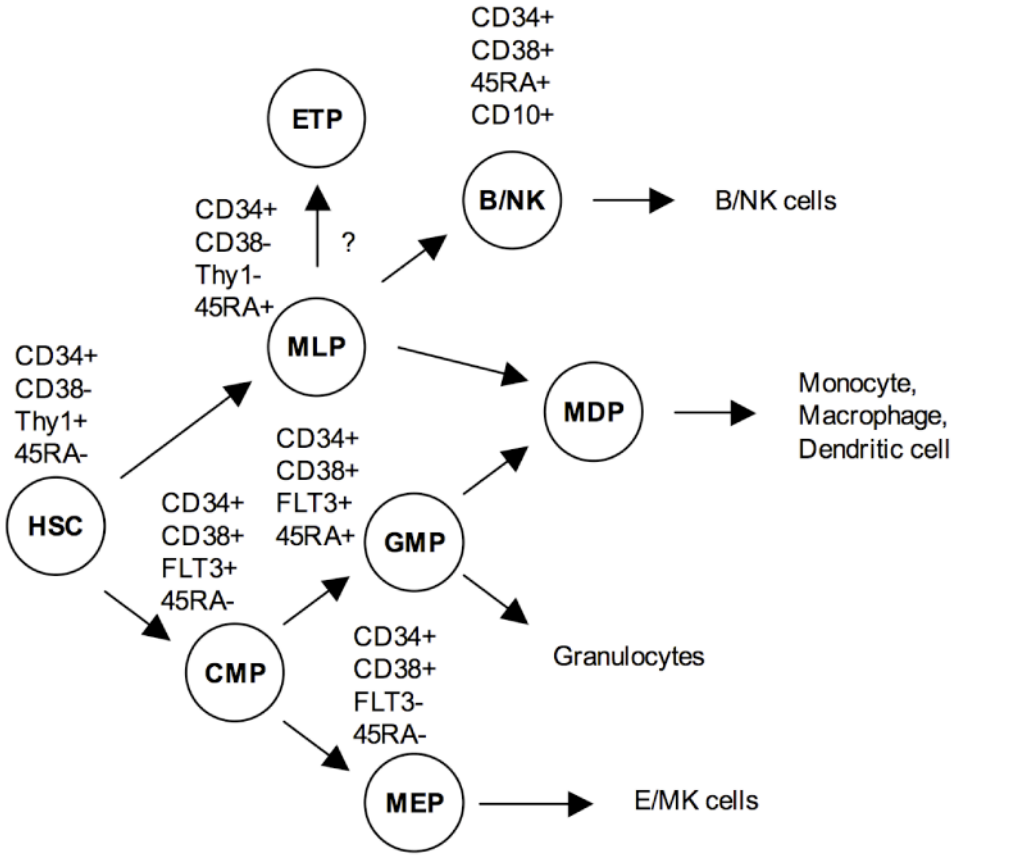

{Doulatov et al., 2010, Nat Immunol, 11, 585-93}

Figure 1.7 The proposed model of human hematopoietic hierarchy
HSC, haematopoietic stem cell; CMP, common myeloid progenitor; MEP, megakaryocyte erythroid progenitor; GMP, granulocyte monocyte progenitor; MLP, multilymphoid progenitor; MDP, macrophage dendritic cell progenitor.

The physiological relevance of the lineage derivation of mouse or human DC, differences in developmental mechanisms and functions, and implications for human disease are not yet clear.

1.7.2 DC precursors in blood

Although it is generally accepted that BM derived DC precursors enter tissues via blood in some form, the identification of these circulating pre-DC in mouse has caused some debate. These have most recently been identified as $CD11c^{+}MHC\text{-}Class\text{-}II^{-}Flt3^{+}$ cells (28), representing 0.03% of PB cells and also present in mouse bone marrow, spleen and lymph node. However, previous study identified two mouse PB pre-DC populations, analogous to human pDC and mDC (70), discussed in 1.3.5. There is also discrepancy in the findings of

circulating early progenitor cells in mice. Despite the identification of haematopoietic stem and progenitor cells in mouse blood (108), circulating MDP and CDP were not specifically identifiable by Liu et al.. It is possible that the ability to identify small numbers of circulating progenitors is dependent on factors such as mouse strain, age or condition and also the kinetics of transfer of cells from bone marrow to peripheral tissue and half life of these cells in blood.

Human tissue DC precursors are known to be bone marrow derived and blood borne from human allogeneic bone marrow transplant recipient studies (109) (73). However, which circulating cell population is responsible for repopulating tissues in this setting is not known. Candidates include PB monocytes or DC. However, unlike the mouse, circulating $CD34^+$ progenitors are consistently found in resting human PB and it is known that culture of these cells can give rise to DC-like populations *in vitro*. The constituent subsets of this $CD34^+$ population and whether these cells contribute to steady-state DC homeostasis *in vivo* is currently unknown.

1.8 Inflammatory versus steady state DC precursors

The observations that monocytes were not necessarily DC precursors in the steady-state, but that activated monocytes share many features with DC, such as high class II expression, the up-regulation of co-stimulatory factors (CD80, CD83, CD86) and the ability to stimulate an MLR, led to a re-examination of the derivation of DC in inflammatory conditions.

1.8.1 Murine LC

The concept that a different homeostatic mechanism for DC maintenance may be required during inflammation, as opposed to the steady-state, has been illustrated most effectively for the murine LC. With the use of minimally perturbed bone marrow transplant and parabiosis models it has been shown that LC can be maintained through self-renewal in the steady-state (80). However, following depletion by uv irradiation, the epidermis is repopulated with LC derived from Gr-1^{high}monocytes (110).

1.8.2 Monocyte as an inflammatory-DC precursor

Similarly to the monocyte dependence of LC repopulation following inflammation, there is evidence to suggest that monocytes play a role in DC differentiation in inflammatory conditions (111), reviewed in (112) and (31). One clear example is the murine $Gr1^{high}$ monocyte which can become a 'TipDC', producing TNFα, nitrogen oxide and reactive oxygen species, and found only in inflammatory tissue, typically in response to *Listeria monocytogenes* infection (113). The development of TipDC is thought to be dependent on GM-CSF (31). For this reason, although it is unknown whether a similar inflammatory monocyte-derived DC exists *in vivo* in humans, parallels are drawn with *in vitro* derived moDC differentiated from $CD14^{+}$monocytes in the presence of GM-CSF and IL-4.

1.9 Growth factor requirement for DC differentiation

The selective effect of a number of cytokines on DC or monocyte/macrophage differentiation and homeostasis is a further line of evidence that these two lineages are independently developed and regulated. Although this has mainly been examined *in vitro* for human cells, the therapeutic use of some growth factors, such as Flt3L and GM-CSF has allowed limited studies of APC following administration of these factors *in vivo*. Murine knock-out models have facilitated the *in vivo* study of the effects of single cytokine or cytokine-receptor deficiency. Several cytokines of key importance have been identified in this way: GM-CSF, Flt3L, M-CSF, IL-4, TNFα and TGFβ, discussed individually below.

1.9.1 GM-CSF

The initial observation that GM-CSF was required for differentiation of both human and mouse monocytes to moDC in culture (43) (114), suggested the dependence of DC on this cytokine. More recently it has been thought to have a prominent role in development of inflammatory DC (reviewed in (115), but may not be required for steady-state homeostasis. This is supported by the fact that mice lacking GM-CSF or its receptor have normal levels of DC in lymphoid

organs (116). GM-CSF administration to humans increases the number and cytotoxicity of monocytes (117) but DC have not been studied.

1.9.2 Flt3 Ligand

The dependence of DC on Flt3 and its ligand, *in vivo* and *in vitro,* is now well recognised. Mice devoid of Flt3 or Flt3L have low levels of pDC and mDC, despite normal monocyte numbers (118). The treatment of mice and humans with Flt3L leads to increased numbers of DC as well as monocytes and granulocytes (119) (120). This suggests the dependence of both plasmacytoid and myeloid DC on Flt3 signaling. Although monocyte expansion can be induced by Flt3L, this is in the context of a general myeloproliferation and these cells appear not to be dependent on Flt3 signaling for differentiation or survival.

1.9.3 M-CSF

In contrast, mononuclear phagocytes, including monocytes, macrophages and osteoclasts, but not DC, are dependent on M-CSF (CSF-1) signaling. CSF-$1^{-/-}$ ($Csf1^{op}/Csf1^{op}$), and CSF-1-$R^{-/-}$ mice, among other abnormalities, have osteopetrosis and reduced numbers of monocytes and tissue macrophages (121). They also have reduced numbers of LC, but not lymphoid DC (110) (122). The presence of M-CSF in culture skews the differentiation of $CD34^{+}$ cells and monocytes towards macrophages.

1.9.4 Additional cytokines

TGFβ null mice show a selective deficiency of LC suggesting the dependence of this cell, but no other monocyte or DC subset, on TGFβ signalling (123). A number of other cytokines, such as IL-4, TNFα and G-CSF may well have more subtle roles in DC homeostasis *in vivo* (33).

1.10 Genetic control of DC development and homeostasis

Cytokines mediated their effects through cytosolic signaling molecules and activation of transcription factors (TFs) which orchestrate gene transcription. Several TFs have been identified, mainly through the study of knock-out mice,

with importance in murine DC differentiation (reviewed in (33). Many of these are required for global DC development, such as STAT3 (124) but some have more subtle effects on specific DC subsets, including RelB, deficiency of which leads to massive reduction of CD8α^-DC. **Figure 1.8** summarises the effect of a number of knockout genes on bone marrow progenitors, DC subsets, monocytes and macrophages where known (125) (33). Rarely is information on all these APC compartments available. Due to the dependence of steady-state and inflammatory DC development on Flt3L and GM-CSF signaling respectively, these pathways are discussed in more detail.

Figure 1.8

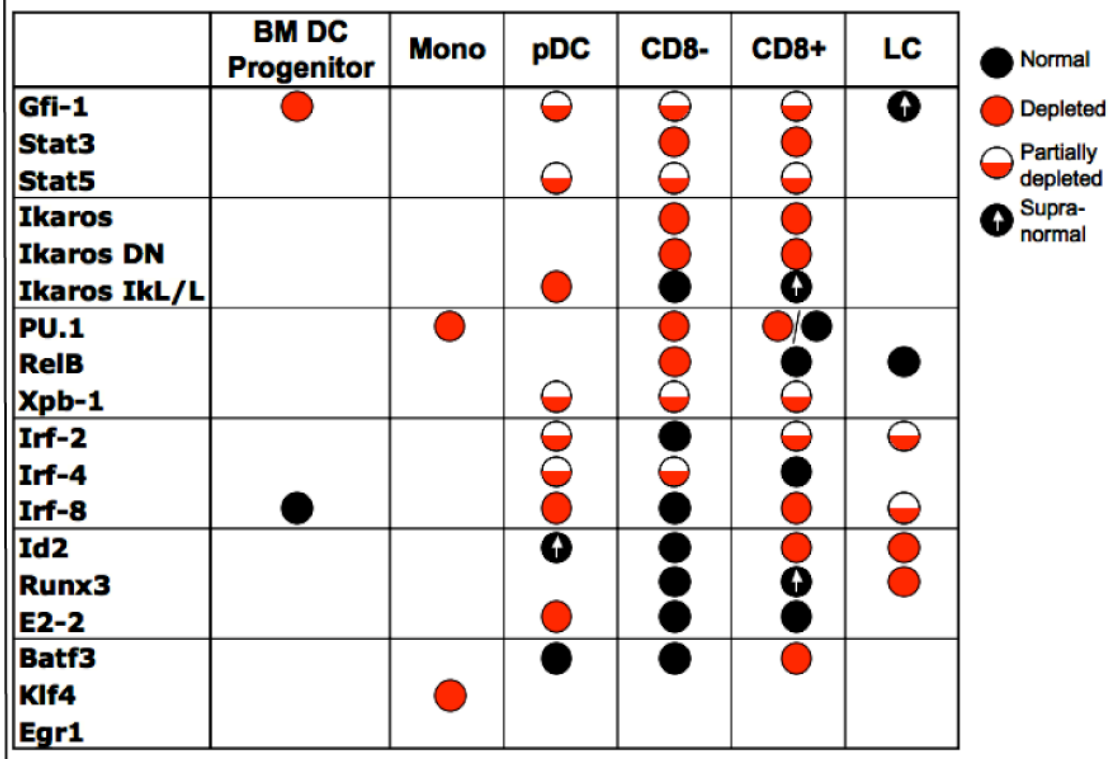

Figure 1.8 Summary of genetic defects affecting DC ontogeny in mice
Adapted from Geissmann et al., 2010, Science, 327, 656-61

1.10.1 Flt3L and GM-CSF signaling pathways

Flt3L and GM-CSF drive DC differentiation through STAT3 and STAT5 signaling, respectively. Deletion of STAT3 in the haematopoietic compartment blocks Flt3L mediated DC differentiation, but not GM-CSF driven development (126). STAT5 directly inhibits IRF8 (and IRF7, SpiB and PU.1) and reduces

pDC development (127). Inhibition by STAT5 is hypothesised to control the balance between pDC and mDC. STAT5 will also activate IRF4 and this is shown to be the predominant route to GM-CSF stimulated DC differentiation *in vitro*, whereas Flt3L signaling relies predominantly on IRF8 (128). Another key TF in the signaling of these cytokines is PU.1. GM-CSF is unable to trigger DC differentiation in progenitors rendered PU.1 deficient (129) and Flt3L signaling up-regulates PU.1 expression (124), suggesting PU.1 is a critical TF for both GM-CSF-driven inflammatory and Flt3L-mediated steady-state DC differentiation (130).

1.10.2 Integration of signaling pathways

As can be seen in the case of Flt3L and GM-CSF signaling pathways, the physiological result of activation of a signaling receptor depends on the integration of intracellular signals with those of other pathways. The relative level of expression of a TF, for example compared to an antagonistic TF, may be as physiologically relevant as whether or not it is present or absent. Another example is seen in monocyte differentiation to either DC or macrophage, where a high expression level of PU.1, compared to a macrophage-driving TF (MafB) is required to induce a DC as opposed to macrophage fate (131). For this reason, results of knockout models may not be subtle enough to reflect true *in vivo* influences.

This concept may also be relevant when considering signaling molecules as haematopoietic stem cell factors and differentiation factors. Early haematopoietic stem cells express Flt3 and it is becoming clear that progenitors previously described as early myeloid or lymphoid can both give rise to DC, yet not every early progenitor follows a DC differentiation path. Over-expression of Flt3, even in progenitors without inherent DC potential (such as MEP), leads to activation of down stream Flt3-associated genes such as STAT3, PU.1 and G-, M- and GM-CSF receptors and differentiation to mDC, pDC and myelomonocytic cells (124). Again, the differentiation outcome of Flt3 signaling may depend on the balance of signals received, PU.1 reduces the DNA binding capacity of GATA-1, a TF critical for megakaryocyte and erythroid development (132), and GATA-1 inhibits the binding of PU.1 to c-jun, a critical PU.1 cofactor

(133). It is therefore possible that physiological expression of Flt3 in haematopoietic progenitors permits differentiation of these cells to DC but the differentiation route taken depends on a balance of signaling from Flt3L and other lineage determining cytokines.

1.10.3 DC-related TF mutations in human disease

A few DC-related TF genes have been found to be mutated in human disease, usually in relation to malignancy. PU.1 and Flt3 mutations have been described in human AML (134) (135) and the involvement of the IKAROS gene in adult and childhood ALL is also recognised (136) (137).

A small number of human germ line mutations affecting DC lineages have been recognised. Pitt-Hopkins syndrome is an autosomal dominant condition associated with mono-allelic loss of function mutations in E2-2, severe mental and motor dysfunction and abnormal craniofacial development. Analysis of pDC in this condition showed normal numbers of cells but abnormal phenotype with reduced CD303 expression and impaired IFNα production in response to CpG *in vitro*. A similar phenotype was seen in E2-2$^{+/-}$ mice (138).
Heterozygous STAT3 mutations are found in the majority of patients with Hyper-IgE syndrome, a rare disorder characterised by recurrent severe bacterial infections, eczema and variably with spontaneous fractures (139). However, the DC profile of patients with this condition has not be examined.

1.11 Embryological origin of some macrophage populations

One further potential ontogenic pathway for APC, specifically long-lived tissue macrophages, has its routes in embryogenesis. Prior to the development of definitive bone marrow haematopoiesis, fetal liver haematopoiesis or even the establishment of a circulatory system, haematopoietic cells can be found in the yolk sac. Yolk sac macrophages may migrate to tissues directly, or via blood once the circulatory system is established.

1.11.1 Microglia

It has recently been shown in mice that microglia, the central nervous system resident macrophages, derive from yolk sac primitive myeloid progenitors that arise before the development of haematopoiesis, and can be maintained throughout life independently of blood-borne precursors (87).

1.11.2 LC

A similar concept has been proposed for epidermal LC (140). HLA-DR$^+$ cells can be detected in embryological developing human epidermis as early as 6-7 weeks gestation (141), and langerin expression detected after week 11 (142). In mice, ATPase$^+$ LC-like cells are present in the subectodermal mesenchyme (future dermis) from as early as E10.5 and will migrate to the epidermis as soon as E16.5, prior to the development of bone marrow haematopoiesis, and show a similar phenotype to yolk-sac derived macrophages with a high proliferative index. They only acquire class II and langerin expression after birth. The contribution of fetal liver monocytes to this process is not clear. The hypothesis that the initial seeding of epidermis is with self-renewing, embryologicaly derived yolk sac cells which may then be supported by blood borne precursors during inflammation and/or in adult tissue, is yet to be proven.

Whether this hypothesis holds true for any other tissue macrophage populations is also not known.

1.12 Primary DC diseases in humans

Disordered DC ontogeny or homeostasis as a primary human disease is recognised in only a few conditions. These include two DC neoplasms, interdigitating DC sarcoma and pDC leukaemia/haematodermic neoplasm, and one condition of disordered DC homeostasis, Langerhans cell histiocytosis (LCH), the malignant nature of which is debated. Of these rare disorders, LCH is the most common and so is considered further.

1.12.1 LCH

LCH presents mainly in children but is also seen in adults. It is characterised by accumulations of Lang$^+$ dendritic-like cells in single or multiple organs. These

'LCH Cells' are found in an inflammatory environment admixed with T cells, eosinophils, macrophages and neutrophils. It commonly affects skin, pituitary gland, bone, liver, lung and brain but may be found in any organ. The natural history ranges from a mild, single-organ, self-limiting disorder to a multi-systems potentially fatal disease. Treatment, when necessary, is with immunosuppressive, immunomodulatory or chemotherapeutic agents and may be required for a number of years. Late sequaelae, directly attributable to the disease, in addition to the side effects of treatment, may be seen particularly in the neurological system.

Due to their langerin expression, it has been generally accepted that LCH cells derive from LC, despite their appearance in tissues where LC are not normally found. However, the discovery of $Lang^{+}$ non-LC cells in mice, raises the question of the exact origin of LCH cells, particularly if langerin expression were found not to be specific to human LC. A number of critical questions remain unanswered in LCH: are LCH cells present as the cause or consequence of the LCH lesion?; how or why do they accumulate?; how do they interact with other cells in the lesion? Determining the origin of these cells is a critical step in the understanding of LCH pathogenesis and may potentially guide treatment strategies.

1.13 Scope of the Thesis

The primary aim of this work is to develop an integrated model of human DC ontogeny and homeostasis through the examination of BM, PB and tissue in health and disease. The key questions considered are: i) Is the homeostasis of peripheral tissue (skin) DC reliant on blood borne precursors in the steady-state? ii) Which circulating cells are capable of supporting tissue DC populations? iii) Are human DC populations capable of self-renewal in steady-state? iv) Can DC progenitors be traced back to the BM? v) What is the lineage derivation of DC and monocytes/macrophages? vi) How is DC development controlled genetically in humans?

1.13.1 Limitations of studies in humans

The understanding of human DC biology lags behind that of the mouse and many hypotheses generated from murine studies have been difficult to test *in vivo* in humans, particularly under steady-state conditions.

Studies of human DC are limited by material resources and the obvious inability to proactively manipulate physiology *in vivo*. However, comparisons between healthy and diseased tissue can allow inferences to be drawn and the study of DC homeostasis during specific treatments, such as haematopoietic stem cell transplantation, growth factor administration or treatment with small molecule inhibitors, are invaluable.

Relevant particularly to DC ontogeny is the difficulty in humans of tracking cellular changes with time, as methods such as bead or fluorescent protein labeling of cells are not possible. Sampling tissues only gives a snap-shot impression and while serial sampling can give a broader picture, it requires more committed subject participation and still requires assumptions of cellular behaviour between sample times. The use of humanised mouse models to study human DC populations *in vivo* goes some way to overcoming these problems but cannot take into account the genetic variation encountered in the human populations, nor the range of environmental stimuli experienced.

Much is yet to be learned about DC and progenitor populations in *ex vivo*, healthy, human tissues and the study of these cells in human diseases.

1.13.2 The study of DC in Healthy human tissue

Work in this thesis examines BM, PB and skin from healthy volunteers. This provides a snap-shot of cellular profiles in steady-state. Studies include the phenotyping and quantification of APC, and analysis of growth factor receptor expression, cell cycle, and mRNA expression patterns.

1.13.3 The study of DC in human disease

In order to specifically probe the relationship between BM progenitors, human PB monocytes/DC and tissue APC populations, new human models, akin to mouse steady-state models, are required. A search was undertaken for subjects with spontaneous and prolonged monocyte or DC deficiency and a thorough analysis of BM, PB and tissue DC and their precursors was undertaken, together with investigation of immune regulatory mechanisms and a search for genetic mutations responsible for the phenotypes.

Finally, following the identification of Lang^{+}DC, distinct from LC in mice, a survey of langerin expression in human tissues is performed. Findings are extended to a study of Langerhans Cell histiocytosis (LCH) lesions. The identity of the LCH cell and how it relates to DC found in normal skin is discussed.

Chapter 2. Materials and Methods

2.1 Cell isolation

Human samples were obtained following informed consent and in accordance with a favorable ethical opinion from North Tyneside and North London Research Ethics Committees.

2.1.1 PB and BM mononuclear cells and neutrophils

Mononuclear cells from fresh blood were isolated according to standard protocols. Briefly, PB (in EDTA: Ethylenediaminetetra-acetic, or heparin) or BM (in EDTA) were diluted 1:2 and 1:4, respectively, Dulbeccos Phosphate Buffered Saline (DPBS) and layered over Lymphoprep (Axis-Shield Diagnostics Ltd.; www.axis-shield.com) then separated by density centrifugation, room temperature at 800g for 15 mins. Cells at the interface of lymphoprep and supernatant were removed and washed in DPBS (500g for 5mins) then again to remove platelets (200g 7.5mins). Cells were counted on Improved Neubauer Haemocytometer and viability assessed by trypan blue (Invitrogen; www.invitrogen.com) staining.

Leukoreduction system filters were obtained in place of buffy coats from NHSBTS. These 'cones' contain white cells which are not returned to the subject after platelet apheresis. They contain up to 2 $x10^9$ total cells in 5-10ml volume, allowing the isolation of approximately 1.5 x 10^9 PMBC (143). To extract the cells, the cone is clamped above a 50ml falcon tube and the bottom tube of the cone is cut, allowing the contents to flow into the falcon. The cone is then flushed from the top with RT DPBS to a total volume of 40ml. The sample is then diluted 1:4 with DPBS and layered over lymphoprep before centrifugation and extraction of PBMC in the same way as for fresh blood (above).

PB Neutrophils for DNA were isolated from the red blood cell (RBC) pellet. The majority of the red cell pellet, particularly the upper portion, was pipetted from underneath the lymphoprep and diluted 1:4 with DPBS. This was mixed with half the volume of 6% Dextran/0.9% NaCl, alliqoted into 15ml tubes and left to

stand for 1hr. The supernatant was then removed and spun, 4^0C at 500g for 12 mins with slow brake. Supernatant was discarded and cells resuspended in 12ml ice-cold distilled water for lysis of remaining RBC. After 20secs 4ml of 0.6M KCL was added and then the solution diluted to 50ml with DPBS. This was spun at 600g for 6mins (4^0C). Lysis steps were repeated if RBC remained. Cells were then pelleted and frozen for later DNA extraction.

2.1.2 Skin

Control skin DC were isolated from 300µm dermatome sections of skin recovered from mammoplasty surgery. 4mm punch or shave biopsies were taken from subjects. Where necessary, epidermal and dermal sheets were prepared by digestion at 37^0C for 1hr with 1mg/ml dispase (Invitrogen; www.invitrogen.com) in RPMI (Roswell Park Memorial Institute; RPMI-1640; Sigma-Aldrich; www.sigmaaldrich.com). Sheets were then separated with forceps and washed in cold RPMI. Single cell suspensions were obtained by the digestion of dermal sheets or whole skin at 37^0C with 0.8mg/ml collagenase (Type IV, Worthington) and epidermal sheets with 0.6mg/ml collagenase, in RPMI with 10% Fetal Calf Serum (FCS) for 8 hours in a bacterial petri dish to prevent adherence of leukocytes. Alternatively, whole skin or dermal sheets were cultured at 37^0C, 5% CO_2, in RPMI or X-Vivo 10, (BioWhittaker™; www.fishersci.com), or epidermal sheets in the same medium supplemented with 500U/ml GM-CSF (SagramostinTM) for collection of migrating DC. Viability of digested cells was usually >95% and of migrated cells >90% by DAPI (4,6-diamidino-2-phenylindole; Partec; www.partec.com) or LIVE/DEAD® dead cell stain (Invitrogen; www.invitrogen.com) exclusion.

For enumeration of LC by whole mount microscopy, epidermal sheets were fixed in acetone for 30mins and then rehydrated in DPBS for 20mins and stored at 4^0C.

2.1.3 Cell sorting

Fluorescence activated cell sorting (FACS) was performed using a BD FACS Aria (custom 100 mW 488 sapphire, 60mW 355 UV, 40 mW 640 red, 50 mW 407 violet, 100 µm nozzle and 20 psi). Cells were stained as for flow cytometry,

washed and suspended in buffer (DPBS + 0.1% FCS + 2mM EDTA). Cells were collected in flow tubes or 1.5ml eppendorfs containing small volumes of RPMI, at 4^0C. Alternatively, skin DC from patient samples were sorted directly onto Shandon Cytoslides® (Thermo scientific; www.thermo.com), into a small drop of buffer for subsequent air-drying, fixation and FISH analysis.

Cells for mRNA analysis were pelleted, lysed and stored at -80^0C in 350μl lysis buffer (50μl β-mercatoethanol in 5ml RLT buffer; Qiagen RNeasy Plus Micro Kit; www.qiagen.com).

2.1.4 Fibroblasts

Dermal fibroblasts (Fb) were isolated from punch or shave biopsies of skin. Deep dermis was digested for 12 hours in RPMI (Invitrogen; www.invitrogen.com), supplemented with glutamine, penicillin and streptomycin + 10% FCS, with collagenase (0.8mg/ml collagenase D Roche; www.roche-aplied-sciences.com). A single cell suspension was obtained by pipetting and was then washed in DPBS. Cells were resuspended in 500μl of RPMI + 20% FCS and transferred to a single well in a 24 well plate. This was incubated for 2-4hrs at 37^0C then the medium replaced with fresh RPMI + 20% FCS. This step was repeated after incubation at 37^0C overnight and then cells left to grow with twice weekly replacement of medium. Once 80% confluence was reached, cells were sub-cultured to bigger tissue culture vessels.

To sub-culture fibroblasts, medium was removed and cells rinsed with DPBS. Cells were covered with Trypsin/EDTA (Trypsin Versene Mixture, Lonza BioWhittaker; www.fishersci.com) for 5 minutes at 37^0C and then FCS, 1/3 the volume of Trypsin/EDTA, added to neutralise the trypsin. Cells were transferred to a universal container and washed with DPBS and re-plated at $2x10^5$ cells in a 25ml tissue culture flask, or $6x10^5$ cells in a 75ml flask, in RPMI + 20% FCS.

2.2 Phenotype analysis

2.2.1 Flow cytometry and FACS sorting

Multiparamater flow cytometry allows rapid and simultaneous analysis of differential antigen expression and physical properties to define populations of cells in suspension. Surface, intracytoplasmic and intranuclear antigens may be

detected, in addition to quantitative assessment of DNA content. Modern instrumentation provides twelve or more fluorescent channels allowing the analysis of a corresponding number of antigens in a single tube. A panel was developed to identify, enumerate and analyse specifically monocytes, DC and CD34+ progenitors and allow comparison with peripheral tissue DC. A second panel catered for the analysis of lymphocytic cells.

PBMC, BM and normal skin preparations, were stained in aliquots of $1x10^6$ cells in 50µl of buffer (DPBS + 2% FCS+ 2mM EDTA; AnalaR®) according to standard protocols. For subject skin biopsies, all available cells were prepared. Flow cytometry was performed on LSRII cytometer (Becton Dickinson; BD) and data analyzed with FlowJo (Treestar).

Antibodies were from BD unless stated otherwise and are denoted as: antigen fluorochrome (clone). CD1a FITC (NA1/34; Dako; www.dako.com); CD1a APC (HI 149); CD1c PE APC (AD5-8E7; MACS/Miltenyi Biotec), CD3 FITC PE APC (UCHT1) PerCPCy5.5 (SK7); CD4 FITC (SK3); CD8 APCCy7 (SK1); CD10 APC (HI10a); CD11c APC V450 (B-ly6); CD14 PE PECy7 (M5E2) and QDOT605 (TuK4; Invitrogen); CD16 FITC PE PECy7 (3G8); CD19 FITC PE PECy7 (SJ25C1); CD25 PE PECy7 (2A3); CD34 APC (8G12) and APCCy7 (581; Biolegend); CD38 PE-Cy7 (HB7); CD45 APCCy7 V450 (2D1); CD45RA FITC (L48) PE (HI100); CD56 FITC PE (NCAM16.2); CD90 Qdot605 (5E10; eBioscience); CD115 PE (61708; R&D Systems), CD117 PE (104D2), CD123 PE (9F5); CD135 PE (4G8); CD141 PE (1A4), CD141 APC (AD5-14H12; MACS/Miltenyi Biotec), HLA-DR PerCP Cy5.5 (L243); Langerin PE (DCGM4; Beckman Coulter). Intracellular staining with FoxP3 APC (PCH101; eBioscience) and Ki-67 PE FITC (B56) and corresponding isotypes, was performed with $2x10^6$ cells/tube after fixation and permeabilisation with BD Cytofix/Cytoperm and Permwash reagents, according to manufacturer's protocols. Absolute counting was performed using 50µl whole blood in BD Trucount™ Tubes according to manufacturer's protocol. Dead cells were excluded by DAPI (4,6-diamidino-2-phenylindole; Partec; www.partec.com) or LIVE/DEAD® dead cell (Invitrogen; www.invitrogen.com) staining. True positive staining was confirmed with the use of isotype controls in a 'fluorescence minus one' system.

Antibody panels are shown in **table 2.1** including PB DC panels, PB lymphoid panel, Skin DC and BM analysis panels. The blue series demonstrates the isotype control setup for a fluorescence minus one system for PB DC.

Table 2.1

		APC-Cy7 638/780	PERCP-Cy5.5 488/710	V500 407/525	V450 407/450	Q605 488/610	PE-Cy7 488/780	APC 638/670	FITC 488/520	PE 532/585
PB	Standard PB DC	CD34	CD123	HLA-DR	CD11c	CD14	CD16	CD141	Lineage	CD1c
	New Antigen	CD34	CD123	HLA-DR	CD11c	CD14	CD16	CD141/ New	Lineage	CD141/ New
	Dead cell dye	CD34	HLA-DR CD123	Amine dye/DR	CD11c/ DAPI	CD14	CD16	CD141/ CD11c	Lineage	CD141/ CD123
	FMO Set	Isotype	CD123	HLA-DR	CD11c	CD14	CD16	CD141	Lineage	CD1c
		CD34	Isotype	HLA-DR	CD11c	CD14	CD16	CD141	Lineage	CD1c
		CD34	CD123	HLA-DR	Isotype	CD14	CD16	CD141	Lineage	CD1c
		CD34	CD123	HLA-DR	CD11c	Isotype	CD16	CD141	Lineage	CD1c
		CD34	CD123	HLA-DR	CD11c	CD14	Isotype	CD141	Lineage	CD1c
		CD34	CD123	HLA-DR	CD11c	CD14	CD16	Isotype	Lineage	CD1c
		CD34	CD123	HLA-DR	CD11c	CD14	CD16	CD141	Lineage	Isotype
	PB Lymph	CD45	CD8	–	–	–	CD19	CD4	CD3	CD56
	PB Treg	CD8	CD3	–	–	–		FoxP3	CD4	CD25
Skin	Skin DC	CD45	HLA-DR	Amine Dye	DAPI/ CD11c	(AF)	CD14	CD1a	AF/ CD1a	Langerin/ GFR
BM	BM CD34+	CD34	CD90/ Thy-1	Amine Dye	HLA-DR	CD45RA	CD38	CD10	Lineage CD3,19, 20,56,	CD135

2.2.2 Immunofluorescence microscopy

Modern epifluorescence microscopy with Z-stack capability can be used to determine accurately the absolute number of cells in small volumes of fixed tissue, giving additional valuable topographical information. The cellular distribution of antigen expression can also be observed. The combination of flow cytometry and fluorescence microscopy allows powerful analysis of small amounts of tissue.

Fluorescence microscopy was performed using a Leica TCS SP2 confocal microscope with HCX Plan Apo x40 NA 0.85 lens and PMTs running Leica LCS v2.61 software (www.leica-microsystems.com) or Zeiss Axioplan 2 microscope EC Plan-neofluar x40 NA 0.75 lens and Axiocam with running Ziess Axiovision v2.8 software (www.zeiss.com). Separated epidermal sheets were fixed in acetone for 20mins and rehydrated in PBS for 20mins before staining. The following primary or directly labeled antibodies were used: anti-CD1a FITC (NA1/34; Dako); anti-HLA-DR FITC (L243 or G46-6; BD), anti-Ki-67 (rabbit monoclonal SP6; Vector Laboratories) followed by Alexa fluor 555 conjugated goat-anti-rabbit IgG (H+L) (Invitrogen). Specimens were mounted in VectaShield containing DAPI (Vector Laboratories).

2.2.3 FISH

Cytospin slides of sorted PB populations at 10-20 thousand cells/slide were made and air-dried. These, or slides supporting directly sorted skin cells were fixed in Carnoy's (methanol:acetic acid 3:1): 100μl of Carnoy's pipetted onto slide and fluid contained by a circle drawn around the cells with ImmEdge Hydrophobic Barrier Pen (Vector Labs; www.vectorlabs.com). Slides were then air-dried before fixing again in Carnoys for 2mins in a coplin jar and again air-drying. XY probe mix (Vysis CEP X SpectrumOrange and CEP X SpectrumGreen DNA probe kit; www.abbottmolecular.com) was combined with CEP buffer at 1:4 and 8μl of this was pipetted onto each slide and a 20x20cm coverslip applied. The edges of the coverslip were sealed with rubber glue. Denaturation (2mins at 73^0C) and hybridization (over night at 37^0C) was performed on a ThermoBrite Statspin Slide Hybridiser. After hybridization, coverslips were removed and slides placed in 2x SSC prior to 2mins at 73^0C in 0.4x SSC. Slides were replaced in 2x SSC at RT for 1 minute before air-drying. Fluorescence was preserved with Vectashield + DAPI, coverslip applied and edges sealed with clear nail varnish. Slides were stored at 4^0C until analysis within 24-48hrs. Subsequently they were stored at -20^0C.

2.3 Molecular biology

2.3.1 DNA preparation for neutrophils and fibroblasts

Cell pellets ($5x10^6$-$1x10^7$ cells) were resuspended with 2ml of nuclear lysis buffer (400mM Tris – HCl, 60mM EDTA, 150mM NaCl, 1% SDS, in distilled water) and transferred to 15ml tubes. 0.5ml of 5M sodium perchlorate was added to each tube then rotary mixed at room temperature for 15 min to fully dissolve the pellet. Tubes were then incubated at 65ºC for 30mins prior to the addition of 2ml Chloroform. The resulting solutions were mixed for 10mins then cetrifuged to break the emulsion. The DNA containing phase (top layer) was transferred to a fresh 15ml tube and 2 volumes of pure ethanol were added down the side of the tube. After gentle mixing the DNA was spooled onto a disposable microbiology loop and air-dried for 10mins. DNA was then dissolved off the loop in 0.2ml TE buffer (10mM Tris, 0.5mM EDTA) at 60ºC overnight.

2.3.2 RNA and cDNA prep (CD34s)

RNA was extracted using the Qiagen Micro kit (for <1x106 cells) as per manufacturer's instructions. Briefly, 350μl of 70% ethanol was added to cells which had been lysed and stored in 350μl lysis buffer, mixed and pipetted onto RNeasy micro column (Qiagen RNeasy Plus Micro Kit; www.qiagen.com) in a 2ml collecting tube, then centrifuged at 8000g for 15secs. 350μl of RW1 buffer was added to column and centrifuged for 15secs at 8000g. DNase in RDD buffer was placed directly onto the silica-gel membrane and incubated at RT for 15mins. This was washed with RW1 buffer and then RPE buffer, centrifuging between each wash. 500μl 80% ethanol was added, followed by centrifugation for 2mins at 8000g then the membrane dried by further centrifugation. RNA was eluted from the membrane with RNase-free water and RNA yield determined spectrophotometrically using a Nanodrop ND-1000 machine (Thermo Scientific; www.nanodrop.com).

Single stranded cDNA was generated: RNA was denatured at 65^0C for 5 mins. cDNA mix was made: 5 x buffer from MMVRT kit (invitrogen, www.invitrogen.com) 166.25μl, deoxyribonucleotide triphosphate (dNTP) (Roche; www.roche.com) 50μl of each in 300μl RNase free water, Random Hexamers (Pharmacia, www.pfizer.com) 105μl, dithiothreitol (DTT) (from

MMVRT kit). To each 10μl sample of RNA was added 11μl cDNA mix, 0.75μl moloney murine leukemia virus (M-MLV) reverse transcriptase (RT) enzyme (Invitrogen) and 0.38μl RNasin (Promega, www.promega.com). This was incubated at 37^{o}C for 2hrs then denatured at 65^{0}C for 10mins. cDNA was stored at -20^{0}C until used.

2.3.3 Quantitative real-time PCR

QPCR was performed with TaqMan® Gene Expression Assays (Applied Biosciences; www.appliedbiosystems.com) according to manufacturer's instructions. These assays contain a mix of two unlabeled PCR primers and one FAM dye-labeled TaqMan MGB Probe. Briefly, 2-5μl of cDNA was diluted with water to total volume of 9μl. 10μl of TaqMan Universal PCR Master Mix and 1μl of gene specific TaqMan Primer/Probe Mix were added to each sample. Each 20μl reaction was pipetted into a well of the MicroAmp® optical 96-well reaction plate (Applied Biosciences), sealed with an optical lid and run on 7900HT Fast Real-Time PCR system (Applied Biosciences). Each gene expression assay was plated in duplicate for each sample. Relative mRNA levels were determined using standard ΔΔ Ct calculations with expression levels of experimental samples normalised to GAPDH.

Quantitative real-time PCR on LCH samples, langerin+ DC and LC (Chapter 7) was performed by Carl Allen in Texas (Dept of pediatrics, Texas Children's Cancer Center and Hematology Service, Baylor College of Medicine, Houston TX 77030). Cells were isolated and stored RNA lysis buffer by the author, prior to dispatch to Texas.
RT Q-PCR discussed in Chapter 6 was performed by the author and members of the laboratory (Naomi McGovern and Sarah Pagan).

2.3.4 ELISA

Quantikine® immunoassays (R&D Systems, www.rndsystems.com) were used for all cytokine ELISA tests (Flt3L, M-CSF, SCF). The assay employs a quantitative sandwich enzyme immunoassay technique whereby a monoclonal antibody specific for the cytokine is pre-coated onto a microplate. Samples are

added and any cytokine present is bound by the immobilised antibody. This is detected by adding an enzyme-linked polyclonal antibody specific for the cytokine, followed by a substrate solution which triggers a colour change in the presence of any cytokine. Tests were run according to manufacturer's instructions. Briefly, standard curves were prepared using manufacturer's supplied standard reagent for each kit. 10 control serums (from healthy volunteers) were used to determine normal ranges for each cytokine. Samples were tested neat and at 1:2, 1:10, 1:20 and 1:40 dilutions. Each sample was run in duplicate in 2 separate experiments.

ELISA results discussed in Chapter 5 were obtained by the author and members of the laboratory (Naomi McGovern and Sarah Pagan).

2.4 Statistical analysis

Graphs were plotted with Prism Version 5.0a (GraphPad Software, Inc.). Mean and SD calculation, paired t tests and linear regression analysis were performed within the graphing software. All p values were two-tailed.

Chapter 3. DC profiling

3.1 Introduction

In order to study the homeostasis of human dendritic cells (DC) in health and disease, it was necessary to be able to identify and quantify, in absolute or relative terms, the DC and monocyte/macrophage subsets in human tissues. The most accessible human tissues included peripheral blood and skin.

Methods were required that could i) positively identify monocytes and DC in peripheral blood (PB) and exclude cells extraneous to the analysis, ii) assess the potential of PB cells as pre-tissue DC, iii) enable the examination of peripheral tissue (skin) for the presence of cells analogous to blood components, iv) determine 'normal ranges' for PB and skin monocyte and DC subsets, against which to compare clinical samples, v) lend themselves to the analysis of limited clinical material.

3.1.1 The necessity of lineage staining

In the flow cytometric analysis of human peripheral blood DC, prior to the identification of specific DC markers, such as blood DC antigens (BDCA) 1-4 (37), the exclusion of cells which could express HLA-DR was necessary. This was achieved by labeling surface antigens of these cells with the same fluorochrome so they could be excluded in a single fluorescence channel. Even with the advent of specific DC markers, the proportions of DC in peripheral blood mononuclear cells (PBMC) are so small (<1%), that exclusion of other cells prior to analysis greatly aids accuracy. Additionally, other cells may express DC markers, such as CD1c (BDCA-1) on approximately 50% of B cells (144) and CD304 (BDCA-4) on some activated T cells (145) and also reported on a subset of lymph node (LN) Treg cells (146).

3.1.2 Lineage options

The 'lineage cocktail' applied to exclude non-DC from the lineage$^-$HLA-DR$^+$ (Lin$^-$ DR$^+$) gate, and so the nature of the cells excluded, varies between publications (37) (38). B cell markers may include CD19 or CD20, NK and T cell markers

CD56, CD3, CD7, CD16 and the inclusion of CD34 is variable. Circulating $CD34^+$ progenitors express medium levels of HLA-DR (at least equivalent to $CD14^+$ monocytes) and so will be included in the DC gate unless specifically removed. In addition, most DC studies exclude monocytes from analysis with the addition of CD14 and CD16 in lineage. Although much attention has been directed at the necessity to exclude cells from DC analysis, less focus has been given to Monocytes/DC which could potentially be excluded from the Lin^-DR^+ gate due to positive lineage staining.

3.1.3 Reports of myeloid cells in NK gates

One group noted that myeloid cells could be found in NK cell gates when using CD16, CD56 and CD7 for NK cell identification (147). $Lin(CD3/14/19)^-CD56^+$ PBMC contained $CD7^+$ NK cells and $CD7^-$ monocyte/DC, the identity of which remained unexplained. The expression of DC antigens on NK cells, particularly when activated, has been previously described and includes CD80, CD86, HLA-DR and CD4, reviewed in (148). However, the expression of NK cell antigens on cells gated from a DC perspective has not. This analysis may reveal the identity of these mystery myeloid cells, without having to redefine them phenotypically or functionally.

3.1.4 Lin^-DR^- cells

In the analysis of Lin^-DR^+ PB DC, the nature of cells which stain positively for lineage is well documented but cells which remain negative for lineage markers and are also $HLA\text{-}DR^-$ have not been characterised. As Lin^-DR^+ cells show a spectrum of HLA-DR expression, it is important to know what cells may be inadvertently included in the lower end of the gate and whether they express any DC-associated antigens which would be included in DC analysis. Also, this population, present in normal PB and not removed by Ficoll treatment, may be important in the analysis of PBMC in disease but without identifying these cells, this information would be lost.

3.1.5 Skin DC

One of the aims of this work was to explore the relationship between blood and skin DC. No simple relationship was apparent with previous analytical methods.

The markers used to classify skin DC, primarily CD1a and CD14, do not related to PB DC as there is no CD1a expression in PB. Conversely, the expression of BDCA markers in skin has not been investigated. Even with more advanced skin DC analysis (73), unclassified populations can be found, such as $CD1a^{+}CD14^{+}$ and $CD1a^{-}CD14^{-}$ (double negative, DN) cells. *In vitro* culture reveals that both markers are inducible on monocytes and $CD34^{+}$ progenitors, further complicating the direct comparison of PB and peripheral tissue leukocytes. In addition, extraction of single cell suspensions from skin requires greater tissue processing than extraction of cells from blood. Skin preparation requires either digestion of tissue, introducing enzyme-related artifacts, or migration of cells, introducing potential *in vitro* culture artifacts. Whilst these problems are impossible to eliminate, they must be taken into account in the analysis of results.

3.1.6 Cross-presenting DC in blood and skin

Recent interest in the PB $CD141^{high}$ mDC as a cross-presenting DC (149), analogous to the $CD8\alpha^{+}$ murine LN DC (66), and the identification of a functionally similar cell in mouse skin (35), begs the question of whether such a cell exists in human skin. Not only are these cells potent DC with the potential to control autoimmunity and protect against viral infection, but their distinct function and antigen expression profile may further the understanding of mouse/human DC homology.

Elucidating the relationships between PB and tissue DC is a critical step towards explaining DC ontogeny and homeostasis.

3.2 Materials and Methods for Chapter 3

3.2.1 Flow cytometry set up

Using LSRII or FACSAriaII, PMT voltages were set on cells stained with single fluorochromes. Compensation was then performed using individual fluorochrome staining of compensation beads (BD CompBead anti-mouse Ig κ) and adjusted manually using BD Diva software. Positive staining was confirmed with isotype controls for all tissues.

3.2.2 Trucount Analysis

To determine the absolute counts of leucocytes in blood (cells/μl), BD TruCOUNT Tubes were used. Each tube contains a known number of fluorescent beads in a lyophilised pellet which dissolves on contact with liquid. A known volume of whole blood is added accurately and leukocytes are identified by staining with conjugated antibodies. The resulting mixture is run on a flow cytometer after a red cell lysis step and thorough mixing. As the number of beads and cells analyzed can be counted, the corresponding volume of blood analyzed can be calculated and the number of cells/μl determined:

(# cells counted/# beads counted) x (# beads in tube/test volume) = absolute count of cell (cells/μl whole blood)

Trucount tubes were stained with CD45, CD3, CD34 and CD14. CD45 was necessary in order to threshold on positively stained cells. Normally FSC parameter would be used for this purpose (to reduce the amount of noise or debris recorded by the flow cytometer as events) but as the beads are smaller than cells, a fluorescence channel is used for trucount tubes. CD3 allowed calculation of T cell numbers, CD14 of $CD14^+$monocytes and CD34 of circulating progenitors. The relative proportions of PBMC cells analyzed in tubes containing any of these antigens could then be used to determine the absolute numbers of all cell populations.

3.2.3 PBSC processing

PBSC from donors harvested after G-CSF administration was generally analyzed directly with no further processing steps. Where red cell contamination was evident, a red cell lysis step was performed using BD FACS lysing solution (10x) diluted with cold distilled water. This was applied to cells using approximately 1ml of diluted lysis solution per $1x10^7$cells for 10mins at RT, followed by a wash in DPBS and subsequent staining in flow buffer.

3.2.4 Skin Digestion at 4^0C

Where described, dermis was digested at 4^0C. Skin was processed as described in Chapter 2 except that after addition of collagenase, it was left at 4^0C overnight. Subsequently, it was placed at 37^0C for 3hrs to complete the digestion. The resulting cell suspension was treated the same way as previously described.

3.3 Results I: PB Analysis

3.3.1 PB APCs

A 12 channel flow protocol was developed to allow, in a single flow cytometry tube, the identification and relative quantification of all DC subsets from PBMC (**Figure 3.1, A),** collected in a single 'APC' gate**.** Firstly, a gate was set on FSC and SSC to include PBMC and exclude residual red cells, platelets, neutrophils or debris (plot i) and doublets excluded using SSC-A v SSC-H (ii). A Lineage channel was used to stain T-cells (CD3), B-cells (CD19 and CD20) and NK cells (CD56). Cells within a Lin^-DR^+ gate were then selected (iii). From this classical (Gate 1), intermediate (Gate 2) and non-classical (Gate 3) monocytes were separated with CD14 and CD16 staining (iv). Cells negative for both these antigens (double negatives 'DN') include PB DC and $CD34^+$ progenitors. pDC (Gate 4) and mDC were identified by their CD123 and CD11c expression respectively (v). mDC were then further split by CD141 (Gate 5) and CD1c (Gate 6) staining (vi). $CD141^{high}$ cells had slightly lower CD11c expression than $CD1c^+$ cells (vii). Circulating progenitors were negative for both these markers and positive for CD34 (viii, Gate 7).

Further analysis of $Lin^-DR^+CD34^+$ cells (**Figure 3.1, B,** ii) showed they were consistently $CD45^{dim}$ (red dots in iii) and, although HLA-DR^+, they expressed lower levels of Class-II than PB DC (red dots in iv, compared to grey cells in Lin^-DR^+ area of the plot). Interestingly, when examining all $CD34^+$ cells found in PBMC (i) small numbers of $Lin^+CD34^+CD45^{bright}$ cells were observed (black dots in iii and iv). Variability was noted in the proportion of $CD34^+$ cells that were Lin^+ but these cells could be found in all Lin^+ areas of the Lin v DR plot and in all samples.

In order to be able to identify all cells in the Lin v DR plot, the Lin^-DR^- gate (**Figure 3.1, A,** iii, gate 8) was analyzed. This contained a population of $CD123^+$ cells with low FSC and SSC, negative for CD14, CD16, CD1c, CD11c, CD304, CD7 and CD10, but positive for CD33, CD13 and CD31 (**Figure 3.1, C**). Cytospin of these sorted cells showed lobulated nuclei with basophilic cytoplasm. These findings were consistent with the phenotype and morphological appearance of basophils. By FACs, cytospin and giemsa staining, the $Lin^-DR^-CD123^-$ material was found to be a combination of debris, small platelet clumps and red blood cells which had not been excluded by the initial 'Cells' gate. This material showed the lowest SSC and FSC profile of all events in the cells gate.

The viability of freshly isolated PBMC was always >99% so a dead cell exclusion dye was not routinely included for this material. However, there was the flexibility to allow its inclusion for previously frozen material; either DAPI in the V450 channel (with CD11c in APC) or amine dye in the V500 channel (with HLA-DR in PERCPCy5.5 and CD123 in PE).

Figure 3.1

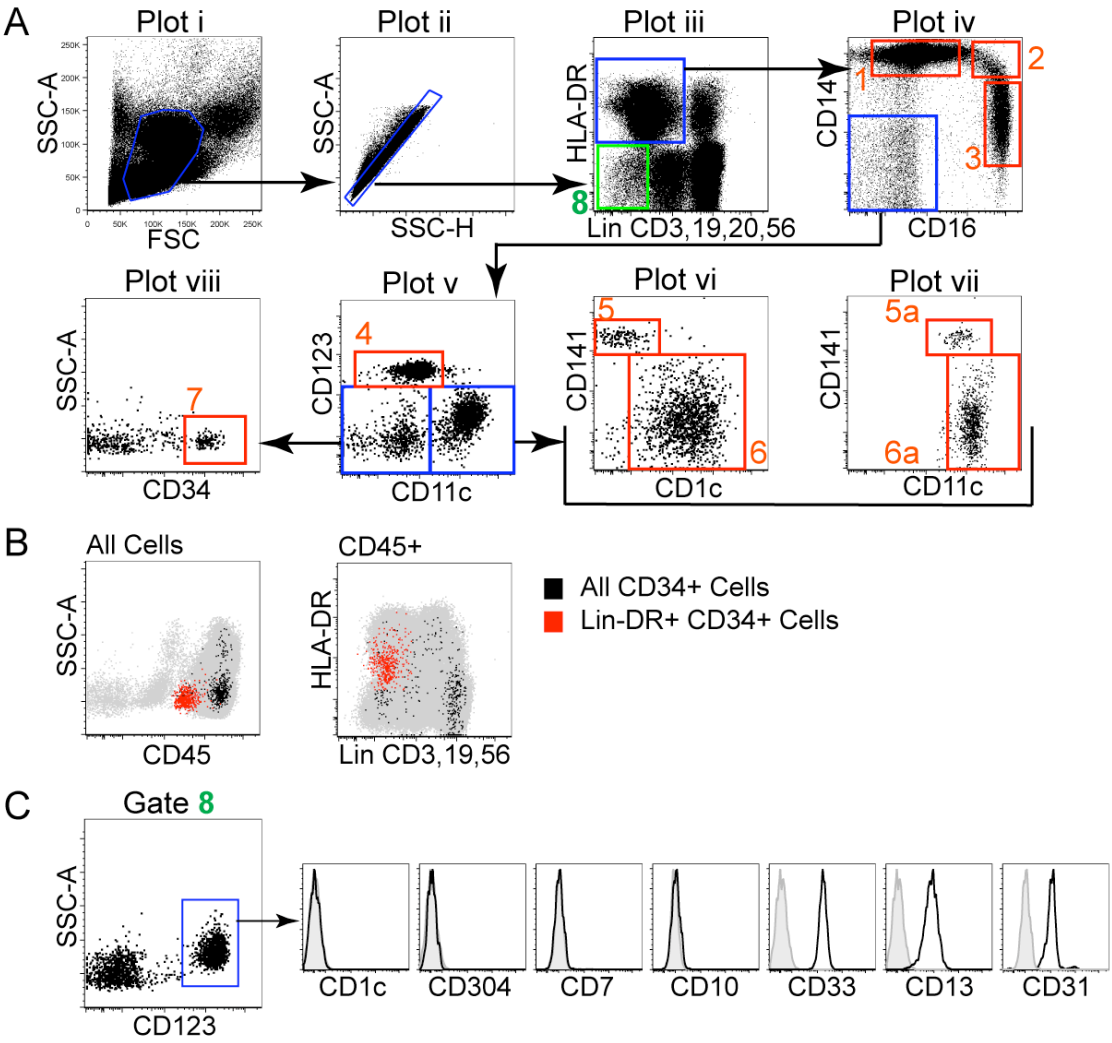

Figure 3.1 Flow cytometry of PBMC to reveal Monocyte and DC subsets
A: Gate 1 CD14+ Monocytes, Gate 2 CD14+CD16+ monocytes, Gate 3 CD16+ monocytes. Gate 4 pDC, Gate 5 CD141-high mDC, Gate 6 CD1c+ mDC, Gate 7 CD34+ progenitors. Gates 5a and 6a show same cells as Gates 5 and 6 but defined without CD1c expression. B: CD34+ progenitors plotted on the left against CD45 and SSC with all PBMC cells shown in grey. Plotted on the right against Lineage and HLA-DR with all CD45+ cells shown in grey. Red dots: Lin-DR+ CD34+ cells; Black dots: All CD34+ cells in PBMC. C: Lin-DR- cells (A: gate 8) plotted CD123 against SSC. Histograms showantigen expression on CD123+ cells. Grey histograms, isotype control; black histograms, antigen. SSC-A/H, side scatter area/height; FSC, forward scatter; Lin (), Lineage (antigens included in lineage cocktail).

3.3.2 Isotypes

True positive staining of antigens on all APC subsets in all tissues examined was confirmed with specific isotype controls. This is particularly necessary in the case of APC as non-specific and Fc-receptor binding can lead to false positive results if compared to other cell types and not isotype controls. **Figure**

3.2 shows the use of isotype controls in PB DC analysis. Here, one conjugated antibody per tube is switched for its relevant isotype whilst the remaining antibodies are unchanged, in a fluorescence minus one (FMO) system (**Table 2.1**). This negates issues related to compensation when more than one antibody is exchanged for an isotype control.

Figure 3.2

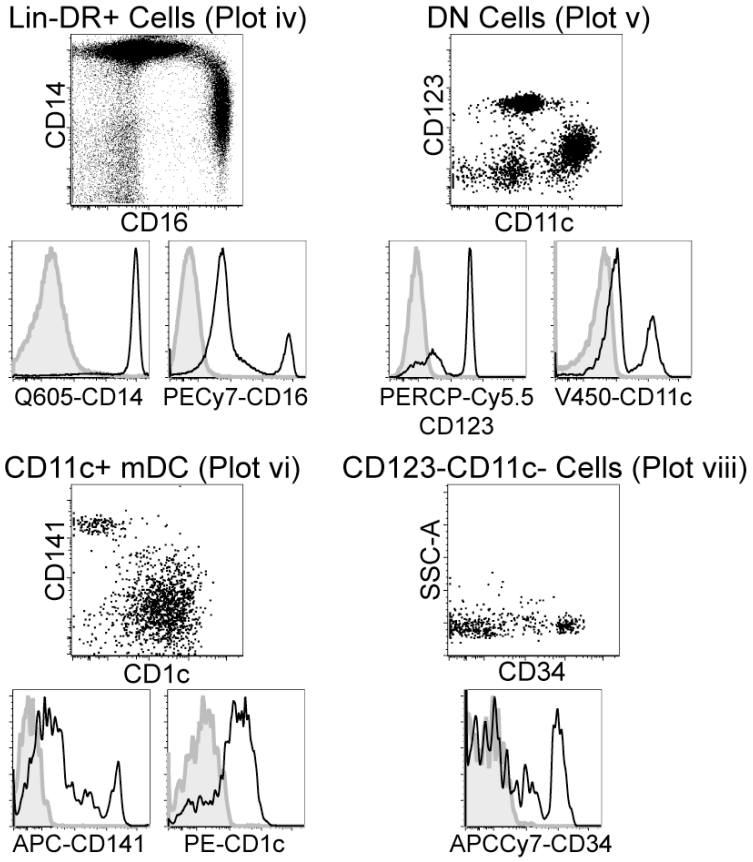

Figure 3.2 Isotype controls as FMO set-up for PB DC analysis
Isotypes: grey histograms; Antigen specific: black histograms. DN, Double negative (CD14-CD16-); Lin, lineage; DR, HLA-DR

3.3.3 Lineage delineation

The use of $Lin^{-}DR^{+}$ gate to identify monocytes/DC relies on good separation of Lin^{+} and HLA-DR^{-} cells from the gate, in order to exclude HLA-DR expressing lymphocytes and $Lin^{-}DR^{-}$ basophils. A bright HLA-DR stain was the first step and although V500 (BD Horizon) was found to give the best separation this was only available in the last few months of work. Up to this point, and for the majority of work PERCPCy5.5 conjugated antibody was used. This ensured

sufficient distinction of HLA-DR^{bright} CD123^{+} pDC from HLA-DR^{-} CD123^{+} basophils.

Staining of B, T and NK cells with specific markers not included in lineage allowed the identification of the position of these cells on the Lineage versus HLA-DR plot (**Figure 3.3, A**). CD19^{+} B cells, gated from total PBMC, stained brightly with lineage containing CD20 (black dots) which increased the separation of these cells from HLA-DR^{+} monocytes/DC (**Figure 3.3, A**). Note the comparison with the third plot in panel A (showing blue dots) where CD20 is not included in lineage. Here there is a cloud of DR^{+} cells in the centre of the plot which are B cells stained only with CD19. CD7 identified both NK and T cells (red dots), showing them to sit in the Lin^{+}DR^{-} area. Blue dots represent CD56^{+} cells gated from total PBMC. The CD56^{+} cells with the brightest lineage fluorescence are likely to represent a mixture of CD56^{+} T cells and CD56^{bright} NK cells, and the Lin^{-}CD56^{+} cells may be CD16^{-} NK cells. The bulk of the CD56^{+} population shows lineage fluorescence in the middle of the axis.
A proportion of both T and NK cells could express HLA-DR when activated. Populations of cells positive for CD7 or CD56 was also noted in the Lin^{-}DR^{+} area, discussed below.

In order to identify myeloid cells that may fall into NK cell gates when CD56 and CD7 were used as NK cell markers, the expression of these antigens on cells in the Lin^{-}DR^{+} gate was examined. It was found that a proportion of CD11c^{+}mDC (14% mean of n=3) and a small proportion (1.6% mean of n=3) of CD14^{+}monocytes expressed CD56 compared to isotype control. In addition, 17% (mean of n=3) of pDC and 11% (mean of n=3) of circulating CD34^{+} progenitors expressed CD7 (**Figure 3.3, B**). The addition of CD7 and CD56 to lineage cocktail increased the brightness of NK cells in the lineage channel and increased the separation from the Lin^{-}DR^{+} gate (**Figure 3.3, C**) but lead to the exclusion of some DC from the Lin^{-} gate. The variation in the shape of the Lin^{-} DR^{+} cell cloud in C compared to A is due to the respective presence and absence of monocytes in this population.

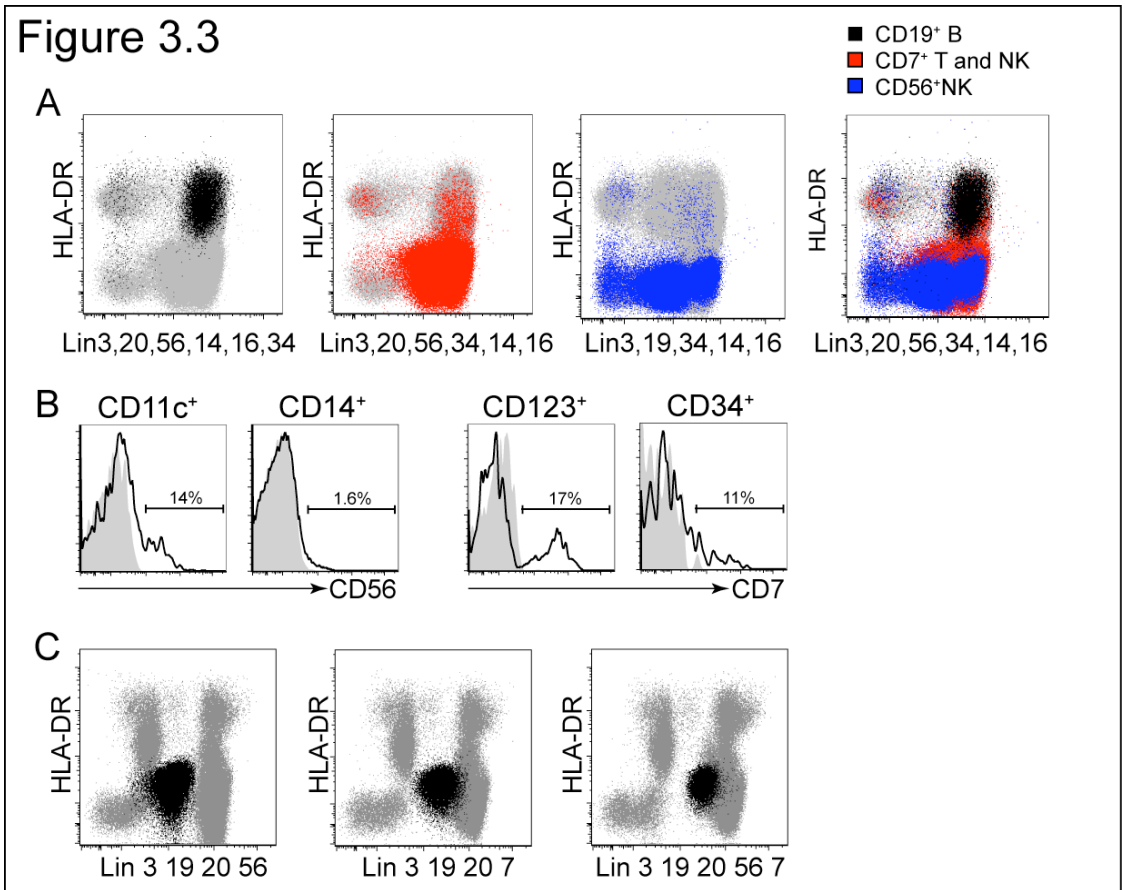

Figure 3.3 Lineage staining in PB DC analysis
A: PBMC stained with lineage including CD3, 20, 56, 34, 14, 16 to show where B, T and NK cells sit in the Lineage versus HLA-DR plot. Black dots show cells gated as $CD19^+$ B cells from total PBMC. Red dots show $CD7^+$ T and NK cells and blue dots where $CD56^+$ NK cells fall when CD56 is not included in lineage. Note CD19 is included in lineage in place of CD20 in this plot. B: the percentage of $CD11c^+$DC and $CD14^+$Mono expressing CD56 and the percentage of $CD123^+$pDC and CD34 progenitors expressing CD7. C: the effect on NK cell (black dots) position in the Lin v DR plot when CD56, CD7 or both are in lineage.

3.3.4 Normal range of PB monocytes/DC relative to Number of cells analyzed

In order to develop a normal range of monocytes/DC in PBMC, blood from twenty-six healthy adult volunteers (age range 24-55yrs) was analyzed**.** APC populations were expressed in relative terms as the percent of mononuclear cells **(Figure 3.4)**. Mononuclear cells were defined as cells falling within both the initial 'Cells' gate **(Figure 3.1, Plot A)** and the subsequent 'singlets' gate **(Figure 3.1, Plot B).**

Figure 3.4

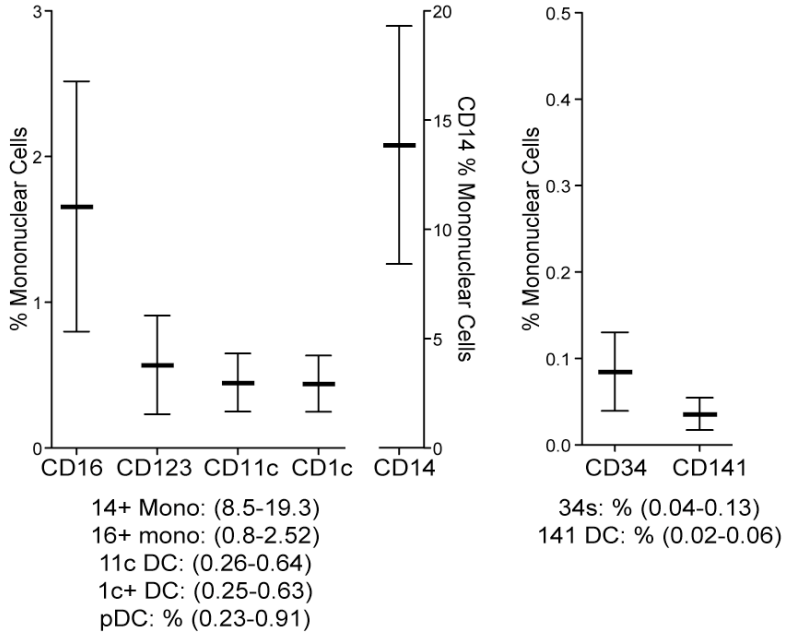

Figure 3.4 Relative quantities of PB Monocytes, DC ad CD34+ progenitors in PBMC.
Bars show mean+/-SD n=28, except CD34 and CD141 n=27

3.3.5 Normal range of PB monocytes/DC in absolute terms

Although a SSC v FSC gate is often used as an initial step in lymphocyte analysis, this is not possible for DC analysis as DC and monocyte subsets have a range of SSC and FSC profiles from the largest $CD14^+$monocytes to the smallest $CD34^+$progenitors **(Figure 3.5, A).** Therefore all cells must be included in the analysis of DC.

In order to derive a normal range of absolute counts (cells/ml whole blood) for monocyte/DC subsets, an additional BD Trucount™ tube of whole blood was run and analyzed alongside twenty-one normal samples. CD45 was included to set a threshold for flow cytometric data recording (only events falling in the $CD45^+$ gate were counted). The inclusion of CD14 and CD34 allowed the proportions of cells in the DC tube to be derived and CD3 was required for quantification of lymphocytes as discussed below. As described in material and methods this allowed the determination of the absolute number of cells in each population (**Figure 3.5, B**).

Figure 3.5

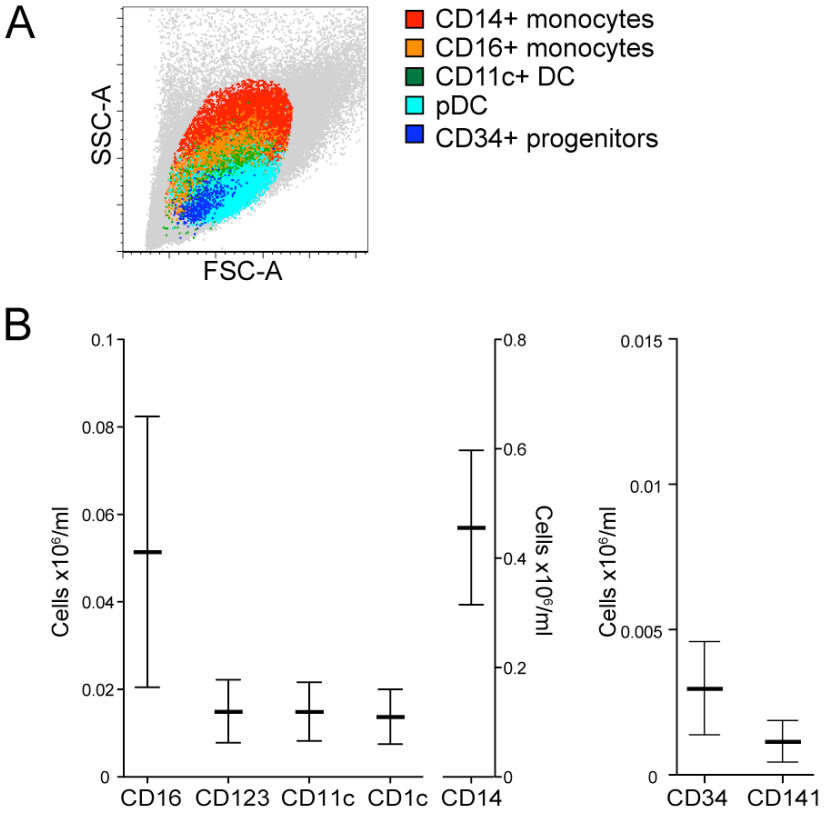

Figure 3.5 Range of absolute counts of PB Monocytes, DC and CD34 progenitors from PBMC

A: PBMC plotted as SSC v FSC showing the profile PB monocyte, DC and CD34+ progenitors. Dotted circle shows the gate position for lymphocyte analysis.
B: Graphs of absolute counts of PB monocytes, DC and CD34+ progentors expressed as Cells/ml. Bars show mean+/-SD n=21
SSC, side scatter; FSC, forward scatter

3.3.6 Lymphocytes

A second panel of conjugated antibodies was designed to quantify, by direct staining, the lineage positive fraction of PBMC (**Figure 3.6, A**), including $CD19^+$ B cells (Gate 1), $CD3^+$ T cells (Gate 2) and $CD56^+$NK cells (Gate 3). CD4 and CD8 were included to differentiate T cell subsets (T cell Plot). In addition to identifying two populations of NK cells (CD56bright, Gate 3a, and $CD56^+$) CD56 could be used to identify activated $CD56^+$ T-cells (Gate 4). CD45 was used to exclude debris as the initial 'cells gate' was close to where this material fell at the origin of SSC versus FSC plot. Also, unlike the analysis of DC where there is an additional positive (Lin^-DR^+) gating step to exclude other cells and debris

prior to quantification, without CD45, the cells gate would be the only gate before lymphocyte quantification.

Again, populations were expressed both as percent of singlet cells in the lymphocyte gate (**Figure 3.6, B**), and as number of cells/ml whole blood through the BD Trucount™ method (**Figure 3.6, C**). Inclusion of CD3 in the trucount tube allowed the quantification of lymphocytes in the lymphocyte analysis tube.

Figure 3.6

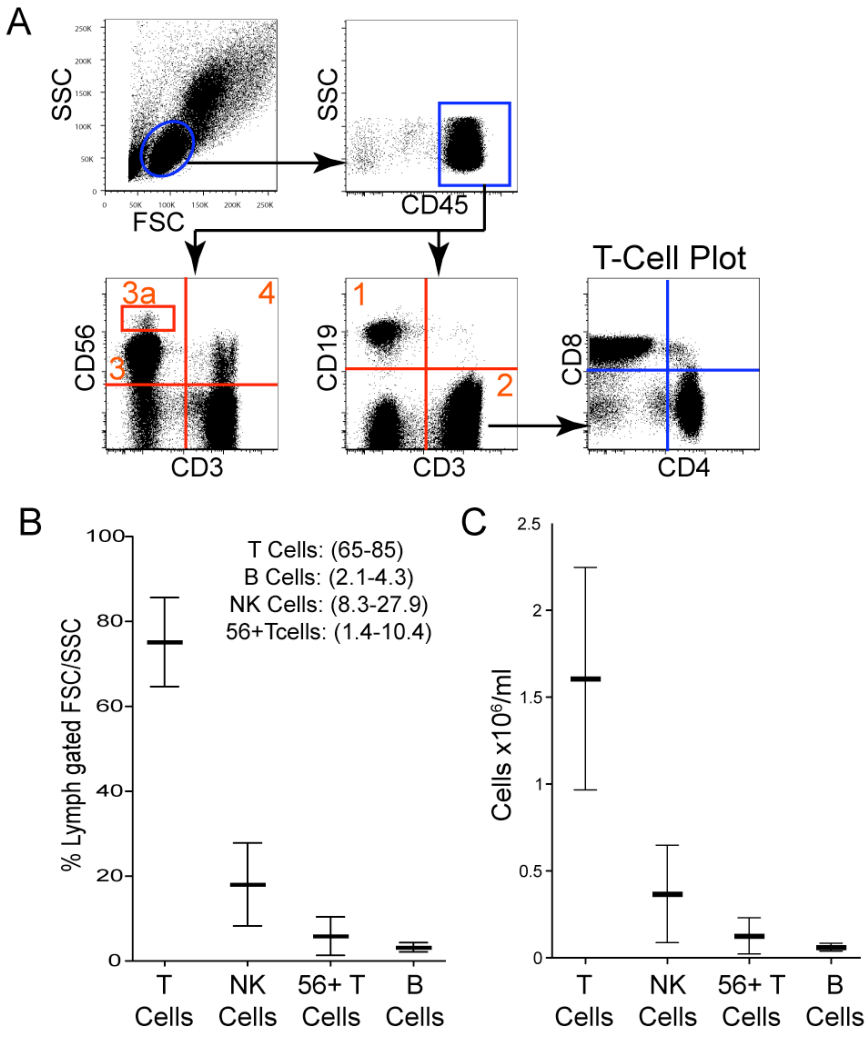

Figure 3.6 Flow cytometric quantification of Lympocytes in PBMC
A: Antigen panel and gating strategy to identify PB lymphocyte subsets
B: Relative quantification of PBMC lymphocytes expressed as % of cells from lymphocyte SSCvFSC gate. Bars show mean+/-SD n=10
C: Absolute numbers of lymphocytes in PBMC expressed as cells/ml.
Bars show mean+/-SD n=10 SSC, side scatter; FSC, forward scatter

3.4 Results II: Skin APC analysis

3.4.1 Flow cytometric analysis of digested and migrated skin APC

Figure 3.7 shows flow cytometric evaluation of APC populations digested and migrated from whole skin, dermis and epidermis. It was found that digesting or migrating thin sections of whole skin allowed isolation of all described populations of both dermal and epidermal APC, which could be then distinguished by flow cytometry.

Leukocytes were identified by positive CD45 staining and APC by their expression of HLA-DR. Dermal macrophages containing melanin granules could be separated from DC by their autofluorescence (AF) in the FITC channel, without additional surface markers. This autofluorescence could also be seen in the other fluorescence channels. These cells were not capable of migration *in vitro* and so were not present in the cells of migrated preparations. From the non-autofluorescent populations several subsets of DC could be identified, including a population of dermal DC (DDC) expressing CD14 but lacking CD1a (Gate 1) and a population expressing CD1a but lacking CD14, $CD14^{+}$DC (Gate 2). From whole skin a population of $CD1a^{bright}$, langerin/$CD207^{+}$ ($Lang^{+}$) cells could be found (Gate 3), representing epidermal LC. The autofluorescent macrophages from digested preps were $CD14^{+}CD1a^{-}$ (Gate 4). A small number of $CD1a^{bright}Lang^{+}$ cells could always be found in digested dermis and represented LC migrating through the dermis.

It was found that digesting epidermis alone with the same concentration of collagenase as for whole skin or dermis resulted in unnecessary disruption of the epidermal architecture causing release of large numbers of keratinocytes into the medium, without increasing the numbers of available LC. Keratinocytes were found to non-specifically bind antibodies and complicate the flow cytometric analysis of LC. A similar problem was observed with the digestion of whole skin if the epidermis remaining after digestion was disrupted through pipetting. A reduction in collagenase concentration (to 0.5mg/ml) for digesting epidermis and care extracting cells from whole skin digests was found to solve the problems.

Figure 3.7

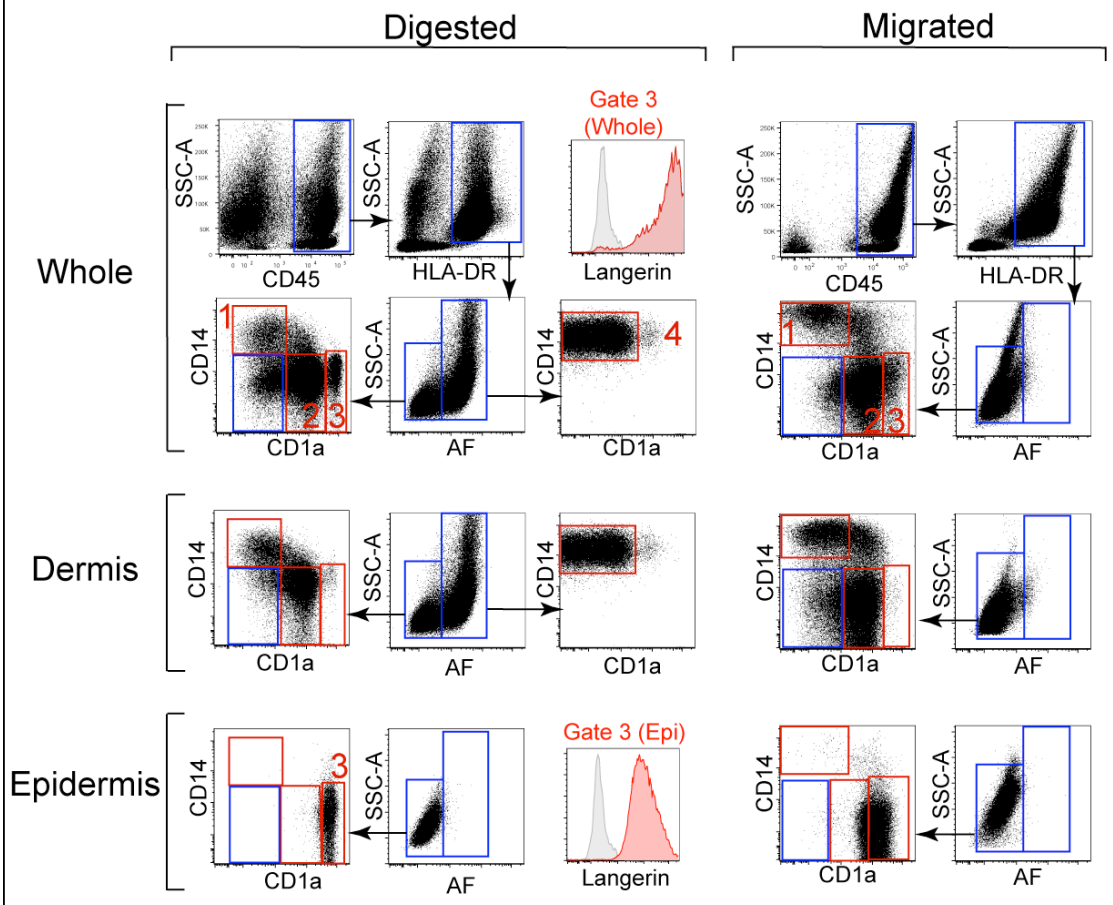

Figure 3.7 Flow cytometric identification of major APC subsets digested and migrated from whole skin, dermis and epidermis.
Gate 1 defines $CD14^+$ cells; Gate 2, $CD1a^+$ DDC; Gate 3, langerin positive LC Gate 4 shows that autofluorescent macrophages are $CD14^+CD1a^-$. They are not present in cells from migrated preps.

3.4.2 Relative quantification of dermal APC

For the study of DC from patient biopsies, the interest was primarily in quantifying the DC subsets. As dermis and epidermis from these samples would be analyzed separately, the dermis from twenty two controls was used to determine a normal range of APC populations expressed as the percent of live cells in the digested dermis (**Figure 3.8**).

Figure 3.8

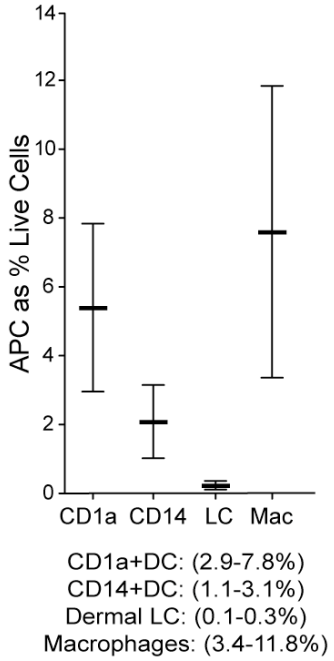

Figure 3.8 Relative quantification of dermal APC
Subsets expressed as a percentage of live cells analysed n=22. Bars show mean +/- SD.

Initially attempts were made to quantify APC relative to fibroblasts present in the digested preps, using CD73 as a fibroblast marker. However, quantifying APC relative to total live cells gave comparative ratios and released a fluorescent channel for additional phenotype analysis. The use of shave biopsies, as opposed to punch biopsies, for clinical samples created a similar thickness of sample to that of the normal skin preparations, so controlling for variations in APC density through the thickness of the dermis.

3.4.3 Quantification of absolute numbers of LC in epidermal sheets

In the epidermis, it was possible to quantify the absolute number of LC/mm^2 by fluorescence microscopy (sections 2.1.2 and 2.2.2). Twelve Controls were analyzed to determine a normal range against which to compare patient samples (**Figure 3.9**). LCs within a minimum area of 0.3mm^2 were included in each count. This equated to approximately three fields at x10 magnification.

Figure 3.9

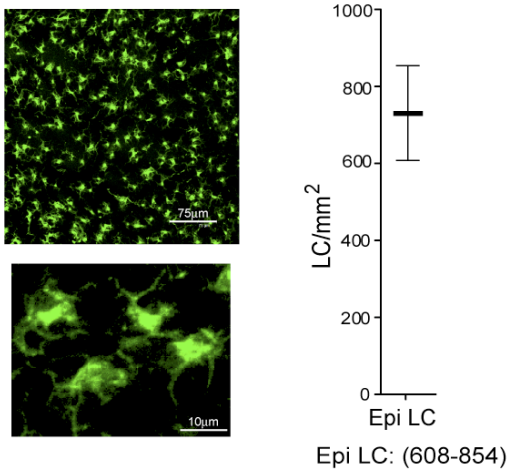

Figure 3.9 Confocal microscopy of epidermal sheets.
Whole mount epidermal sheets of controls, stained with anti-CD1a-FITC and imaged with Leica TCS SP2 confocal microscope. Graph shows mean +/- SD of n=12 LC counts expressed as LC/mm^2.

3.4.4 CD141^{high} cells in skin

In order to determine whether any cells with phenotypic similarities to PB mDC could be found in skin, CD141 and CD11c expression on skin DC was examined. A population of CD141^{high}CD11c^{low} cells was found in the DC gate (CD45$^+$HLA-DR$^+$AF$^-$) of both digested whole skin and dermis (**Figure 3.10, A,** i). These cells represented 0.8-1% of all live cells analyzed (n=3 dermis; n=4 whole skin) (**B**). Within this population there was a spectrum of CD1c and CD1a expression (**A**, ii, blue dots) up to the level of antigen expression seen in DDC (background grey dots). All 141^{high} cells expressing CD1a also expressed CD1c while some CD1c^{low}CD1a$^-$ cells were present. None of the CD141^{high} cells expressed CD14 or fell in the CD1a^{bright} LC gate (**A,** iii). There was no langerin expression in this population, compared to isotype control (**A,** blue histogram Gate 1). Conversely, the population of CD11c^{low}CD141^{low} cells (**A,** Gate 2) expressed high levels of langerin and fell in the CD1a^{bright} gate (**A,** green histogram, Gate 2), identifying them as LC. The same populations were found in digested dermis, suggesting that these cells were not epidermal in origin. The only difference was the smaller number of LC in this preparation, as seen in all digested dermal preps.

CD141^{high} cells were also found among DC migrated from skin, (shown in **C** plotted against CD1a) and displayed a similar spectrum of CD1a expression as cells from digested skin (**C**). However, in the migrated prep, CD14^{+} cells had to be excluded from the analysis (**C**, ii) as they expressed levels of CD141 akin to the CD141^{high} cells (**C**, blue histogram, Gate 3a). This is examined further in section 3.4.6. Once these cells were removed, CD14^{-}CD141^{high} cells could still be clearly identified.

Figure 3.10

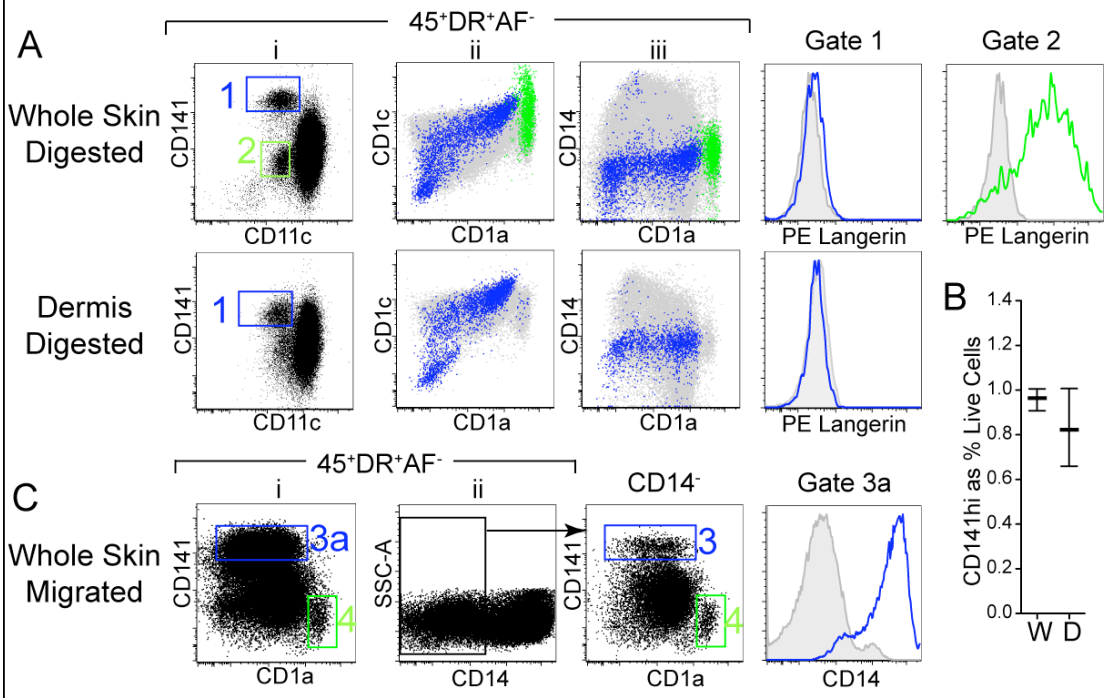

Figure 3.10 CD141^{high} cells in skin
A: CD141^{high}CD11c^{low} cells (Gate 1) in digested whole skin and dermis. Plot i shows all CD45^{+}HLA-DR^{+}AF^{-} cells in black. Gate 2 contains CD11c^{low} cells which are negative/low for CD141 expression but are postive for langerin (histogram Gate 2), identifying them as LC. Plots ii and iii show all CD45^{+}HLA-DR^{+}AF^{-} in grey. CD141^{high} from Gate 1 are shown in blue and LC in green.There is no langerin expression on CD141^{high} from Gate 1 (histogram Gate 1). B: Percentage of live cells analysed contained in Gate 1 (CD141^{high}CD11c^{low} cells) from digested whole (W) skin (n=4) and dermis (D) (n=3). C: CD45^{+}HLA-DR^{+}AF^{-} cells migrated from whole skin. The majority of cells in Gate 3a (plot i) are CD14^{+} (black histogram Gate 3a). If CD14^{-} cells are selected from CD45^{+}HLA-DR^{+}AF^{-} (plot ii), CD141^{high} cells can then be identified (Gate 3).

3.4.5 Comparison of CD141 expression in Skin and Blood DC

If PB mDC can contribute to skin DC homeostasis, it is likely that cells phenotypically comparable to PB mDC would be found in skin. As CD141^{high}

cells have been identified in skin, a direct flow cytometric comparison of CD141, CD11c, and CD1c expression was made between blood mDC and skin DDC (**Figure 3.11**). As there was no CD16 or CD123 expression in skin, cells expressing these markers in blood ($CD16^+$monocytes and $CD123^+$pDC) were excluded from the PB analysis. $CD11c^+CD141^{high}CD1c^-$ and $CD11c^+CD141^{neg/low}CD1c^+$ cells could be found in both tissues. When $CD1a^+$cells were excluded from the skin analysis (DN DC were gated), the proportions of the two mDC populations in skin became very close to the proportions found in PB. As there is no CD1a expression on PB mDC, this comparison is perhaps more relevant to identifying cells which may have recently emigrated from PB into skin.

Figure 3.11

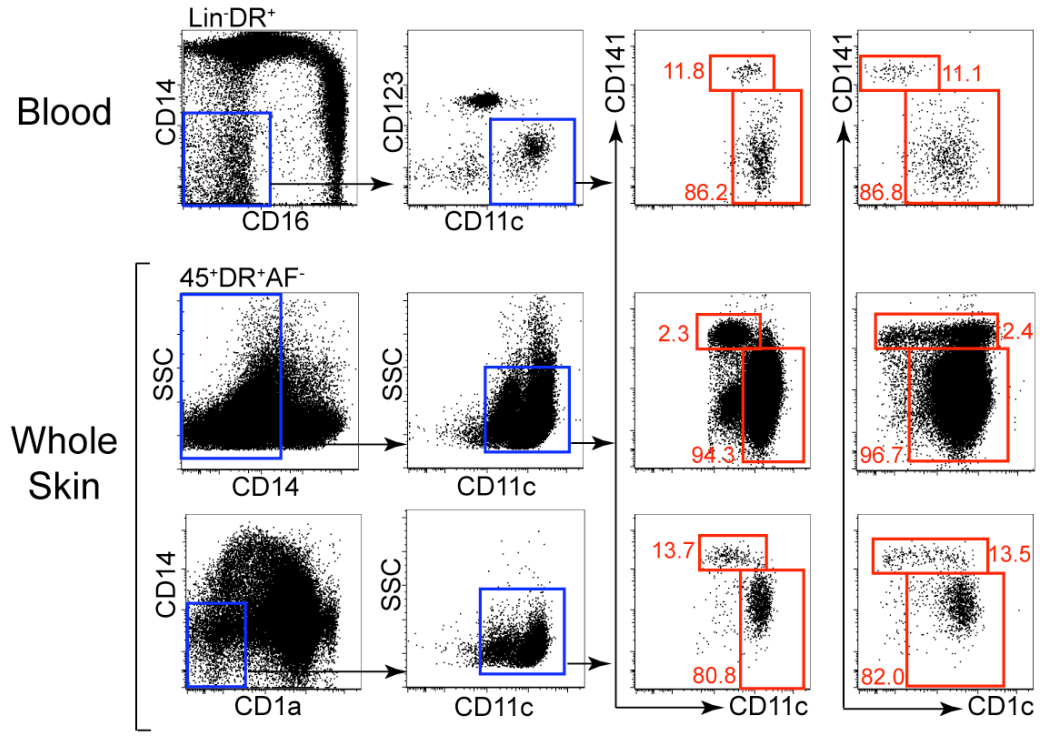

Figure 3.11 Comparison of CD141 expression in PB and skin
Blood: Lin^-DR^+ PB cells. DC selected by their CD14 and CD16 negativity. $CD123^+$pDC excluded from the analysis. $CD11c^+$mDC displayed as CD11c v CD141 and CD1c v CD141. Whole Skin: $CD14^-$DC selected from $CD45^+DR^+AF^-$ cells. Similarly to PB, $CD11c^+$ cells selected and then shown plotted as CD11c or CD1c against CD141. Bottom panel shows the same analysis but with the initial gate set to exclude both $CD14^-$ and $CD1a^+$ DC.Numbers represent percent of cells from the plot contained within the gate.

3.4.6 CD141 up-regulation in blood and skin

As CD141 appears to be a critical marker in the identification of a specific subset of cross-presenting DC, it's expression by other cells in PB and skin was important to examine. In addition, during the preparation of skin, enzyme digestion may remove sensitive antigens and the short culture step (overnight at 37^0C) may be sufficient to induce expression of some antigens.

In blood, all monocyte/DC subsets were found to express CD141 at a lower level to CD141^{high}mDC. (**Figure 3.12, A,** black histograms compared to grey isotype control). However, it was noted that PB cells that had been left overnight in EDTA at room temperature before PBMC isolation, for example during transport, expressed higher levels of CD141 (**A,** red histograms). Neither the proportion of CD141^{high}mDC, nor the level of their CD141 expression was altered under these conditions.

Similarly, in skin, all APC, including dermal macrophages, showed some expression of CD141 compared to isotype control after overnight collagenase digestion at 37^0C (**B,** red histograms). To determine whether preparation conditions affected the level of CD141 expression, half of the same skin preparation was collagenase digested overnight at 4^0C, followed by 3hrs at 37^0C to complete the digestion (**B,** black histograms). The level of CD141 expression on DC and macrophages was lower after digestion at 4^0C than 37^0C. However, the expression of CD141 by the CD11c^{low} cells was reduced in the dermal preparation digested at 37^0C. This resulted in the histogram of CD141 expression for these populations showing only one peak. However, the cells could still be distinguished by their level of CD11c expression (**C**) Interestingly, preservation of CD141 expression on these cells was observed in skin digested whole at 37^0C, possibly due to protection by the epidermis.

Figure 3.12

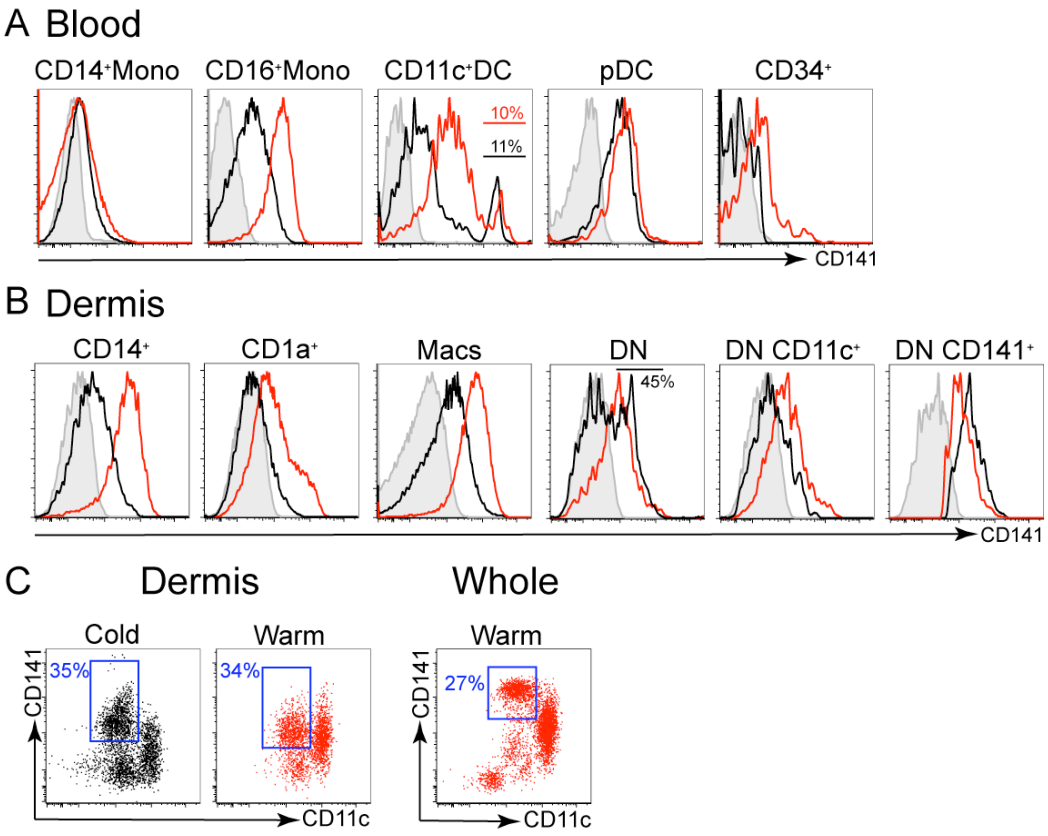

Figure 3.12 CD141 expression on APC of blood and skin
A: Expression of CD141 on fresh PB $Lin^{-}DR^{+}$ monocytes and DC (black histograms) (n=28) and after transport overnight at room temperature (red histograms) (n=1). Isotype controls shown in grey. Numbers represent the % of $CD141^{high}$ cells in the myeloid DC gate. B: Expression of CD141 on $CD45^{+}DR^{+}AF^{-}$ dermal APC after digestion of dermis at $4^{0}C$ (black histograms) (n=1) and $37^{0}C$ (red histograms) (n=2). Isotype controls shown in grey. Number represents the % of $CD141^{high}$ cells in the $CD14^{-}CD1a^{-}$ (DN) gate of dermis digested at $4^{0}C$.
C: Dots plots showing the expression of CD141 and CD11c on $AF^{-}CD1a^{-}CD14^{-}$ cells from dermis digested at $4^{0}C$ (Cold, black dots) and $37^{0}C$ (Warm, red dots) and on DN cells from whole skin (n=2) digested at $37^{0}C$. Blue gates show the position of $CD11c^{low}$ cells on the CD141 axis and numbers represent % of cells from the plot that fall within the gate.

3.5 Discussion

Through the development of techniques to enable the profiling of PB and skin DC a number of important biological observations have been made. These are critical not only to the ability to accurately identify DC but they also have direct relevance to the study of DC ontogeny and homeostasis. Most important of these is the observation that cells analogous to PB mDC can be found in skin.

3.5. Identification of PB DC

In practice, the DC profile panel was developed over the course of the project as issues, such as the brightness of HLA-DR, came to light. The necessity to have a bright channel (PE or APC) available for the staining of other antigens of interest, whilst conserving the ability to positively identify all PB DC subsets, lead to the omission of CD1c when necessary. An additional advantage of the final set-up is the common use of PE and APC as commercially available conjugates for antigen specific antibodies. In fact, a recent paper (36), published after development of the PB flow cytometry panels used in this study, shows an example of how flow cytometry panels can be expanded to include the simultaneous analysis of up to 12 different antigens.

However, as well as allowing the creation of normal ranges specific to the reagents and techniques used here, enabling direct comparison of clinical samples and controls, the development of the panel has facilitated in a number of key observations, discussed below.

3.5.2 Identification of myeloid cells expressing NK cell markers.

CD7 is an antigen present on NK and T cells. In the recent paper by Milush et al., (147) it was used to distinguish between $CD56^+$ NK cells and $CD56^+$ 'myeloid cells', This was necessary as activated NK cells can also express DC-associated markers such as HLA-DR, CD4, CD80 and CD86. This group showed that $CD56^+CD7^-$ cells had myeloid characteristics including CD33 and CD13 expression, and the FSC and SSC profile of lymphocytes in flow cytometric analysis. Examining the expression of CD56 cells from a DC perspective revealed that these cells are $CD11c^+$mDC, approximately 15% of which express CD56. In keeping with previous reports of CD56 expression on small numbers of both freshly isolated $CD14^+$monocytes and those in culture (150) (151), CD56 expression was identified on 1.6% of $CD14^+$monocytes. In addition the data show that CD34 and CD123 should also be included in lineage for NK cell analysis which relies on NK expression of CD7 as a proportion of both these cell populations also express CD7.

From a DC analysis perspective, although the addition of CD7 to the lineage cocktail increases the separation of NK cells from the Lin^-DR^+ APC gate, and therefore reduces the likelihood of $CD16^+DR^+$ NK cells falling in the monocyte/DC gate, the loss of $CD7^+$pDC to the Lin^+ area of the plot precludes it's routine use as a lineage marker. Although some mDC express CD56, this expression is relatively dim and so it was still possible to include these cells in the Lin^-DR^+ gate with CD56 in lineage. Compared to other NK cell markers, CD56 in lineage was the least disruptive to monocyte/DC analysis, as the inclusion of CD16 would have largely prevented analysis of $CD16^+DR^+$ cells.

The observation that some NK cells, as well as B cells, share antigens (for example CD11c) in common with DC is of interest. Functionally, DC and B cells are both professional APC. NK cells have been shown to have the ability to present antigen in the context of MHC-Class II (152). Although not without controversy, a mouse cell co-expressing markers associated with DC and NK cells has been designated as an interferon producing killer dendritic cell (IKDC) (153). Whether human DC expressing NK markers might have a similar role is not known. In order to determine whether these cells have a specific physiological role, further phenotypic and functional work is required.

The reports of DC arising from a common lymphoid progenitor suggest that at least some of these cells may share an origin with NK and B cells. This will be discussed further in Chapter 5.

3.5.3 Normal ranges

Normal ranges for PB subsets were developed to allow the comparison of clinical samples with normal controls, with the specific techniques and materials used in this work. Whilst quantifying cells populations, as a proportion of cells analyzed is sufficiently accurate for normal controls, as soon as numbers of specific populations become altered in clinical samples, the comparisons become less valid.

In terms of DC analysis, this is particularly the case if the number of lymphocytes changes, as this affects the denominator. Although it can be

argued that this form of analysis still reflects important quantitative relationships between immune cell types, to negate the problems encountered in relative values, a normal range based on actual cell counts per ml of blood was also derived.

However, when analyzing small populations in PB, it is not practical to work with whole blood as there are so many cells extraneous to the analysis. For this reason the Trucount™ method was used to convert counts in whole blood to counts in PBMC. The assumption, inherent in the use of the Trucount™ method, is that Ficoll treatment results in isolation of PBMC populations in equivalent proportions to whole blood. This allows the absolute count of one cell type in the Trucount™ tube to be used to determine the absolute count of all others cells in PBMC according to their compositional proportions. However, providing patient samples are processed in the same way as control samples, both the relative and absolute normal ranges will be valid for comparison between the two.

3.5.7 The identification of novel DC subsets in skin

The novel finding of $CD141^{high}CD11c^{low}$ cells, comparable to PB $CD141^{high}$mDC, has been described in digested and migrated skin and is of particular interest in relation to peripheral tissue DC homeostasis. Unlike the PB $CD141^{high}$mDC, the skin population includes cells with a spectrum of dual expression of CD1c and CD1a. As $CD1c^{-}CD1a^{-}$ cells are also present within this population, and the staining pattern of both antigens is a spectrum from negative to positive, it is tempting to speculate that these could be blood derived mDC which acquire CD1c and CD1a on entry to the skin compartment. Without longitudinal studies to examine the acquisition or loss of antigen expression, it is impossible to be sure whether $CD141^{high}$ cells are gaining or loosing CD1a and CD1c expression, but the presence of these antigens on the majority of dermal DC makes the latter less likely. Further work is needed to characterise these cells, in particular whether, like their potential PB counterparts, they express CLEC9A and XCR1 and are capable of antigen cross-presentation (68) (66).

What has not been formally excluded in this analysis is whether the cells identified in digested skin preparations could be from PB contamination. However, this is unlikely, at least as a non-physiological process, as other constituents found in PB, such as B cells and pDC, which represent greater proportions of PBMC than mDC, are not found in these skin preps.

3.5.8 Level of CD141 expression on skin DC subsets

Although the $CD141^{high}CD11c^{low}$ cells can be detected in digested dermis and whole skin, the level of CD141 expression on these cells is lower in dermis digested alone, even though CD141 is still expressed up to a similar brightness on the other DC subsets. A possible explanation for this is that there are two competing forces determining CD141 expression in this setup: firstly, the overnight culture at 37^0C allows up-regulation of CD141 on DDC; secondly, there is some collagenase sensitivity of CD141 expression on the $CD11c^{low}$ cells. The presence of the epidermis in the whole skin digest may provide protection against collagenase digestion of the CD141 antigen on the $CD11c^{low}$ cells, either physically or through cell-cell or soluble factor communication.

CD141/BDCA-3 is also known as thrombomodulin. In the clotting cascade, this protein acts as an anti-coagulant through its action as a cofactor in the thrombin induced activation of protein C. However, its role in DC biology is completely unknown. As such, the physiological relevance of this marker on cross presenting DC and the mechanism and consequence of CD141 up-regulation either in cultured skin or older PB cells remains to be determined.

3.6. Further work

3.6.1 PB DC and NK cell biology

The functional relationship between DC and NK cells, particularly those DC expressing NK cell markers, is of interest. Whether these cells express other 'NK cell specific' markers, such as Killer-cell immunoglobulin-like receptors (KIRs), NKp46, NKG2 and NKG2D will be explored. Whether these cells have any specific physiological role, or any similarities with mouse IKDC, such as type 1-IFN or IFNγ production can be investigated.

3.6.2. Characterization of skin DN DC

Work will aim to further characterise the skin DN DC including the $CD141^{high}$ and $CD11c^{+}$ cells. As this DN population potentially houses the blood-derived DDC 'precursors', phenotypical and functional comparisons will be made between these cells and PB DC through the examination of mRNA and antigen expression levels, including TLRs, CLEC9A, XCR1 and GFRs. In addition, their anatomical positioning within the dermis, their ability to enter the cell cycle and to cross present antigen will be explored.

Chapter 4. DC ontogeny and Homeostasis in Health

4.1 Introduction

There are three distinct but overlapping potential compartments of steady-state DC development. These have not been clearly mapped *in vivo* in humans.

1. The bone marrow haematopoietic progenitor compartment
2. Circulating 'pre-tissue DC' progenitors
3. Progenitors which replenish DC from within tissues

4.1.1 DC Precursors in BM

As discussed in Chapter 1, there has been some progress in mapping steps in murine DC haematopoiesis, but fewer successful attempts to dissect the human $CD34^+$ DC progenitor compartment.

The study of haematopoietic progenitors is a massive field, which is approached from every angle of biology, including work ranging from inflammatory disease and malignancy to aging and regenerative medicine. Even studies specific to DC ontogeny show some conflicting or at least incompatible results, due in part to lack of common nomenclature, varying *in vitro* and *in vivo* techniques and different cellular endpoints. Most recently, the description of a myeloid/lymphoid split later in haematopoiesis than originally thought has allowed a paradigm shift of understanding of potential routes of DC development (100) (104). The identification of TF important in DC differentiation in mice has fueled an expansion in the understanding of signaling pathways necessary for DC development and expanded the options for identifying DC precursors (33).

As studies in human DC ontogeny are not as far advanced, it was necessary to find a starting point from which to develop the analysis of human $CD34^+$ DC progenitors in health and disease. The recent study by Doulatov et al., (89) provided a manageable protocol, applicable to small clinical samples, and had the advantage of an accompanying *in vitro* functional analysis of each $CD34^+$ progenitor subset, establishing which subsets had monocyte/DC potential. This study identified in human cord blood and adult bone marrow of two $CD34^+$ populations able to give rise to DC; the MLP (multilymphoid progenitor) and the

GMP (Granulocyte monocyte progenitor). Whether these cells play a role in human DC homeostasis *in vivo*, and in what relationship to each other, is unexplored.

4.1.2 Circulating pre-tissue DC progenitors

Whilst it is assumed that tissue DC rely on blood-borne precursors to maintain their numbers, the identity of these precursors is unclear. The monocyte has previously been considered the most likely candidate in part due to its ability to differentiate into DC-like cells *in vitro* (43). However, it is becoming more generally accepted that its role as a DC-precursor *in vivo* may relate only to inflammatory environments, possibly under the control of GM-CSF (112).

Identifying the steady-state circulating DC precursor is therefore critical. Exactly which PB cells have the potential to become tissue DC, and under what conditions, remains undetermined. Either or both mDC subsets ($CD141^{high}$ or $CD1c^{+}$) could reasonably be proposed as tissue DC precursors. Data from the previous chapter showed the presence of phenotypically similar cells in human skin. mDC have the ability to migrate across endothelium *in vitro*, without any chemotactic stimuli (154) and they express CLA (cutaneous lymphocyte antigen), a molecule responsible for T cell homing to skin via interaction with ELAM-1 on endothelial cells (155). In comparison, pDC, although they express CLA, require chemokine stimulation for migration across endothelium and have not been identified in non-lymphoid healthy peripheral tissues.

$CD34^{+}$ progenitors circulate in human PB in steady-state. They are $HLA\text{-}DR^{+}$ and known to have DC differentiation potential from *in vitro* culture systems. It has also been noted that a subset of these cells express CLA (156). Whether this population contains cells with the capacity to replenish tissue DC *in vivo* is unknown. However, the observation in mice that $CD34^{+}$ cells circulate from BM via blood to extramedullary tissues, where they are able to proliferate within tissues and differentiate into myeloid cells, including DC (108), suggests that the DC potential of circulating human $CD34^{+}$ progenitors is worth examining.

The phenotyping of these cells in a comparative fashion to BM $CD34^+$ progenitors, in un-stimulated, steady-state PB, has not been undertaken but would go some way to assessing their potential as pre-tissue DC.

4.1.3 Growth factor (GF) receptor expression

One simple way to determine lineage relationships between cells may relate to their growth factor receptor expression profile. The observation of the differential dependence of DC and monocytes on Flt3 and M-CSF signaling respectively, suggests that the expression of receptors for these cytokines may be helpful in determining relationships between DC and monocyte subsets in different tissues. Direct comparison of GF receptor expression on PB and skin APC has not been made.

4.1.4 Local self-renewal of DC populations

Another potential mechanism for the maintenance of tissue DC is the local proliferation of DC or their immediate precursors. This may either reduce the dependence on, or requirement for, blood-borne precursors for tissue DC homeostasis, or render the population independent of the bone marrow entirely, at least in the steady-state. Murine LC have been shown to be maintained in steady-state through self-renewal and independently of the BM. Evidence shows that a proportion of tissue DC populations are also in cell cycle (reviewed in (157)).

Whether human tissue DC or potential pre-tissue DC are in cell cycle, or have the potential to enter cell cycle, has not been examined systematically in skin or PB.

4.2 Materials and Methods for Chapter 4

4.2.1 Antibodies use in the Flow cytometric analysis of $CD34^+$ progenitors

Table 4.1 shows the fluorochrome panel used for the flow cytometric analysis of $CD34^+$ progenitors. It was necessary to have the flexibility to add a dead cell dye as previously frozen clinical samples were analyzed. Cells were stained at

a concentration of 1-2 x 10^6 cells in 50μl of flow buffer. Antibody volumes used in this staining volume were as follows: CD45RA, 1μl; CD34, HLA-DR, CD38, Lineage, 5μl; CD90, CD10, 10μl; CD135, 15μl.

Table 4.1

	APC-Cy7 638/780	PERCP-Cy5.5 488/710	V500 407/525	V450 407/450	Q605 488/610	PE-Cy7 488/780	APC 638/670	FITC 488/520	PE 532/585
Standard	CD34	CD90	Dead Cell	DR/CD45	CD45RA	CD38	CD10	Lineage	CD115
New Antigen	CD34	CD90	Dead/DR	DR/CD11c	CD45RA	CD38	CD10	Lineage	New antigen

The major technical concern encountered was the difficulty of compensation between CD14 Q605 (488/610) and the PE channel (532/585), despite the use of the blue and green laser respectively, as the Qdot is excited by all lasers. This meant it was critical to include FMO isotype in the PE channel for any new PE-conjugated antigen to detect and confirm, in particular, small shifts in fluorescence intensity.

4.2.2 Cell cycle analysis by Ki-67 and DNA content staining

PBMC or skin cells from digested skin in a single cell suspension were surface stained as previously described. After staining, cells were washed in flow buffer, pelleted and mixed with 200μl of BD Cytofix/Cytoperm solution. This was left for 20mins at RT in the dark before washing in diluted 10x BD permwash buffer, and resuspending the pellet in BD Cytoperm Plus buffer, 200μl, for 10mins on ice, washing in permwash, resuspending again in BD Cytofix/Cytoperm solution for 5mins at RT in the dark and a further permwash. Pelleted cells were resuspended in 50μl of permwash, blocked for 10mins with normal mouse serum, and stained with Ki-67 or isotype control at 4^0C in the dark. Cells were washed again in permwash and then resuspended in flow buffer containing 1:4 DAPI (Partec), prior to analysis on flow cytometer. Other methods, such as ethanol fixation and Caltag reagents (www.caltagmedsystems.co.uk), were tried for intracellular staining, but the BD reagents were found to give the best preservation of surface staining and autofluorescence in macrophages. **Figure 4.1** shows a diagrammatic representation of the stages of the cell cycle (A) from Thermo Scientific; SJ Hong and how this relates to the phase of cell cycle as described by Ki-67 staining and DNA content analysis, Panel B.

Figure 4.1

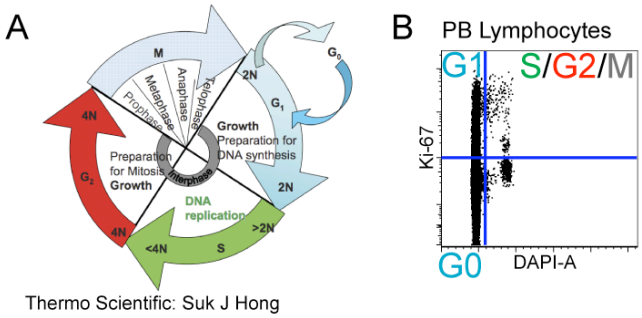

Thermo Scientific: Suk J Hong

Figure 4.1 Flow cytometric cell cycle analysis by Ki-67 and DNA content (DAPI) staining

A: Diagramatic representation of the stages in cell cycle. B: Stages of cell cycle as described by Ki-67 and DAPI staining. Ki-67$^-$ single DNA gate contains cells in G0. Ki-67$^+$ single DNA gate contains cells in G1 and Ki-67$^+$ double DNA gate shows cells which have replicated DNA and are in S, G2 or M phases.

4.2.3 Ki-67 staining of epidermal sheets

Fixed epidermal sheets were stained with anti-Ki-67 (rabbit monoclonal SP6; Vector Laboratories) at 1:200 in 100μl DPBS+0.1% Triton, overnight at 4^0C. This was then washed in DPBS+0.1% Triton in a 6 well plate for 40mins. Alexa fluor 555 conjugated goat-anti-rabbit IgG (H+L) (Invitrogen) was added at a concentration of 1:500 with anti-CD1a FITC (NA1/34; Dako) at 1:10 in 100μl of DPBS. A further 40min wash in DPBS was performed before mounting the sheet in a drop of VectaShield (Vector Laboratories) containing DAPI, with dermis side of the epidermis facing upwards and covering with a coverslip.

4.2.4 Amine dead dye

Where the V450 channel was used for antigen analysis, in place of DAPI, Invitrogen LIVE/DEAD® fixable dead cell stain was used (www.invitrogen.com), aqua yellow in the V525 channel. As this stains cellular amines, with greater uptake in dead cells where permeation of the compromised cell membrane allows intracellular staining, it cannot be used in the presence of any protein or antibodies. Cells therefore have to be stained with amine dye, in plain DPBS, prior to fluorescent antibody staining of surface (or intracellular) antigens. After cell isolation and washing, cells were resuspended at a concentration of $1x10^6$

cells in 1ml DPBS and 1μl of amine dye added. This was incubated in the dark at 4^0C for 30mins before washing in DPBS. Cells were then resuspended in flow buffer (containing 2% FCS) and surface or intracellular staining performed as previously described.

4.3 Results I: Stem Cell compartment/CD34$^+$ Progenitors

A basic understanding of the haematopoietic stem cell compartment is a critical step in tracing DC ontogeny. It was necessary to be able to identify cells within the CD34$^+$ compartment thought to have DC potential as previously defined, and the method published by Doulatov et al., (89) was adopted for this purpose. This then allowed comparison of CD34$^+$ subsets in BM and PB to identify the DC-potential contained in the circulating population, and later with populations in human disease.

4.3.1 Identification of CD34$^+$ progenitor subsets in Bone Marrow, resting Peripheral Blood and G-CSF mobilised peripheral blood.

The first tissue analyzed was BM. The gating strategy for identification of CD34$^+$ subsets is shown in **Figure 4.2, BM**. A CD45$^+$ gate was used to exclude material such as debris, red cells and platelets. The CD34$^+$ cells were then selected (Gate 1). Gate 2 defined CD38$^+$ cells and was arbitrarily but consistently set to include 25% of CD34$^+$ cells. This was found to include the majority of relevant cells and gave the most consistent results across normal controls (n=6). Gate 3 defined CD38$^-$ cells and again was arbitrarily but consistently set to include 17% of CD34$^+$ cells. From the CD38$^+$ cells B/NK progenitors were classified as CD10$^+$. The CD10$^-$ cells (Gate 4) could be further subdivided into CD45RA$^-$Flt3$^-$ Megakaryocyte erythroid progenitors (MEP), CD45RA$^-$Flt3$^+$ common myeloid progenitor (CMP) and CD45RA$^+$Flt3$^+$ granulocyte monocyte progenitor (GMP). From the more primitive CD38$^-$ cells, Haematopoietic stem cells (HSC) were gated as CD45RA$^-$CD90(Thy-1)$^+$, Multi-potential progenitor (MPP) as CD45RA$^-$CD90$^-$ and multi-lymphoid progenitor (MLP) as CD45RA$^+$CD90$^{-/low}$. All populations were HLA-DR$^+$ (not shown) in keeping with the finding of CD34$^+$ cells in the Lin$^-$DR$^+$ gate during DC analysis.

The second panel in **Figure 4.2** shows the analysis of G-CSF mobilised PBSC and third shows circulating CD34$^+$ progenitors from peripheral blood.

Figure 4.2

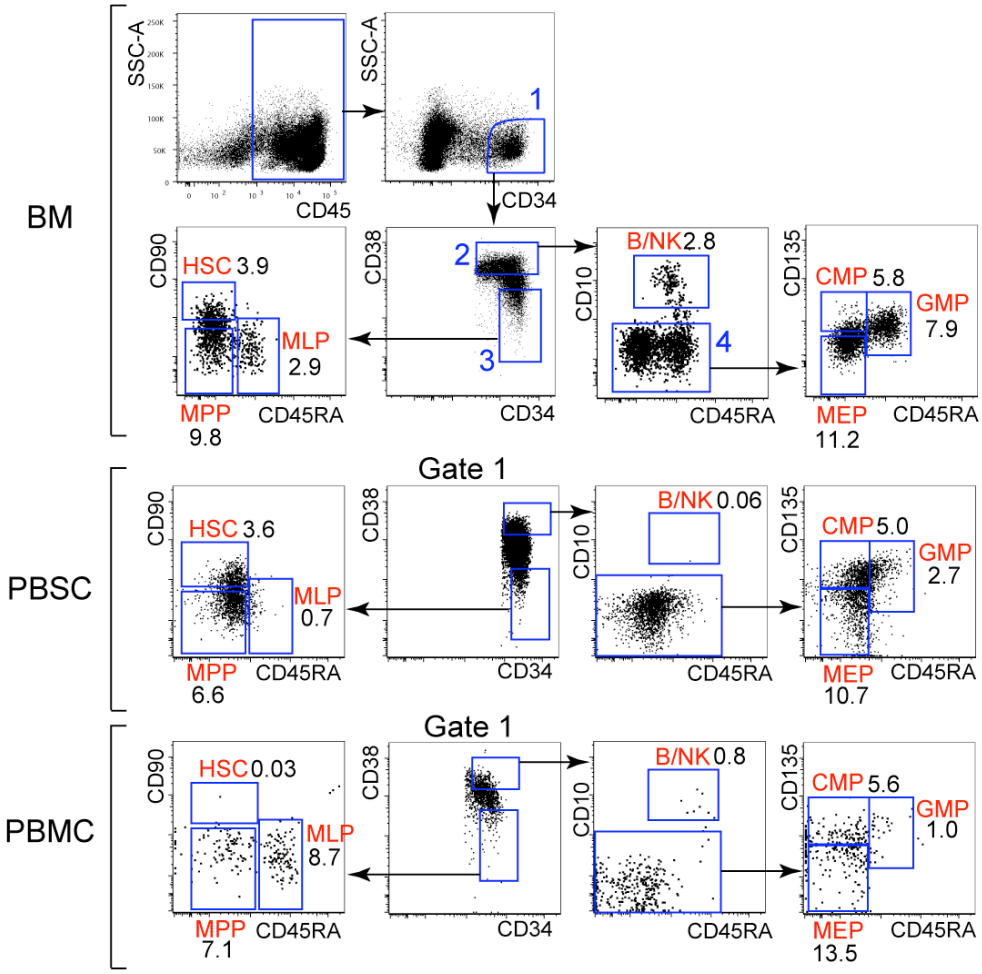

Figure 4.2 Subset analysis of BM, PBSC and PBMC CD34$^+$ progenitors
Black numbers represent number of cells in each subset as % of total CD34$^+$ cells in sample (Gate 1). HSC, Haematopoietic stem cells; MPP, Multipotent progenitors; MLP, multilymphoid progenitors; CMP, common myeloid progenitors; MEP, megakaryocyte erythroid progenitors; GMP, granulocyte monocyte progenitors.

4.3.2 The proportion of CD34 subsets in BM, PBMC and PBSC

In order to determine whether there was any skew in the composition of CD34$^+$ progenitors in G-CSF-mobilised PBSC (n=1) and resting PBMC (n=2) compared to BM (n=6), the proportion of cells in each tissue was analyzed. Specific to DC homeostasis was the question of whether circulating GMP or MLP could be found in resting PB.

The first clear difference was in the proportion of HSC, which represented 3.5-4% of $CD34^+$ cells in BM and PBSC, while virtually no HSC were found in resting PBMC from healthy volunteers (**Figure 4.3**). B/NK were found predominantly in BM (2.8%) compared to 0.06% in PBSC and 0.8% in PBMC. All other subsets were represented in all three conditions. Of note, MLP were relatively enriched in PBMC (8.7% versus 2.9% in BM and 0.7% in PBSC) while GMP constituted a relatively smaller population (1% in PBMC versus 7.9% in BM and 2.7% in PBSC).

Figure 4.3

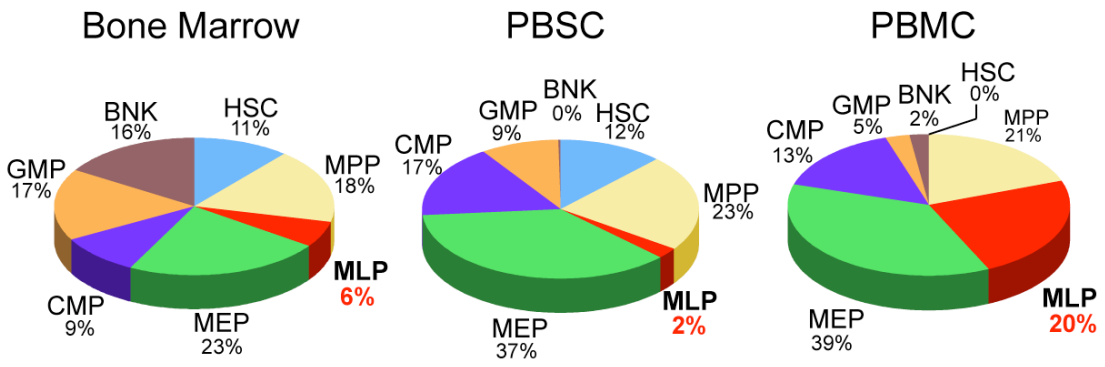

Figure 4.3 Comparison of proportions of $CD34^+$ subsets in BM, PBSC and PBMC
BM, n=6; PBSC, n=1; PBMC, n=2. Numbers represent number of cells in each CD34+ subset as % of cells included CD34+CD38+ and CD34+CD38- gates (Figure 4.2, gates 2+3)

4.3.3 $CD34^+$ progenitors are found in skin

In light of the observation in mouse that haematopoietic progenitors are found in peripheral tissues, and the current finding that MLP and GMP, thought to house DC potential, were found circulating in resting human blood, human skin was examined for the presence of $CD34^+$ cells. These were sought in the $CD45^+HLA\text{-}DR^+$ APC compartment of skin as CD34 is known to be abundant on skin CD45- cells, such as endothelial cells. These were found (compared to isotype control for anti-CD34 antibody) in digested dermis (n=4) and digested whole skin (n=1, not shown). Many of these $CD34^+$ cells were found in the $CD14^-CD1a^-$ DC gate, but $CD34^+$ cells were also identified in all other DC gates

(**Figure 4.4, A**), including $CD14^+CD1a^-$ ($CD14^+$DC) and $CD14^-CD1a^+$ (DDC) (**A**, Gate 1). In addition, $CD34^+$ cells were found in the AF^+ gate (**A**, Gate 2) and expressed CD14 but not CD1a, similarly to macrophages. Like their $CD34^-$ counterparts, $CD34^+$ cells in the AF^- gate had lower SSC than those in AF^+ gate. There was no CD34 expression in $CD45^+$ $HLA\text{-}DR^+$ cells migrated from skin (**B**, Gate 3). The findings in digested skin are comparable with PB where the majority of $CD34^+$ cells are $CD45^+HLA\text{-}DR^+$ but negative for all lineage and DC markers. However, as seen in 3.3.1, some Lin^+ $CD34^+$ cells are always found.

Unsurprisingly, $CD34^+$ cells were abundant in the $CD45^-$ population of skin as this antigen is known to be present on endothelial cells, and cells around adnexal structures, such as hair follicles and sweat ducts. They showed low expression of HLA-DR, and no expression CD1a or CD14 (**C**).

Figure 4.4

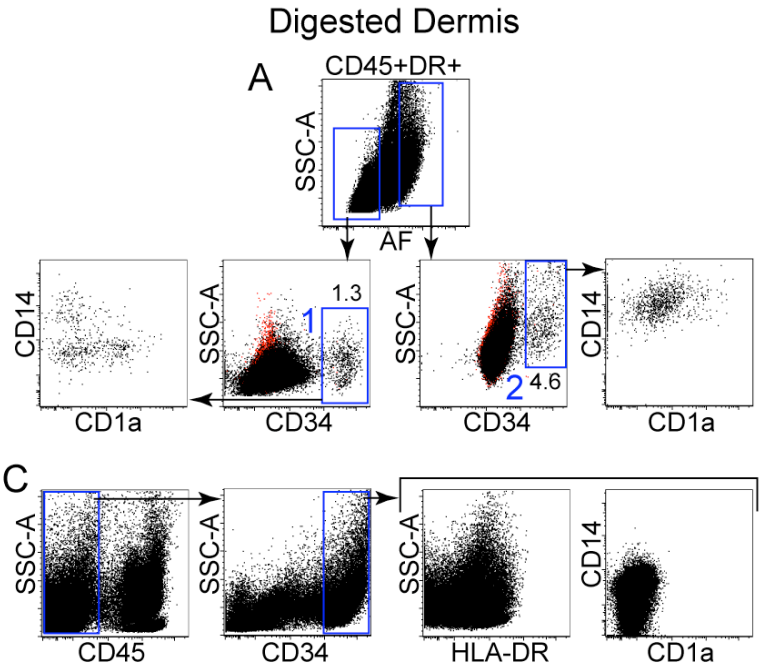

Figure 4.4 Flow cytometric analysis of CD34 expression in skin
A: CD14 and CD1a expression on $CD34^+$ cells from digested dermis (n=4) gated as AF^- (Gate 1) and AF^+ (Gate 2). Isotype shown in underlying red dots. B: CD34 expression in migrated whole skin IGate 3) (n=1). Isotype in red. Numbers represent % of cells within gate. C: CD14, CD1a and HLA-DR expression on $CD34^+$ cells in the $CD45^-$ compartment of digested dermis.

4.4 Results II: DC Ontogeny and homeostasis in Health

Attributes expected of pre-tissue DC were sought on potential DC precursors and tissue DC subsets. These included growth factor receptor expression profiles and analysis of DC populations in cell cycle.

4.4.1 Growth factor receptor expression on CD34$^+$ Progenitors

The expression of CD135/Flt3, CD115/M-CSF-R and CD117/SCF-R was examined on the CD34$^+$ compartment of BM and PBMC (**Figure 4.5**). All BM and PBMC CD34$^+$ subsets expressed CD117 with the exception of B/NK. CD115 expression was negative on BM and PBMC CD34$^+$. FLt3 was seen at a low level on total CD34+ cells.

Figure 4.5

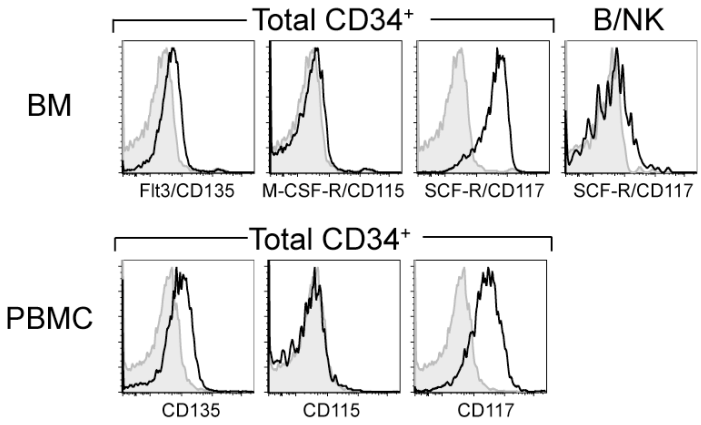

Figure 4.5 Growth factor expression on CD34$^+$ progenitors from BM and PB
BM, n=3; PBMC, n=2
Antigen staining, black histograms; Isotype controls, grey histograms

4.4.2 Growth Factor receptor expression on PB and skin DC

The observation in mice that DC differentiation is dependent on Flt3L signaling, while signaling through the M-CSF-R drives differentiation towards a monocytic phenotype, suggests that the expression of these receptors may go some way to defining the lineage potential or lineage derivation of cells in DC ontogeny. The expression of Flt3 and M-CSFR was therefore examined on human PB monocytes and PB and skin DC (**Figure 4.6**). Flt3 expression was seen on both myeloid and plasmacytoid PB DC, and on dermal CD1a$^+$DC, DN (CD1a$^-$CD14$^-$

)DC and epidermal LC from digested and migrated whole skin, but was not seen on any $CD14^+$ cells. In direct contrast, M-CSF-R was expressed on PB $CD14^+$monocytes and dermal $CD14^+$DC but none of the other DC populations. Dermal macrophages also expressed a low level of M-CSF-R compared to isotype control.

Figure 4.6

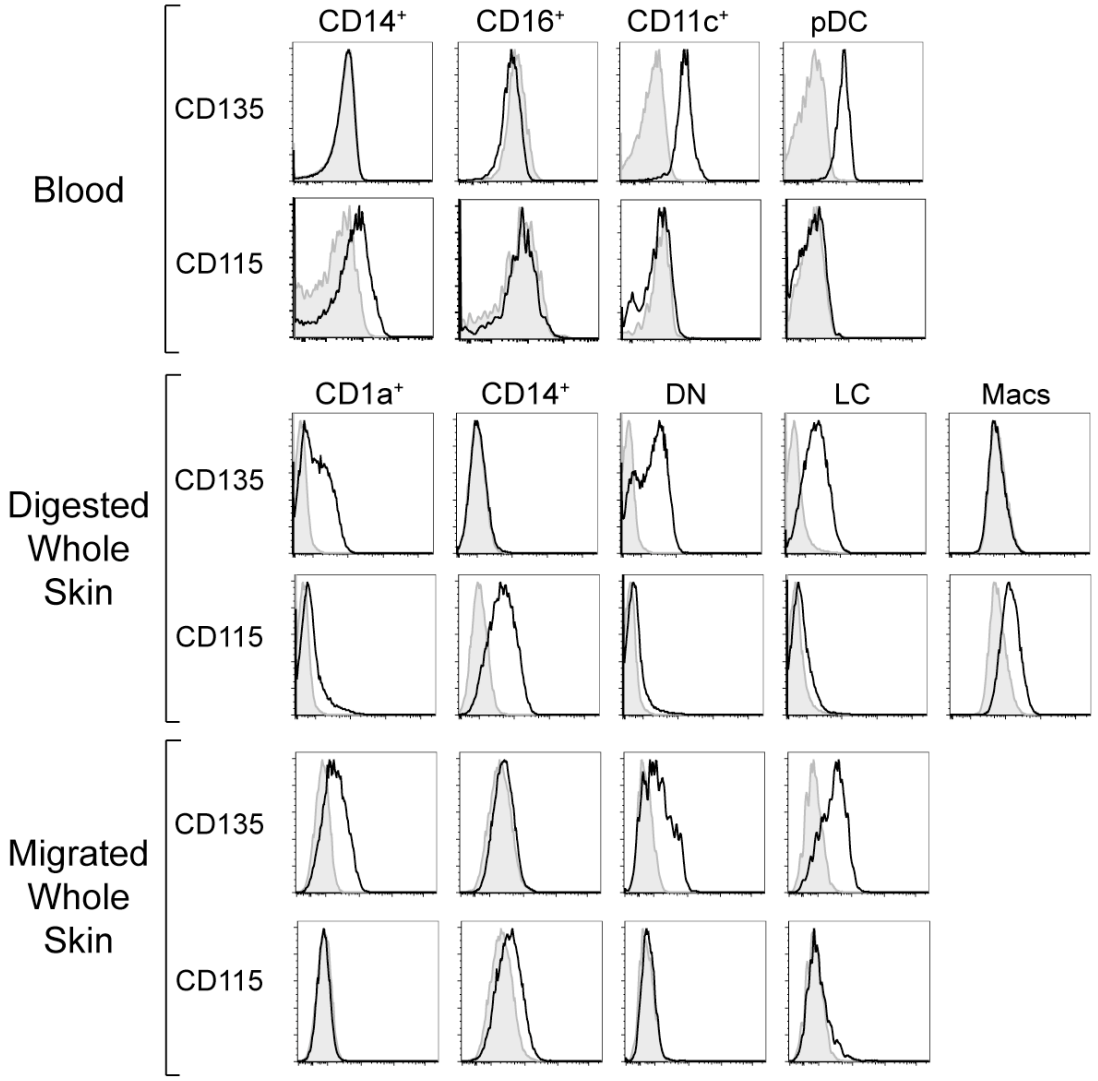

Figure 4.6 Growth factor expression on PB and Skin DC
Antigen staining, black histograms; Isotype controls, grey histograms.
Blood: $CD14^+$ and $CD16^+$ Monocytes, $CD11c^+$mDC and pDC (n=2). Digested Whole Skin (n=2) and Migrated Whole Skin (n=1) $CD1a^+$DDC, $CD14^+$DC, $CD1a^-CD14^-$ (DN) DC, LC, Macrophagess. No macrophages were present in the migrated cell population.

4.4.3 Cell Cycle in PB

To determine whether any populations of PB DC showed evidence of active cell cycling, a feature that might be expected in cells capable of supporting tissue DC populations, flow cytometric analysis of Ki-67 and DAPI staining in PB monocytes and DC subsets was undertaken (**Figure 4.7**). PBMC were sourced from whole-blood leukoreduction chambers, or 'cones'. There was no Ki-67 positivity in either monocyte subset. However, myeloid DC, $CD34^+$ progenitors and pDC showed Ki-67 expression compared to isotype control; 21%, 30% and 2.2% respectively, in keeping with their having proliferative potential. In all three populations, the $Ki\text{-}67^+$ cells were diploid by DAPI staining, with no evidence of DNA replication at the time of analysis. By contrast, T cells from the same cone (gated on $Lin^{bright}DR^-$ cells) showed 0.62% $Ki\text{-}67^+$ but with 3.3% of these cells in S/G2/M phases by DAPI staining.

Figure 4.7

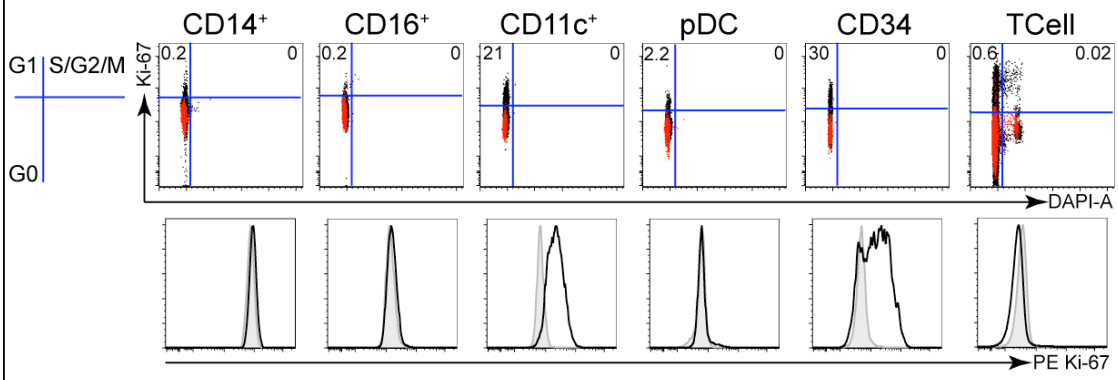

Figure 4.7 Cell cycle analysis in PB Monocytes, DC, $CD34^+$ progenitors and T cells

Flow cytometric cell cycle analysis by Ki-67 antigen and DAPI DNA staining Ki-67 antigen, black dots and histograms; Ki-67 Isotype control, red dots and grey histograms (n=2). Blue gates delineate: horizontal, $Ki\text{-}67^{+/-}$ cells; vertical, DAPI staining of 2N/>2N nuclei. Top left hand diagramme depicts cell cycle stage by Ki-67 and DAPI staining. T cells were taken as $Lin^{bright}DR^-$ cells.

4.4.4 Cell Cycle in Skin APC

Similarly, skin DC and macrophage populations were examined for evidence of active cell cycling by flow cytometry, with Ki-67 and DAPI staining (**Figure 4.8, A**). From the dermis there were virtually no $Ki\text{-}67^+$ cells in the $CD14^+$DC or macrophage populations (mean of n=7: 0.25% and 0.05% respectively) and

very few in the migrating LC population from the dermis (mean of n=5: 0.4%) (**B**). $CD1a^{-}CD14^{-}$ (DN) DC showed up to 6% $Ki\text{-}67^{+}$ (mean of n=5: 2.5%) and $CD1a^{+}$ DDC had a mean Ki-67 positivity of 0.9% (n=7). LC from digested epidermis contained the highest proportion of $Ki\text{-}67^{+}$ cells with a mean of 6.2% (n=6). Unlike PB, over half $Ki\text{-}67^{+}$ cells in skin showed evidence of active DNA replication by DAPI staining, suggesting their position in S, G2 or M phases of the cell cycle.

To verify the proportion of epidermal LC in cell cycle, nuclear Ki-67 expression was assessed by fluorescence microscopy of fixed epidermal sheets (**C**). A minimum of 100 nuclei from $HLA\text{-}DR^{+}$ LC (green) were assessed for Ki-67 positivity (Dual Red-Ki-67 and Blue-DAPI) in each sample. The mean percentage $Ki\text{-}67^{+}$ LC from epidermal sheets was 5.5% (n=3: range 4-7%) (**D**).

Figure 4.8

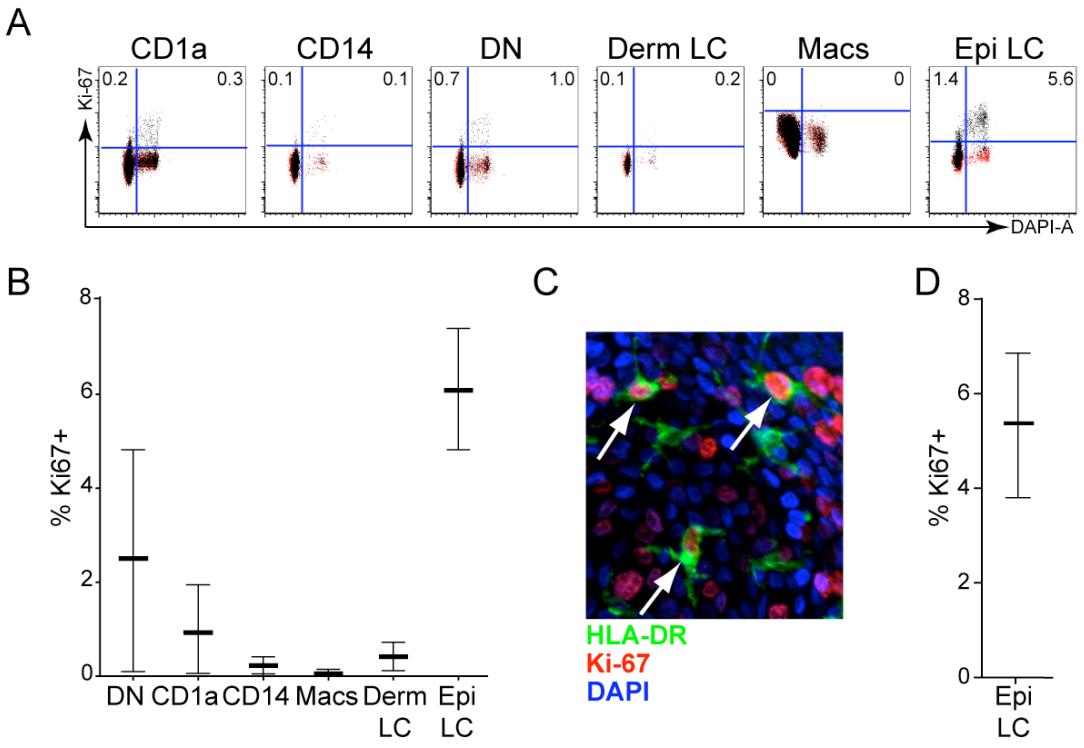

Figure 4.8 Cell cycle analysis in skin DC
A: Flow cytometric analysis of cell cycle by Ki-67 antgen and DAPI DNA staining Ki-67 antigen, black dots; Ki-67 Isotype control, red dots. B: Summary of cells in G1/S/G2/M by Ki-67 positivity: CD1a+DDC, CD14+DC and Macs n=7. DN DC and migrating LC n=5. Epidermal LC, n=6. C: Fluorescence microscopy showing Ki-67 positivity in the nuclei of LC in a fixed epidermal sheet. HLA-DR, green; Ki-67, red; DAPI, blue. D: Summary of Ki-67 positivity in LC by fluorescence microscopy of epidermal sheets n=3.

4.5 Discussion

To further explore the pre-tissue DC potential of circulating CD34+ progenitors and PB DC, their growth factor receptor expression profile and proliferative capacity have been examined and compared to tissue DC. PB was also analyzed for the presence of circulating $CD34^+$ cells which may carry DC potential, and the presence of $CD34^+$ progenitors in skin was sought.

4.5.1 $CD34^+$ progenitors as immediate tissue DC precursors

$CD34^+$ progenitors from PB are known to differentiate to DC *in vitro* (158), in the presence of GM-CSF and TNFα, over a time course of 12-14 days. However, whether tissue DC maintenance by circulating $CD34^+$ cells occurs *in vivo* is unknown.

With the techniques employed, it was possible to examine sufficient cells from clinical BM or PB samples to undertake $CD34^+$ subset analysis. This allowed the phenotypic identification of the eight subsets described by Doulatov et al., (89). One of the two populations shown *in vitro* to have DC potential, the MLP, was found in relatively enriched proportions in PB. Although no functional studies have yet been performed on this PB $CD34^+$ subset, it is tempting to speculate that the relative enrichment may have physiological relevance, particularly in relation to DC ontogeny and homeostasis. Doulatov demonstrated that MLP from BM and cord blood could readily form DC and monocytes/macrophages in culture and in an *in vivo* mouse model. It is therefore possible that PB cells identified by the same expression profile may behave similarly *in vivo*. As $CD45^+$HLA-DR^+CD34^+ cells (similar to the total $CD45^+$HLA-DR^+CD34^+ population found in PB) have now been identified in skin, it is plausible that these cells may enter tissue directly. In addition, cytokines known to stimulate DC differentiation of CD34+ progenitors *in vitro*, including GM-CSF and TNFα, are produced by cells in skin, such as keratinocytes (159) (160). Further work is required to ascertain whether the DC-antigen negative $CD34^+$ cells in tissue can be assigned to any recognised $CD34^+$ subset and whether these cells isolated from PB have DC potential.

Of additional interest, $CD34^+$ cells were found in every dermal APC gate. This mirrors *in vitro* culture results where $CD34^+$ cells differentiate to $CD1a^+$ and/or $CD14^+$ DC with GM-CSF and TNFα (161), and to macrophages with M-CSF (162). It is also note worthy that $CD34^+$ cells are not found in cells migrated from skin. This is possibly due to the transient expression of CD34 on these cells once DC-related antigens are expressed, with the 60hr migration providing sufficient time for down-regulation CD34. Alternatively, $CD34^+$ progenitors may be unable to migrate out of skin. However, the findings in mouse that haematopoietic progenitors can be found in lymphatics draining peripheral tissues suggests that these cells can maintain migratory capacity (108).

The hypothesis that PB MLP may be able to support tissue DC maintenance would not negate the potential for GMP to play a role in DC homeostasis, as described by the model illustrating two routes to a DC/monocyte progenitor (MDP), via GMP or MLP (89). This could either occur again through the entry of GMP directly to tissue or, particularly given the reduced proportions of GMP found in normal PB, by differentiation to 'pre-tissue DC', hypothetically PB mDC, possibly in bone marrow, prior to entry into blood or tissues. Alternatively, one or other subset (GMP or MLP) may have a more prominent role in monocyte ontogeny in steady-state or inflammatory conditions.

4.5.2 GF receptor expression highlights potential lineage relationships between PB and tissue APC.

The bright expression of Flt3 by PB mDC and pDC is in keeping with their Flt3L dependence as described in mice and humans (163). This is in contrast to the relatively dim expression of this receptor on all $CD34^+$ progenitor subsets, possibly revealing a quantitative or qualitative difference in signaling requirements for FL acting as a haematopoietic factor and as a 'DC-poietin'. It is recognised that Flt3 expression is negatively regulated by Flt3L exposure, possibly through a mechanism involving receptor internalization or ligand blockade of antibody binding (164). However, this is unlikely to account for the different levels of Flt3 expression seen in PB $CD34^+$ cells and DC as both

populations, at least in PB, are exposed to the same serum concentration of Flt3L.

As Flt3 expression is thought to be essential for differentiation to DC (124), the expression of this receptor on PB DC, skin $CD1a^+$DDC, $CD11c^+$DN cells and epidermal LC suggests these populations are derived from a DC lineage. PB $CD14^+$monocytes, dermal $CD14^+$DC and macrophages do not express Flt3 but are positive for CD115/M-CSF-R, possibly indicating a shared origin or developmental pathway for these three populations. The expression of Flt3 on $CD34^+$ progenitors may reflect their stem cell phenotype but may also indicate the potential for DC differentiation.

The observation that GF receptor expression is maintained in migrated cells leads to the possibility that these receptors also play a role in cell maintenance or survival. It shows that expression of GF receptors is not a transient phenomenon suggesting their role may not be purely to direct differentiation pathways at a single point in the cell's fate.

4.5.3 Cell cycle

It has been shown in mice that LC maintain their numbers in steady-state through self-renewal. It is therefore possible that other DC populations may have similar capabilities. Although peripheral tissue DC are thought to be continuously recruited from blood borne precursors, it has been shown in mice that up to 20% of non-lymphoid (non-LC) tissue DC are dividing in the steady-state (157). Analysis of cell cycle in human skin was therefore undertaken, and studies expanded to include PB DC.

Before considering the physiological relevance of the results it is necessary to consider the potential pitfalls of Ki-67 analysis. Despite its now routine use in the assessment of the proliferative index of tumours, the exact physiological function of the Ki-67 protein remains unclear. One critical consideration when using Ki-67 to assess cellular participation in the cell cycle, is the kinetics of expression. Study of a normal human fetus cell line showed that Ki-67 is expressed in cells from G1, through S, G2 and M phases (165). After arrest of

cell cycle in G1, induced by serum deprivation, Ki-67 remained positive for approximately 24hrs. It has been reported to disappear approximately 1hr after mitosis in the promyelocytic leukaemic cell line studied (HL-60) (166). The exact kinetics of Ki-67 expression in normal adult tissue DC *in vivo* is not known, but when Ki-67 expression is accompanied by an increase in DNA content of cells by DAPI staining, it is highly suggestive of active cell cycling. Where DNA replication is not seen, Ki-67 positivity may indicate the potential for cell division and is likely to indicate cells in G1 phase of the cell cycle as only cells in G0 are Ki-67 negative (167). The relevance of this to DC analysis is discussed below.

Perhaps unsurprisingly, given the findings in mice, the peripheral tissue DC population containing the highest proportion of Ki-67$^+$ dividing cells was the LC. This was shown both by flow cytometric analysis and fluorescence microscopy. However, a proportion of DN DC (mean 2.5%) and a smaller proportion of CD1a$^+$DC (mean 0.9%) were also in cell cycle. There was no Ki-67 positivity in CD14$^+$DC or macrophages. In PB a large proportion of mDC (21%) and CD34$^+$ progenitors (30%) were Ki-67$^+$, together with a small proportion of pDC (2.2%). There was no evidence of cell cycling in monocytes.

It is perhaps striking that the populations which show evidence of proliferative potential are those that are Flt3$^+$, in contrast to the CD14$^+$ APC which neither express Flt3 nor show signs of Ki-67 positivity. It has been shown *in vitro* that Flt3L induces CD34$^+$ cell proliferation (168) and Flt3L administration *in vivo* results in expansion of Flt3$^+$ progenitors as well as DC (119). Although the increase in DC numbers during Flt3L administration may be due in part to progenitor expansion and subsequent DC differentiation, lymphoid tissue DC expansion has been shown to occur through Flt3L induced cell cycling of DC themselves, (28). It is therefore possible that the expression of Flt3 on PB and skin DC may not only have directed their differentiation to DC but may also facilitate the entry of these cells into cell cycle, and contribute to their potential ability to self-renew.

Another point of interest is that, aside from the LC, the skin DC population with the highest proportion of proliferating cells, up to 6%, was the CD1a$^-$CD14$^-$ compartment. This, by phenotypic analysis, is where CD14$^-$ (non-monocyte)

tissue DC progenitors from PB may be found as there is no CD1a expression in PB. In keeping with this, it is where the majority of $CD141^{high}$ and $CD1c^{+}CD11c^{+}$ cells, with equivalent phenotypes to PB mDC, were found (chapter 3). The DN population also contains the $CD34^{+}$ cells which do not express DC-related antigens. Further dissection of this compartment is required to identify exactly which populations house the ki-67 positivity and so the proliferation potential.

One puzzle is why PB mDC and $CD34^{+}$ cells, despite a significant proportion being positive for Ki-67, show no evidence of DNA replication *ex vivo*. There are several possible explanations. Firstly, they may be poised in G1, awaiting a signal to enter the DNA replication stages of cell cycle, on entry to tissues. A less attractive alternative is that they have recently divided and temporarily remain $Ki\text{-}67^{+}$. Finally, it is possible that the lack of DNA replication, and potential arrest in G1 phase, is an *ex vivo* artifact related to the processing of cells in leukoreduction chamber. Cells are stored in a massively concentrated suspension and may well result in conditions able to cause cell cycle arrest (165). It is less likely that Ki-67 expression is an *ex vivo* artifact as no conditions, apart from the entry of cells into cell cycle, are known to induce its expression. Analysis of freshly isolated PBMC is necessary to rule out *ex vivo* processing as a cause arrest of these cells in G1.

4.5.4 Towards a unified hypothesis of DC homeostasis

The reliance on either replenishment by blood borne precursors or local self-renewal for tissue DC homeostasis may not be mutually exclusive, even in steady-state. It is conceivable that relative dependence on either mechanism could be specific to particular tissues or even particular DC populations. Along similar lines, it is conceivable that more than one blood-borne precursor population is involved in tissue DC homeostasis, either in a redundant or parallel fashion.

The environmental circumstances may also influence the mechanism required for maintenance of DC numbers. For example, during inflammation the kinetics of DC activation and migration due to increased antigen exposure may necessitate a greater reliance on immediately available blood borne precursors,

possibly also drawing on 'inflammation-specific' populations, conceivably the monocyte. This has been shown in the case of LC which are able to self-renew in steady-state in mice, show increased proliferation in some inflammatory situations, such as atopic dermatitis in humans (169) but are replaced by monocytes in conditions severe enough to cause radical depletion of murine LC (110). Monocyte derived inflammatory tissue DC, or TipDC, are also recognised in mice (111) (113).

4.5.5 Further work

Further work will aim to clarify the tissue DC potential of PB cells in greater detail, including the $CD141^{high}$DC and $CD1c^{+}$DC and $CD34^{+}$ progenitor subsets. More detailed Ki-67 and Growth factor expression analysis will be undertaken. Whether these cells are able to take on a tissue DC phenotype or enter cell cycle *ex vivo* will be examined in culture, using specific cytokines and skin conditioned medium. mRNA expression analysis in $CD34^{+}$ and DC subsets from PB and skin may also suggest relationships between the cell populations.

In vivo, circulating $CD34^{+}$ and PB DC subsets will be monitored following allogeneic SCT, in parallel with DC phenotyping and CD34 expression analysis in patient skin. Determination of the kinetics of chimerism conversion in these populations, with specific focus on potential pre-DC compartments, may shed light on the repopulation of tissue DC compartments following HSCT.

Chapter 5. DC Monocyte and B/NK lymphoid deficiency

5.1 Introduction

Studies of kinetics of tissue DC repopulation following haematopoietic stem cell transplant (HSCT) have shown that human tissue DC are bone marrow derived (73) (109). However, it has not been possible to probe the distal relationships between monocytes and DC, or prove the independence of LC from BM, in human steady-state conditions. To recapitulate mouse models of DC or monocyte depletion, subjects with spontaneous and sustained monocytopenia or DC deficiency are required.

5.1.1 The predicted effects of monocytopenia on DC homeostasis

The identification of cases with isolated monocytopenia would allow the role of these cells in tissue DC homeostasis to be elucidated. Any populations able to maintain their numbers independently of monocytes, for example through self renewal, could be identified and the developmental relationship between monocytes and other potential pre-tissue DC, including PB mDC, could be interrogated. Whether clinical monocytopenia ever occurs independently of PB DC deficiency is entirely unknown as DC are not measured by routine automated blood counters.

5.1.2 Immune regulation by DC

The study of subjects with monocytopenia or DC deficiency would also allow the investigation of their role in immune regulation. The role of DC in controlling tolerance is receiving increasing attention. In particular, a direct homeostatic balance has been found between the frequency of murine DC and Treg. This is linked to changes in concentration of Flt3L (30). Depletion of Tregs increases DC proliferation in a Flt3L-dependent mechanism (27) (28), administration of exogenous FL induces Treg proliferation as a direct result of DC expansion and DC depletion in Flt3L KO mice leads to reduced numbers of Treg, with autoimmune sequelae (29). The proliferation of Treg *in vivo* is dependent on MHC Class II expression on DC (30). The homeostatic balance between DC, Treg and FL has not been tested in humans.

5.1.3 The identification of monocytopenic patients

As PB DC are not measured in routine clinical practice, the most practical way to screen for potential APC deficiency was through the identification of monocytopenic patients. Clinical monocytopenia is found in a number of primary chronic haematological conditions, such as hairy cell leukaemia and aplastic anaemia. The initial thought was to investigate DC homeostasis in these diseases. However, a small group of 5 patients was identified, with a clinically-apparent, isolated monocytopenia. The main presenting features included mycobacterial infections, human papilloma virus (HPV) infection, pulmonary alveolar proteinosis and autoimmunity. Detailed analysis of PB, BM and tissue DC compartments was undertaken in all five subjects. During the course of the work the clinical details of a series of eighteen similar cases were published (170).

The cases in this series were also identified through their susceptibility to non-tuberculous mycobacterial, viral and fungal infections accompanied by profound monocytopenia and reduced B and NK cell numbers. In addition, ten patients developed malignancies, the majority of which were leukaemias, and five developed pulmonary alveolar proteinosis (PAP), a condition characterised by accumulation of proteinaceous material in alveolar spaces resulting in reduced gasseous exchange and respiratory failure. PAP is most commonly associated with reduced numbers or function of alveolar macrophages related to antibodies to or mutations in GM-CSF-R. Within these eighteen cases, five families were identified with 2 affected generations, and a pattern of inheritance in keeping with an autosomal dominant mode of transmission.

5.2 Materials & Methods for Chapter 5

5.2.1 Treg staining

PBMC were alliquoted at $1x10^6$ cells/tube and surface stained as previously described. Cells were then washed in flow buffer and fixed and permeabilised in ebioscience reagents (www.ebioscience.com), as per manufacturer's instructions. Cells were then blocked with rat serum for 10mins prior to

Intracellular FoxP3, or isotype, staining at 4^0C in the dark. Cells were washed with permeabilisation buffer (diluted 1:10) and resuspended in flow buffer prior to flow cytometric analysis.

5.2.3 Bronchoalveolar Lavage (BAL) Fluid

Cells from lung wash out were obtained from subject 4 during a routine clinical procedure. The fluid was centrifuged at 500g for 5 mins and the resulting pellet resuspended in DPBS prior to flow cytometric analysis or cytospin preparation.

5.2.3 BM and Lung CD68 immunohistochemistry

Formalin fixed, paraffin embedded tissue was sectioned and stained with anti-CD68 K (clone KP1) in the NHS pathology laboratories, according to standard protocols. Images were attained using a Zeiss Axioplan 2 microscope EC Plan-neofluar x10 lens and Axiocam running Ziess Axiovision v2.8 software (www.zeiss.com).

5.3 Results I: Clinical presentation

There was a diverse range of presenting symptoms among the five subjects but all presented with clinical problems included in the case series (170). Human papilloma virus (HPV) infection was the most common symptom but not the primary presenting feature in any case.

5.3.1 Clinical Symptoms

Subject 1 presented at the age of 12 with disseminated BCG following routine vaccination. Subject 2 was diagnosed at the age of 27 with spontaneous Mycobacterium *kansasii* infection and HPV infection of hands and feet. Subject 3 developed respiratory failure at age 21 due to PAP and had concurrent perineal HPV infection. Subject 4 presented with recurrent erythema nodosum and HPV infection of hands at age 23. Subject 5 presented at the age of 10 weeks with disseminated BCG following routine vaccination, in addition to oral candidiasis and cachexia. Subjects 1, 2, 4 and 5 had no clinically affected

relatives, while subject 3 reported two generations of ancestors dying of early respiratory death or leukaemia, in keeping with an autosomal dominant pattern of inheritance. **Table 5.1** shows a summary of the clinical details.

Table 5.1

	Subject 1	Subject 2	Subject 3	Subject 4	Subject 5
Age at presentation	12	27	21	23	10 weeks
Age at analysis	15	31	23	33	6 months
Presenting feature	Disseminated BCG following vaccine diagnosed on skin biopsies.	Spontaneous mycobacterium kansasii diagnosed from BM and spleen aspirates.	Pulmonary alveolar proteinosis and respiratory failure.	Recurrent erythema nodosum, human papilloma virus infection	Disseminated BCG following vaccine diagnosed on lymph node biopsie. Myeloproliferation
Skin rash (at time of biopsy or previously)	Yes, at time of biopsy. Macroscopically unaffected skin taken.	No	No	Yes, previously.. Macroscopically unaffected skin taken.	No
Autoimmune symptoms	No	No	No	Un	No
HPV	No	Yes (hands and feet)	Yes (perineum)	Yes (hands)	No
BM histology	Mild hypocellularity for age (taken whilst on anti-tuberculous drug treatment) but normal maturation of megakaryocytic, erythropoietic and myeloid lineages. No dysplastic features.	Normocellular bone marrow with normal trilineage maturation. Ill defined granuloma in which acid fast bacilli were identified. No dysplastic features.	High-normal cellularity (taken during active pulmonary infection) with normal trilineage maturation. No dysplastic features.	Normocellular with normal trilineage maturation.	Hypercellular, even for age. Massive expansion of myeloid compartment. Erythro- and megakaryopoiesis present. No dysplastic features. Ill defined granuloma in first sample.
BM cytogenetics	Normal	Normal	Normal	Normal	Normal
Definitive treatment	Matched unrelated HSCT	-	Matched unrelated HSCT	-	Matched unrelated HSCT
Outcome	Alive and well 2yrs post HSCT	Death from H1N1 virus infection	Alive and well 40 days post HSCT	-	Alive and well 1yr post HSCT
Family History	No	No	Yes. 2 generations of death <40yrs from leukaemia or respiratory illness	No	No

5.3.2 Clinical Investigations

The subjects' full blood counts (FBC) at the time of analysis are shown in **Table 5.2**. Subjects 1, 2 and 4 had no significant anaemia, thrombocytopenia, leukopenia or myeloproliferation but showed a near absolute monocytopenia and variable reduction in lymphocytes. Subject 3 had values in keeping with an active systemic infection as counts were taken during an episode of pulmonary sepsis. Subject 5 initially presented with a marked anaemia (Hb 4.6) and mild thrombocytopenia (plt 66) in addition to myeloproliferation with WBCs 125. However, this was in the setting of severe illness requiring intensive care support. Blood count at the time of PB and tissue DC analysis still showed

evidence of anaemia, mild thrombocytopenia and myeloproliferation, but by this time treatment had been received for systemic BCG infection.

Table 5.2

	Hb (g/dl)	Plts (x 10^9/l)	WBC (x 10^9/l)	Neuts (x 10^9/l)	Monos (x 10^9/l)	Lymphs (x 10^9/l)	Eosins (x 10^9/l)	Basos (x 10^9/l)
Normal Range	13.5 - 17.5	150 - 450	4.5 - 13.0	1.8 - 8.0	0.2 - 0.8	1.2 - 5.2	0.04 - 0.4	0.0 - 0.1
Subject 1	**13**	**271**	**3.8**	**3.05**	**0.01**	**0.52**	**0.18**	**0.04**
Subject 2	**15.3**	**123**	**3.9**	**3.35**	**0.02**	**0.43**	**0.09**	**0.02**
Subject 3	**10.6**	**431**	**5.23**	**3.42**	**0.03**	**1.21**	**0.49**	**0.08**
Subject 4	**14.1**	**163**	**6.4**	**3.29**	**0.03**	**2.09**	**0.95**	**0.04**
Subject 5	**7.3**	**100**	**16.9**	**12.3**	**0.01**	**4.13**	**0.24**	**0.08**

Bone marrow examination in subjects 1-4 was normal by standard clinical haematological methods including morphology, histology and cytogenetics, with the exception of subject 2 who's first BM trephine showed ill formed granulomata positive for acid fast bacilli in keeping with mycobacterium kansasii infection. Subsequent marrow testing in this subject was normal. Subject 5, however, showed marked expansion of myelopoiesis with preservation of erythropoiesis and megakaryopoiesis (**Figure 5.1**). There were also granulomata seen in the first BM sample taken, which cleared after treatment for BCG infection.

Figure 5.1

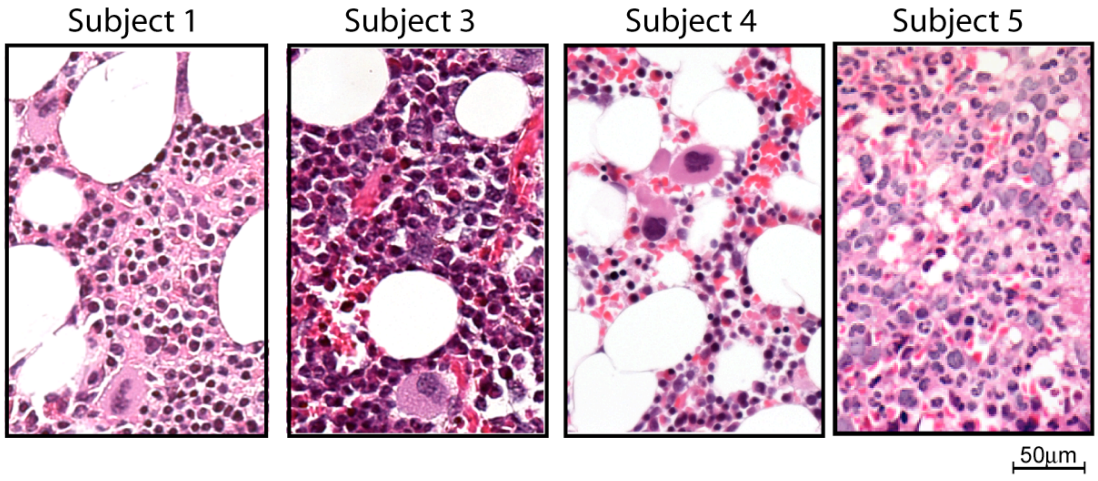

Figure 5.1 Bone Marrow Histology
Images of of intertrabecular spaces taken at x20 magnification on Zeiss Axioplan 2 microscope. Hematoxylin and Eosin stain by Pathology Department, Newcastle upon Tyne Hospitals NHS Trust.

Due to the myeloproliferative picture in subject 5, blood and BM were tested for Philadelphia chromosome, found in the myeloproliferative disorder 'Chronic Myeloid Leukaemia', but this was not detected. The subject also underwent biopsy of an enlarged axillary lymph node which revealed granulomata, in keeping with BCG infection, together with evidence of myeloid hyperplasia.

5.4 Results II: Detailed Cellular Phenotype Analysis

5.4.1 Flow cytometric evaluation of PB APC

Detailed flow cytometric analysis of PBMC monocytes and DC from all five subjects showed a massive reduction of cells in the Lin^-DR^+ gate with very few $CD14^+$ or $CD16^+$ monocytes. In addition, all subjects showed a virtual absence of both pDC and mDC. The residual cells in the lin^-DR^+ gate were $CD34^+$ progenitors (**Figure 5.2, A**). Flow cytometry of lymphocytes from PBMC revealed a more mixed picture with marked reduction, or near absence of $CD19^+CD3^-$ B cells and $CD56^+CD3^-$ and $CD56^{bright}CD3^-$ NK cells in subjects 1-4 but preservation of near normal B and NK cell proportions in subject 5 (**B**).

Figure 5.2

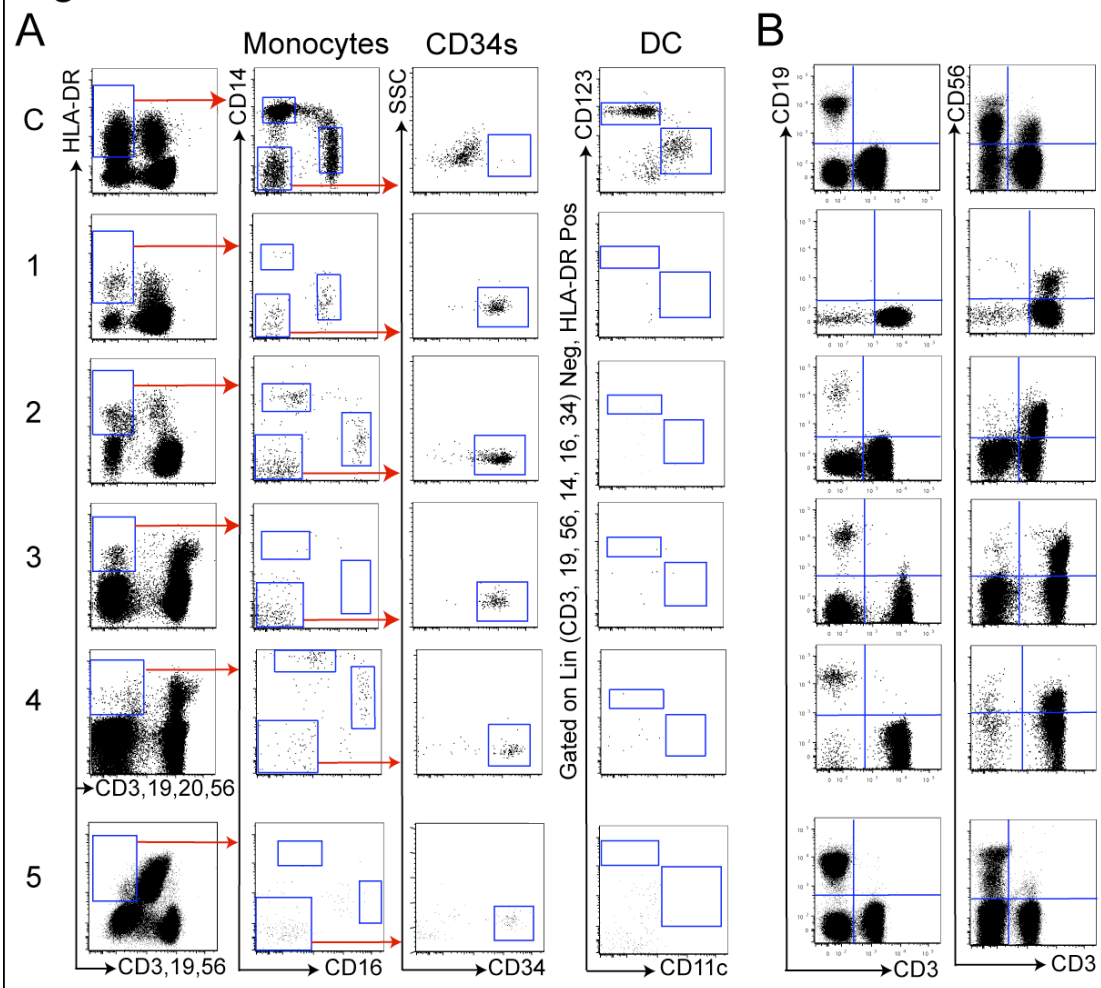

Figure 5.2 Flow cytometric analysis of PB DC, Monocytes and lymphoid cells
C, Control; 1-5, subjects 1-5. Plots show equivalent numbers of cells analysed (65,000 for lymphocytes and 75,000 for DC). A: Lineage, CD3,19,20,56; except for Subject 5, CD3,19,56. $Lin^{-}HLA\text{-}DR^{+}$ compartment divided into $CD14^{+}$ and $CD16^{+}$ monocytes and $CD14^{-}CD16^{-}$ cells which contain $CD34^{+}$ progenitors, $CD123^{+}$pDC and $CD11c^{+}$mDC. B: $CD19^{+}CD3^{-}$, B cells; $CD19^{-}CD3^{+}$, T cells; $CD56^{+}CD3^{-}$, NK cells; $CD56^{+}CD3^{+}$, $CD56^{+}$T cells. SSC, Side scatter.

5.4.2 PB of subjects compared to normal controls

The proportions of monocytes, DC and lymphocytes in subjects were directly compared to normal controls. Monocyte subsets were severely depleted in all subjects. $CD14^{+}$monocytes were between 0.1% and 5.5% of median normal values. $CD16^{+}$monocytes were more variable ranging from 0.2% to 24.2% of normal median values. Of note, both monocyte subsets were virtually undetectable in subject 5. $CD123^{+}$pDC and $CD11c^{+}$mDC were virtually absent in all subjects. $CD11c^{+}$ cells may normally be subdivided into $CD141^{high}$ and $CD1c^{+}$ fractions but neither was detectable (not shown). The only remaining Lin^{-}

DR$^+$ cells were CD34$^+$ progenitor cells, which were relatively expanded (**Figure 5.3, A**).

Subjects 1-4 showed preservation of T cell frequencies but low or virtually absent NK and B cells with the exception of subject 4 who had B cells at the low end of the normal range. Subject 5, however, had preserved B and NK cells and a slightly reduced proportion of T cells (**B**).

Figure 5.3

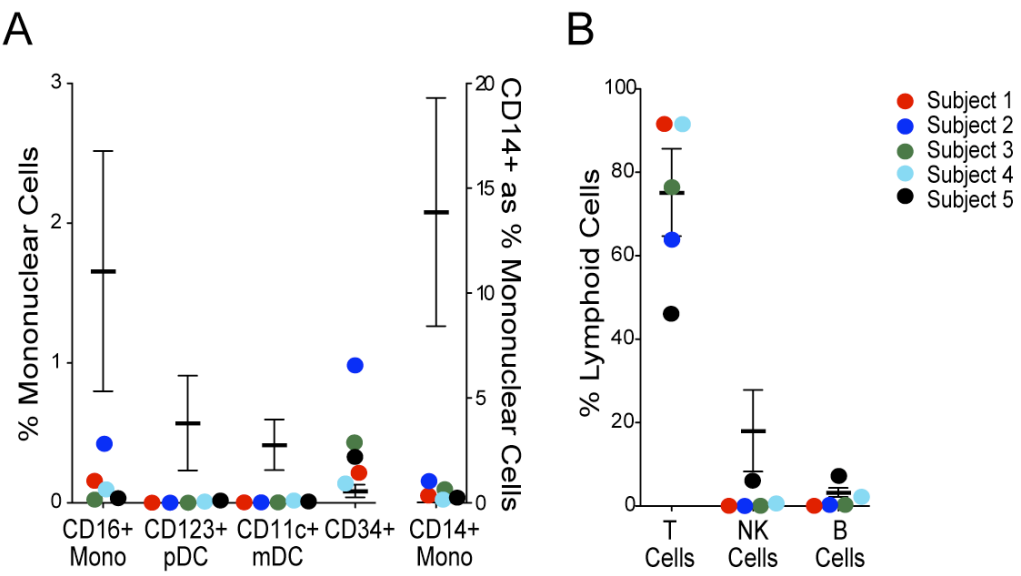

Figure 5.3 Comparison of PB DC, Monocyte and lymphocyte subsets with normal controls
Subject 1, red; subject 2, blue; subject 3, green; subject 4, turquoise; subject 5, black. A: Proportion of CD16$^+$ Monocytes, pDC, mDC, CD34$^+$ progenitors and CD14$^+$ monocytes expressed as % of PBMC. Controls n=28 B: Proportion of CD3$^+$ T cells, CD56$^+$CD3$^-$ NK cells and CD19$^+$ B cells expressed as % of cells in the lymphoid SSC/FSC gate. Contorls n=11. Error bars indicate mean+/-SD

5.4.3 Functional consequences of cellular defect

Data from Dr Rainer Doffinger, Principle Clinical Scientist, Department of Clinical Biochemistry and Immunology, Addenbrookes Hospital, Cambridge.

Cytokines released into the supernatant were measured after whole blood was stimulated *in vitro* with LPS supplemented in turn with IL-12 or IFNγ. A paired 'travel control' was run with each subject. Subjects 1-4 and their travel controls

were analyzed at least twice. Subject 5 and travel controls were analyzed 3 times. **Figure 5.4** shows results as mean+/-SD for all controls, subjects 1-4 and subject 5, each from one experiment.

Subjects showed some reduction of IFNγ production in response to LPS and IL-12 compared to controls. However, there was a significant difference observed between all subjects compared to controls for IL-12 release after stimulation with LPS and IFNγ. TNFα and IL-6 release after LPS stimulation were also significantly lower in subjects.

Figure 5.4

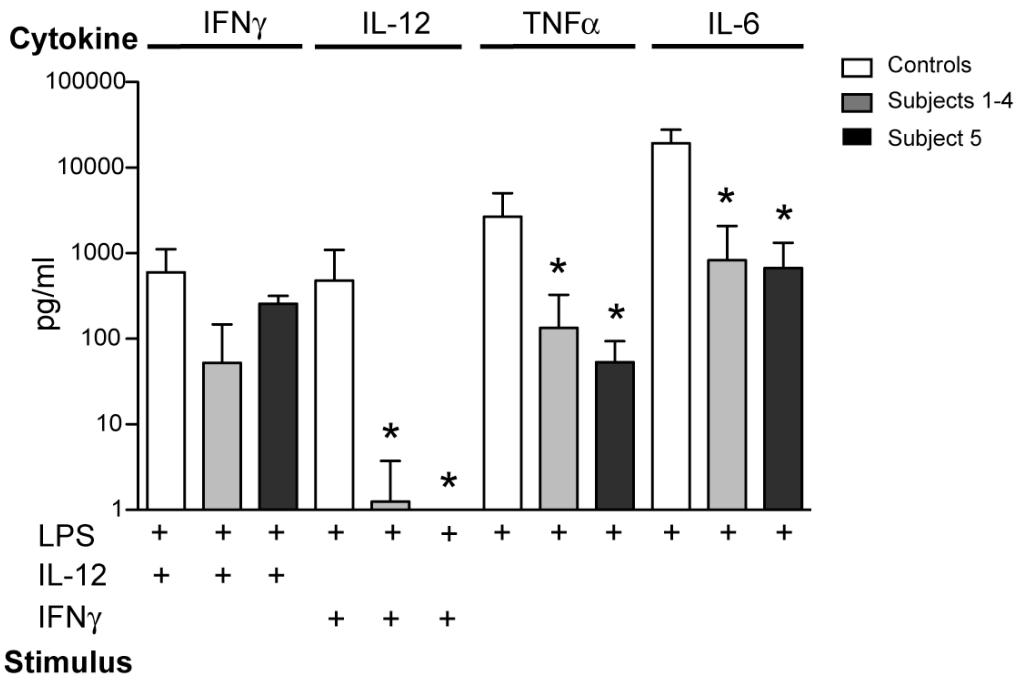

Figure 5.4 Functional Study of whole blood
Cytokine (above graph) release into supernatant after whole blood stimulation *in vitro* with LPS, IL-12 or IFNγ or combination as indicated under graph.
Bars show mean +/-SD. White, travel controls; Grey, subjects 1-4 inclusive; Black, subject 5. * $p < 0.05$ (paired t test) subjects 1-4 or subject 5 compared to control
IFNγ, interferon gamma; IL-12, interleukin-12; TNFα, tumour necrosis factor α; IL-6, interleukin-6; LPS, lipopolysaccharide.
Data couresy of Dr R Doffinger, Cambridge

5.4.4 Flow cytometric analysis of Dermis

Having observed almost complete loss of DC and monocytes from the blood, macroscopically healthy skin was examined to determine if tissue DC were similarly affected. Flow cytometry of collagenase-digested dermis was

performed. The $CD45^{+}HLA\text{-}DR^{+}AF^{-}$ DC compartment was markedly depleted (**Figure 5.5, A, Gate 1**), and $CD14^{+}$ and $CD1a^{+}$ DC were virtually absent (**B**). There remained detectable $CD1a^{bright}Lang^{+}$ cells, which represented migratory LC passing through the dermis. $CD45^{+}HLA\text{-}DR^{+}AF^{+}$ dermal macrophages were also present (**A, Gate 2**) but variably depleted compared with normal (**B**).

Figure 5.5

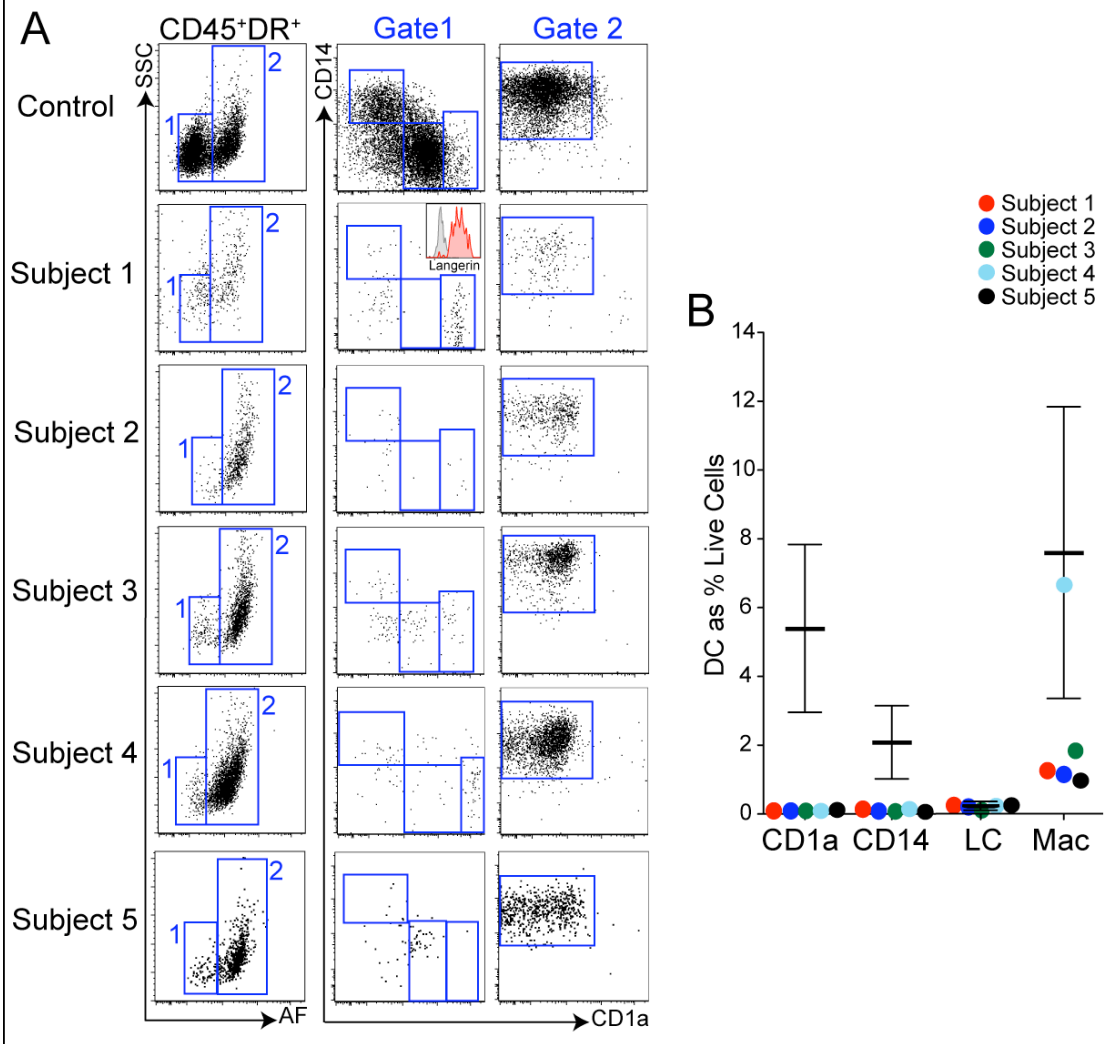

Figure 5.5 Flow cytometric assessment of Digested Dermis
A: Plots show equivalent numbers of cells analysed (40,000).
Gate 1: AF^{-} DDC. Histogram subject 1 shows langerin positivity of CD1a bright cells.Gate 2: Dermal macrophages. B: Dermal APC populations expressed as % of live cells compared to normal controls (n=22). Bars show mean+/-SD.
SSC, side scatter; AF, autofluorescence; CD1a, DDC; CD14, CD14+DC, LC, Langerhans cells; Mac, macrophages.

5.4.5 Whole mount fluorescence microscopy of Epidermis

To see whether epidermal LC, the population showing the highest proliferative proportion in normal skin, were able to survive independently of other monocyte or DC subsets, examination of intact epidermal sheets by whole mount microscopy with anti-CD1a antibodies was performed. This confirmed the presence of an intact LC network in subjects 1, 3, 4 and 5 (**figure 5.6, A**). LC density was reduced in subjects 2 and 3 (**C**) and subject 2 showed patchy disruption of the network. Proliferating LC, as demonstrated by Ki-67 nuclear staining of HLA-DR^+ cells in epidermal sheets, were found in all subjects (**B**) in similar or greater proportions than controls (**D**).

Figure 5.6

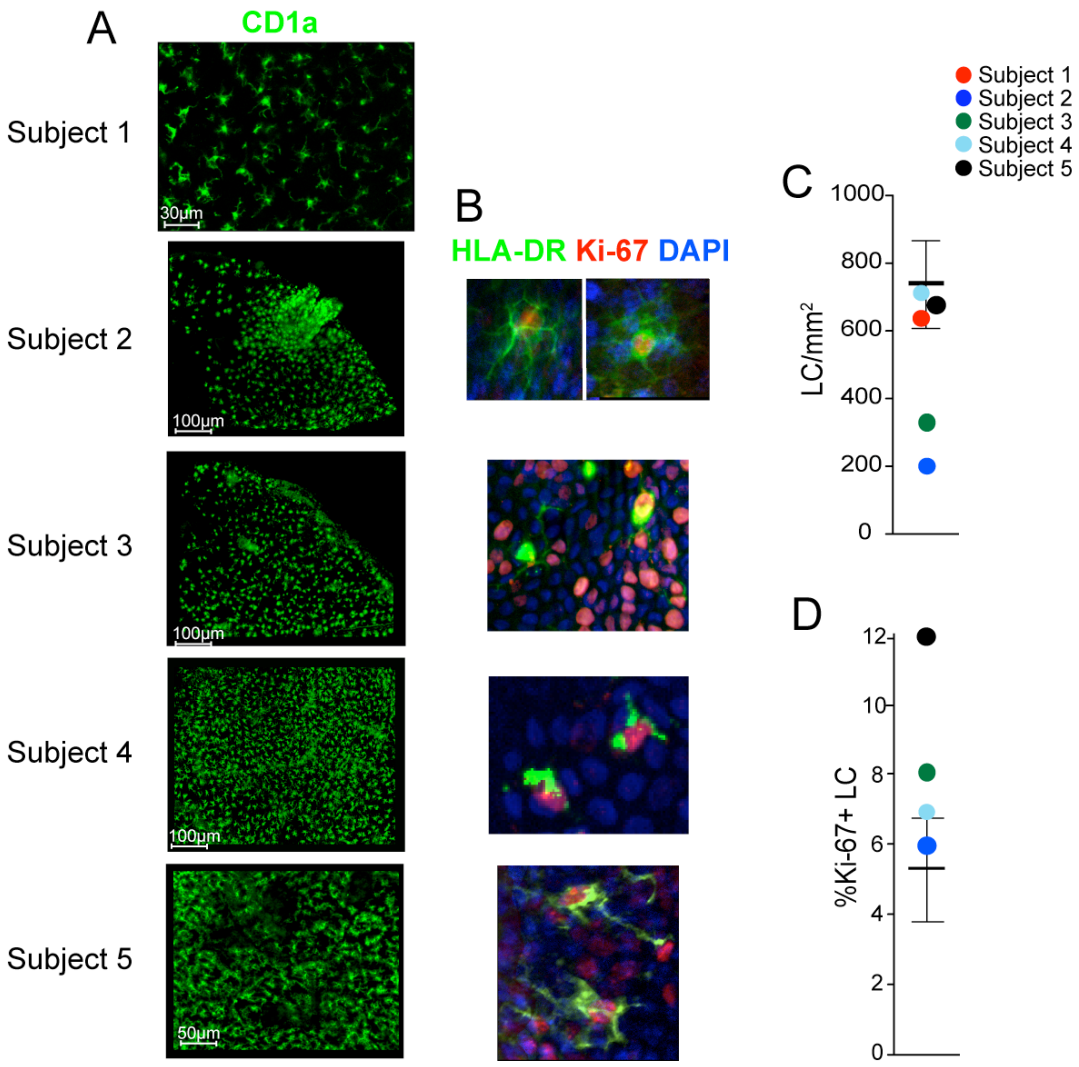

Figure 5.6 Preservation of Epidermal LC
A: Whole mount immunofluorescence staining of epidermal sheets with anti-CD1a Representative fields from each subject, imaged with Leica TCS SP2 confocal microscope or Zeiss Axioplan 2 microscope. B: Immunofluorescence staining for Ki-67 (red), HLA-DR (green) and nuclei (DAPI-blue) of epidermal sheets. Examples of Ki-67$^+$ LC are shown (white arrows). C: Total LC counts averaged from the entire low power image of epidermis from subjects, relative to controls (n=12). Bars show mean+/-SD. D: Proportion of LC in cycle as determined by Ki-67$^+$ nuclei in whole mount epidermal sheets (controls n=3)

5.4.6 Macrophages in BAL, BM and lung (and LN)

The surprising observation of relative preservation of dermal macrophages, despite PB monocytopenia, and in contrast to dermal DC, prompted the search for macrophages in other tissues.

Flow cytometry of cells from broncheo-alveolar lavage (BAL) fluid (subject 3) revealed two populations of $CD45^{+}HLA\text{-}DR^{+}AF^{+}$ macrophages; $CD14^{+}$ and $CD14^{-}$. Immunohistochemical staining for $CD68^{+}$ macrophages in lung biopsy from the same patient confirmed essentially normal numbers of these cells in alveolae (**Figure 5.7**). Bone marrow macrophages were also detectable by immunohistochemistry in subject 3. CD68 staining in dermis confirmed the presence of macrophages in this tissue, in keeping with results from flow cytometry (subject 1).

Figure 5.7

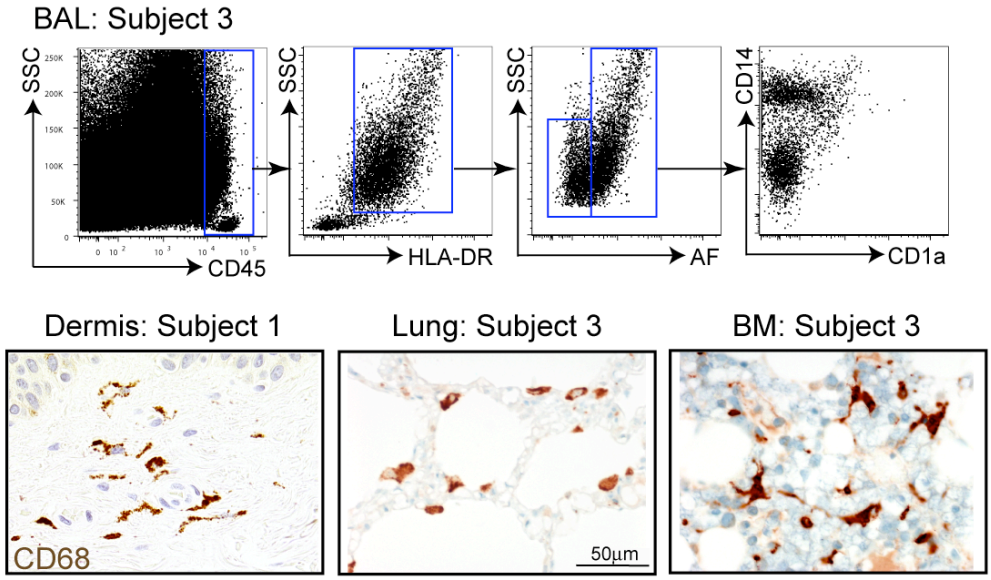

Figure 5.7 Identification of Tissue Macrophages
Top Panel: Flow cytometry of Bronchoalveolar Fluid (Subject 3) to detect $CD45^{+}HLA\text{-}DR^{+}AF^{+}$ macrophages. Bottom Panel: Immunohistochemical staining of $CD68^{+}$ macrophages in Dermis (Subject 1), Lung Biopsy (Subject 3) and Bone Marrow (Subject 3). Brown, anti-CD68K. SSC, side scatter; AF, autofluorescence. Immunohistochemical staining performed by Pathology Department, Newcastle upon Tyne Hospitals NHS Trust.

5.5 Results III: Role of DC in Immune Regulation

The virtual absence of PB and tissue DC afforded an ideal opportunity to test the relationship between these cells, Tregs and Flt3L. The mouse model predicts that loss of DC should result in reduced numbers of Tregs and high Flt3L concentrations (30). Serum Flt3L levels were measured and the numbers of Treg in PB was determined. As Flt3L is a stem cell factor as well as a DC-poietin, the levels of stem cell factor were also measured. Due to the

accompanying monocytopenia, M-SCF concentrations were also tested as this cytokine has been shown to be necessary for monocyte development (122). The corresponding growth factor receptor expression was measured on $CD34^+$ progenitors.

5.5.1 Cytokine ELISAs and GF receptor expression on CD34s

To assess the relationship between DC depletion and Flt3L, serum levels of this cytokine were measured by ELISA. Flt3L could be detected in normal serum but subjects 1-4 were found to have up to 100-fold elevation of Flt3L compared to controls. Subject 5 showed a 2 fold increase in Flt3L concentration. M-CSF levels were elevated in subjects 1-3 and at the upper limits of normal in subject 4. SCF concentrations were entirely normal compared to controls (**Figure 5.8, A**). Neither M-CSF nor SCF was measured in subject 5 due to lack of available material.

Expression of Flt3/CD135 was not detectable on BM $CD34^+$ cells from subjects tested (1 and 3) or on PB $CD34^+$ from subject 5 (**B**). CD117/c-kit expression was unaffected on BM $CD34^+$ cells but, similarly to controls, CD115/M-CSFR was not detectable in the subject tested (subject 3).

Figure 5.8

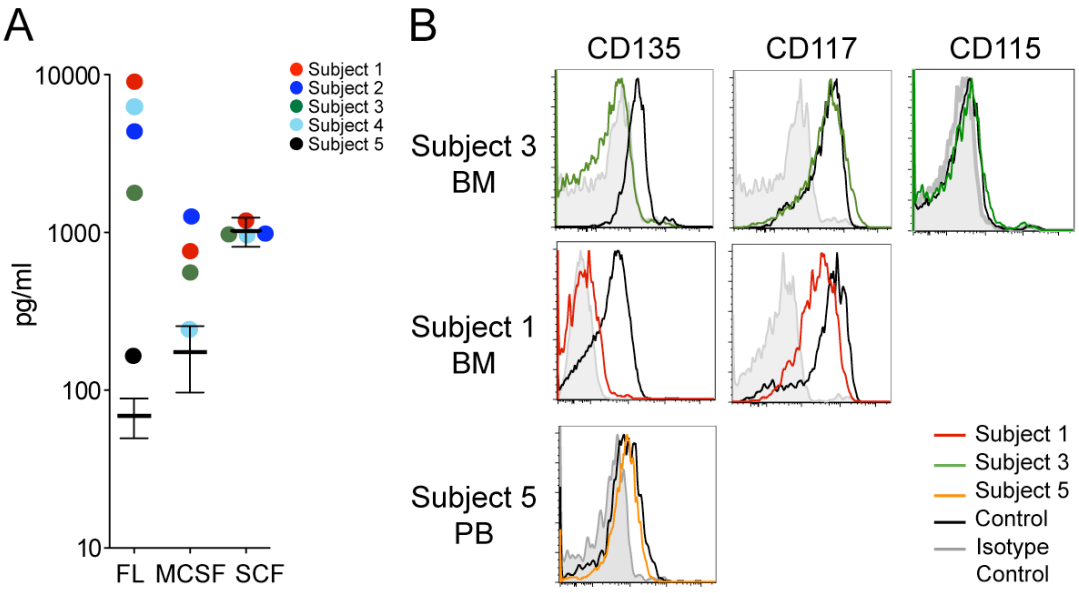

Figure 5.8 Serum growth factor concentrations and CD34+ Growth factor receptor expression
A: Serum FL, M-CSF and SCF concentrations measured by ELISA. Testing performed in the laboratory by Sarah Pagan and Naomi McGovern. B: Expression of Flt3, c-kit and M-CSFR on CD34+ cells from BM (Subjects 3 and 1) or PB (subject 5). Normal controls, black histograms; subjects, coloured histograms as per key; isotype controls, grey histograms. FL, Flt3 Ligand; MCSF, macrophage colony stimulating factor; SCF, stem cell factorCD135, Flt3; CD117, c-kit; CD115, M-CSF Receptor.

5.5.2 Relationship between DC and Treg and assessment of T cell phenotype

DC depletion and massive elevation of Flt3L in subjects lead to the prediction that Treg numbers would be reduced.

Figure 5.9, A shows the flow cytometric analysis of Tregs in a normal control. From PBMC a lymphocyte SSC v FSC gate was taken. $CD3^{+}CD4^{+}$ cells were gated and the number of these cells with dual expression of FoxP3 and bright CD25 was assessed. The figure shows the expression of these markers on $CD4^{+}$ T cells from a control and subject 1. The absolute number of Tregs per ml of whole blood was calculated using the BD Trucount™ method as previously described. Where cells were analyzed after a freezing step, dead cells were excluded from the analysis with a dead cell dye.

Initially, twenty one healthy volunteers we were studied as the *in vivo* relationship of DC and Treg in healthy humans had not previously been examined. A positive correlation was found between the absolute frequency of $Lin^{-}HLA\text{-}DR^{+}$ cells (DC, monocytes and $CD34^{+}$ cells) and $CD4^{+}CD25^{hi}FoxP3^{+}$ Tregs in peripheral blood ($p=0.0369$). Analysis of Treg numbers in four subjects revealed that severe DC deficiency was associated with marked depletion of Tregs (**B**). Plotting the four subjects together with normal blood profiles increased the significance of the relationship between DC and Tregs, without changing the slope of the regression ($p<0.0001$). The subjects had a 53-88% reduction in Treg count compared with the normal median value of 0.041 x 10^{6}/ml. There was no statistically significant correlation between Treg numbers and specific DC subsets.

An increase in the proportion of activated T cells has also been observed when mice are rendered Treg deficient, directly or via DC depletion (27, 30, 171, 172). T cells from subjects were therefore examined for evidence of increased activation by their expression of CD56 and CD25. The ratio of $CD4^{+}$ to $CD8^{+}$ T cells was not significantly perturbed but there was an increase in the proportion of activated $CD56^{+}$ $CD3^{+}$ T cells and $CD25^{+}$ $CD3^{+}$ T cells in subjects 1-4, compared to normal controls (**C**). Subject 5 was not tested due to lack of material available.

Figure 5.9

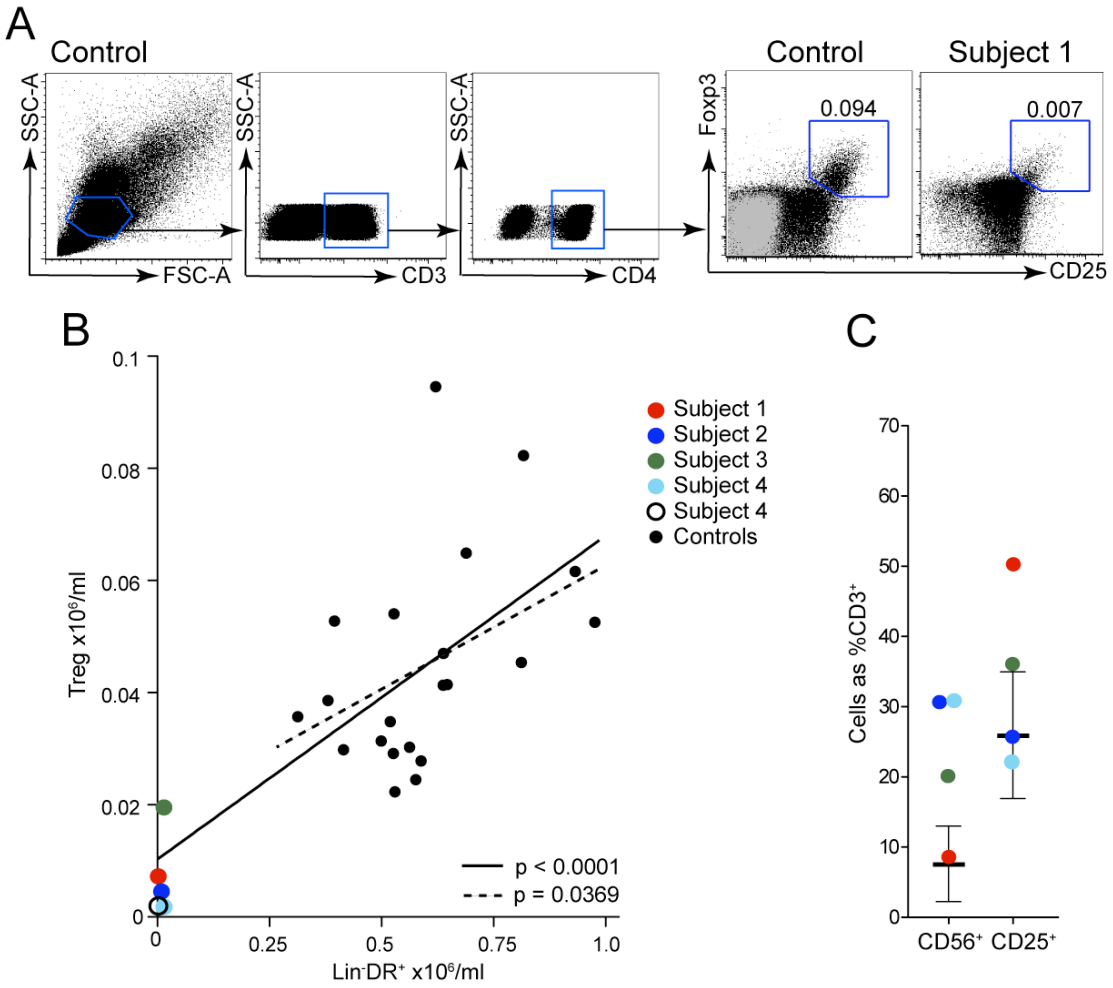

Figure 5.9 Treg and DC analysis
A: Flow cytometric analysis of Treg numbers, representative control and subject 1 shown. Isotype control for CD25-PE-Cy7 and FoxP3-APC shown in grey against normal control. B: Absolute number of CD3+CD4+CD25-highFoxP3+Tregs plotted against Lineage- HLA-DR+cells. Controls (n=21), filled black dots and hashed linear regression line. Subjects, in coloured dots and solid linear regression line. C: Proportion of $CD56^+$ and $CD25^+$ $CD3^+$ T cells relative to controls (n=10). SSC-A, side scatter area; FSC-A, forward scatter area, Lin, lineage (CD3,19,56,20); Treg, regulatory T cell.

5.6 Results IV: Recovery post bone marrow transplant

Subjects 1, 3 and 5 received definitive treatment with haematopoietic stem cell transplantation to treat potentially fatal complications of the condition. These were respectively: disseminated BCG infection, not curable with anti-microbial treatment; end stage respiratory failure due to PAP; progressive myeloproliferation with concerns about potential transformation to leukaemia. To examine whether DC were able to repopulate tissues following HSCT, PB

and skin were re-examined. Material was available post-transplant from subjects 1 and 3.

5.6.1 PB

Peripheral blood from subjects 1 and 3 was examined 130 and 40 days post transplant, respectively. Reconstitution of all PB monocyte and DC subsets was seen in both subjects (**Figure 5.10, A**) with proportions similar to controls at 40 days post transplant for other haematological conditions (**B**). By 130 days subject 1 had also recovered normal numbers of B, T and NK cells (**C**). Subject 3 at day 40 had NK cells, a few T cells but no B cells, which is in keeping with the expected course of recovery following HSCT.

Figure 5.10

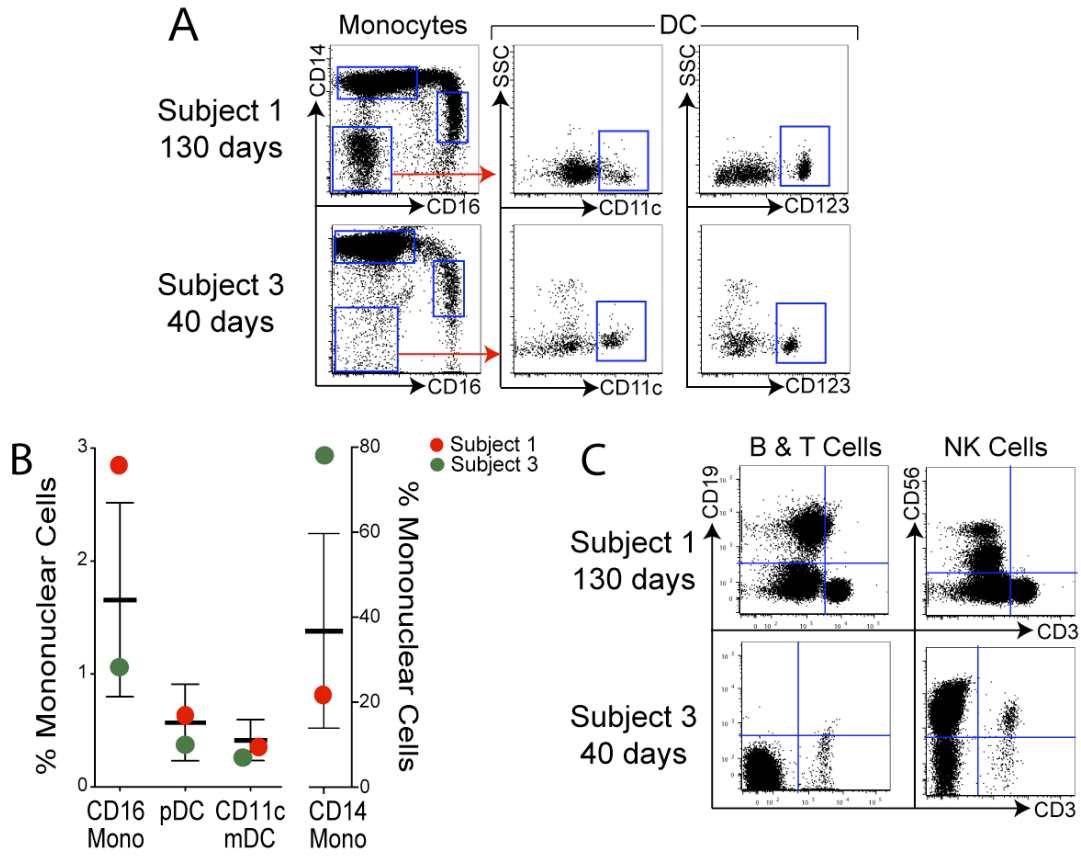

Figure 5.10 Peripheral Blood DC and lymphocyte analysis post BMT
A: Flow cytometric analysis of PBMC Monocytes, pDC and mDC. Subject 1, 130 days post BMT; subject 3, 40 days post BMT. B: Subject monocyte and DC subsets shown as % of PBMC, compared to controls taken 40days post BMT (n=7). Bars represent mean+/-SD. C: Flow cytometric analysis of PBMC lymphocytes. Subjects as for A

5.6.2 Skin

Skin biopsy from subject 1 was also taken at Day 130 post transplant. The dermis was found to be repopulated with all DC subsets (**Figure 5.11, A**) and macrophages, to near normal proportions (**B**). The epidermis, as assessed by immunofluorescent microscopy of whole mount epidermis, remained well populated with LC (**C**). Chimerism assessment of skin APC populations by examination of X and Y chromosome distribution was not possible as both the donor and recipient were male.

Figure 5.11

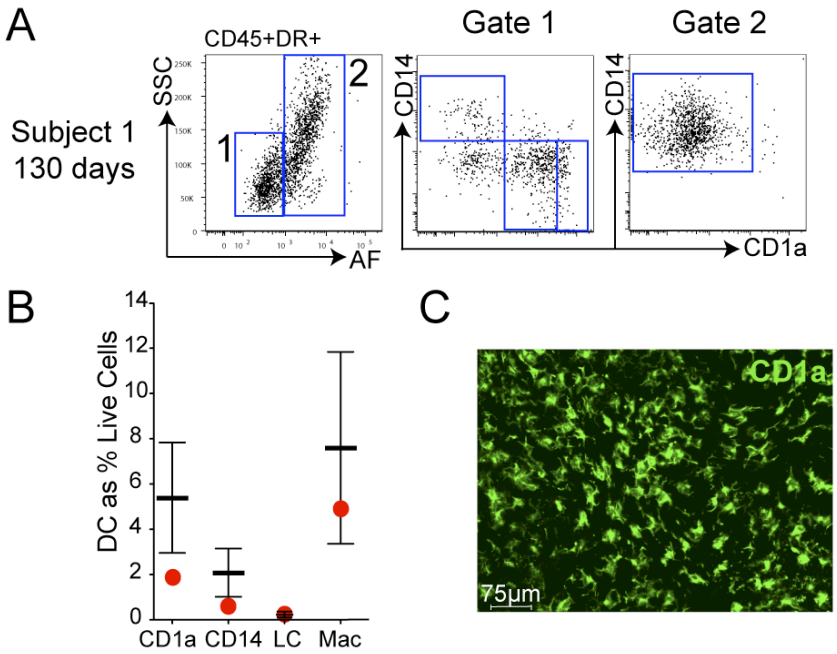

Figure 5.11 Skin APC analysis post BMT
A: Flow cytometric analysis of digested dermis from Subject 1, 130 days post BMT B: Subject 1 dermis APC, expressed as % live cells, compared to normal controls. Bars show mean+/-SD. C: Whole mount epidermal sheet from Subject 1 130 days post BMT, stained with anti-CD1a-FITC

5.7 Discussion

The phenotypic study of subjects with the newly recognised syndrome of monocyte, DC and mixed lymphoid deficiency, now referred to as DCML deficiency, has revealed a number of novel insights to *in vivo* human DC homeostasis. Specifically, it has shown that tissue DC are reliant on blood-borne precursors with the notable exception of LC which have now been shown

to maintain their numbers independently of the bone marrow in steady-state. Surprisingly, tissue macrophages were also still present. Finally, it has allowed the testing of a murine-derived model of DC and Treg homeostasis and shown that this model may hold true *in vivo* in humans.

5.7.1 Discrepancies between subjects 1-4 and subject 5

The clinical aspects of subjects 1-4 fit with those of the eighteen cases described in the recent publication (170) and, since the finding of DC deficiency in addition to monocyte and lymphocyte depletion, will be referred to as DCML deficiency.

Subject 5, however, showed a striking dissimilarity with a presentation at 10 weeks of age, as opposed to the mean age of presentation of DCML deficiency at 31yrs. The cellular phenotype was also different, although still encompassing severe monocyte and DC deficiency, B, T and NK cells were preserved and there was a marked accompanying myeloproliferation see in PB and BM. This suggests the possibility of a different pathophysiology underlying the clinical features in subject 5 and the early age of presentation raises suspicion of a congenital genetic mutation. This is discussed in more detail in Chapter 6.

5.7.2 Functional consequences of the DCML phenotype

The susceptibility to mycobacterial infections inevitably draws a comparison with a well recognised primary immune deficiency 'mendelian susceptibility to mycobacterial disease' (MSMD). In this condition, there is no gross cellular phenotype but there is disruption of the IFNγ/IL-12 signaling pathway. Causative genetic mutations within this pathway have been described in at least 6 genes, and may have a recessive (autosomal or X-linked) or autosomal dominant pattern of inheritance (173). The susceptibility to mycobacterial infection is due to either impaired IL-12 dependent production of IFNγ from T/NK cells or impaired monocytic cellular responses to IFNγ (174).

The severe reduction of IL-12 and reduction of IFNγ production in whole blood with LPS challenge suggested a disruption in the IL-12/IFNγ axis also in these

subjects. This correlates with their *in vivo* susceptibility to mycobacterial infection but is entirely explicable by the severe reduction of monocytes in PB. Some residual TNFα and IL-6 release is seen, which may be due to activation of neutrophils by LPS (175).

5.7.3 Tissue DC homeostasis

The most striking observation in terms of DC homeostasis was the presence of near-normal numbers (50-100%) of epidermal LC, despite the marked reduction of potential circulating precursors. In direct comparison, subjects 1, 3, 4 and 5 had as few as 0.1% $CD14^+$ and 0.2% $CD16^+$ monocytes, and no dermal blood DC, but LC networks remained intact. The patchy distribution of LC in subject 2 could potentially relate to previous skin inflammation. This suggests that human LC are able to maintain their numbers independently of bone marrow in steady-state. This is most likely to be due to self-renewal as Ki-67^+ LC were found in high normal or increased numbers in epidermal sheets from subjects.

The absence of dermal DC, with the exception of migrating LC, suggests that tissue DC share a common origin with PB $Lin^-HLA\text{-}DR^+$ cells. As both monocytes and DC were depleted, it is not possible to determine which plays the prominent role in steady-state tissue DC homeostasis. Another cell that cannot be excluded as a potential DC precursor is the circulating $CD34^+$ cell. The phenotype of near global absence of monocytes and DC suggests that haematopoietic progenitors are unable to differentiate along a monocyte/DC path. Therefore, even though $CD34^+$ cells can be found in subjects' PB, even in increased numbers, these cells may be unable to differentiate to tissue DC in DCML deficiency.

5.7.4 Macrophages

The presence of $CD68^+$ macrophage populations in dermis, alveolar spaces and BM show that these cells can also persist independently of blood monocytes. However, at least in the case of alveolar macrophages, it is possible that these cells have impaired function as subject 3 developed severe PAP despite the histological and flow cytometric evidence of the presence of good numbers of alveolar macrophages.

There are several conceivable explanations for why macrophages persist despite the absence of monocytes. Firstly, uncertainty about the natural history of the syndrome, at least in subjects 1-4, adds complexity. It is possible that these subjects had circulating monocytes at some time and macrophages can be very long lived (176) (73). However, at presentation, subjects 1-4 had documented monocytopenia for at least 3 to 14yrs, and most likely longer as initial blood counts were taken incidentally. As subject 5 presented at only 10 weeks of age, it is possible that circulating monocytes were never present, but tissue macrophages were still found.

Secondly, at least a subset of adult tissue macrophages originate independently of BM. It has recently been shown that murine microglia arise from the embryonic yolksac (87) and yolksac phagocytes, prior to the development of liver haematopoiesis, are seen to populate other tissues within the embryo including lung and liver (177), reviewed in (178). To what extent these embryonic tissue phagocytes play a role in the adult is not clear. However, it is conceivable that tissue macrophages found in these subjects could be of embryological origin.

A final route that cannot be excluded is the differentiation of macrophages directly from circulating $CD34^+$ cells. It is known from *in vitro* culture that different cytokines, and therefore potentially different signaling pathways, are required to direct $CD34^+$ progenitors to differentiate to macrophages rather than DC (162), however whether differentiation to macrophages has to be via a $CD14^+$ monocytic cell is not clear. It is conceivable that conditions favouring the differentiation pathway from $CD34^+$ cells to macrophages could exist in these subjects and that $CD34^+$ progenitors retain their macrophage potential, despite their being no circulating monocytes. Further work is required to characterise the phenotype and function of macrophages present in DCML deficiency, compared to normal tissues.

5.7.5 Elevated Flt3L and M-CSF with normal SCF levels

As with DC depleted mouse models, massive elevation of Ftl3L was found in DCML deficiency. Not only was there depletion of cells which would normally express Flt3 but Flt3 could not be detected on the surface of subjects' $CD34^+$ progenitor cells. An elevation of Flt3L has been seen in the treatment of mice with a small-molecule Flt3 inhibitor (164). This caused depletion of tissue DC, massive increase of serum Flt3L and undetectable surface Flt3 on lineage negative BM cells, suggesting a feedback regulatory loop between Flt3 expression and Flt3L concentration. This may explain the absent Flt3 on CD34+ progenitors. This mechanism as the explanation for absent Flt3 on haematopoietic progenitors is supported by the fact that normal erythropoiesis, megakaryopoiesis and granulopoiesis was observed, suggesting that the lack of Flt3 on haematopoietic progenitors did not have a quantitative effect on the haematopoietic stem cell compartment. Similarly, SCF levels were normal, possibly reflecting a quantitatively normal stem cell population.

In comparison, subject 5, despite only a modest 2 fold elevation of serum Flt3L demonstrated a marked myeloproliferation. In mice lacking $CD11c^+$ DC, myeloproliferation is also found in association with elevated Flt3L (171). The lack of myeloproliferation in subjects 1-4, despite 10-100 fold increases in serum Flt3L suggests a differentiation block at an earlier stage of haematopoiesis than in subject 5. The modest elevation of Flt3L in subject 5, as opposed to the huge elevations seen in DCML deficiency, may be explained by the presence, due to myeloproliferation, of large numbers of cells expressing Flt3.

Serum M-CSF was also raised in subjects 1-3 and high normal in subject 4. Subject 5 was not tested as material was not available. The corresponding receptor, M-CSF-R, was not present on $CD34^+$ progenitors, nor on any other PB cell as the populations normally expressing this receptor, namely monocytes, were absent. Similarly to Flt3/Flt3L regulation, CSF-1 receptor (the murine homologue to M-CSF-R) knockout mice, have elevated serum CSF-1 (M-CSF) levels (122) and CSF-1 receptor is down regulated by internalization on binding CSF-1 (179). However, in these cases, it is possible that the raised M-CSF serum levels are related to loss of receptor expression secondary to

lack of cells. It is therefore not clear whether the primary loss is of M-CSF-R expressing cells, or M-CSF-R itself. Whether the tissue macrophages found in these subjects express M-CSF-R has not yet been investigated.

The implications of these observations on potential causative genetic defects will be discussed in chapter 6.

5.7.6 DC in immune regulation

The observation of spontaneous DC deficiency with elevated serum Flt3L presented a unique opportunity to examine human DC-Treg co-regulation *in vivo*. As predicted by the mouse models, Treg were found to be depleted. The model was also found to hold true in normal volunteers suggesting that inter-individual variation in humans is sufficient to demonstrate this relationship.

The fact that there was no significant relationship identified between individual DC subsets and Treg may be due to the small number of controls or to the possibility that Treg homeostasis occurs in an MHC class II dependent fashion, as predicted by the mouse model (30).

Approximately one quarter of patients with DCML deficiency, including the fourth subject in this study, developed autoimmune syndromes (170). Treg depletion as a consequence of DC deficiency may contribute to this phenomenon.

5.7.7 Post transplant

In subjects 1 and 3 both PB and tissue DC subsets were restored following haematopoietic stem cell transplantation. Subject 5 also recovered PB counts as measured by routine clinical parameters. This suggests that, not only is the defect not of stromal origin, but that it is a primary bone marrow haematopoietic disorder.

The genetic aetiology of DCML deficiency and the phenotype of subject 5 is considered in the next chapter.

Chapter 6. Genetic Regulation of DC and Monocyte Development

6.1 Introduction

Haematopoiesis is characterised by a progressive restriction of differentiation potential in progenitor populations. This process is orchestrated through transcription factor (TF) activity which, among other things, controls the expression of growth factor receptors and so the responsiveness of cells to growth factor (GF) signaling. Disordered haematopoiesis may therefore result from defects in TFs, GFs or GF-receptors. Following the identification of subjects with absent peripheral DC and monocytes, the opportunity was taken to establish whether any specific defects existed in the haematopoietic progenitor compartment and whether any causative genetic mutations could be identified.

6.1.1 Stem cell compartment

There is much current interest in tracing monocyte/macrophage and DC ontogeny back through the stem cell compartment in mouse with at least two specific subsets identified with DC potential. Recent studies, using adoptive transfer models, have mapped the myeloid element of monocyte/DC differentiation. This pathway includes the GMP, which retains granulopoietic potential and gives rise to the MDP (monocyte dendritic cell progenitor). This cell has monocyte and DC potential. The CDP (common DC precursor), also from the GMP and possibly downstream of the MDP, gives rise to only pDC and mDC (101) (102) (180). Similarly, presumed lymphoid precursors (CLP) have been shown to be able to give rise to myeloid DC (96) (105).

In DCML deficiency subjects, repopulation of missing cell compartments following HSCT would indicate that the defect causing the clinical phenotype lies in the haematopoietic stem cell compartment. To examine whether there were any identifiable defects in progenitor cell subsets, $CD34^+$ cells from BM and PB were examined. Of particular interest, given the cellular phenotype of subjects 1-4, were previous reports of human $CD34^+$ populations able to give rise to DC/monocyte, B and NK cells (106) (107). A cell with similar potential

was also recently identified in human cord blood and adult BM by Doulatov et al., (89). The flow cytometric protocol used in this study was adapted for progenitor cell analysis in DCML deficiency.

6.1.2 Genetic work-up

A number of TFs have been found to be essential for monocyte and/or DC development in mice (33). These include factors involved in the signal transduction of Flt3L and GM-CSF (181). Although M-CSF is known to play an important role in monocyte development, less is know about the TFs involved. **Figure 1.8 (Chapter 1)** summaries the current known genetic defects affecting DC ontogeny in mice (33) (125).

The key signalling molecule directing DC differentiation in steady-state is Flt3L (182). This signals via STAT3 (183), whose downstream targets include PU.1, IRF8, M-CSF-R and Flt3 itself (126). GM-CSF signals through STAT5 which in turn activates STAT3 and IRF4 and may inhibit IRF8 (128) (127). Mutations in all these genes have been shown to cause monocyte/macrophage and/or DC deficiencies in mice.

Many mutations lead to some selectivity in deficiency of DC subtypes, either reflecting the role of the gene in differentiation or the consequence of redundancy in unaffected populations. Whether monocytes are affected is not commonly documented and BM DC progenitors have been examined only in the case of Gfi-1 and IRF8 knockout models, revealing depletion and preservation of DC progenitors, respectively.

Based on the comparison of subjects' phenotypes and published mouse genetic models a number of candidate genes were sent for sequencing or sequenced locally.

6.1.3 Family History

Subject 5 presented in infancy suggesting an inherited or de novo constitutional genetic defect. In contrast, DCML deficiency subjects, including those in the case series from Vinh et al., (170), present mainly in adulthood with

heterogeneous phenotypes. Some are sporadic, with no family history while five pedigrees, with autosomal dominant pattern of inheritance, were identified in the case series.

The identification of genetic mutations in sporadic genetic disorders through a candidate gene approach is frequently unrewarding. The availability of DNA from affected and unaffected members would allow much more powerful classical or post-genomic analysis. For this reason, and for the direct clinical benefit of potentially affected relatives, the kindred of subject 3 was explored to identify living undiagnosed individuals and to include unaffected family members.

6.1.4 Inclusion of data from laboratory members and other collaborating laboratories

Gene sequencing was carried out by a number of different laboratories, and some of the molecular genetic work by members of the Collin laboratory. The data are included here as results are central to the discussion and critically influence further work. Where this is the case, it is clearly indicated in the text and figure legends.

6.2 Materials and Methods for Chapter 6

6.2.1 Purification of $CD34^+$ cells from PBMC

Unmobilised circulating PB $CD34^+$ cells were purified from PBMC by FACS. Control PBMC were isolated as previously described and stained with CD34 PE alone. Progenitor cells were identified by their CD34 expression and low SSC. Cells were sorted into 100μl RPMI in 1.5ml eppendorf at 4^0C and then kept on ice for transfer to the laboratory. They were pelleted and lysed in RNA lysis buffer, then stored at -80^0C until used to generate cDNA for QPCR analysis.

6.2.2 PU.1 Gene sequencing

PU.1 primers were designed from sequence data available at www.ncbi.nlm.nih.gov, tagged with M13 primers and synthesised by Sigma Life

Science Oligos (www.sigmaaldrich.com). The minimal tiling path contained 10 probes and covered the five exons, the majority of the introns and the promoter region (**Figure 6.1**). Forward and reverse primer optimization was performed at 1, 2 and 3mM $MgCl_2$ concentrations and temperatures ranging from 60-70^{0}C on a PCR block, PTC-225 DNA Engine Tetrad Thermal Cycler (MJ Research/Bio-Rad; www.bio-rad.com). Amplification and purity was checked by gel electrophoresis on a 2% agarose gel. DNA was isolated from both fibroblasts and neutrophils from control and subject 3, was amplified on a PTC-225 DNA Engine Tetrad Thermal Cycler (MJ Research/Bio-Rad; www.bio-rad.com) with a PCR program consisting of step 1, 94^{0}C for 4 mins; step 2, 94^{0}C for 30secs; step 3 Anneal 30secs; step 4, 72^{0}C 30secs; step 5, 72^{0}C 4 mins; with steps 2-4 repeated for 34 cycles. Removal of excess primer and nucleotides was performed with ExoSAP-IT and incubated on PCR block at 37^{0}C for 15mins to degrade singlestranded DNA, then 80^{0}C for 15mins to inactivate ExoSAP-IT. Cleaned, amplified PCR product was then sent, with M13 tagged primers to DNA Sequencing and Services, College of Life Sciences, University of Dundee, Scotland DD1 5EH for sequencing on a 3730 Capillary DNA Analyzer (www.appliedbiosystems.com). Data was retrieved as .ab1 files and viewed with Chromas Lite Software. The sequence was then pasted into http://www.ncbi.nlm.nih.gov/ and run on the BLAST program. Known Single Nucleotide Polymorphisms (SNPs) were identified and mapped using the ensembl genome browser at http://www.ensembl.org/index.html. Information about the SNPs was gathered using links from ensembl to the ncbi SNP database at http://www.ncbi.nlm.nih.gov/SNP/. Data were analyzed by laboratory member, Rachel Dickinson.

Figure 6.1

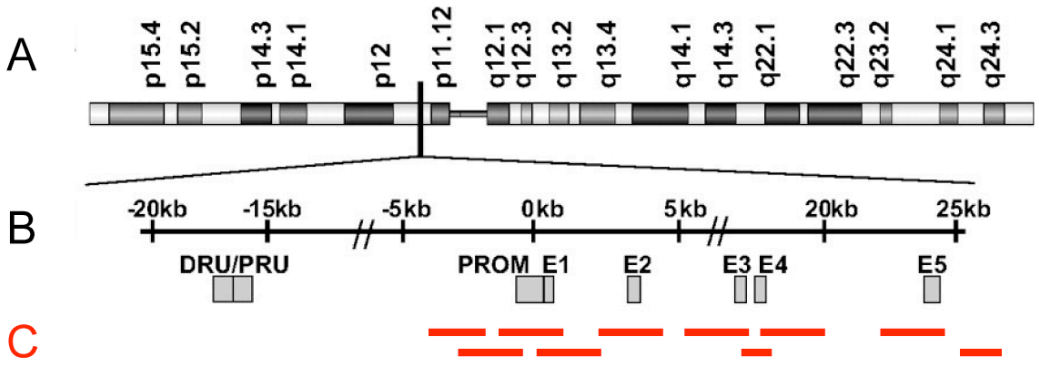

D

ncbi PROBE name	FORWARD_PRIMER	REVERSE_PRIMER	START	STOP
Pr001256093.1	tgtaaaacgacggccagtCGCTCTGTGTCATTGGTCCTCA	caggaaacagctatgaccTTCGCCTCCCTCCAGGACTC	47376253	47376605
Pr001256775.1	tgtaaaacgacggccagtCCGCTGAACTGGTAGGTGAGCTT	caggaaacagctatgaccCCGCAGGCAGCAAGAAGAAG	47376830	47377103
Pr001256975.1	tgtaaaacgacggccagtGTCAGTTGGCCTGGCTGGGT	caggaaacagctatgaccAACGCACCGGTCCCTAGCAT	47380316	47380914
Pr001269489.1	tgtaaaacgacggccagtGCTGGCCTGGGAAGCCAT	caggaaacagctatgaccTGGTGGATAGGCAAGAAAGGTTTG	47400225	47400824
Pr001271566.1	tgtaaaacgacggccagtCAGGAGGGCCCACAACAAGG	caggaaacagctatgaccCATGCAGGTGGCGAGGGTTA	47381125	47381724
Pr001274294.1	tgtaaaacgacggccagtCACGGGTTGGGCTGGTGG	caggaaacagctatgaccTGAGGTGACTGTTGGCTACATAGGG	47399824	47400422
Pr001274535.1	tgtaaaacgacggccagtCAGGCACACCCACACACTGC	caggaaacagctatgaccTCAGATGAGGAGGAGGGCGA	47379904	47380497
Pr001275037.1	tgtaaaacgacggccagtCCCGCACCTTGACACACTGC	caggaaacagctatgaccCCCAGTTCCAGGCAGAGGGA	47396971	47397425
Pr001275038.1	tgtaaaacgacggccagtGCCTTCACCATCCTCAGCCC	caggaaacagctatgaccGGGACTATCTCCCAGCGGCA	47399543	47400129
Pr001275040.1	tgtaaaacgacggccagtCATGGGCTTCCCTACCACCA	caggaaacagctatgaccTGGGTGGATGAGTGGACTGG	47400636	47401234

Figure 6.1 PU.1 Gene Sequencing, Gene structure and Primers
A and B from Bonadies, N. et al. Blood 2010;115:331-334. D from www.ncbi.nlm.nih.gov A: Diagram of Chromosome 11 showing location of PU.1/SPI1 gene at the centromeric part of the short arm (11p11.2).
B: Diagramatic representation of PU.1 gene showing Distal regulatory unit (DRU), Proximal regulatory unit (PRU) Promoter region (PROM), exons 1-5 (E1-5).
C: Minimal tiling path represented by 10 probes (red lines) showing approximate location of start and end sequences (not to scale). D: Details of probes used to amplify and sequence DNA. Lower case letters represent M13 primers.

6.3 Results I: Human IRF8 Deficiency

Subject 5 showed a phenotype distinct from subjects 1-4 with preservation of lymphocytes and a myeloproliferation accompanying the monocyte and DC deficiency. In addition, the presentation as an infant highlighted the possibility of a congenital genetic mutation as a cause of the phenotype.

6.3.1 Analysis of $CD34^+$ progenitors in Subject 5

In order to characterise the haematopoietic compartment more fully, and potentially identify where in DC and monocyte ontogeny a defect had occurred,

CD34$^+$ progenitor subsets were analyzed as previously described. BM was not available from subject 5, but as CD34$^+$ populations similar to BM are seen in normal PB, circulating CD34$^+$ cells were analyzed in their place.

An accumulation of both MLP (1.4 fold increase) and GMP (10 fold increase) was seen in PB (**Figure 6.2**). Some B/NK were detectable, but in relatively reduced proportions. Unlike PB from controls, circulating HSC were also detectable, constituting 1.4% of CD34$^+$ cells.

Figure 6.2

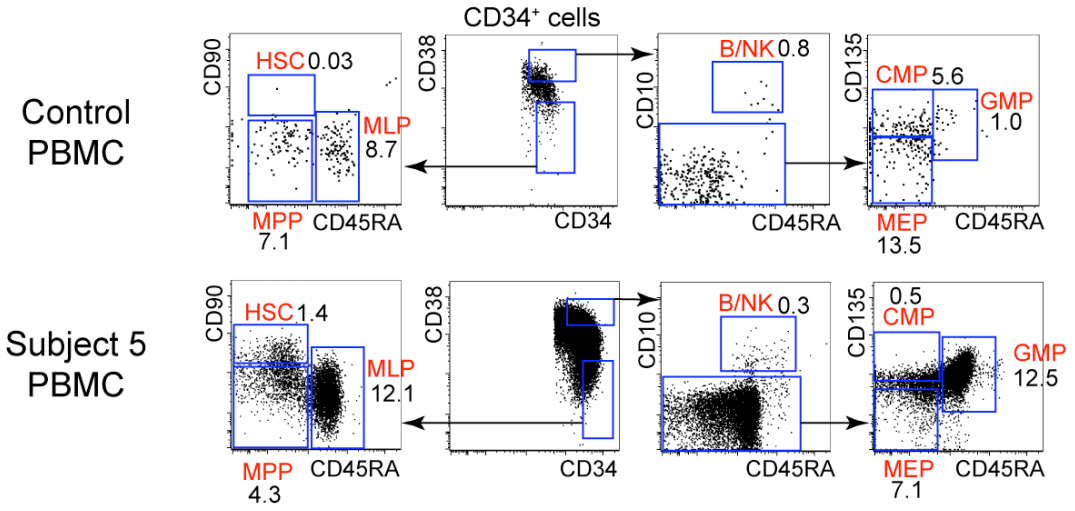

Figure 6.2 IRF8 Flow cytometric analysis of circulating CD34$^+$ progenitors in Control and Subject 5
Top panel shows CD34$^+$ subset analysis in control PBMC. Bottom panel shows CD34$^+$ susbset analysis in PBMC from Subject 5. Numbers in black type indicate % of CD34$^+$ cells in each gate. HSC, hematopoietic stem cell; MPP, multi-potent progenitor; MLP, multi-lymphoid progenitor; B/NK, committed B/NK precursor; CMP, common myeloid progenitor; MEP, megakaryocyte/erythroid progenitor.

6.3.2 IRF8 deficiency in subject 5

The similarity between the combination of DC deficiency and myeloproliferation and mice with mutations in interferon regulatory factor 8 (*IRF8*; also known as *ICSBP*) was noted by Dr Sophie Hambleton. Genomic DNA from subject 5 was sent to Philippe Gros' laboratory (Department of Biochemistry, McGill University, Montreal, Canada) and was sequenced by Sandra Salem. Sequencing revealed homozygosity for a point mutation in *IRF8* leading to a

lysine to glutamic acid substitution at position 108 (K108E), within the DNA binding domain (DBD) (**Figure 6.3, A**).

Molecular modeling by David Burk and Albert Berghuis (McGill University, Montreal, Canada), mapped K108 to a short beta strand running parallel to the major DNA-binding alpha helix (**B** by kind permission of Albert Berghuis). The mutation was shown to disrupt the hydrogen bonding, and thus binding, to DNA. This would have the effect of preventing the downstream transcriptional responses to IRF8.

Figure 6.3

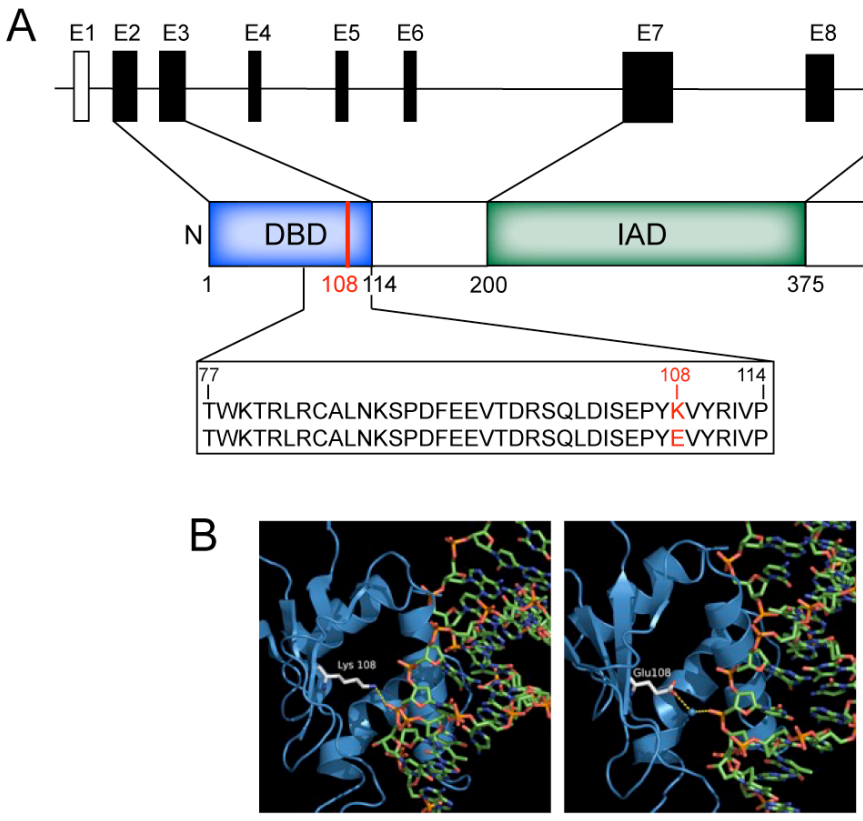

Figure: Schematic of K108E mutation in IRF8 gene.
A: Sandra Salem and Phillipe Gros
B: David Burk and Albert Berghuis
Department of Biochemistry, McGill University, Montreal, Canada

Figure 6.3 IRF8 mutation in subject 5
A: schematic representation of human IRF8 gene, including 9 exons (non-coding, empty; coding, filled), and the major structural features DBD (DNA Binding domain) and IAD (IRF association domain). Site of K108E Mutation (red) in DMD is illustrated with corresponding amino acid sequence. B: Model of DNA binding domain of IRF8 showing disruption caused by K108E mutation.

6.3.3 Inheritance of K108E mutation

In order to establish the inheritance pattern of the IRF8 K108E mutation, genomic DNA from both parents and the subject's sibling (6yrs old at time of analysis) was also sequenced in Philippe Gros' laboratory.

Whilst DNA was being analyzed, PB phenotyping of subject 5's parents and sibling was undertaken (**Figure 6.4, A and B**). At the time of testing, both sibling and mother were well. Father was being investigated for mild, asymptomatic lymphadenopathy, biopsy of which was shown to be negative for infection and malignancy, with no further investigation planned. There was no evidence of depletion of monocytes, DC or lymphocytes in parents or sibling.

Heterozygosity for the K108E allele was confirmed in both parents (who were unrelated but originated from the same part of Ireland). The sibling was wild type. This confirms the classical recessive inheritance of the K108E mutation, demonstrating that heterozygosity for K108E mutation does not confer an abnormal phenotype (**C**).

Figure 6.4

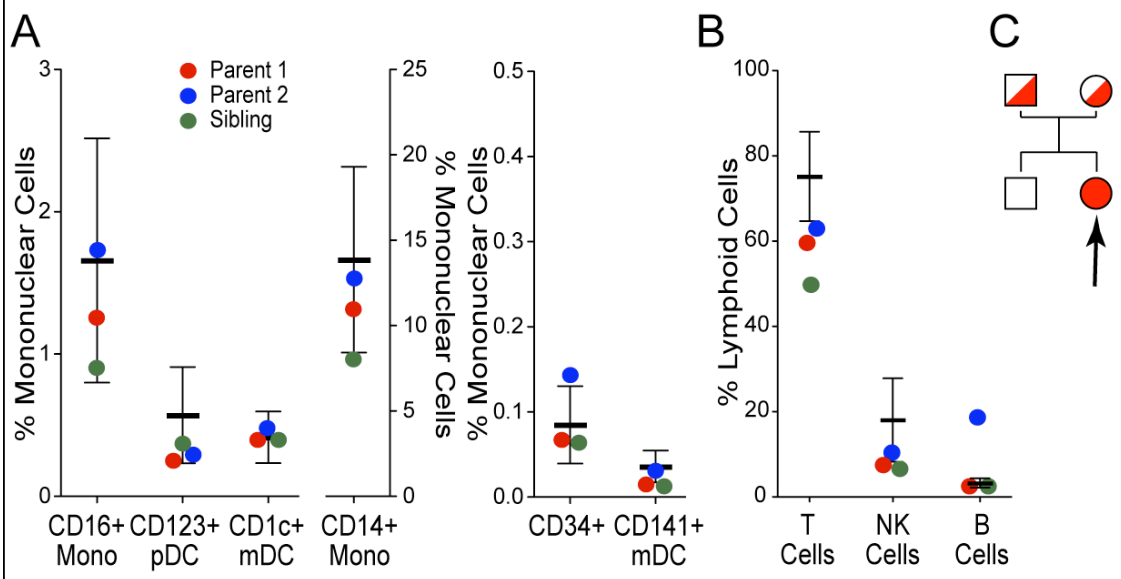

Figure 6.4 Comparison of Subject 5 Relatives' PB DC, Monocyte and CD34⁺ subsets with normal controls

Parent 1, red; Parent 2, blue; sibling, green. A: Proportion of CD16⁺monocytes, pDC, CD1c⁺mDC and CD14⁺monocytes, CD34⁺ progenitors and CD141^{high}mDC expressed as % of PBMC. Controls n=28. B: Proportion of CD3⁺ T cells, CD56⁺CD3⁻ NK cells and CD19⁺ B cells expressed as % of cells in the lymphoid SSC/FSC gate. Contorls n=11. C: Pedigree of subject 5 (indicated with arrow). Square, male; Circle, female; red filled, homozygous IRF8 mutation; empty, unaffected; half-filled, heterozygous for IRF8 mutation. Error bars indicate mean+/-SD

6.4 Results II: DCML Deficiency; genetic work up of subjects 1-4

In contrast to IRF8 deficiency in which there is myeloproliferation, patients with DCML deficiency had normal BM cellularity (**Figure 5.1**). To understand the genetic basis of DCML deficiency and the differences between this disorder and IRF8 deficiency, the CD34⁺ compartment from these subjects was analyzed as described, and steps were taken to identify any causative genetic mutations.

6.4.1 CD34⁺ Compartment in DCML Deficiency

Bone marrow was available for analysis from subjects 1, 3 and 4 (**Figure 6.5, A**). Total BM mononuclear cells analyzed are shown. The minimum number of CD34⁺ cells analyzed was 4500. Numbers in black type indicate % of CD34⁺ cells in each gate. All definitions are as described in Chapter 4. However, in this analysis it was not possible to separate Flt3⁺ CMP from Flt3⁻ MEP as Flt3 was not expressed by CD34⁺ cells in the subjects 1-4, therefore CMP and MEP

were analyzed in a combined gate. Total $CD34^+$ cells are depicted ('Live $CD34^+$') in the central panel.
In DCML deficiency, a complete absence of MLP from gate 2 was seen. In keeping with this, an immediate progeny of the MLP, the $CD10^+$ B/NK precursor, was also absent. GMP were depleted by between 72% and 95%.

To determine whether these deficiencies in BM were reflected in PB, circulating $CD34^+$ cells from subject 3 were also analyzed (**B**). This was found to be the case as MLP and B/NK were virtually absent from PB and GMP were markedly reduced. All other populations were identifiable, including a small number of HSC, in contrast to normal PB (**Figure 4.2**).

Figure 6.5

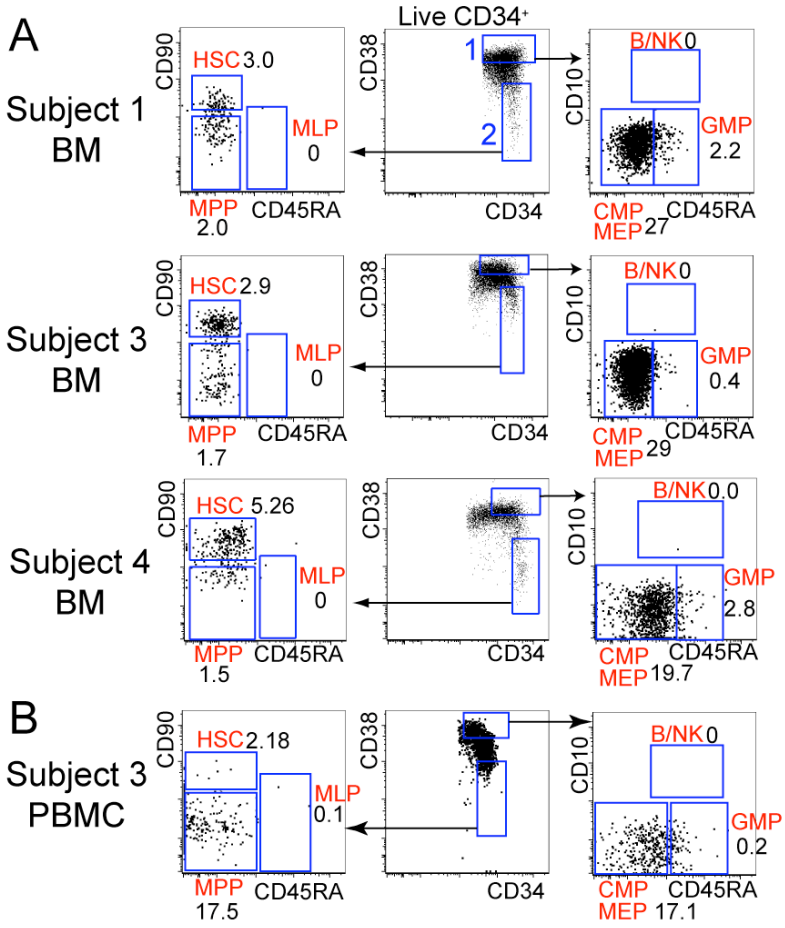

Figure 6.5 DCML 34s Flow cytometric analysis of BM and PBMC CD34⁺ Subsets in DCML Deficiency
A: BM analysis of Subject 1, 3, 4. Gate 1: more mature CD38⁺ fraction from live CD34⁺ cells; Gate 2: primitive CD38⁻ fraction. B: PBMC analysis of Subject 3, gating similarly to BM analysis Numbers in black type indicate % of CD34⁺ cells in each gate. HSC, hematopoietic stem cell; MPP, multi-potent progenitor; MLP, multi-lymphoid progenitor; B/NK, committed B/NK precursor; CMP, common myeloid progenitor; MEP, megakaryocyte/erythroid progenitor.

6.4.2 Familial case of DCML Deficiency: Subject 3

Having identified the same distinct defect in haematopoiesis in all DCML subjects analyzed, despite their clinical heterogeneity, the possibility that this condition might be caused by a similar mutation in all subjects arose. Aside from individually sequencing candidate genes, the search for potential genetic cause of DCML deficiency would be significantly assisted by a complete pedigree of affected and unaffected relatives.

In the pedigree of subject 3, five individuals were identified as potentially affected according to their clinical history (**Figure 6.6**). All were deceased. The subject's father was treated for arthritis and died approximately 40yrs old of 'lung problems'. The other affected relatives died of 'leukaemia' or 'cancer' around their 4th decade. As yet, there is no preserved genetic material available from deceased relatives.

Figure 6.6

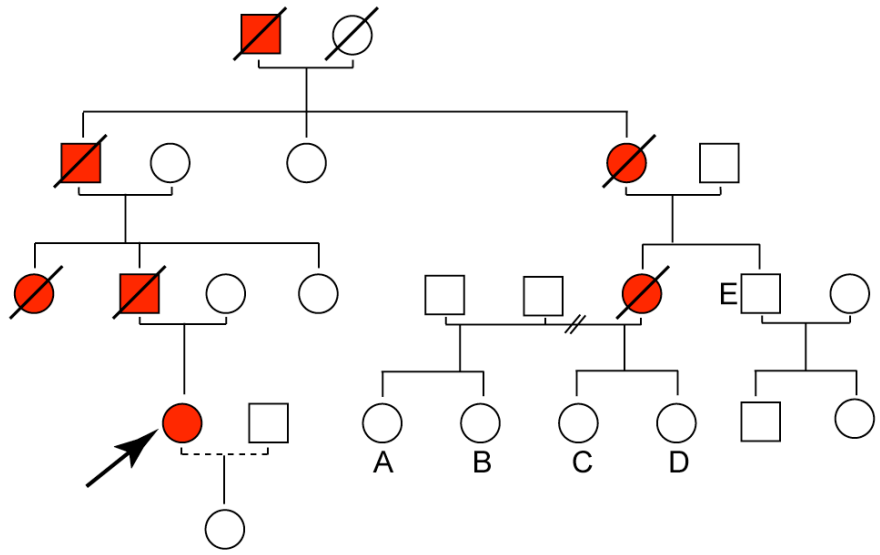

Figure 6.6 Family tree of Subject 3
Subject 3 indicated by arrow. Second cousins, labelled 'A-D'. Cousin once removed, labelled 'E'. Square, male; circle, female; red filled, affected individual; diagonal line, deceased.

Subject 3's mother, four second-cousins (A-D) and a cousin-once-removed (E) were available for phenotype analysis but had no symptoms relating to DCML deficiency at the time of analysis. E was 44yrs old with 2 healthy children (aged 6 and 9yrs), born at term. 2nd cousins A-D were 25yrs, 23yrs, 22yrs and 18yrs old with no medical problems. A had 2 young, healthy children also born at term.

The subject's daughter was born prematurely at 28 weeks. This is a recognised complication of DCML deficiency as described by Vinh et al., 2010. At the age of 3yrs old there were still respiratory and nutritional problems relating to prematurity, but several full blood counts, taken during routine clinical care, showed no evidence of monocytopenia or lymphopenia.

None of the other subjects had any relevant medical family history.

6.4.3 Phenotype of Subject 3's relatives

PB Monocyte, DC and lymphocyte subsets were analyzed for subject 3's mother, four second-cousins and a cousin-once-removed (**Figure 6.7, A and B**). As the positive family history came from the paternal side, the mother was expected to be normal. Interestingly, she had a $CD14^+$ monocyte count below the normal range but was clinically entirely asymptomatic from this. The remaining members of the family tested had results at the lower end of the normal range (dotted lines in **Figure 6.7**). All were well at the time of testing.

In addition to phenotype analysis, granulocyte pellets were frozen for future DNA analysis.

Figure 6.7

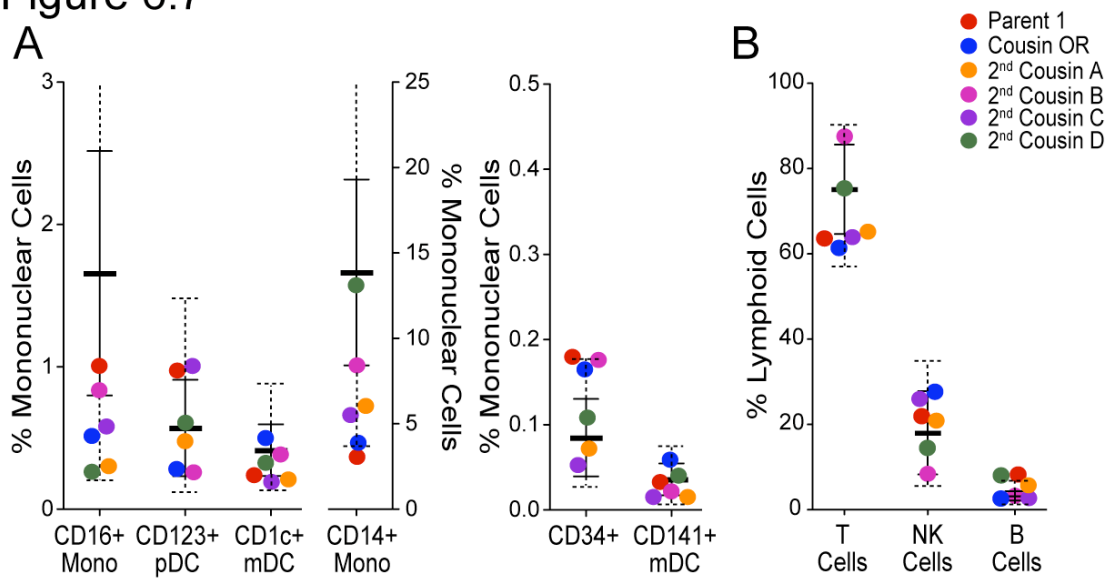

Figure 6.7 PB APC and lymphocyte quantitation for Subject 3's Relatives
Parent 1, red; Cousin one removed (OR), blue; 2nd cousin A, orange; 2nd cousin B, pink; 2nd cousin C, purple; 2nd cousin D, green.
A: Proportion of $CD16^+$monocytes, pDC, $CD1c^+$mDC and $CD14^+$monocytes, $CD34^+$ progenitors and $CD141^{high}$mDC expressed as % of PBMC. Controls n=28
B: Proportion of $CD3^+$ T cells, $CD56^+CD3^-$ NK cells and $CD19^+$ B cells expressed as % of cells in the lymphoid SSC/FSC gate. Contorls n=11. Error bars indicate mean+/-SD. Dashed bars represent range of normal values.

6.4.4 Gene expression in $CD34^+$ compartment

Based on genes found to be important in murine DC development, the consequences of their disruption, and the observation of elevated serum Flt3L

and M-CSF levels in the subjects, PB $CD34^+$ cells, from subjects 3 and 4, were analyzed for mRNA expression of a number of genes. $CD34^+$ cells from PBMC were flow sorted by FACS from subjects 3 and 4, and 2 healthy controls. **Figure 6.8** shows the results of Q-PCR for STAT3, IRF8, Flt3, PU.1 and M-CSF-R. The results are expressed as mean of 2 subjects normalised against mean of 2 controls, with each analysis performed twice. M-CSF-R mRNA, although detectable in controls, was undetectable in subjects (equivalent to <0.8% of controls). IRF8 expression was markedly reduced while Flt3 and PU.1 mRNA levels were approximately half that of controls. STAT3 was mildly reduced at 78% of normal.

Figure 6.8

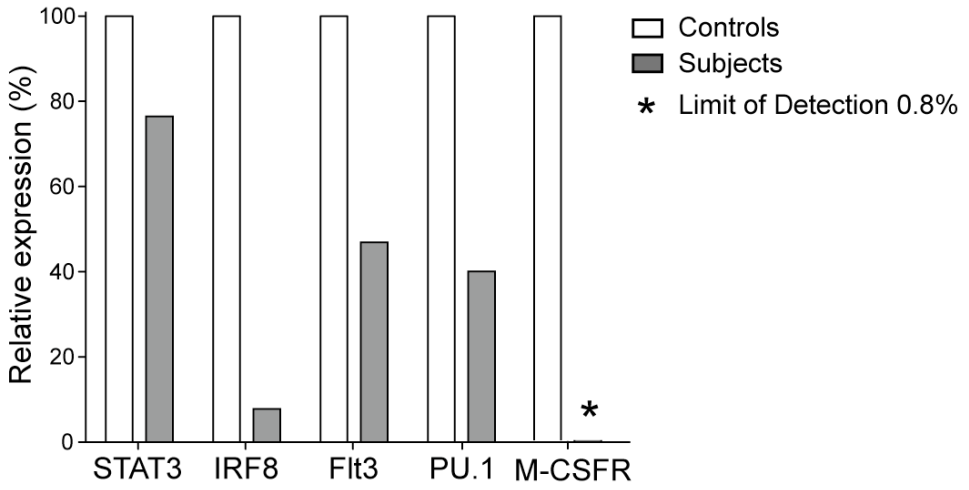

Figure 6.8 QPCR mRNA expression analysis in PB $CD34^+$ cells of subjects 3 and 4, compared to normal controls.
Grey bars indicate the mean relative expression of subjects 3 and 4. Unfilled bars indicate mean of controls, normalised to 100% expression. STAT3, signal transducer and actiator of transcription 3; IRF8, interferon response element 8; Flt3, fms-like tyrosin kinase 3; PU.1/SPI1; M-CSFR, macrophage colony stimulating factor receptor.

6.4.5 Gene sequencing

A number of candidate genes have been sequenced in the DCML subjects. Subject 1's DNA was sent for IRF1 and IRF8 sequencing (Philippe Gros' laboratory, Department of Biochemistry, McGill University, Montreal, Canada), and Flt3, Flt3L and Gfi-1 sequencing (Jacques van Dongen's laboratory, Department of Immunology, Erasmus Medical Centre, Rotterdam, The

Netherlands). SPI1/PU.1 gene in subject 3's granulocyte and fibroblast DNA was prepared in our laboratory (Sarah Pagan and Rachel Dickinson) and sequenced in Dundee (see **Figure 6.1**). No mutations have yet been identified. However, the upstream regulatory element (URE; proximal and distal units – PRU and DRU), located 17kb upstream of the transcription start site, has not yet been sequenced.

6.5 Discussion

The phenotyping of subject 5 lead directly to the diagnosis of autosomal recessive IRF8 deficiency, the first recognised genetic cause of DC deficiency in humans. Although very similar, the phenotype of DCML deficiency suggests an alternative defect which is yet to be identified. Meanwhile, analysis of the $CD34^+$ compartment in these disorders has revealed not only further differences between the two conditions but also allows some inferences about DC and monocyte haematopoiesis to be drawn.

6.5.1 IRF8 deficiency

IRF8, a member of the Interferon Regulatory Factor family, is expressed at highest levels in DC (184) and plays a role both in DC differentiation (185) and the transcription response to interferons (186) and toll like receptor agonists (187). The IRF8 sequence is highly conserved across species and $IRF8^{-/-}$ mice have a very similar phenotype; they lack monocytes, pDC, and mDC and show marked myeloproliferation (85).

As IRF8 is expressed almost exclusively in the haematopoietic system, it was likely that HSCT would be curative for IRF8 mutation, and no further consequences of germ line IRF8 mutation would be expected. Subject 5 received a matched unrelated donor cord blood transplant at the age of 9 months and is alive and well at 1yr post-transplant. There was no overt clinical or cellular phenotype associated with K108E heterozygosity, confirming the true recessive nature of this condition.

6.5.2 CD34$^+$ progenitor compartment

It has previously been demonstrated that DC potential resides in both myeloid and lymphoid compartments in humans (106) (188). Doulatov et al., have recently described the MLP, able to form DC, macrophages and lymphoid cells at a single cell level, but lacking erythroid, granulocyte or megakaryocyte potential.

In keeping with the cellular phenotype of DCML deficiency, the MLP population in subjects 1-4 was absent. The GMP subset was also markedly reduced. Although clearly being able to support granulopoiesis, as the subjects had normal numbers of circulating neutrophils and eosinophils, they were unable to give rise to monocytes or DC.

The phenotype in the CD34$^+$ progenitor cell compartment proves that DCML deficiency arises as the result of a defect in bone marrow haematopoiesis. It also suggests that MLP at least contribute to the normal homeostasis of DC and monocytes and is consistent with models of haematopoiesis in which DC and monocytes may arise from both lymphoid (MLP) and myeloid (GM) origins (106), (188), (89).

In comparison, IRF8 deficiency results in a defect later in DC ontogeny, as accumulation of MLP and GMP is seen. It is likely that myeloproliferation, driven by raised Flt3L, occurs as GMP are present in large numbers, are unable to differentiate down the DC/monocyte route but maintain their granulocyte differentiation potential. DCML deficiency subjects, despite massive elevation of Flt3L, are not myeloproliferative, again suggesting an earlier block in differentiation with either reduced responsiveness to Flt3L or insufficient numbers of GMP to allow myeloproliferation.

6.5.3 Genetic work-up of DCML deficiency: Hereditability

In order to observe the complete absence of a haematopoietic cell population due to a genetic lesion, the defect must be germ line or haematopoiesis must be clonal, having acquired a somatic mutation that confers a selective proliferative advantage. It is also conceivable that a germ line mutation may predispose to the development of clonal haematopoiesis through a

predisposition to the acquisition of a further mutation(s), such as in the case of Fanconi's anaemia. This is an autosomal or X-linked recessive disorder of DNA repair that leads bone marrow failure, and the development of haematological and/or solid tumours, probably due to the acquisition of further mutations.

Another explanation is that the DCML mutation causes a stromal defect which renders the tissues unable to support DC. This was ruled out as both subjects 1 and 3 showed complete repopulation of PB and tissue DC and monocyte subsets following haematopoietic stem cell transplantation.

The family pedigree of subject 3 strongly suggests an autosomal dominant inheritance of a germ line mutation. The potential contradiction in this family tree is that none of the four second-cousins appear to be affected. In an autosomal dominantly inherited condition, the chance of four unaffected children being born to an affected parent is 6.25%. As the youngest is only 18yrs and presentation of DCML deficiency can be as late as the 5^{th} decade, it is possible that the phenotype is not yet apparent. However, subject 3 had a documented monocytopenia from the age of 10yrs and all affected relatives died in their 30s or early 40s with a prodromal illness of some years.

The other three cases appear sporadic with no parental history of relevant illness. One pedigree shown in the case series by Vinh et al., (170) describes an affected individual who had clinically unaffected parents but produced a son who had severe HPV infection and died of leukaemia at the age of 17yrs, symptoms suggesting he also had DCML deficiency. This implies that the sporadic mutation in this case, originated at meiosis, giving rise to a germline mutation. The children of our subjects (subject 3, 1 child; subject 4, 2 children) have not been tested as all are under 10 years old and clinically well.

It is hoped that comparison of DNA from fibroblasts and the haematopoietic system (available for subjects 3 and 4) may reveal whether any potential mutations were constitutional or acquired somatic mutations restricted to the haematopoietic compartment. Whether a molecular recessive mutation is sufficient to acquire the disorder, or whether a homozygous state is required is not clear at present. Inheritance that is consistent with an autosomal dominant

trait but recessive molecular pathology is shown by many cancer genes, for example retinoblastoma (189).

There is some variation in the age of presentation, even within kindreds, and a significant variation in the type of symptoms experienced, despite a remarkably similar cellular phenotype. This phenomenon is also seen in paediatric immune deficiencies where mutations in one gene can be associated with a number of different phenotypes (190). However, the reverse is also true where several different genetic mutations can result in a similar phenotype. The phenotypic differences in DCML deficiency may therefore reflect the different environmental challenges encountered, the different consequences of mutations within one gene or suggest different genetic mutations which happen to result in a similar cellular phenotype.

6.5.4 Genetic work-up of DCML deficiency: Candidate genes

A number of candidate genes were sequenced in DCML deficiency subjects. The initial prime candidate was Flt3 as it has been shown to be essential for mouse DC development. Although high Flt3L levels can lead to down-regulation of Flt3 (164), a mutation of Flt3 could have been the primary defect. However, Flt3 mRNA was detectable in PB $CD34^+$ progenitors by Q-PCR, at 40.1% of normal and no mutation was found on sequencing the gene.

Figure 6.9 shows a diagramatic representation of the potential integration of signalling pathways for FLt3L, GM-CSF and M-CSF based in part on a figure from (191). Flt3 signalling is dependent on STAT3 (183) which in turn activates PU.1 and Flt3 itself. IRF8 and M-CSF-R are also downstream targets (126) (130). Stat3 and PU.1 mRNA were detectable in PB CD34+ cells at 76.5 and 46.9% of normal, respectively, and no PU.1 mutation was detected on gene sequencing. IRF8 and M-CSF-R are also downstream targets of Stat3 signalling. mRNA analysis, again from PB CD34 progenitors, showed a marked reduction in IRF8 mRNA (7.8% of control levels) and M-CSF-R was virtually undetectable (threshold 0.8%). However, IRF8 gene was sequenced in one DCML subject and found to be wild type. M-CSF-R mutation as a primary lesion is less likely as mice with CSF-1R deficiency show primarily macrophage

deficiencies, including osteopetrosis, and also lack LC. Interpretation of mRNA levels is slightly complicated by the absence of MLP and reduced numbers of GMP in DCML deficiency subjects compared to controls. It is therefore difficult to assess whether reduced levels of a particular mRNA are due to absence of a cell subset or due to reduced gene expression in all cells.

Figure 6.9

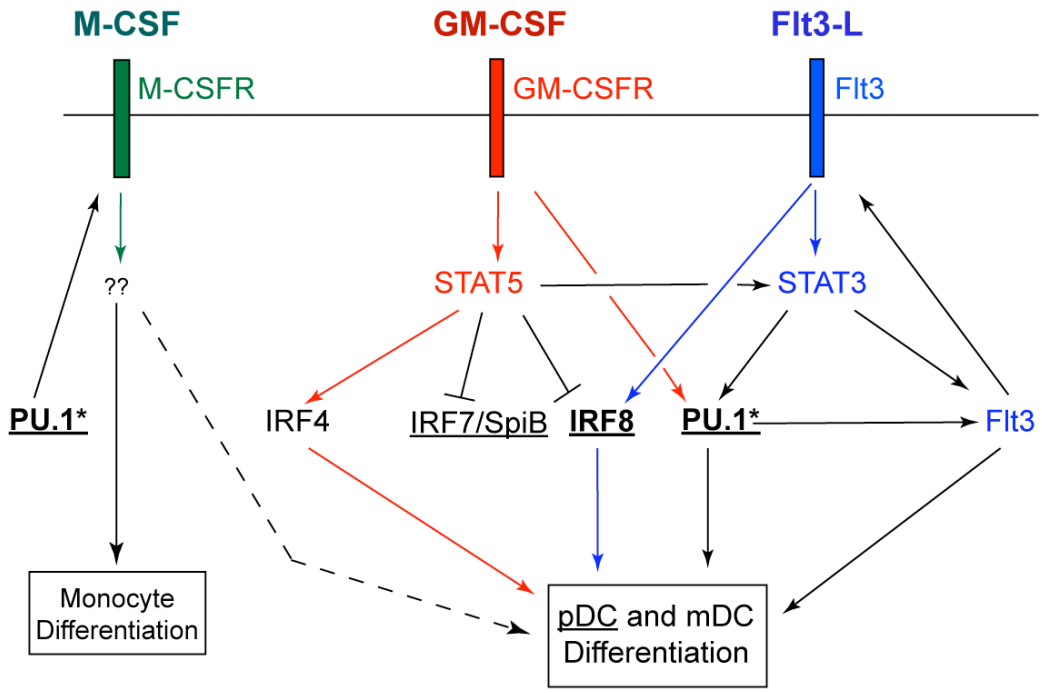

Figure 6.9: Integration of Growth Factor signalling pathways
Direcly adapted from Onai and Manz, 2008, Immunity. Underlined TFs indicate those important for pDC development in mouse.

A number of other candidate genes have been sequenced in DCML deficiency, both in our subjects and those described by Vinh et al.. (170). In our subjects, the list of genes sequenced to date, with no mutations identified, includes PU.1, Flt3, Flt3L, Gfi-1, IRF1 and IRF8. Vinh et al., also sequenced the following genes: IL12Rb1, IFNGR1, IFNGR2, Stat1, Stat2, JAK2, GNB2L1, CSF2, CSF2RB, C/EBPA, C/EBPB, C/EBPD, C/EBPE, RUNX1, IRF4, ICSBP1, PDGFRB, RhoH, HSP90AB1, CXCL14, CCR5, CSCR4, CSCL12 (SDF-1) with no mutations found. A number of potential candidates have therefore not yet been sequenced, including stat3, stat5, IRF2 and Id2.

Another area of particular interest is the upstream regulatory element (URE) of PU.1. Targeted disruption of this URE has been shown to reduce PU.1 expression by 80% (134). Sequencing of this region is in progress.

Work on the genetic basis of DCML deficiency is therefore ongoing.

6.5.5 Further biological implications

The absence of DC, B- and NK-cells in DCML deficiency, together with the absence of the MLP, suggests that at least some of these cells share a common origin from HSC up to, and including, the MLP. These observations are in keeping with the hypothesis that a divide into myeloid and lymphoid lineages is not the first step in haematopoiesis and that myeloid and lymphoid progenitors may loose erythrocyte and megakaryocyte potential prior to the myeloid/lymphoid division.

This may have implications for the pathophysiology of a number of haematological malignancies. These include biphenotypic leukaemia, characterised by leukaemic blasts expressing both myeloid and lymphoid antigens. Hairy Cell Leukaemia (HCL) presents typically with an absolute monocytopenia by standard blood counting methods, and the presence in PB and BM of leukaemic cells with DC-like cytoplasmic villi, expressing both DC and B cell antigens. Finally, the pathological cells of Hodgkin's Disease also express DC and B cell markers. Defining whether these diseases developed as disorders of stem cell differentiation, or due to the clonal expansion of more mature cells, may lead to identification of signaling pathways and potentially genes involved and would help define more specific treatment strategies.

6.6 Further work

Further work will aim to discover the genetic basis for DCML deficiency.

The following strategies are being taken:

1. Collaboration with John Dick's group (Division of Cell and Molecular Biology, University Health Network and Department of Molecular Genetics, University of Toronto, Toronto, Ontario M5G 1L7, Canada). Expression array data from

$CD34^+$ progenitor subsets has been collected and a list compiled of genes expressed preferentially in MLP and GMP, and a list of those in HSC, MLP and GMP.

2. 'Exomics' analysis of PB granulocytes and skin fibroblasts from subjects 3 and 4. The exomic sections of DNA from these samples will be sequenced and screened for mutations in candidate genes identified from the literature and the lists from John Dick's laboratory.

3. More detailed history of subject 3's family will be undertaken and any material suitable for genetic analysis from apparently affected relatives will be sought.

Chapter 7. Langerin Positive Dendritic Cells

7.1 Introduction

Langerin was so named after its discovery on Langerhans cells. It was believed to be specific to LC until the recent description of $Lang^+$DC subsets, independent of LC, in mouse spleen and peripheral tissues. Whether $Lang^+$ DC can be found in humans has not been examined.

7.1.1 Langerin History

Langerin has been presumed to be specific to LC as it was first identified on these cells, and so named, in 1999 by Valladeau et al. (192). It was shown to be C-type lectin, recognizing glycosylated moieties on pathogens. It is an endocytic receptor which, when internalised, associates with Birbeck Granules (71). Langerin is expressed on the cell surface, intracellularly in the endosomal recycling compartment and together with CD1a in Birbeck granules; tennis racket-shaped, cytoplasmic organelles (193).

7.1.2 Langerin expression in the mouse

As discussed in Chapter 1, langerin expression in mice is not specific to epithelial LC. It is also found on $CD8^+$ LN resident DC and on a proportion of interstitial skin, lung, liver and kidney $CD8^-CD103^+$ migratory DC (35). These $Lang^+$DC subsets have been shown in mice to be independent of LC by their GF requirement and different repopulation kinetics following bone marrow transplant (34). Work with KO mice has demonstrated the dependence of epidermal LC on M-CSF-R (110) and TGFβ (194), where $Lang^+$ dermal DC are dependent on Flt3 signaling (33) (195). $Lang^+$ DC were also distinguishable by their lack of expression of other LC markers, such as EpCam and E-Cadherin, both cell adhesion molecules, thought to be LC-specific (196) (197).

7.1.3 In vitro induction of human langerin expression

A number of *in vitro* systems have been shown to induce langerin expression on human cells. A proportion of $CD34^+$ cells, cultured with either GM-CSF and TNFα, or under the influence of TGFβ, show langerin expression. However, the

phenotype of langerin expressing cells, cultured with TNFα, more closely resembles that of a DC due to their expression of CD1c and CD11c and virtual lack of E-Cadherin (75).

Similarly, monocytes cultured with GM-CSF, IL-4 and TGFβ, but not those without TGFβ, express E-cadherin (83). However, $Lang^+$ cells differentiated from monocytes *in vitro*, unlike freshly isolated LC, were able to produce IL-12 in response to LPS stimulation (198), a function typical of DC (199). Whether these $Lang^+$ cells derived *in vitro* are LC, LC-like, or whether they are Langerin expressing DC is not clear.

7.1.4 Langerhans Cell Histiocytosis

Whether langerin is specific to LC has direct relevance to the pathophysiology of Langerhans cells histiocytosis (LCH). This rare, but potentially fatal condition is characterised by the accumulation of $Lang^+CD1a^+$ cells (LCH cells), admixed with lymphocytes, eosinophils, neutrophils and macrophages, in tissues including bone, bone marrow, skin, pituitary and central nervous system, liver, lung and gastrointestinal tract. Due to their langerin expression, LCH cells have been presumed to arise from LC. However, if langerin expression is not confined to epidermal LC, the cellular origin of the LCH cell may be questioned. Determining the origin of LCH cells is a critical step in the understanding of LCH pathogenesis and may potentially guide treatment strategies.

7.2 Materials and Methods for Chapter 7

7.2.1 FACS sorting of Langerin$^+$ skin cells from control skin

Whole skin, cut with a size 8 dermatome knife, was collagenase digested as previously described. Cells were filtered through a 100micron mesh and stained for flow cytometry with the equivalent of 1-2x10^6 cells in 50μl of flow buffer with 5μl of each antibody. After washing and resuspending the cells, DNAse I (Roche, www.roche.com) was added at 0.1mg/ml, to prevent cell clumping due to DNA release from dying cells during the 2-3hr sorting process. Cells were collected into RPMI and immediately pelleted and lysed in RNA lysis buffer prior

to dispatch on ice to Texas (Carl Allen, Texas Children's Cancer Center, Baylor College of Medicine, Houston, TX 77030) for QPCR analysis.

7.2.2 FACS sorting of Langerin$^+$ skin cells from clinical samples

Typically, a maximum of 100,000 cells would be available from a digested clinical skin biopsy, of which approximately 60% would be CD45$^+$, half of these HLA-DR$^+$ and 2/3 of these DC. Due to their rarity, cells were sorted directly onto glass slides, into a drop of buffer. Slides were allowed to air dry prior to fixing with cold methanol. This was achieved by pipetting 100μl drop of methanol onto the slide and allowing it to air-dry prior to 2mins in methanol in a coplin jar. The number of cells varied with the size of the biopsy and efficiency of the digestion.

7.2.3 LCH sample preparation

LCH lesions were processed to a single cells suspension for flow cytometric analysis. Lesion 1, vitreous fluid, was dissociated with a 20G needle and syringe and stained directly. Lesions 2, 3 and 5, biopsy of a neck mass, mouth lesion and sphenoid were dissected into pieces approximately 2mm diameter and digested in RF10 with 0.8mg/ml collagenase at 37^{0}C for 4hrs. These were then filtered through a 100micron filter and stained for flow cytometry. Lesion 4 was processed identically to all other skin samples as previously described.

7.3 Results I: Langerin positive Dermal DC

Langerin expression in humans has only been described on epidermal LC. Following the description of Lang$^+$DC in mouse dermis, the distribution of langerin expression in human skin was re-examined.

7.3.1 Flow cytometric analysis of langerin expression in skin

To determine whether human peripheral tissue DC populations, other than LC, expressed langerin in healthy tissue, whole skin was collagenase-digested and stained for flow cytometry with fluorescent antibodies against CD45, HLA-DR, CD14, CD1a and langerin, with a channel free for autofluorescence. The CD45$^+$HLA-DR$^+$AF$^-$ DC compartment of digested whole skin contained a population of CD1a^{bright} Lang$^+$ cells, consistent with the phenotype of LC (**Figure**

7.1, red gate). There was also a proportion of $CD1a^+$ cells seen to express langerin (**blue gate**) above background levels as defined by isotype control. This $Lang^+DC$ population (LDC) represented 1.47-7.53% (mean 3.67%, n=15) of $CD14^-$ cells in whole skin. There was no langerin expression seen in the $CD14^+DC$ or macrophage populations (not shown).

Figure 7.1

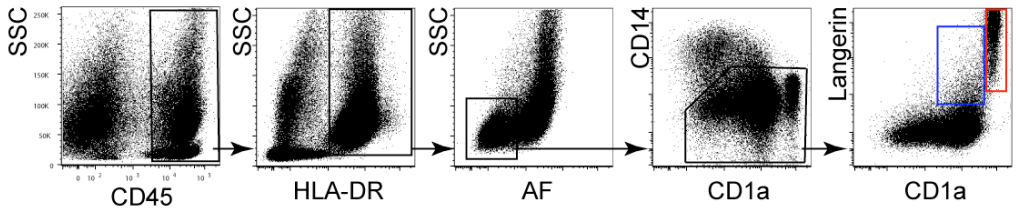

Figure 7.1 Gating strategy to identify LDC
Flow cytometric analysis of digested whole skin stained with anti- CD45, HLA-DR, CD14, CD1a and Langerin. Blue gate identifies $langerin^+DC$; Red gate includes $CD1a^{bright}$, $langerin^+$ LC; AF, autofluorescence.

7.3.2 Langerin$^+$ DC distribution in healthy skin

Having identified two possibly independent $Lang^+$ populations in whole skin, the compartmental distribution of these cells was examined. Dermis and epidermis were digested and analyzed separately. In addition to cells obtained through digestion, migrated cells were studied to assess the stability of the phenotype and the migratory ability of LDC. As both LDC and LC expressed CD1a, albeit at different intensities, Epithelial Cell Adhesion Molecule (EpCam), shown in mice to be specific to LC, was investigated as an antigen to distinguish between the two $Lang^+$ cells types.

$CD1a^+Lang^+$ LDC could be identified in digested dermis, but not in epidermis (**Figure 7.2, A**). In contrast to LC, and as predicted by mouse, LDC did not express EpCam. Identification of LDC by EpCam and Langerin expression demonstrated similar numbers of cells as by CD1a and Langerin expression, suggesting the same population was being described. When migrated cells were examined, similar proportions of LDC were found as to when the same skin preparation was digested (n=5). Migratory $CD1a^+Lang^+EpCam^-$ LDC could

be identified from dermis and whole skin, but not epidermis. CD1a and langerin expression were found to be slightly less intense on all migrated cells (**A**). LDC and LC were still distinguishable by their differing levels of CD1a and contrasting EpCam expression. The stability of the LDC phenotype during migration suggests that this population may constitute a DC subset independent of LC.

The ratio of number of LDC:LC in digested skin compartments, identified by CD1a and EpCam expression, suggested a compartmental independence of the two cell subsets (**B**). The highest ratio was found in digested dermis, where most LC had been removed when the epidermis was removed; the only remaining LC being those migrating via dermal lymphatics to skin-draining LNs. The lowest ratio was in epidermis, where only LC were found. Whole digested skin contained both subsets.

Figure 7.2

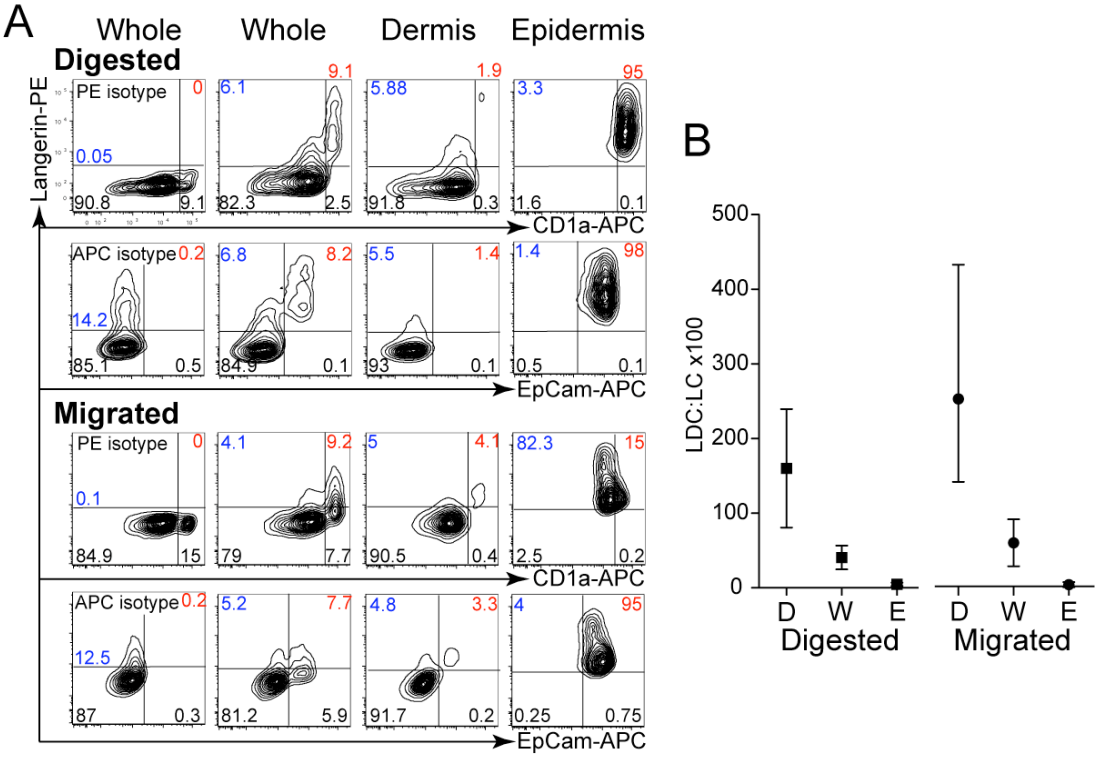

Figure 7.2 Flow cytometric comparison of LDC populations in Whole skin, Dermis and Epidermis

A: LDC populations identified by CD1a and langerin expression (top row) and EpCam and langerin expression (second row) from a single skin preparation digested as whole skin, dermis or epidermis. Isotype controls for PE (Langerin) and APC (CD1a and EpCam) shown in the first column.

Bottom 2 rows: identical analysis but of cells migrated from a single skin preparation as whole skin, dermis or epidermis. Representative example of 5 experiments.

Blue numbers: % of $CD45^{+}DR^{+}AF^{-}CD14^{-}$ cells falling in LDC gate

Red numbers: % of $CD45^{+}DR^{+}AF^{-}CD14^{-}$ cells falling in LC gate

Black numbers: % of $CD45^{+}DR^{+}AF^{-}CD14^{-}$ cells falling in DDC gate ($CD1a^{lower}$ $EpCam^{-}Lang^{-}$) and remainder. Contour plots are set at 5% probability.

B: Ratio of LDC:LC found in digested and migrated Dermis (D), Whole skin (W) and Epidermis (E). Bars show mean and range of n=4

7.3.3 Intracellular Langerin

As well as being expressed on the cell surface, langerin is known to exist intracellularly in endosomes and BGs in LC. Analysis of intracellular langerin in LDC was undertaken. Intracellular langerin staining identified similar proportions of LC and LDC as extracellular langerin staining in digested whole skin with CD1a or EpCam included (**Figure 7.3**).

Figure 7.3

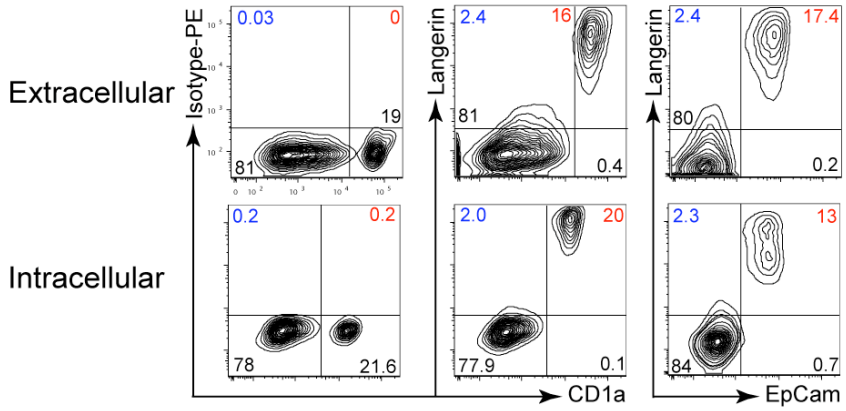

Figure 7.3: Flow cytometric analysis of Intra- and extracellular langerin expression in whole skin LDC and LC
1st column shows CD1a against extracellular (top row) and intracellular (bottom row) PE-IgG1k isotype control. Middle column shows CD1a expression against extra- and intracellular langerin. Last column shows EpCam expression against extra- and intracellular langerin. Numbers represent % of $CD45^{+}DR^{+}AF^{-}CD14^{-}$ cells falling in each quadrant: Red, LC; Blue, LDC; Black, DDC ($CD1a^{lower}EpCam^{-}Lang^{-}$) and remainder. Contour plots are set at 5% probability.

7.3.4 Distinct antigen expression profile of LDC compared to LC

In order to identify any antigens, besides EpCam, expressed discrepantly by LDC and LC, cells were examined for surface protein and cytoplasmic mRNA expression of a panel of DC- and myeloid-related antigens.

As part of an ongoing collaboration, LDC, LC and $CD1a^{+}$DDC populations were sorted locally by FACS and sent as RNA lysate to Carl Allen, Texas Children's Cancer Center and Hematology Service, Baylor College of Medicine, Houston, TX 77030, where they were interrogated with QPCR techniques to reveal mRNA expression differences (**Figure 7.4, B**).

While LDC showed surface expression of CD13, CD31, CD11c and CD11b, LC were negative for these antigens (**Figure 7.4, A**). When plotted against langerin, similar proportions of LDC were identified with these antigens as with CD1a or EpCam. mRNA expression results were concordant for these antigens, as well as CD207/langerin and EpCam. Although it was not possible to confirm the expression of E-Cadherin by flow cytometry, mRNA analysis showed greater expression in LC.

Figure 7.4

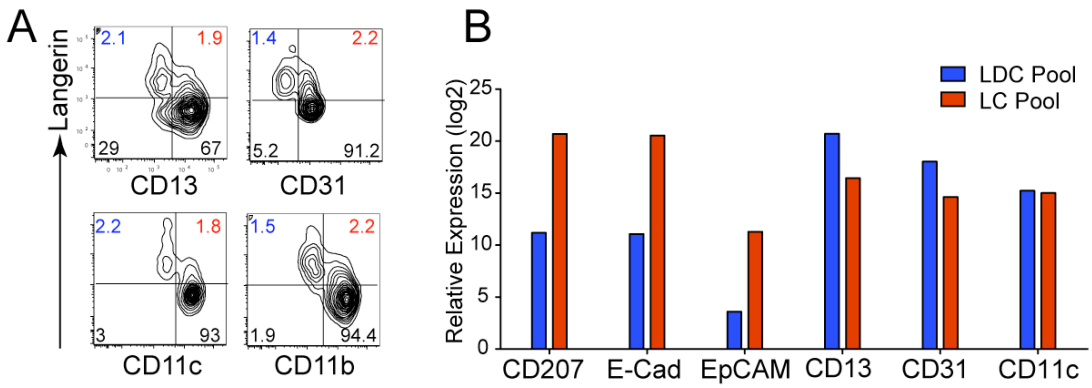

Figure 7.4 Protein and mRNA expression of antigens differing between LDC and LC

A: Flow cytometric analysis of CD13, CD31, CD11c and CD11b expression on $CD45^+DR^+AF^-CD14^-$ LC and LDC as defined by langerin expression. Contours are set at 5% probability.

Blue numbers: % of $CD45^+DR^+AF^-CD14^-$ cells falling in LDC gate

Red numbers: % of $CD45^+DR^+AF^-CD14^-$ cells falling in LC gate

Black numbers: % of$CD45^+DR^+AF^-CD14^-$ cells falling remaining gates.

B: QPCR data from Carl Allen, Texas Children's Cancer Center and Hematology Service, Baylor College of Medicine, Houston, TX 77030. Normal skin cellular material sorted and supplied by author. mRNA expression of Langerin (CD207), E-Cadherin (E-Cad), EpCam, CD14, CD31 and CD11c in FACS cell sorted, pooled LDC (blue bars) and LC (red bars) subsets (n=3). Data presented as expression relative to GAPDH, on log2 scale.

7.3.5 Microscopy of LDC and LC

To examine the cellular distribution of langerin in LDC and LC, these populations, together with $CD1a^+$DDC, underwent FACS cell sorting, according to the gating strategy in **figure 7.1**, using a panel of antibodies including mouse-clonal-anti-langerin antibody. The sorted cells were cytospun onto slides and then stained for cytology with giemsa staining, or immunofluorescence microscopy with goat-polyclonal-anti-langerin and rabbit-anti-goat-secondary, anti-HLA-DR and DAPI and imaged with Zeiss axioplan 2 microscope.

This revealed differences between LDC and LC in both the cellular morphology and the cellular distribution of langerin. Morphological differences were seen with giemsa staining **(Figure 7.5)**. $CD1a^+$DDC and LDC had similar appearances with more compact chromatin within the nucleus and a higher nuclear:cytoplasmic ratio than LC. LC were more likely to have preserved

dendrites. By fluorescence microscopy, examination of langerin expression revealed that LC had a distinct perinuclear distribution of langerin, particularly concentrated in the golgi zone, while LDC had a more diffuse cytoplasmic staining pattern. $CD1a^{+}$DDC showed no expression of langerin by microscopy.

Figure 7.5

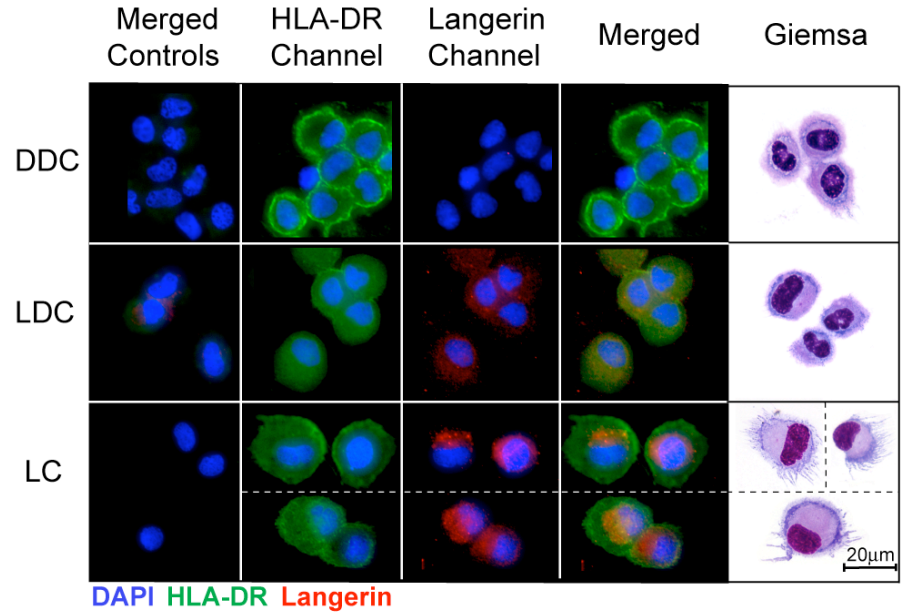

Figure 7.5 Fluorescence microscopy and Giemsa staining of DDC, LDC and LC
Cytospins of FACs sorted CD1a+DDC, Langerin+DC and LC from whole skin digest. Stained for fluorescence microscopy with DAPI, anti-HLA-DR-FITC, goat anti-langerin 1° + rabbit-anti-goat-555 2°. 1st panel shows staining with rabbit-anti-goat-IgG-555, IgG_{2Ak}-FITC and DAPI. Last panel shows giemsa staining of same sorted populations. Dotted lines indicate separate fields of view Fluorescence and light fields imaged with Zeiss axioplan 2 microscope.

7.3.6 Kinetics of LDC and LC chimerism following haematopoietic stem cell transplantation

Differing kinetics of APC donor chimerism have been seen at D40 following human HSCT when DDC are mainly donor in origin while LC remain predominantly recipient (73). In order to determine whether the homeostasis of LDC following HSCT was more similar to DDC or LC, the chimerism of skin LC (n=4), LDC (n=4) and $CD1a^{+}$DDC (n=2) was examined at Day 40 (D40) following sex-mismatched, reduced intensity conditioned, human HSCT. Patients had no prior or concurrent graft versus host disease (GvHD). This was

compared to the chimerism of peripheral blood monocyte and DC in paired samples. Peripheral blood $CD14^+$ and $CD16^+$ monocytes, mDC and pDC were sorted according to the gating strategy in **figure 7.6, A**. Whole skin shave biopsies from HSCT subjects were collagenase digested overnight and then cell populations sorted directly onto glass slides. From $CD45^+HLA\text{-}DR^+AF^-$ cells LC, LDC and $CD1a^+$DDC were identified as depicted in **Figure 7.6, B** (red, blue and green gates respectively). The number of cells sorted and fixed onto slides was variable. LC ranged from 4-349 cells/slide, LDC from 84-229 and DDC from 115-545 (**Table 7.1**).

Table 7.1

	Cell	No Collected	No examined by FISH	%Donor
1	LC	24	24	5.8%
	LDC	84	70	78.5%
2	LC	4	3	0%
	LDC	253	100	99%
3	LC	86	11	9%
	LDC	229	4	100%
	1a+DC	115	47	100%
4	LC	349	85	37%
	LDC	227	30	93%
	1a+DC	545	74	90%

These were examined by Fluorescence in situ hybridization (FISH) for X and Y-chromosomes. A minimum of 100 cells was counted, where possible, otherwise all cells present on the slide were assessed.

PB monocytes and DC were 100% donor at D40 in all patients studied. In skin, LDC and $CD1a^+$DDC had a mean % donor chimerism of 92.6% and 95.0% respectively, while LC showed a mean of 12.9% donor chimerism, significantly lower than LDC ($p=0.004$; paired t-test). The homeostasis of LDC following HSCT therefore more closely resembles that of DDC than LC, suggesting that these cells have a physiological behavior more in keeping with DDC.

Figure 7.6

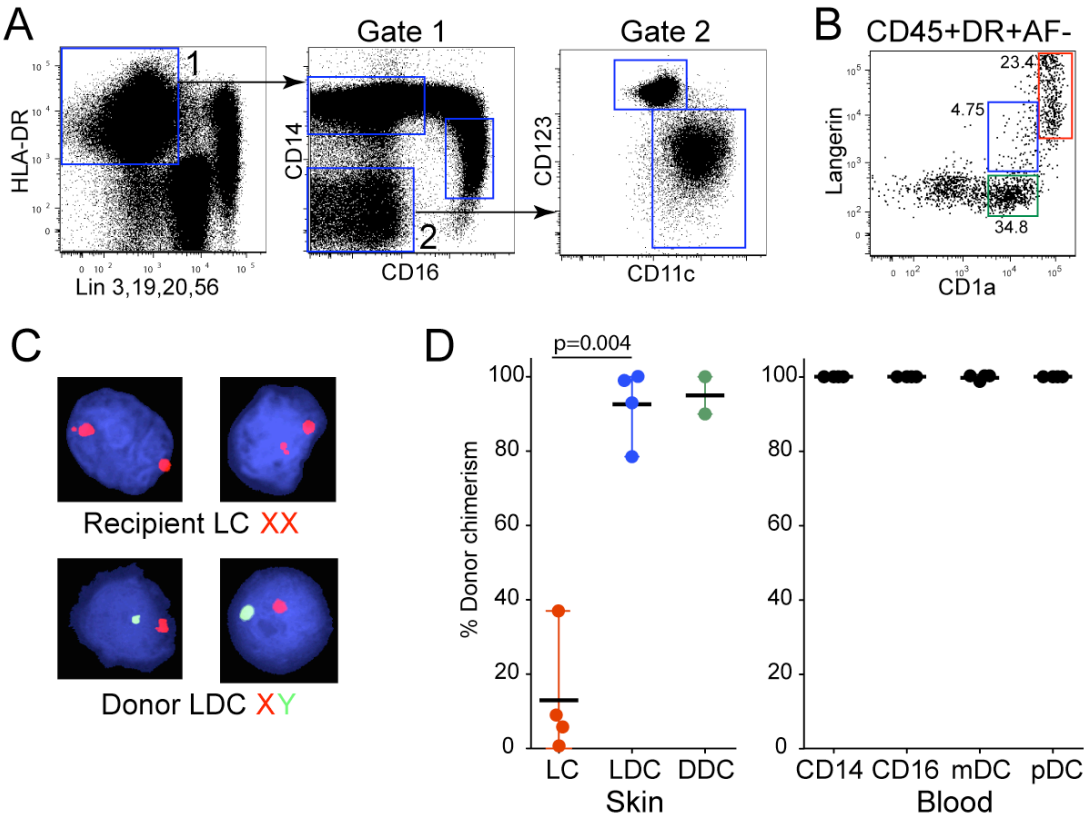

Figure 7.6 Chimerism kinetics of DDC, LDC and LC following BMT
A: Gating strategy for FACS sorting of PB Mono ($CD14^+$ and $CD16^+$) and DC subsets ($CD123^+$ pDC and $CD11c^+$ mDC) post-BMT.
B: Gating strategy for FACS sorting of $CD45^+DR^+AF^-$ cells from digested whole skin biopsy. Green gate, $CD1a^+$DDC; Blue gate, LDC; Red gate, LC. Numbers represent % of cells within each gate. C: FISH for X and Y chromosomes in two representative sorted skin LC and LDC from 1 sample. Red, X; Green, Y; Blue, DAPI. D: % of cells with donor chimerism in skin DC and PB monoctyes and DC, taken at D40 post BMT and assessed by X/Y chromosome FISH. >100 nuclei assessed where sufficient cells, otherwise all cells analysed. LC, Langerhans cells (red) n=4; LDC, $Lang^+$DC (blue) n=4; DDC, dermal DC (green) n=2 CD14, $CD14^+$ monocytes; CD16, $CD16^+$ monocytes; mDC, $CD11c^+$mDC; pDC, $CD123^+$pDC.

7.3.7 Langerin expression in dermis of DCML deficiency patients

As discussed in Chapter 5, DCML deficiency subjects maintain their LC population in the absence of other PB or dermal DC populations. Again to examine whether LDC and LC were homeostatically independent, the skin of DCML subjects was examined for the presence LDC.

Figure 7.7 shows $CD45^+HLA\text{-}DR^+AF^-CD14^-$ DC from digested dermis of subjects 1 and 4 compared to control (the same control as in **Figure 7.2**) with CD1a plotted against Langerin. As previously, $CD1a^{bright}Lang^+$ LC are gated in

red and CD1a^{+}Lang^{+} LDC in blue. Plots are normalised to display the same number of cells in the LC gate (30 cells). Subjects 1 and 4, despite the finding of migrating LC in the dermis, had no LDC. This is in marked contrast to digested dermis control where the ratio of LDC:LC was 3:1.

Figure 7.7

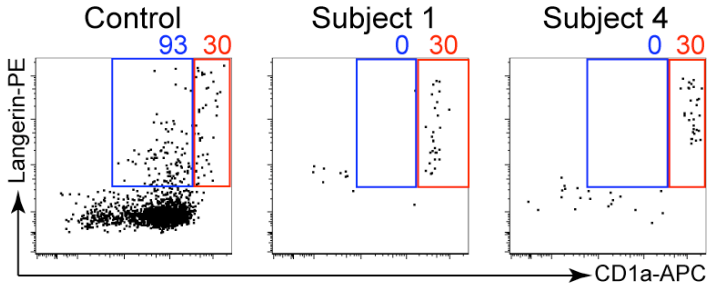

Figure 7.7 Langerin distribution in dermis of DCML deficiency subjects
CD45^{+}DR^{+}AF^{-}CD14^{-}DC from digested dermis of control and DCML deficiency subjects 1 and 4. Plots show CD1a against langerin. CD1a^{bright}langerin^{+} LC gated in red; CD1a^{lower}langerin^{+} LDC gated in blue. Numbers represent cells in the gate. Number of events displayed was adjusted to show 30 cells within LC gate.

7.3.8 Lung tissue

To examine the biological independence of LDC from LC, tissue with no resident LC population was examined. Macroscopically normal lung parenchyma from tumour resection specimens was examined. This was collagenase digested and analyzed with the same fluorochrome panel and gating strategy as for skin DC (**Figure 7.8, A**). As expected, no CD1a^{bright}Lang^{+} LC were present (red gate) but CD1a^{+}Lang^{+} LDC were found, representing 10.4% (mean of n=3, range 7.9-13.5%) of CD45^{+}HLA-DR^{+}AF^{-}CD14^{-} lung DC. Similarly to LDC in skin, these cells were negative for EpCam expression (**B**).

Figure 7.8

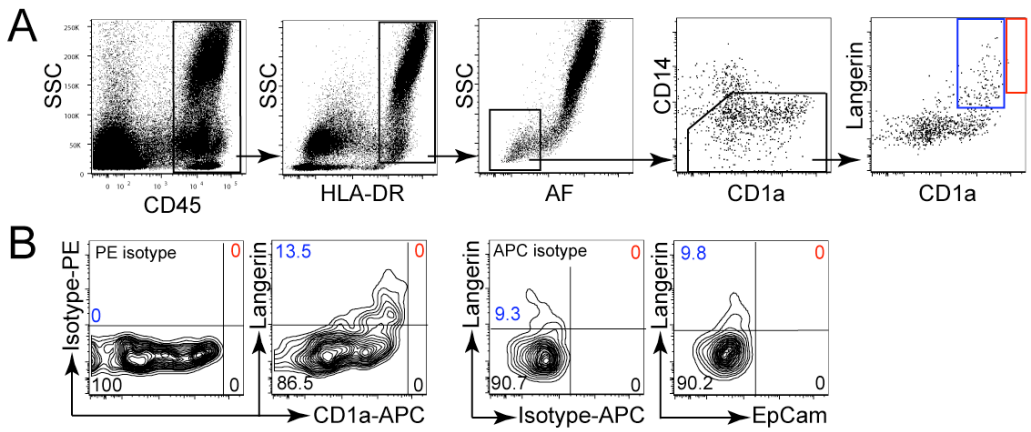

Figure 7.8 Lang^{+}DC in Lung parenchyma
Flow cytometric analysis of digested normal lung parenchyma.
A: similarly to DC gating strategy in skin, CD45^{+}DR^{+}AF^{-}CD14^{-} cells are identified. CD1a^{lower}Lang^{+} LDC (blue gate); CD1a^{high}Langerin+ LC (Red gate).
B: CD45^{+}DR^{+}AF^{-}CD14^{-} cells showing CD1a against PE-isotype control and langerin, and APC-Isotype control and EpCam against langerin. Numbers represent % of CD45^{+}DR^{+}AF^{-}CD14^{-} cells falling in each quadrant: Red, LC; Blue, LDC; Black, DDC (CD1a^{lower}EpCam^{-}Lang^{-}) and remainder. Contour plots are set at 5% probability.SSC, Side scatter; AF, autofluorescence

7.3.9 Langerin expression in PB

No langerin expression was seen on PB monocytes or DC in freshly isolated, ficoll-prepared PBMC. However, when cells from a leukoreduction chamber, or 'cone' were examined, 1.2% of CD11c^{+}mDC showed langerin expression (n=2) (**Figure 7.9**). No langerin was seen on monocytes or pDC, compared to isotype control. The Lang^{+} mDC were negative for CD1a expression.

Figure 7.9

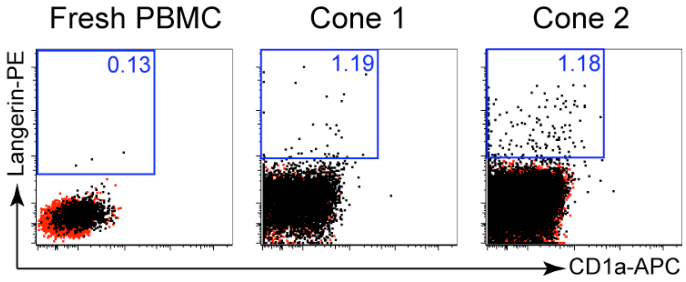

Figure 7.9 Langerin expression in CD11c+mDC from fresh PBMC and leukoreduction chambers
$Lin^{-}DR^{+}CD14^{-}CD16^{-}CD11c^{+}$ mDC plotted as CD1a against langerin. Cells from freshly isolated PBMC and 2 cones (Black dots); PE and APC isotype controls (Red dots). $Lang^{+}$ cells gated according to isotype (blue gate). Numbers represent % of mDC expressing langerin. Lin, lineage (CD3, 19, 20, 56); DR, HLA-DR; mDC, myeloid DC.

7.4 Results II: Analysis of LCH lesions

In order to explore whether LCH cells may more closely resemble LDC than LC, flow cytometry was used to further phenotype LCH cells and to compare them with the two $Lang^{+}$ cells subsets found in healthy skin: LDC and LC. In addition, the immunohistological diagnosis of LCH in routine clinical practice takes approximately 4-5 days. With the methodology available to extract single cells from tissues and analyse langerin-expressing cells by flow cytometry, the possibility of obtaining a diagnosis in a few hours became apparent.

7.4.1 Flow cytometric analysis of LCH lesions

Five lesions from four patients, suspected on clinical grounds to have LCH, were examined for the presence of $CD45^{+}HLA\text{-}DR^{+}CD1a^{+}Lang^{+}$ LCH cells by flow cytometry. Where sufficient material permitted, analysis for surface expression of DC-associated markers was undertaken. Clinical details of patients and anatomical locations of lesions are given in **table 7.2**. All material was from diagnostic biopsies of suspected LCH cases, with no prior treatment. Where solid material was received (lesions 2-5), this was collagenase digested for 4-12hrs prior to analysis. Where material was viscous (lesion 1) this was dissociated mechanically with needle and syringe prior to analysis.

Table 7.2

	Lesion 1	Lesion 2	Lesion 3	Lesion 4	Lesion 5
Age at presentation	3yrs	4yrs	Same patient as in 2	3yrs	2yrs
Anatomical location of lesion biopsied	Vitreous fluid	Neck mass	Mouth lesion	Skin lesion	Sphenoidal mass
Presenting features	Unilateral proptosis	Diabetes insipidus, neck swelling and mouth lesions	Diabetes insipidus, neck swelling and mouth lesions	Diabetes insipidus, scalp lesions and bone marrow involvement	Diabetes insipidus. Sphenoidal mass on MRI

Figure 7.10 shows flow cytometric analysis of five lesions, revealing in all samples $CD45^{+}DR^{+}AF^{-}CD1a^{+}Lang^{+}$ cells with a phenotype in keeping with LCH cells. Gated in this way $CD1a^{+}Lang^{+}$ LCH cells constituted 46-82% of lesional DC cells.

Figure 7.10

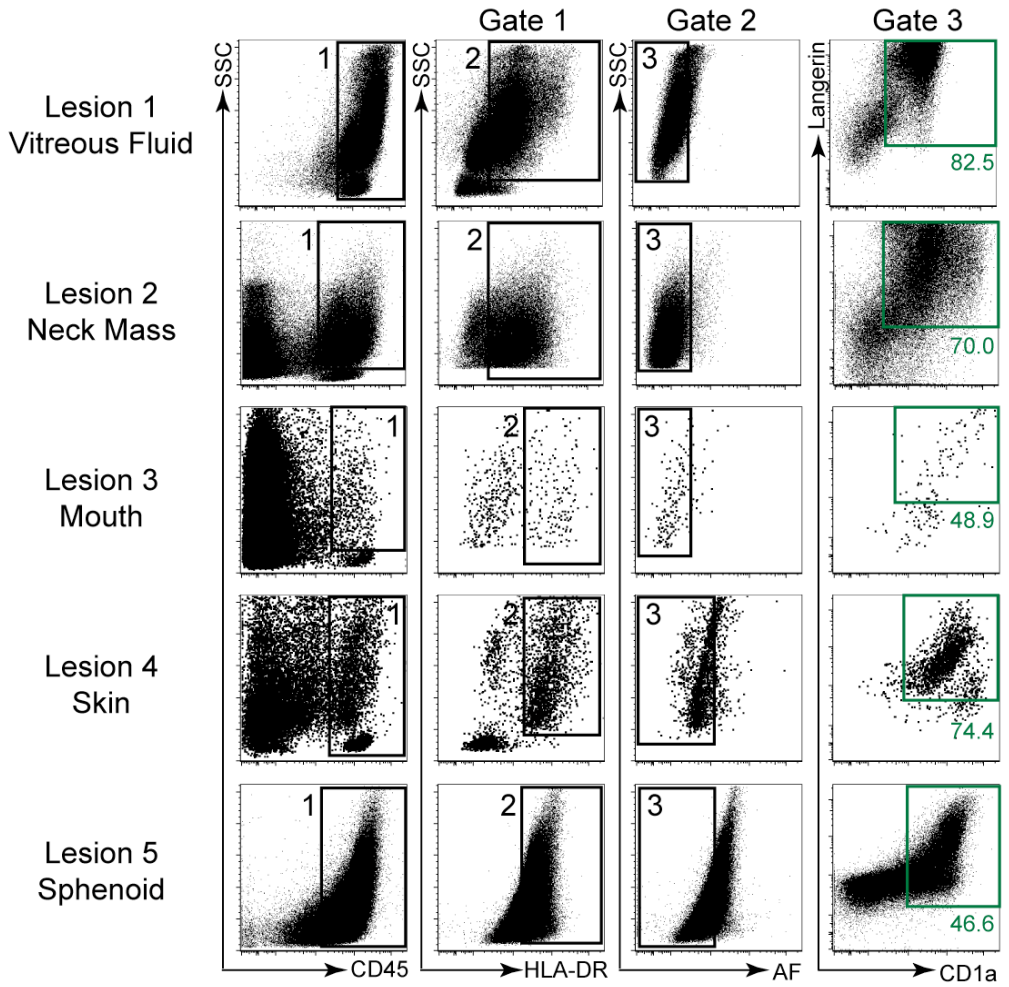

Figure 7.10 Flow cytometric diagnosis and analysis of 5 LCH lesions
Similarly to skin DC gating, CD45$^+$ (gate 1) HLA-DR$^+$ (gate 2) AF$^-$ (gate 3) cells were selected. LCH cells were identified as CD1a$^+$Langerin$^+$ (green gate). Green numbers represent % of cells in the LCH gate. SSC, side scatter; FSC, forward scatter; AF, autofluorescence

7.4.2 Antigen expression profile of LCH cells compared to LC and LDC

To determine whether LCH cells shared any phenotypic characteristics, other than langerin expression, with LC or LDC, the cell surface expression and mRNA levels of antigens found to be discrepant between LDC and LC were analyzed.

Phenotypic similarities of LCH cells to LDC by flow cytometry included the level of CD1a and CD11c expression and negativity for EpCam. Similarities with LC included lower expression of CD11b and CD13 (**Figure 7.11, A**). The intensity

of langerin expression on LCH cells fell between that of LC and LDC while expression of CD14 varied between lesions.

When interrogated by QPCR, results were concordant with surface expression of Langerin, EpCam and CD13. In addition QPCR for E-Cadherin and CD31 showed mRNA levels in LCH cells similar to LDC and $CD1a^{+}$DDC. No Langerin or EpCam mRNA was detected in the DDC pool (**Figure 7.11, B**). There was discrepancy between surface expression and QPCR results for CD11c. By flow cytometry, LC were clearly negative while LDC and LCH cells (and $CD1a^{+}$DDC, shown previously, **figure 3.10**) were positive. QPCR showed a greater similarity in CD11c mRNA although LCH cells were closest to $CD1a^{+}$DDC.

Figure 7.11

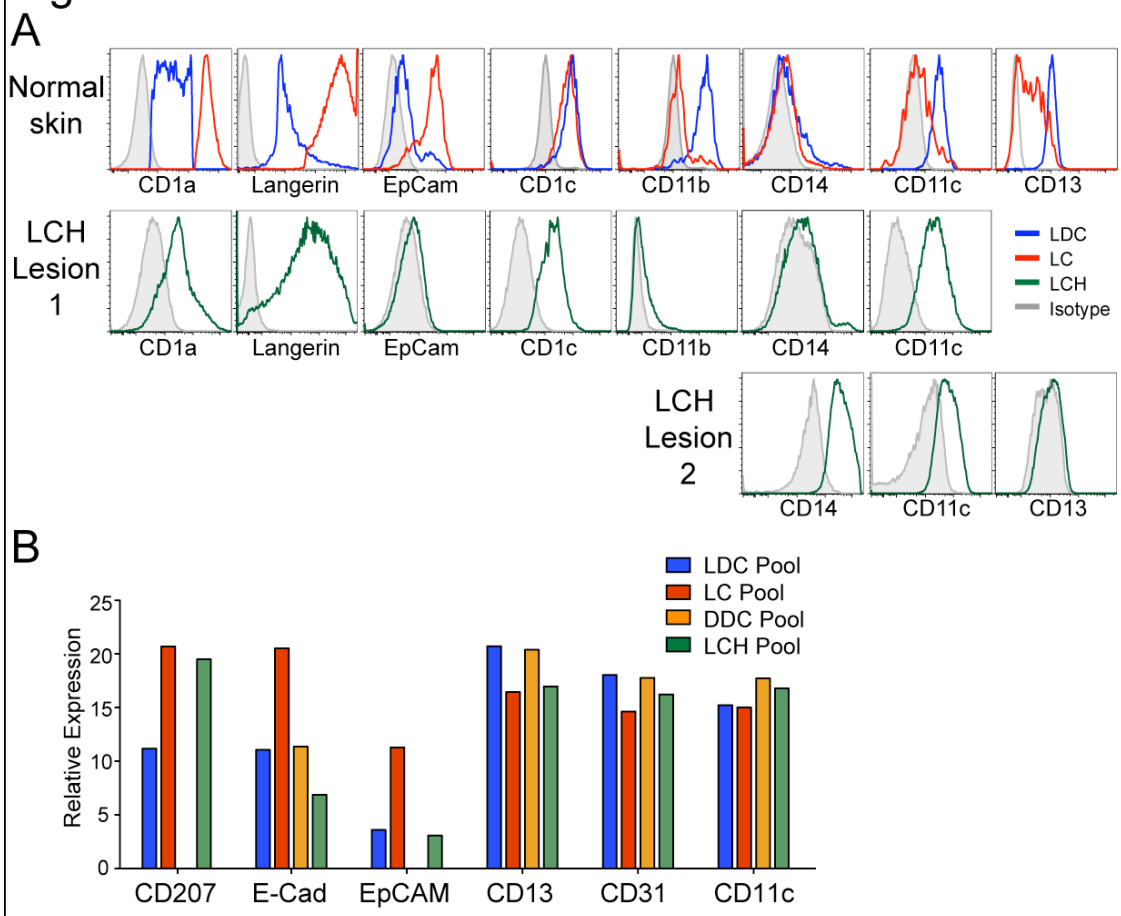

Figure 7.11 Surface antigen and mRNA expression in LCH compared to normal skin DC

A: Flow cytometric analysis of surface antigen expression of LCH compared to normal skin. LDC (blue histograms) and LC (red histograms). Isotype controls (grey histograms). 2 LCH lesions are included, LCH lesion 1 (neck mass), LCH lesion 2 (sphenoidal mass). B: QPCR data from Carl Allen, Texas Children's Cancer Center and Hematology Service, Baylor College of Medicine, Houston, TX 77030. Normal skin cellular material sorted and supplied by author. QPCR of pooled LDC (blue bars), LC (red bars) and CD1a$^+$DDC (orange bars) samples compared to Lang$^+$ cells from LCH samples (green bars) for langerin (CD207), E-Cadherin (E-Cad), EpCam, CD13, CD31 and CD11c. Normal skin LDC and DDC n=3 ; normal skin LC n=2 ; LCH n=4 Data presented as expression relative to GAPDH: 20-(Ct(N)-Ct(GAPDH)).

7.4.3 Cell cycle in LCH cells

Sufficient cells were available from lesion 2 (neck mass) for cell cycle assessment by Ki-67 and DAPI staining (**Figure 7.12**). Once again LCH cells were identified as CD45$^+$HLA-DR$^+$CD1a$^+$Langerin$^+$ and then singlets excluded by gating DAPI-area versus DAPI-width. 9.5% of LCH cells were found to be Ki-67$^+$ corresponding with cells in G1, S, G2 or M phase. However, there was

some background staining with isotype control so subtracting this gave a figure of 6.7% in cell cycle.

Figure 7.12

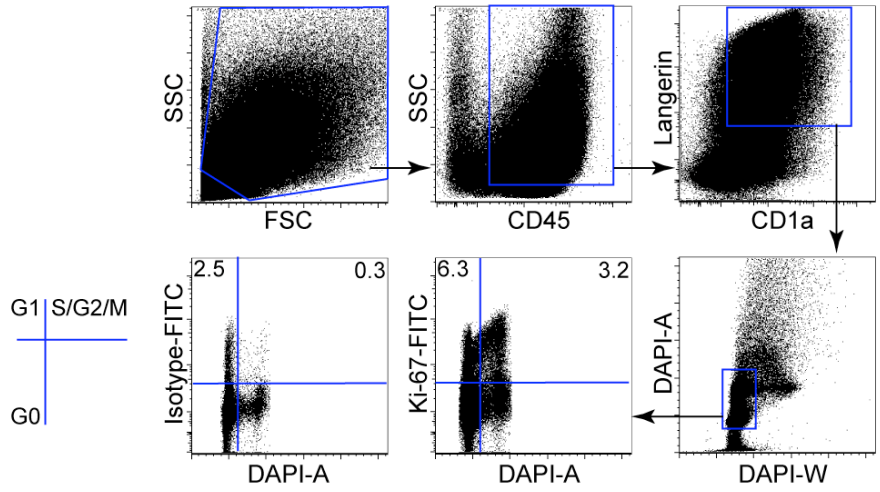

Figure 7.12 Flow cytometric Cell Cycle analysis by Ki-67 and DAPI staining
$CD45^+CD1a^+Lang^+$ cells selected. Doublets excluded by DAPI area versus width gating. Ki-67+ in G1, S, G2, M phase. FITC isotype shown bottom left plot.

7.5 Discussion

Langerin expression has been found on a subset of human dermal DC which have phenotypic distinctions from LC and appear to show different homeostatic mechanisms in disease. Furthermore, analysis of the $Lang^+$ LCH cell has shown it to be at least as closely related to this newly described LDC as to LC.

7.5.1 LDC represent a subset of DC distinct from LC

LDC appear phenotypically and homeostatically distinct from LC and may be more closely related to $CD1a^+$ dermal DC. Langerin expression in LDC is found to be genuine as it was seen by flow cytometry above background, compared to isotype controls, was found intracellularly, detected by microscopy and mRNA expression confirmed by QPCR. The distinction of LDC from LC is seen on a number of levels. LDC and LC show phenotypic differences in antigen expression, are found in distinct anatomical compartments, are able to exist and

maintain their numbers independently in different tissues and show distinct kinetics following HSCT. In contrast, LDC have phenotypic and homeostatic similarities with $CD1a^{+}$DDC as they express $CD11c^{+}$, $CD13^{+}$, $CD31^{+}$, $CD11b^{+}$, have similar morphological features and are replaced by donor cells at a similar rate following HSCT.

The identification of $Lang^{+}EpCam^{-}CD1a^{+}$DC in digested whole skin and dermis, and their absence from epidermis, suggests that these cells are anatomically distinct from $EpCam^{+}CD1a^{bright}$ LC of the epidermis. This is corroborated by the presence of LDC in lung parenchyma where LC are not found. The reverse is seen in the skin of DCML deficiency subjects who are able to maintain LC numbers despite the absence of DDC, including LDC.

Although the concept of LDC as LC precursors cannot be disproved, their presence in tissue devoid of LC, and their absence in DCML deficiency argues against this, at least as their inevitable fate. It is possible that the small numbers of cells available in DCML deficiency patient biopsies were below the level of detection, but were they necessary to maintain LC numbers they might be expected to be present in relatively increased proportions due to the absence of all other DDC subsets, whereas the reverse is seen.

In addition, LDC could be found in similar sized shave biopsies from patients who had undergone HSCT. Although this experiment was technically challenging, sufficient LDC could be sorted for successful analysis by FISH. The % donor chimerism found in LC and DDC is in keeping with a previous published study of the turnover of dermal DC following reduced intensity haematopoietic stem cell transplantation in the absence of GvHD, where the mean donor chimerism of $CD14^{-}$DDC at Day 40 was 91.0% and of LC was 43.1% (73). LDC in the four patients analyzed therefore compare more closely to DDC with a mean percent donor chimerism of 92.6% and 95.0%, respectively. In contrast, in the same experiment, LC were only 12.9% donor.

If DDC are reliant on blood borne precursors for maintenance of their numbers, as suggested by DCML deficiency and HSCT experiments, and as there is no langerin expression in fresh PB, it is likely that LDC up-regulate langerin in the

tissues. It will be critical to identify any factors that drive or trigger langerin expression, and whether this langerin-expressing potential is pre-programmed and inherent to a particular cell type, or dependent entirely on the microenvironment. Of interest is the observation of langerin expression on >1% of mDC isolated from cones. These cells have a very different *ex vivo* history from freshly isolated PBMC. Leukocytes are filtered into the cone during the 2-3hr platelet apheresis procedure, for which time cells in the cone will be at or near 37^0C. Following isolation of the cone from the apheresis circuit, it is stored at room temperature over night. Up to 2 $x10^9$ total cells and 1.5 x 10^9 PMBC can be isolated from a cone, from a volume of approximately 5-10ml (143). Cells are therefore massively concentrated both during their 2-3hrs at 37^0C and during storage overnight at room temperature. This inflammatory cellular suspension might be expected to have phenotypic differences to freshly isolated PBMC. Literature published on the viability and activity of cells has shown good results but in general cells have been analyzed 3hrs after the apheresis procedure, in contrast to the cones available for general use (200).

The ability to express langerin *in vitro* is seen in $CD14^+$ monocytes and $CD34^+$ progenitors in culture with inflammatory cytokines including GM-CSF and TNFα. As discussed previously, these culture conditions lead to the differentiation of cells to a phenotype more similar to LDC than LC; $CD11c^+CD1c^+CD1a^+$ and E-Cadherin negative/low (75). It may be that the addition of TGFβ is necessary for induction of more LC-like cells in terms of CD1a, Langerin and E-Cadherin expression (83) (201). Regardless of the semantics, the ability of non-LC cells to up-regulated langerin in culture or *ex vivo*, and independently of other antigens specific to LC, suggests that its expression is not sufficient to confer an LC phenotype.

7.5.2 Comparison with Murine Lang$^+$DC

Although $Lang^+$DC are found in mouse dermis, the expression of langerin on human LDC is not be sufficient to assign these cells the status of murine dermal $Lang^+$DC counterparts. In contrast to LC, both mouse and human dermal $Lang^+$DC express CD11c (77) but human LDC constitute a smaller population of dermal DC than in mouse. Murine $Lang^+CD8^-$ dermal DC represent 10% total

dermal DC and 2% of total dermal leukocytes (34). In contrast, LDC represent only 3.7% of $CD14^-$DC (3% of all DDC) and approximately 1% of total dermal leukocytes.

It has been shown that murine dermal $Lang^+CD8^-$ DC are related to $Lang^+CD8^+$ LN resident DC, by their dependence on Flt3 and IRF8 and their ability to cross-present antigen (35). More recently, this LN resident DC has been found to be similar to the human $CD141^{high}$ PB mDC in humans as both cell types express CLEC9A and XCR1 and can cross-present antigen (67). However, LDC do not fall in the human dermal $CD141^{high}$ cell populations identified in Chapter 3, as $CD141^{high}$ cells are all langerin negative (**Figure 3.10**). To determine whether there is functional homology between the langerin expressing DC subsets in mouse and human, further functional and phenotypic analysis of human LDC is required to determine whether these cells express CLEC9A and XCR1 and whether they are able to cross-present antigen.

7.5.3 LCH

The presence in LCH cells of langerin and CD1a on the surface, and Birbeck Granules intra-cellularly, has lead to the precept that these cells must originate from LC. Several key points raise the possibility that an alternative route to the LCH cell may be possible. For example, LCH cells may be inflammatory DC which have up-regulated Langerin, suggested by the following points: the demonstration of langerin on dermal DC independently of LC; the concept that langerin expression may be inducible; the known inflammatory nature of the LCH lesion and the tissue distribution of LCH lesions which it is not limited to tissues with resident LC populations.

Limited phenotypic and mRNA expression analysis of LDC, LC and LCH cells have shown that LCH cells are at least as similar to LDC, or even DDC, as they are to LC by the intensity of their expression of CD1a, CD11c, CD13 and lack of EpCam and E-Cadherin.

A critical step to taking this argument further will be to identify which cellular or soluble factors can induce expression of langerin in situations such as the cone

(and the LCH lesion). The study of PB monocytes and DC in patients with LCH, both their phenotype *ex vivo* and their culture responses *in vitro* may also shed light on potential circulating LCH cell precursors.

During the course of these studies, a flow cytometry technique has been developed for the diagnosis of LCH. This technique is fast, 4-12hrs from biopsy to result, as opposed to 4-5 days for immunohistochemistry, can be applied to any tissue biopsy, allows simultaneous analysis of large numbers of all lesional cell types and has the flexibility to add further diagnostic markers as LCH becomes better understood. However, it does not give the additional anatomical information afforded by histology. Further work is required to validate the results against standard histological findings and to test the negative predictive value of the test.

7.6 Further work

Further work will aim to:

i) Identify cellular or soluble factors involved in langerin expression and test their ability to induce langerin expression on potential DC precursors *in vitro*.

ii) Examine other normal tissues, including liver, gut and lymphoid tissue, to develop a map of langerin expression in humans.

iii) Examine human LDC for their expression of CLEC9A and XCR1 and ability to cross present antigen.

iii) Examine non-LCH inflammatory lesions to determine whether langerin up-regulation may be specific to LCH or seen also in other inflammatory conditions. For example, lesions of lichen planus have been shown to contain increased numbers of $Lang^+$ cells (202).

iv) LCH work will include analysis of PB for potential LCH cell precursors, analysis of lesions for soluble factors/cytokines and *in vitro* culture of potential precursors. The flow-cytometric diagnostic analysis will also be validated.

Chapter 8. Summaries, Conclusions and Further Work

8.1 Summary of novel findings

This work explores the homeostasis of DC and LC in health and disease. In the course of these studies methods to examine human peripheral blood, skin and progenitor cell compartments were developed to study the distribution of DC and their potential precursors. Whilst the identity of human DC-restricted BM progenitors and blood borne tissue-DC precursors remain unproven, a number of novel observations concerning DC homeostasis were made:

i) Cells phenotypically analogous to PB mDC and CD34$^+$ progenitors are found in the DC compartment of skin. These cells show characteristics which might be expected in 'pre-tissue DC' including expression of Flt3 and the potential to enter into cell cycle as demonstrated by Ki-67 expression.

ii) Autosomal recessive IRF8 deficiency presents in infancy and results in a near absence of monocytes and tissue DC. This demonstrates the *in vivo* reliance of DC and monocyte ontogeny on IRF8 signaling. The haematopoietic defect can be traced back to the progenitor cell compartment where accumulation of two CD34$^+$ populations, MLP and GMP, is seen, suggesting these cells may normally play a role in DC/monocyte ontogeny. Myeloproliferation is seen in association with raised Flt3L and expanded GMP compartment.

iii) The novel syndrome DCML deficiency presents in early adulthood with a propensity to mycobacterial and viral infections, is characterised by near absolute DC and monocyte deficiency in PB, with marked reduction in B and NK cells, and DC deficiency in tissues. Specific defects in bone marrow haematopoietic stem cell compartments are seen with absence of MLP and marked reduction in GMP, advancing the idea of a potential dual myeloid and lymphoid origin of DC. Despite massive elevation of serum Fl3L, there is no accompanying myeloproliferation suggesting a block in haematopoiesis earlier than seen in IRF8 deficiency.

iv) Human LC homeostasis is independent of PB precursors in the steady-state. IRF8 and DCML deficiency reveal that LC are able to self-maintain in the absence of potential blood-borne precursors. Demonstration of Ki-67^{+} LC suggests the mechanism of LC homeostasis involves self-renewal.

v) The model illustrating interdependence of Treg and DC homeostasis and Flt3L in mouse holds true in humans. In both IRF8 and DCML deficiency, depletion of DC is associated with reduction in Treg numbers and elevation of Flt3L, in keeping with the model proposed in mice.

vi) A population of Lang^{+}DC, independent of LC, is found in human peripheral tissues. A subset of DC in dermis and lung express langerin. They are shown to be most closely related to mDC through phenotypic analysis, and to be independent of LC by their differing homeostatic mechanisms in DCML deficiency and following HSCT.

vii) The pathognomonic Langerhans cell histiocytosis cell is at least as closely related to a dermal DC as to an LC. LCH cells share phenotypic characteristics with LDC and LC. This crucially influences the understanding of the origin of LCH cells and changes the emphasis of LCH research.

8.2 PB mDC as pre-tissue DC

The exact physiological function of PB mDC remains to be determined. They are unlikely to be able to interact directly with T cells in blood, requiring cell-cell contact. Therefore, in order to function as DC, they must be able to enter either peripheral or lymphoid tissue where they can encounter antigen and/or T cells. This has been shown for pDC which are found in lymphoid tissue but rarely in peripheral tissues, suggesting they transit directly from PB to lymphoid tissue.

A number of observations from this work have strengthened this argument: i) a significant proportion of PB mDC are Ki-67^{+} suggesting they have the potential to enter cell cycle. ii) Cells analogous to CD11c^{+}CD141^{high} and CD11c^{+}CD1c^{+} mDC are found in the CD1a^{-}CD14^{-} DC compartment of skin; iv) this skin compartment is where the highest proportion of cells in cell cycle is found,

excluding epidermal LC; v) When analyzing the CD141^{high} cells in skin, there is a spectrum of CD1c and CD1a expression, tempting speculation that these cells are able to acquire these markers, perhaps during maturation in tissues.

It is therefore conceivable that mDC act as pre-tissue DC in the steady state and are able to divide on receiving further signaling, potentially from tissues. Once in tissues, they are able to up-regulate 'traditional skin DC markers' including CD1a and CD1c.

Further work will aim to build evidence to support or refute this hypothesis through *in vitro* culture work, further analysis of the precise nature of cells in cell-cycle in the skin, detailed analysis of repopulation of dermal compartments following HSCT and comparative gene expression array analysis of PB and skin counterparts.

8.3 Circulating CD34$^+$ progenitors as immediate tissue DC precursors

It has been shown in mice that circulating progenitors can be found in peripheral tissues where they are able to divide and differentiate into myeloid cells, or even re-enter the circulation via the lymphatics (108). Work in this thesis has shown that CD34$^+$ progenitors are found in human skin where they are apparently able to express DC-related antigens, possibly before down-regulating CD34, as suggested by the absence of CD34 expression in migrating cell populations.

The circulating CD34$^+$ progenitors are enriched relative to BM for a subset hypothesised as a DC progenitor population, the MLP. Whether this subset is preferentially able to enter tissue will be the subject of further research.

Future studies will explore whether these circulating CD34$^+$ progenitors are able to contribute to the blood-derived support of tissue DC in the steady-state, possibly in a redundant or complementary system with PB mDC, and aim to clarify which specific CD34$^+$ subsets are able to perform this role *in vivo*. The contribution of monocytes to this steady-state process also requires investigation.

8.4 Autosomal recessive IRF8 deficiency

Through the DC profiling work, characterization of the first genetically identified defect associated with human DC deficiency has been made. Flow cytometric confirmation of the absence of monocytes and DC, in association with a myeloproliferation, led to the comparison of the phenotype with that seen in the murine model, and so to the diagnosis of IRF8 deficiency. In addition, the techniques were able to demonstrate that the heterozygous form of this IRF8 mutation is not associated with a cellular phenotype.

The cellular phenotype of IRF8 deficiency revealed the dependence of tissue DC but independence of LC and tissue macrophages on IRF8 signaling for their differentiation or survival. It also highlights the ability of LC to self-renew in steady-state and shows that this is not an IRF8 dependent phenomenon.

The accumulation of MLP and GMP suggests that IRF8 signaling is necessary beyond this stage of differentiation. However, the myeloproliferation shows that granulopoiesis is not dependent on IRF8 signaling and is likely to be driven by Flt3L signaling in the expanded GMP population.

Further work will examine the *in vitro* potential of IRF8 deficient $CD34^+$ progenitors to differentiate along DC and monocyte/macrophage pathways that may be relevant in steady-state or inflammation and examine responses to cytokines and growth factors in an attempt to further understand the IRF8 signaling pathways. In particular, the preservation of tissue macrophages in the absence of monocytes begs the question as to whether CD34+ progenitors can differentiate to macrophages without monocyte intermediates, even in IRF8 deficiency.

8.5 DCML Deficiency

In contrast to IRF8 deficiency, DCML deficiency was associated with an absence of MLP and marked reduction in GMP, suggesting a distinct but as yet unidentified genetic abnormality, likely earlier in the differentiation pathway. This haematopoietic phenotype was reflected in the circulating $CD34^+$ populations

which, despite a relative increase in numbers, was also depleted of MLP and GMP. The deficiency of MLP was, not unexpectedly, associated with reduced numbers of B and NK cells. Although granulopoiesis was maintained, there was no evidence of myeloproliferation, despite massive elevation of serum Flt3L concentrations, suggesting some reduction in granulopoietic potential, at least in response to Flt3L.

The preservation of LC despite the lack of circulating progenitors once again demonstrates the self-renewing capacity of LC. Again, some tissue macrophages could be identified, seemingly in reasonable numbers. However, the development of PAP, generally associated with poor alveolar macrophage function, suggests that these cells may have impaired function in DCML deficiency, at least in lung.

One very tangible consequence of the description of DCML deficiency and its identification as a bone marrow defect is the justification of therapeutic HSCT for patients with serious complications of the disease. This is proven by two of the four cases experiencing resolution of symptoms following HSCT. In contrast, one subject who was treated conservatively succumbed suddenly and unexpectedly to H1N1 influenza. In conversation with colleagues two similar cases came to light, although not proven to be DCML deficiency, they presented with PAP in association with clinical monocytopenia and died from their pulmonary failure due to progressive and untreatable alveolar proteinosis. Likewise, the early death of relatives of subject 3, if shown to be due to the same disorder, illustrates the fatal nature of this condition if left untreated. It is hoped that increased awareness of the disorder will allow other patients the opportunity for this curative treatment.

Further work will aim to:

i) Identify the genetic defect in DCML deficiency through ‘Exomics’ analysis, family DNA comparisons and, if necessary, other approaches such as microRNA analysis.

ii) Examine the *in vitro* potential of DCML deficiency $CD34^+$ progenitor subsets to differentiate to monocytes/DC under a variety of cytokine conditions, compared to IRF8 deficiency and normal controls.

iii) Analyse in more detail the tissue macrophage subsets present and assess their function.

iv) Follow cases of DCML deficiency longitudinally, through the early identification of any affected family members. Were the underlying genetic abnormality(ies) to be identified, this may allow diagnosis prior to the development of symptoms, or even potentially prior to the detection of a cellular phenotype, depending on the early natural history of the disorder and the compartmental localization of the genetic abnormality (germ line or somatic).

v) Disseminate knowledge of the disease for earlier identification and treatment of patients.

8.6 Flt3L concentration, Treg and DC homeostasis are interdependently regulated.

Analysis of Treg numbers and FLt3L concentrations in DC deficiency syndromes in humans has revealed the likely interdependence of these elements, as predicted by mouse models. In humans with varied genetic backgrounds and environmental influences, this relationship holds true in normal volunteers without the extremes of DC depletion or exogenous Flt3L administration. Further work will examine the influence of individual DC subsets to this relationship through the inclusion of larger numbers of controls and analysis of greater numbers of cells/control. In addition, Treg and Flt3L concentrations in conditions conferring loss of specific subsets of monocytes or DC (for example, hairy cell leukaemia – discussed later) will be examined.

8.7 Langerin expression is not specific to LC in humans

Langerin expression has not previously been knowingly described on any human non-LC cell. Work in the thesis has led to the suggestion that the langerin expressing DC in dermis is unrelated to the LC and more likely to represent a proportion of dermal $CD1a^+$ DC. This has been shown through both phenotypic analysis and observation of the different homeostatic behaviours in DCML deficiency and following HSCT. The presence of LDC in tissues lacking LC populations, and their presence in cell populations migrated from skin,

suggests that this is a relatively stable phenotype and not an immediate or inevitable precursor of LC.

Whether the human LDC bares any phylogenetic relationship to the murine $CD103^{+}Lang^{+}$ dermal DC remains to be studied. The murine $CD103^{+}$DC is know to cross-present antigen, express CLEC9A and XCR1, similarly to the human PB $CD141^{high}$ mDC. The expression of these antigens will be tested in human LDC and $CD141^{high}$ skin DC by mRNA expression analysis to determine if either or both subsets show any functional similarities with the murine $CD103^{+}Lang^{+}$DC.

Although langerin has been presumed to be a 'lineage marker' of LC, its expression on a subset of DC suggests this is not the case. In addition, langerin expression can be induced *in vitro* on monocytes or $CD34^{+}$ progenitors as they differentiate in response to inflammatory cytokines (including TNFα), or in response to TGFβ. Finally, the observation of langerin expression on $CD11c^{+}$ DC extracted from 'cones', and the unpublished observation of others, that langerin can be induced on PB mDC on overnight culture in the absence of any cytokines (38), suggests that induction of langerin expression is not necessarily specific to a single DC subset.

Further work will investigate factors triggering langerin expression, and the cell subsets in which this can occur, *in vitro*, particularly without the necessity for further cellular differentiation. Increased langerin expression is reported in some inflammatory conditions, such as in the lung of patients with smoking related 'Chronic Obstructive Pulmonary Disease' (203), and in some inflammatory skin diseases such as *lichen planus* (204). Further characterization of $Lang^{+}$ cells in these and related conditions may reveal them to be LDC, rather than LC, perhaps enabling comparisons to be drawn with LCH lesions and subsequently leading to insights into the regulations of langerin expression in tissues.

8.8 Langerhans Cell Histiocytosis

The origin of the LCH cells is of key interest when attempting to elucidate the pathophysiology of the LCH lesion. The possibility that the LCH cell is not a direct derivative of the LC highlights the relevance of studying other monocyte and DC compartments in the disease. We now have techniques to thoroughly and quantitatively interrogate all tissue DC compartments in patients with LCH and potentially identify any subtle changes in proportions or phenotype that may indicate aberrant homeostasis in 'DC-poiesis'.

Why some LCH cases present with a single lesion and some with multifocal or multisystem disease is entirely unknown. Mechanisms may include i) the dissemination of disease from an original focus, in a similar manner to metastatic cancer; ii) may reflect the normal tissue tropism of the LCH cell 'precursor'; iii) may be related to tissue factors which cause recruitment of LCH and other inflammatory cells at a local level. In any of these cases, a careful examination of PB populations, and their behaviour in inflammatory conditions, may shed light on circulating cells able to cause or respond to these conditions.

Whether LCH contains a malignant component, and if so, whether this is the driving force of the disease, is still debated. It is conceivable that a lesion, which may start as an inflammatory focus causing upregulation of langerin on a local or recruited monocyte/DC population, leads to the proliferation of these cells which have inherent ability to enter into cell cycle in tissues. This continuous polyclonal proliferation, under the constant stimulus of inflammatory cytokines, may result in the development of a malignant clone. If this were the case, it might be expected that individual lesions within one case of multisystem disease would have the potential to generate different malignant clones. However, this is not something that has been examined *in vivo* as, traditionally, only one affected site would be biopsied to make a diagnosis.

The recent identification of recurrent BRAF mutations in 57% of LCH lesions (205) lends weight to the argument that a malignant component can exist in LCH. Identifying whether the same mutation was present in all LCH lesions from one case would greatly enhance our understanding of the role of clonality and malignancy in LCH pathogenesis.

Further work will concentrate on:

i) Validating flow cytometric analysis as a rapid diagnostic test for LCH by comparison with traditional histopathological methods

ii) Defining and characterizing the cells in LCH lesions

iii) Further detailed comparison of LCH cell with *ex vivo* skin, PB DC/monocytes and cells differentiated under inflammatory conditions *in vitro*.

iv) Analysis of soluble mediators in serum and *in vitro* conditioned medium of LCH lesions to better understand the pathophysiology of LCH and identify potential disease markers or prognostic factors of use in the clinical setting.

v) Assessment of clonality and search for BRAF mutations, ideally in lesions from >1 site in individual cases. Additionally, the malignant potential of LCH cells or monocyte/DC from LCH patients (and normal controls) after long-term *in vitro* culture will be assessed.

8.9 Human lymphoid tissue

The clear next step in classifying human DC populations is to examine LN and splenic tissue. While normal human LN is rarely available, normal spleen is more commonly accessible as splenectomy may be performed due to trauma or therapeutically for disorders such as structural red cell abnormalities or immune related cytopenias. This would allow a far greater understanding of the dynamics of human DC populations and allow direct comparisons between the PB, peripheral tissue and lymphoid tissue populations.

8.10 Further avenues

Some of the concepts developed in this thesis have a broad application to both basic science and clinical medicine. In particular, the analysis of the bone marrow stem cell compartment, identification of specific defects leading to clearly defined cellular phenotypes and the concept of a myeloid/lymphoid split later in ontogeny than previously thought have implications in the pathology of haematological diseases and malignancies.

In particular, hairy cell leukaemia (HCL) is characterised by malignant cells expressing both B cell and DC markers. This raises the possibility that it could be related to an MLP defect, particularly as it is typically accompanied by an absolute monocytopenia as defined by automated blood counters. Investigation of the presence or absence of monocyte and DC subsets in this condition, further phenotyping of HCL cells and detailed analysis of the BM compartment may lead to insights into the pathophysiology of this disease and the genetic pathways of DC/monocyte ontogeny.

Chronic myeloid leukaemia (CML) is a myeloproliferative disorder defined by the presence of the t(9;22) translocation, or 'Philadelphia chromosome' (Ph) in malignant cells. As cells from the malignant myeloid clone are able to differentiate to apparently normal end-stage cells, it might be predicted that tissue DC, replenished by myeloid precursors, would also become Ph^+. Many groups have shown the ability of Ph^+ monocytes to differentiate to moDC *in vitro* but whether DC are involved in the malignant clone *in vivo* has not been studied. Using the Ph chromosome as a 'lineage marker' may provide insights into the lineage derivation of these cells, particularly with regard to the myeloid versus lymphoid haematopoietic divide.

8.11 Conclusion

Future work will aim to test the hypothesis that:

Human peripheral tissue DC are maintained in the steady state through replenishment by PB mDC and circulating $CD34^+$ progenitors in a redundant or complementary fashion. This process is amplified by the ability of precursors to proliferate within tissues. In perturbed situations, such as inflammation, where these mechanisms may be insufficient to support increased DC migration, or DC possessing specific functions are required, alternative precursors, such as the PB monocyte, may be recruited. The exception is the LC which has now been shown to be independent of blood-borne precursors in the steady-state with maintenance of numbers through self-renewal.

Advance, and never halt, for advancing is perfection.
Advance and do not fear the thorns in the path, for they draw only corrupt blood.
Khalil Gibran (1883-1931)

Somewhere, something incredible is waiting to be known.
Carl Sagan (1934 - 1996)

References

1. Gordon S. The role of the macrophage in immune regulation. Res Immunol. 1998;149:685-688.
2. Gordon S, Taylor PR. Monocyte and macrophage heterogeneity. Nat Rev Immunol. 2005;5:953-964.
3. McCusker K, Hoidal J. Characterization of scavenger receptor activity in resident human lung macrophages. Exp Lung Res. 1989;15:651-661.
4. Quinn JM, Gillespie MT. Modulation of osteoclast formation. Biochem Biophys Res Commun. 2005;328:739-745.
5. Guardiola J, Maffei A. Control of MHC class II gene expression in autoimmune, infectious, and neoplastic diseases. Crit Rev Immunol. 1993;13:247-268.
6. Trombetta ES, Mellman I. Cell biology of antigen processing in vitro and in vivo. Annu Rev Immunol. 2005;23:975-1028.
7. Steinman RM, Banchereau J. Taking dendritic cells into medicine. Nature. 2007;449:419-426.
8. Katz SI, Tamaki K, Sachs DH. Epidermal Langerhans cells are derived from cells originating in bone marrow. Nature. 1979;282:324-326.
9. Steinman RM, Cohn ZA. Identification of a novel cell type in peripheral lymphoid organs of mice. I. Morphology, quantitation, tissue distribution. J Exp Med. 1973;137:1142-1162.
10. Steinman RM, Witmer MD. Lymphoid dendritic cells are potent stimulators of the primary mixed leukocyte reaction in mice. Proc Natl Acad Sci U S A. 1978;75:5132-5136.
11. Schuler G, Steinman RM. Murine epidermal Langerhans cells mature into potent immunostimulatory dendritic cells in vitro. J Exp Med. 1985;161:526-546.
12. Witmer-Pack MD, Olivier W, Valinsky J, Schuler G, Steinman RM. Granulocyte/macrophage colony-stimulating factor is essential for the viability and function of cultured murine epidermal Langerhans cells. J Exp Med. 1987;166:1484-1498.
13. Cella M, Engering A, Pinet V, Pieters J, Lanzavecchia A. Inflammatory stimuli induce accumulation of MHC class II complexes on dendritic cells. Nature. 1997;388:782-787.
14. Robinson MJ, Sancho D, Slack EC, LeibundGut-Landmann S, Reis e Sousa C. Myeloid C-type lectins in innate immunity. Nat Immunol. 2006;7:1258-1265.

15. Janeway CAJ, Medzhitov R. Innate immune recognition. Annu Rev Immunol. 2002;20:197-216.
16. Itano AA, Jenkins MK. Antigen presentation to naive CD4 T cells in the lymph node. Nat Immunol. 2003;4:733-739.
17. Badovinac VP, Messingham KA, Jabbari A, Haring JS, Harty JT. Accelerated CD8+ T-cell memory and prime-boost response after dendritic-cell vaccination. Nat Med. 2005;11:748-756.
18. Macatonia SE, Hosken NA, Litton M et al. Dendritic cells produce IL-12 and direct the development of Th1 cells from naive CD4+ T cells. J Immunol. 1995;154:5071-5079.
19. Langrish CL, Chen Y, Blumenschein WM et al. IL-23 drives a pathogenic T cell population that induces autoimmune inflammation. J Exp Med. 2005;201:233-240.
20. Kapsenberg ML. Dendritic-cell control of pathogen-driven T-cell polarization. Nat Rev Immunol. 2003;3:984-993.
21. Villadangos JA, Schnorrer P. Intrinsic and cooperative antigen-presenting functions of dendritic-cell subsets in vivo. Nat Rev Immunol. 2007;7:543-555.
22. Hawiger D, Inaba K, Dorsett Y et al. Dendritic cells induce peripheral T cell unresponsiveness under steady state conditions in vivo. J Exp Med. 2001;194:769-779.
23. Brocker T, Riedinger M, Karjalainen K. Targeted expression of major histocompatibility complex (MHC) class II molecules demonstrates that dendritic cells can induce negative but not positive selection of thymocytes in vivo. J Exp Med. 1997;185:541-550.
24. Steinman RM, Turley S, Mellman I, Inaba K. The induction of tolerance by dendritic cells that have captured apoptotic cells. J Exp Med. 2000;191:411-416.
25. Albert ML, Jegathesan M, Darnell RB. Dendritic cell maturation is required for the cross-tolerization of CD8+ T cells. Nat Immunol. 2001;2:1010-1017.
26. Sakaguchi S, Ono M, Setoguchi R et al. Foxp3+ CD25+ CD4+ natural regulatory T cells in dominant self-tolerance and autoimmune disease. Immunol Rev. 2006;212:8-27.
27. Kim JM, Rasmussen JP, Rudensky AY. Regulatory T cells prevent catastrophic autoimmunity throughout the lifespan of mice. Nat Immunol. 2007;8:191-197.
28. Liu K, Victora GD, Schwickert TA et al. In vivo analysis of dendritic cell development and homeostasis. Science. 2009;324:392-397.

29. Swee LK, Bosco N, Malissen B, Ceredig R, Rolink A. Expansion of peripheral naturally occurring T regulatory cells by Fms-like tyrosine kinase 3 ligand treatment. Blood. 2009;113:6277-6287.
30. Darrasse-Jeze G, Deroubaix S, Mouquet H et al. Feedback control of regulatory T cell homeostasis by dendritic cells in vivo. J Exp Med. 2009;206:1853-1862.
31. Shortman K, Naik SH. Steady-state and inflammatory dendritic-cell development. Nat Rev Immunol. 2007;7:19-30.
32. Ardavin C, Wu L, Li CL, Shortman K. Thymic dendritic cells and T cells develop simultaneously in the thymus from a common precursor population. Nature. 1993;362:761-763.
33. Merad M, Manz MG. Dendritic cell homeostasis. Blood. 2009;113:3418-3427.
34. Ginhoux F, Collin MP, Bogunovic M et al. Blood-derived dermal langerin+ dendritic cells survey the skin in the steady state. J Exp Med. 2007;204:3133-3146.
35. Ginhoux F, Liu K, Helft J et al. The origin and development of nonlymphoid tissue CD103+ DCs. J Exp Med. 2009;206:3115-3130.
36. Autissier P, Soulas C, Burdo TH, Williams KC. Evaluation of a 12-color flow cytometry panel to study lymphocyte, monocyte, and dendritic cell subsets in humans. Cytometry A. 2010
37. Dzionek A, Fuchs A, Schmidt P et al. BDCA-2, BDCA-3, and BDCA-4: three markers for distinct subsets of dendritic cells in human peripheral blood. J Immunol. 2000;165:6037-6046.
38. MacDonald KP, Munster DJ, Clark GJ, Dzionek A, Schmitz J, Hart DN. Characterization of human blood dendritic cell subsets. Blood. 2002;100:4512-4520.
39. Ziegler-Heitbrock L, Ancuta P, Crowe S et al. Nomenclature of monocytes and dendritic cells in blood. Blood. 2010
40. van Furth R, Cohn ZA. The origin and kinetics of mononuclear phagocytes. J Exp Med. 1968;128:415-435.
41. Passlick B, Flieger D, Ziegler-Heitbrock HW. Identification and characterization of a novel monocyte subpopulation in human peripheral blood. Blood. 1989;74:2527-2534.
42. Almeida J, Bueno C, Alguero MC et al. Comparative analysis of the morphological, cytochemical, immunophenotypical, and functional characteristics of normal human peripheral blood lineage(-)/CD16(+)/HLA-DR(+)/CD14(-/lo)

cells, CD14(+) monocytes, and CD16(-) dendritic cells. Clin Immunol. 2001;100:325-338.

43. Sallusto F, Lanzavecchia A. Efficient presentation of soluble antigen by cultured human dendritic cells is maintained by granulocyte/macrophage colony-stimulating factor plus interleukin 4 and downregulated by tumor necrosis factor alpha. J Exp Med. 1994;179:1109-1118.
44. Sanchez-Torres C, Garcia-Romo GS, Cornejo-Cortes MA, Rivas-Carvalho A, Sanchez-Schmitz G. CD16+ and CD16- human blood monocyte subsets differentiate in vitro to dendritic cells with different abilities to stimulate CD4+ T cells. Int Immunol. 2001;13:1571-1581.
45. Becker S, Warren MK, Haskill S. Colony-stimulating factor-induced monocyte survival and differentiation into macrophages in serum-free cultures. J Immunol. 1987;139:3703-3709.
46. Takahashi K, Naito M, Takeya M. Development and heterogeneity of macrophages and their related cells through their differentiation pathways. Pathol Int. 1996;46:473-485.
47. Randolph GJ, Sanchez-Schmitz G, Liebman RM, Schakel K. The CD16(+) (FcgammaRIII(+)) subset of human monocytes preferentially becomes migratory dendritic cells in a model tissue setting. J Exp Med. 2002;196:517-527.
48. Cros J, Cagnard N, Woollard K et al. Human CD14dim monocytes patrol and sense nucleic acids and viruses via TLR7 and TLR8 receptors. Immunity. 2010;33:375-386.
49. Robbins SH, Walzer T, Dembele D et al. Novel insights into the relationships between dendritic cell subsets in human and mouse revealed by genome-wide expression profiling. Genome Biol. 2008;9:R17.
50. Ancuta P, Liu KY, Misra V et al. Transcriptional profiling reveals developmental relationship and distinct biological functions of CD16+ and CD16- monocyte subsets. BMC Genomics. 2009;10:403.
51. Fingerle G, Pforte A, Passlick B, Blumenstein M, Strobel M, Ziegler-Heitbrock HW. The novel subset of CD14+/CD16+ blood monocytes is expanded in sepsis patients. Blood. 1993;82:3170-3176.
52. Fingerle-Rowson G, Auers J, Kreuzer E, Fraunberger P, Blumenstein M, Ziegler-Heitbrock LH. Expansion of CD14+CD16+ monocytes in critically ill cardiac surgery patients. Inflammation. 1998;22:367-379.

53. Schakel K, von Kietzell M, Hansel A et al. Human 6-sulfo LacNAc-expressing dendritic cells are principal producers of early interleukin-12 and are controlled by erythrocytes. Immunity. 2006;24:767-777.
54. Skrzeczynska-Moncznik J, Bzowska M, Loseke S, Grage-Griebenow E, Zembala M, Pryjma J. Peripheral blood CD14high CD16+ monocytes are main producers of IL-10. Scand J Immunol. 2008;67:152-159.
55. Moniuszko M, Bodzenta-Lukaszyk A, Kowal K, Lenczewska D, Dabrowska M. Enhanced frequencies of CD14++CD16+, but not CD14+CD16+, peripheral blood monocytes in severe asthmatic patients. Clin Immunol. 2009;130:338-346.
56. Ross R. The pathogenesis of atherosclerosis: a perspective for the 1990s. Nature. 1993;362:801-809.
57. Geissmann F, Jung S, Littman DR. Blood monocytes consist of two principal subsets with distinct migratory properties. Immunity. 2003;19:71-82.
58. Auffray C, Fogg D, Garfa M et al. Monitoring of blood vessels and tissues by a population of monocytes with patrolling behavior. Science. 2007;317:666-670.
59. Randolph GJ, Ochando J, Partida-Sanchez S. Migration of dendritic cell subsets and their precursors. Annu Rev Immunol. 2008;26:293-316.
60. Perussia B, Fanning V, Trinchieri G. A leukocyte subset bearing HLA-DR antigens is responsible for in vitro alpha interferon production in response to viruses. Nat Immun Cell Growth Regul. 1985;4:120-137.
61. Cella M, Jarrossay D, Facchetti F et al. Plasmacytoid monocytes migrate to inflamed lymph nodes and produce large amounts of type I interferon. Nat Med. 1999;5:919-923.
62. Masten BJ, Olson GK, Tarleton CA et al. Characterization of myeloid and plasmacytoid dendritic cells in human lung. J Immunol. 2006;177:7784-7793.
63. Woltman AM, de Fijter JW, Zuidwijk K et al. Quantification of dendritic cell subsets in human renal tissue under normal and pathological conditions. Kidney Int. 2007;71:1001-1008.
64. Kohrgruber N, Halanek N, Groger M et al. Survival, maturation, and function of CD11c- and CD11c+ peripheral blood dendritic cells are differentially regulated by cytokines. J Immunol. 1999;163:3250-3259.
65. Piccioli D, Tavarini S, Borgogni E et al. Functional specialization of human circulating CD16 and CD1c myeloid dendritic-cell subsets. Blood. 2007;109:5371-5379.

66. Bachem A, Guttler S, Hartung E et al. Superior antigen cross-presentation and XCR1 expression define human CD11c+CD141+ cells as homologues of mouse CD8+ dendritic cells. J Exp Med. 2010;207:1273-1281.
67. Villadangos JA, Shortman K. Found in translation: the human equivalent of mouse CD8+ dendritic cells. J Exp Med. 2010;207:1131-1134.
68. Poulin LF, Salio M, Griessinger E et al. Characterization of human DNGR-1+ BDCA3+ leukocytes as putative equivalents of mouse CD8{alpha}+ dendritic cells. J Exp Med. 2010
69. Crozat K, Guiton R, Contreras V et al. The XC chemokine receptor 1 is a conserved selective marker of mammalian cells homologous to mouse CD8alpha+ dendritic cells. J Exp Med. 2010;207:1283-1292.
70. O'Keeffe M, Hochrein H, Vremec D et al. Dendritic cell precursor populations of mouse blood: identification of the murine homologues of human blood plasmacytoid pre-DC2 and CD11c+ DC1 precursors. Blood. 2003;101:1453-1459.
71. Valladeau J, Ravel O, Dezutter-Dambuyant C et al. Langerin, a novel C-type lectin specific to Langerhans cells, is an endocytic receptor that induces the formation of Birbeck granules. Immunity. 2000;12:71-81.
72. Mizumoto N, Takashima A. CD1a and langerin: acting as more than Langerhans cell markers. J Clin Invest. 2004;113:658-660.
73. Haniffa M, Ginhoux F, Wang XN et al. Differential rates of replacement of human dermal dendritic cells and macrophages during hematopoietic stem cell transplantation. J Exp Med. 2009;206:371-385.
74. Angel CE, Lala A, Chen CJ, Edgar SG, Ostrovsky LL, Dunbar PR. CD14+ antigen-presenting cells in human dermis are less mature than their CD1a+ counterparts. Int Immunol. 2007;19:1271-1279.
75. Klechevsky E, Morita R, Liu M et al. Functional specializations of human epidermal Langerhans cells and CD14+ dermal dendritic cells. Immunity. 2008;29:497-510.
76. Kissenpfennig A, Henri S, Dubois B et al. Dynamics and function of Langerhans cells in vivo: dermal dendritic cells colonize lymph node areas distinct from slower migrating Langerhans cells. Immunity. 2005;22:643-654.
77. Poulin LF, Henri S, de Bovis B, Devilard E, Kissenpfennig A, Malissen B. The dermis contains langerin+ dendritic cells that develop and function independently of epidermal Langerhans cells. J Exp Med. 2007;204:3119-3131.

78. Bursch LS, Wang L, Igyarto B et al. Identification of a novel population of Langerin+ dendritic cells. J Exp Med. 2007;204:3147-3156.
79. Stoitzner P, Holzmann S, McLellan AD et al. Visualization and characterization of migratory Langerhans cells in murine skin and lymph nodes by antibodies against Langerin/CD207. J Invest Dermatol. 2003;120:266-274.
80. Merad M, Manz MG, Karsunky H et al. Langerhans cells renew in the skin throughout life under steady-state conditions. Nat Immunol. 2002;3:1135-1141.
81. Tripp CH, Chang-Rodriguez S, Stoitzner P et al. Ontogeny of Langerin/CD207 expression in the epidermis of mice. J Invest Dermatol. 2004;122:670-672.
82. Caux C, Dezutter-Dambuyant C, Schmitt D, Banchereau J. GM-CSF and TNF-alpha cooperate in the generation of dendritic Langerhans cells. Nature. 1992;360:258-261.
83. Geissmann F, Prost C, Monnet JP, Dy M, Brousse N, Hermine O. Transforming growth factor beta1, in the presence of granulocyte/macrophage colony-stimulating factor and interleukin 4, induces differentiation of human peripheral blood monocytes into dendritic Langerhans cells. J Exp Med. 1998;187:961-966.
84. Peters JH, Ruppert J, Gieseler RK, Najar HM, Xu H. Differentiation of human monocytes into CD14 negative accessory cells: do dendritic cells derive from the monocytic lineage? Pathobiology. 1991;59:122-126.
85. Schiavoni G, Mattei F, Borghi P et al. ICSBP is critically involved in the normal development and trafficking of Langerhans cells and dermal dendritic cells. Blood. 2004;103:2221-2228.
86. Kaplan DH, Jenison MC, Saeland S, Shlomchik WD, Shlomchik MJ. Epidermal langerhans cell-deficient mice develop enhanced contact hypersensitivity. Immunity. 2005;23:611-620.
87. Ginhoux F, Greter M, Leboeuf M et al. Fate Mapping Analysis Reveals That Adult Microglia Derive from Primitive Macrophages. Science. 2010
88. Dick JE, Bhatia M, Gan O, Kapp U, Wang JC. Assay of human stem cells by repopulation of NOD/SCID mice. Stem Cells. 1997;15 Suppl 1:199-203; discussion 204-7.
89. Doulatov S, Notta F, Eppert K, Nguyen LT, Ohashi PS, Dick JE. Revised map of the human progenitor hierarchy shows the origin of macrophages and dendritic cells in early lymphoid development. Nat Immunol. 2010;11:585-593.
90. Rongvaux A, Willinger T, Takizawa H et al. Human thrombopoietin knockin mice efficiently support human hematopoiesis in vivo. Proc Natl Acad Sci U S A. 2011

91. Chapuis F, Rosenzwajg M, Yagello M, Ekman M, Biberfeld P, Gluckman JC. Differentiation of human dendritic cells from monocytes in vitro. Eur J Immunol. 1997;27:431-441.
92. Randolph GJ, Beaulieu S, Lebecque S, Steinman RM, Muller WA. Differentiation of monocytes into dendritic cells in a model of transendothelial trafficking. Science. 1998;282:480-483.
93. Randolph GJ, Inaba K, Robbiani DF, Steinman RM, Muller WA. Differentiation of phagocytic monocytes into lymph node dendritic cells in vivo. Immunity. 1999;11:753-761.
94. Varol C, Landsman L, Fogg DK et al. Monocytes give rise to mucosal, but not splenic, conventional dendritic cells. J Exp Med. 2007;204:171-180.
95. Naik SH, Metcalf D, van Nieuwenhuijze A et al. Intrasplenic steady-state dendritic cell precursors that are distinct from monocytes. Nat Immunol. 2006;7:663-671.
96. Manz MG, Traver D, Miyamoto T, Weissman IL, Akashi K. Dendritic cell potentials of early lymphoid and myeloid progenitors. Blood. 2001;97:3333-3341.
97. Shortman K, Liu YJ. Mouse and human dendritic cell subtypes. Nat Rev Immunol. 2002;2:151-161.
98. Corcoran L, Ferrero I, Vremec D et al. The lymphoid past of mouse plasmacytoid cells and thymic dendritic cells. J Immunol. 2003;170:4926-4932.
99. Lai AY, Kondo M. Asymmetrical lymphoid and myeloid lineage commitment in multipotent hematopoietic progenitors. J Exp Med. 2006;203:1867-1873.
100. Traver D, Akashi K, Manz M et al. Development of CD8alpha-positive dendritic cells from a common myeloid progenitor. Science. 2000;290:2152-2154.
101. Karsunky H, Merad M, Mende I, Manz MG, Engleman EG, Weissman IL. Developmental origin of interferon-alpha-producing dendritic cells from hematopoietic precursors. Exp Hematol. 2005;33:173-181.
102. Auffray C, Fogg DK, Narni-Mancinelli E et al. CX3CR1+ CD115+ CD135+ common macrophage/DC precursors and the role of CX3CR1 in their response to inflammation. J Exp Med. 2009;206:595-606.
103. Liu K, Nussenzweig MC. Origin and development of dendritic cells. Immunol Rev. 2010;234:45-54.
104. Manz MG, Traver D, Akashi K et al. Dendritic cell development from common myeloid progenitors. Ann N Y Acad Sci. 2001;938:167-73; discussion 173-4.

105. Wu L, D'Amico A, Hochrein H, O'Keeffe M, Shortman K, Lucas K. Development of thymic and splenic dendritic cell populations from different hemopoietic precursors. Blood. 2001;98:3376-3382.
106. Galy A, Travis M, Cen D, Chen B. Human T, B, natural killer, and dendritic cells arise from a common bone marrow progenitor cell subset. Immunity. 1995;3:459-473.
107. Miller JS, McCullar V, Punzel M, Lemischka IR, Moore KA. Single adult human CD34(+)/Lin-/CD38(-) progenitors give rise to natural killer cells, B-lineage cells, dendritic cells, and myeloid cells. Blood. 1999;93:96-106.
108. Massberg S, Schaerli P, Knezevic-Maramica I et al. Immunosurveillance by hematopoietic progenitor cells trafficking through blood, lymph, and peripheral tissues. Cell. 2007;131:994-1008.
109. Collin MP, Hart DN, Jackson GH et al. The fate of human Langerhans cells in hematopoietic stem cell transplantation. J Exp Med. 2006;203:27-33.
110. Ginhoux F, Tacke F, Angeli V et al. Langerhans cells arise from monocytes in vivo. Nat Immunol. 2006;7:265-273.
111. Leon B, Lopez-Bravo M, Ardavin C. Monocyte-derived dendritic cells formed at the infection site control the induction of protective T helper 1 responses against Leishmania. Immunity. 2007;26:519-531.
112. Geissmann F, Auffray C, Palframan R et al. Blood monocytes: distinct subsets, how they relate to dendritic cells, and their possible roles in the regulation of T-cell responses. Immunol Cell Biol. 2008;86:398-408.
113. Serbina NV, Salazar-Mather TP, Biron CA, Kuziel WA, Pamer EG. TNF/iNOS-producing dendritic cells mediate innate immune defense against bacterial infection. Immunity. 2003;19:59-70.
114. Inaba K, Inaba M, Romani N et al. Generation of large numbers of dendritic cells from mouse bone marrow cultures supplemented with granulocyte/macrophage colony-stimulating factor. J Exp Med. 1992;176:1693-1702.
115. Hamilton JA. GM-CSF in inflammation and autoimmunity. Trends Immunol. 2002;23:403-408.
116. Vremec D, Lieschke GJ, Dunn AR, Robb L, Metcalf D, Shortman K. The influence of granulocyte/macrophage colony-stimulating factor on dendritic cell levels in mouse lymphoid organs. Eur J Immunol. 1997;27:40-44.
117. Wing EJ, Magee DM, Whiteside TL, Kaplan SS, Shadduck RK. Recombinant human granulocyte/macrophage colony-stimulating factor enhances monocyte

cytotoxicity and secretion of tumor necrosis factor alpha and interferon in cancer patients. Blood. 1989;73:643-646.

118. Waskow C, Liu K, Darrasse-Jèze G et al. FMS-like tyrosine kinase 3 is required for dendritic cell development in peripheral lymphoid tissues. Nature immunology. 2008;9:676.
119. Maraskovsky E, Brasel K, Teepe M et al. Dramatic increase in the numbers of functionally mature dendritic cells in Flt3 ligand-treated mice: multiple dendritic cell subpopulations identified. J Exp Med. 1996;184:1953-1962.
120. Pulendran B, Banchereau J, Burkeholder S et al. Flt3-ligand and granulocyte colony-stimulating factor mobilize distinct human dendritic cell subsets in vivo. J Immunol. 2000;165:566-572.
121. Cecchini MG, Dominguez MG, Mocci S et al. Role of colony stimulating factor-1 in the establishment and regulation of tissue macrophages during postnatal development of the mouse. Development. 1994;120:1357-1372.
122. Dai XM, Ryan GR, Hapel AJ et al. Targeted disruption of the mouse colony-stimulating factor 1 receptor gene results in osteopetrosis, mononuclear phagocyte deficiency, increased primitive progenitor cell frequencies, and reproductive defects. Blood. 2002;99:111-120.
123. Borkowski TA, Letterio JJ, Mackall CL et al. A role for TGFbeta1 in langerhans cell biology. Further characterization of the epidermal Langerhans cell defect in TGFbeta1 null mice. J Clin Invest. 1997;100:575-581.
124. Onai N, Obata-Onai A, Tussiwand R, Lanzavecchia A, Manz MG. Activation of the Flt3 signal transduction cascade rescues and enhances type I interferon-producing and dendritic cell development. J Exp Med. 2006;203:227-238.
125. Geissmann F, Manz MG, Jung S, Sieweke MH, Merad M, Ley K. Development of monocytes, macrophages, and dendritic cells. Science. 2010;327:656-661.
126. Laouar Y, Welte T, Fu XY, Flavell RA. STAT3 is required for Flt3L-dependent dendritic cell differentiation. Immunity. 2003;19:903-912.
127. Esashi E, Wang YH, Perng O, Qin XF, Liu YJ, Watowich SS. The signal transducer STAT5 inhibits plasmacytoid dendritic cell development by suppressing transcription factor IRF8. Immunity. 2008;28:509-520.
128. Tamura T, Tailor P, Yamaoka K et al. IFN regulatory factor-4 and -8 govern dendritic cell subset development and their functional diversity. J Immunol. 2005;174:2573-2581.

129. Anderson KL, Nelson SL, Perkin HB, Smith KA, Klemsz MJ, Torbett BE. PU.1 is a lineage-specific regulator of tyrosine phosphatase CD45. J Biol Chem. 2001;276:7637-7642.
130. Carotta S, Dakic A, D'Amico A et al. The transcription factor PU.1 controls dendritic cell development and Flt3 cytokine receptor expression in a dose-dependent manner. Immunity. 2010;32:628-641.
131. Bakri Y, Sarrazin S, Mayer UP et al. Balance of MafB and PU.1 specifies alternative macrophage or dendritic cell fate. Blood. 2005;105:2707-2716.
132. Zhang P, Zhang X, Iwama A et al. PU.1 inhibits GATA-1 function and erythroid differentiation by blocking GATA-1 DNA binding. Blood. 2000;96:2641-2648.
133. Nerlov C, Querfurth E, Kulessa H, Graf T. GATA-1 interacts with the myeloid PU.1 transcription factor and represses PU.1-dependent transcription. Blood. 2000;95:2543-2551.
134. Bonadies N, Pabst T, Mueller BU. Heterozygous deletion of the PU.1 locus in human AML. Blood. 2010;115:331-334.
135. Small D. FLT3 mutations: biology and treatment. Hematology Am Soc Hematol Educ Program. 2006;178-184.
136. Takanashi M, Yagi T, Imamura T et al. Expression of the Ikaros gene family in childhood acute lymphoblastic leukaemia. Br J Haematol. 2002;117:525-530.
137. Nakase K, Ishimaru F, Avitahl N et al. Dominant negative isoform of the Ikaros gene in patients with adult B-cell acute lymphoblastic leukemia. Cancer Res. 2000;60:4062-4065.
138. Cisse B, Caton ML, Lehner M et al. Transcription factor E2-2 is an essential and specific regulator of plasmacytoid dendritic cell development. Cell. 2008;135:37-48.
139. Renner ED, Torgerson TR, Rylaarsdam S et al. STAT3 mutation in the original patient with Job's syndrome. N Engl J Med. 2007;357:1667-1668.
140. Ginhoux F, Merad M. Ontogeny and homeostasis of Langerhans cells. Immunol Cell Biol. 2010
141. Foster CA, Holbrook KA, Farr AG. Ontogeny of Langerhans cells in human embryonic and fetal skin: expression of HLA-DR and OKT-6 determinants. J Invest Dermatol. 1986;86:240-243.
142. Schuster C, Vaculik C, Fiala C et al. HLA-DR+ leukocytes acquire CD1 antigens in embryonic and fetal human skin and contain functional antigen-presenting cells. J Exp Med. 2009

143. Neron S, Thibault L, Dussault N et al. Characterization of mononuclear cells remaining in the leukoreduction system chambers of apheresis instruments after routine platelet collection: a new source of viable human blood cells. Transfusion. 2007;47:1042-1049.
144. Delia D, Cattoretti G, Polli N et al. CD1c but neither CD1a nor CD1b molecules are expressed on normal, activated, and malignant human B cells: identification of a new B-cell subset. Blood. 1988;72:241-247.
145. Milpied P, Renand A, Bruneau J et al. Neuropilin-1 is not a marker of human Foxp3+ Treg. Eur J Immunol. 2009;39:1466-1471.
146. Battaglia A, Buzzonetti A, Monego G et al. Neuropilin-1 expression identifies a subset of regulatory T cells in human lymph nodes that is modulated by preoperative chemoradiation therapy in cervical cancer. Immunology. 2008;123:129-138.
147. Milush JM, Long BR, Snyder-Cappione JE et al. Functionally distinct subsets of human NK cells and monocyte/DC-like cells identified by coexpression of CD56, CD7, and CD4. Blood. 2009;114:4823-4831.
148. Spits H, Lanier LL. Natural killer or dendritic: what's in a name? Immunity. 2007;26:11-16.
149. Jongbloed SL, Kassianos AJ, McDonald KJ et al. Human CD141+ (BDCA-3)+ dendritic cells (DCs) represent a unique myeloid DC subset that cross-presents necrotic cell antigens. J Exp Med. 2010
150. Gruenbacher G, Gander H, Rahm A, Nussbaumer W, Romani N, Thurnher M. CD56+ human blood dendritic cells effectively promote TH1-type gammadelta T-cell responses. Blood. 2009;114:4422-4431.
151. Sconocchia G, Keyvanfar K, El Ouriaghli F et al. Phenotype and function of a CD56+ peripheral blood monocyte. Leukemia. 2005;19:69-76.
152. Hanna J, Gonen-Gross T, Fitchett J et al. Novel APC-like properties of human NK cells directly regulate T cell activation. J Clin Invest. 2004;114:1612-1623.
153. Chan CW, Crafton E, Fan HN et al. Interferon-producing killer dendritic cells provide a link between innate and adaptive immunity. Nat Med. 2006;12:207-213.
154. de la Rosa G, Longo N, Rodriguez-Fernandez JL et al. Migration of human blood dendritic cells across endothelial cell monolayers: adhesion molecules and chemokines involved in subset-specific transmigration. J Leukoc Biol. 2003;73:639-649.

155. Robert C, Fuhlbrigge RC, Kieffer JD et al. Interaction of dendritic cells with skin endothelium: A new perspective on immunosurveillance. J Exp Med. 1999;189:627-636.
156. Strunk D, Egger C, Leitner G, Hanau D, Stingl G. A skin homing molecule defines the langerhans cell progenitor in human peripheral blood. J Exp Med. 1997;185:1131-1136.
157. Helft J, Ginhoux F, Bogunovic M, Merad M. Origin and functional heterogeneity of non-lymphoid tissue dendritic cells in mice. Immunol Rev. 2010;234:55-75.
158. Herbst B, Kohler G, Mackensen A et al. In vitro differentiation of CD34+ hematopoietic progenitor cells toward distinct dendritic cell subsets of the birbeck granule and MIIC-positive Langerhans cell and the interdigitating dendritic cell type. Blood. 1996;88:2541-2548.
159. Kupper TS, Horowitz M, Birchall N et al. Hematopoietic, lymphopoietic, and proinflammatory cytokines produced by human and murine keratinocytes. Ann N Y Acad Sci. 1988;548:262-270.
160. Chodakewitz JA, Lacy J, Edwards SE, Birchall N, Coleman DL. Macrophage colony-stimulating factor production by murine and human keratinocytes. Enhancement by bacterial lipopolysaccharide. J Immunol. 1990;144:2190-2196.
161. Caux C, Vanbervliet B, Massacrier C et al. CD34+ hematopoietic progenitors from human cord blood differentiate along two independent dendritic cell pathways in response to GM-CSF+TNF alpha. J Exp Med. 1996;184:695-706.
162. Szabolcs P, Avigan D, Gezelter S et al. Dendritic cells and macrophages can mature independently from a human bone marrow-derived, post-colony-forming unit intermediate. Blood. 1996;87:4520-4530.
163. Karsunky H, Merad M, Cozzio A, Weissman IL, Manz MG. Flt3 ligand regulates dendritic cell development from Flt3+ lymphoid and myeloid-committed progenitors to Flt3+ dendritic cells in vivo. J Exp Med. 2003;198:305-313.
164. Tussiwand R, Onai N, Mazzucchelli L, Manz MG. Inhibition of natural type I IFN-producing and dendritic cell development by a small molecule receptor tyrosine kinase inhibitor with Flt3 affinity. J Immunol. 2005;175:3674-3680.
165. Littleton RJ, Baker GM, Soomro IN, Adams RL, Whimster WF. Kinetic aspects of Ki-67 antigen expression in a normal cell line. Virchows Arch B Cell Pathol Incl Mol Pathol. 1991;60:15-19.

166. Bruno S, Darzynkiewicz Z. Cell cycle dependent expression and stability of the nuclear protein detected by Ki-67 antibody in HL-60 cells. Cell Prolif. 1992;25:31-40.
167. Scholzen T, Gerdes J. The Ki-67 protein: from the known and the unknown. J Cell Physiol. 2000;182:311-322.
168. Shah AJ, Smogorzewska EM, Hannum C, Crooks GM. Flt3 ligand induces proliferation of quiescent human bone marrow CD34+CD38- cells and maintains progenitor cells in vitro. Blood. 1996;87:3563-3570.
169. Chorro L, Sarde A, Li M et al. Langerhans cell (LC) proliferation mediates neonatal development, homeostasis, and inflammation-associated expansion of the epidermal LC network. J Exp Med. 2009;206:3089-3100.
170. Vinh DC, Patel SY, Uzel G et al. Autosomal dominant and sporadic monocytopenia with susceptibility to mycobacteria, fungi, papillomaviruses, and myelodysplasia. Blood. 2010;115:1519-1529.
171. Birnberg T, Bar-On L, Sapoznikov A et al. Lack of conventional dendritic cells is compatible with normal development and T cell homeostasis, but causes myeloid proliferative syndrome. Immunity. 2008;29:986-997.
172. Ohnmacht C, Pullner A, King SB et al. Constitutive ablation of dendritic cells breaks self-tolerance of CD4 T cells and results in spontaneous fatal autoimmunity. J Exp Med. 2009;206:549-559.
173. Al-Muhsen S, Casanova JL. The genetic heterogeneity of mendelian susceptibility to mycobacterial diseases. J Allergy Clin Immunol. 2008;122:1043-51; quiz 1052-3.
174. Zhang SY, Boisson-Dupuis S, Chapgier A et al. Inborn errors of interferon (IFN)-mediated immunity in humans: insights into the respective roles of IFN-alpha/beta, IFN-gamma, and IFN-lambda in host defense. Immunol Rev. 2008;226:29-40.
175. Jozsef L, Khreiss T, El Kebir D, Filep JG. Activation of TLR-9 induces IL-8 secretion through peroxynitrite signaling in human neutrophils. J Immunol. 2006;176:1195-1202.
176. Murphy J, Summer R, Wilson AA, Kotton DN, Fine A. The prolonged life-span of alveolar macrophages. Am J Respir Cell Mol Biol. 2008;38:380-385.
177. Sorokin SP, McNelly NA, Hoyt RFJ. CFU-rAM, the origin of lung macrophages, and the macrophage lineage. Am J Physiol. 1992;263:L299-307.

178. Shepard JL, Zon LI. Developmental derivation of embryonic and adult macrophages. Curr Opin Hematol. 2000;7:3-8.
179. Li W, Stanley ER. Role of dimerization and modification of the CSF-1 receptor in its activation and internalization during the CSF-1 response. EMBO J. 1991;10:277-288.
180. Onai N, Manz MG, Schmid MA. Isolation of common dendritic cell progenitors (CDP) from mouse bone marrow. Methods Mol Biol. 2010;595:195-203.
181. Kingston D, Schmid MA, Onai N, Obata-Onai A, Baumjohann D, Manz MG. The concerted action of GM-CSF and Flt3-ligand on in vivo dendritic cell homeostasis. Blood. 2009;114:835-843.
182. Waskow C, Liu K, Darrasse-Jeze G et al. The receptor tyrosine kinase Flt3 is required for dendritic cell development in peripheral lymphoid tissues. Nat Immunol. 2008;9:676-683.
183. Schiavoni G, Mattei F, Sestili P et al. ICSBP is essential for the development of mouse type I interferon-producing cells and for the generation and activation of CD8alpha(+) dendritic cells. J Exp Med. 2002;196:1415-1425.
184. Crozat K, Guiton R, Guilliams M et al. Comparative genomics as a tool to reveal functional equivalences between human and mouse dendritic cell subsets. Immunol Rev. 2010;234:177-198.
185. Aliberti J, Schulz O, Pennington DJ et al. Essential role for ICSBP in the in vivo development of murine CD8alpha + dendritic cells. Blood. 2003;101:305-310.
186. Tailor P, Tamura T, Kong HJ et al. The feedback phase of type I interferon induction in dendritic cells requires interferon regulatory factor 8. Immunity. 2007;27:228-239.
187. Tsujimura H, Tamura T, Kong HJ et al. Toll-like receptor 9 signaling activates NF-kappaB through IFN regulatory factor-8/IFN consensus sequence binding protein in dendritic cells. J Immunol. 2004;172:6820-6827.
188. Chicha L, Jarrossay D, Manz MG. Clonal type I interferon-producing and dendritic cell precursors are contained in both human lymphoid and myeloid progenitor populations. J Exp Med. 2004;200:1519-1524.
189. Hogg A, Bia B, Onadim Z, Cowell JK. Molecular mechanisms of oncogenic mutations in tumors from patients with bilateral and unilateral retinoblastoma. Proc Natl Acad Sci U S A. 1993;90:7351-7355.
190. Fischer A. Human primary immunodeficiency diseases. Immunity. 2007;27:835-845.

191. Onai N, Manz MG. The STATs on dendritic cell development. Immunity. 2008;28:490-492.
192. Valladeau J, Duvert-Frances V, Pin JJ et al. The monoclonal antibody DCGM4 recognizes Langerin, a protein specific of Langerhans cells, and is rapidly internalized from the cell surface. Eur J Immunol. 1999;29:2695-2704.
193. Mc Dermott R, Ziylan U, Spehner D et al. Birbeck granules are subdomains of endosomal recycling compartment in human epidermal Langerhans cells, which form where Langerin accumulates. Mol Biol Cell. 2002;13:317-335.
194. Borkowski TA, Letterio JJ, Farr AG, Udey MC. A role for endogenous transforming growth factor beta 1 in Langerhans cell biology: the skin of transforming growth factor beta 1 null mice is devoid of epidermal Langerhans cells. J Exp Med. 1996;184:2417-2422.
195. Stoitzner P, Stingl G, Merad M, Romani N. Langerhans cells at the interface of medicine, science, and industry. J Invest Dermatol. 2010;130:331-335.
196. Nagao K, Ginhoux F, Leitner WW et al. Murine epidermal Langerhans cells and langerin-expressing dermal dendritic cells are unrelated and exhibit distinct functions. Proc Natl Acad Sci U S A. 2009;106:3312-3317.
197. Tang A, Amagai M, Granger LG, Stanley JR, Udey MC. Adhesion of epidermal Langerhans cells to keratinocytes mediated by E-cadherin. Nature. 1993;361:82-85.
198. Peiser M, Wanner R, Kolde G. Human epidermal Langerhans cells differ from monocyte-derived Langerhans cells in CD80 expression and in secretion of IL-12 after CD40 cross-linking. J Leukoc Biol. 2004;76:616-622.
199. Heufler C, Koch F, Stanzl U et al. Interleukin-12 is produced by dendritic cells and mediates T helper 1 development as well as interferon-gamma production by T helper 1 cells. Eur J Immunol. 1996;26:659-668.
200. Dietz AB, Bulur PA, Emery RL et al. A novel source of viable peripheral blood mononuclear cells from leukoreduction system chambers. Transfusion. 2006;46:2083-2089.
201. Barbaroux JB, Kwan WH, Allam JP et al. Tumor necrosis factor-alpha- and IL-4-independent development of Langerhans cell-like dendritic cells from M-CSF-conditioned precursors. J Invest Dermatol. 2006;126:114-120.
202. Santoro A, Majorana A, Roversi L et al. Recruitment of dendritic cells in oral lichen planus. J Pathol. 2005;205:426-434.

203. Van Pottelberge GR, Bracke KR, Demedts IK et al. Selective accumulation of langerhans-type dendritic cells in small airways of patients with COPD. Respir Res. 2010;11:35.
204. Musso T, Scutera S, Vermi W et al. Activin a induces langerhans cell differentiation in vitro and in human skin explants. PLoS ONE. 2008;3:e3271.
205. Badalian-Very G, Vergilio JA, Degar BA et al. Recurrent BRAF mutations in Langerhans cell histiocytosis. Blood. 2010